# GROWTH FACTOR PRIMING OF MURINE MESENCHYMAL STEM CELLS CRITICALLY DETERMINES THEIR FUNCTIONALITY

by

**SHANKAR SURESH**


A thesis submitted to
The University of Birmingham
For the degree of
**DOCTOR OF PHILOSOPHY**

Centre for Liver Research
School of Immunity and Infection
College of Medical and Dental Sciences
University of Birmingham
September 2014

## Abstract

Mesenchymal stem cells (MSCs) are a subset of multipotent cells with a variety of trophic and immunosuppressive functions. Isolation of murine MSCs has traditionally been hampered by the presence of contaminating cells in culture. In this study, I prospectively isolate murine MSCs based on the co-expression of platelet-derived growth factor (PDGF) receptor alpha and stem cell antigen-1 (PαS MSCs) and present novel data regarding their *in vitro* phenotype, karyotype and immunomodulatory functions. However, PαS MSCs undergo senescence after extended culture, resulting in a loss of function. Addition of fibroblast growth factor 2 (FGF2), PDGF-BB or transforming growth factor-beta 1 (TGF-β1) was able to overcome senescence in MSC cultures. These factors also 'lineage primed' MSCs down specific fates at the genetic and phenotypic levels, with un-supplemented MSCs primed towards bone, FGF2 or PDGF-BB supplemented cells primed towards fat, and FGF2 supplemented cells primed towards cartilage. TGF-β1 supplementation attenuated tri-lineage differentiation of PαS MSCs but maintained their immunosuppressive functions. These findings were confirmed in a mouse model of inflammatory liver injury, with late-passage TGF-β1 MSCs improving liver injury compared to controls. In summary, these results have significant translational relevance as I reveal that culture conditions can functionally 'prime' MSCs down specific fates.

*This thesis is dedicated to my parents, who believed in my choices and supported me unfailingly throughout my studies.*

## Acknowledgements

This project would not have been possible without the assistance and guidance of several other researchers and friends. I would like to take this opportunity to firstly thank my two supervisors, Professor Philip Newsome and Professor Jon Frampton, for their friendship, mentorship, and scientific input in driving this project forward.

I would also like to acknowledge past and present colleagues at the Centre for Liver Research for creating such a friendly and welcoming work environment. In particular, I would like to thank Dr Diarmaid Houlihan for his supervision, help, training and friendship throughout my studies. He has been a constant source of ideas and this body of work would not have been possible without him. I am also indebted to other colleagues including Dr Roberts, Dr Hopkins, Dr Liaskou, Dr Chen and Dr Patten for their friendship, generosity, scientific input and training in various laboratory protocols.

Research is by principle a shared effort and I would like to express my thanks and gratitude to the collaborators that worked on this project. The cartilage differentiation experiments would not have been possible without Dr Zhang and Prof. Hollander (Bristol University). Karyotype analysis was performed in collaboration with Ms. Strachan, Dr Dyer and Prof. Griffiths (West Midlands Regional Genetics Laboratory). Bioinformatics was performed by Dr Wei (University of Birmingham). Finally, my *in vivo* work would not have been possible without the help of technical and veterinary staff of the BMSU (University of Birmingham).

# Table of Contents

# List of Figures

## GROWTH FACTOR PRIMING OF PAS MSCS



## IN VIVO EFFICACY IN A MOUSE MODEL OF ALLOIMMUNE LIVER INJURY

# List of Tables

## List of Abbreviations

| | |
|---|---|
| **αMEM** | α-modified Minimum Essential Media |
| **1-MT** | 1-methyltryptophan |
| **ACI** | Autologous chondrocyte implantation |
| **AIH** | Autoimmune hepatitis |
| **ALP** | Alkaline phosphatase |
| **ALT** | Alanine transaminase |
| **Ang-1** | Angiopoietin-1 |
| **APC** | Antigen presenting cell |
| **B-ONC** | BRDU-overnight colcemid |
| **BM** | Bone marrow |
| **$CCL_4$** | Carbon tetrachloride |
| **CFU-F** | Colony forming unit - fibroblastic |
| **CM** | Conditioned medium |
| **Col1** | Collagen type I |
| **Col2** | Collagen type II |
| **ConA** | Concanavalin A |
| **CTV** | Cell Trace Violet |
| **DAB** | 3,3'-Diaminobenzidine |
| **DMB** | Dimethyl methylene blue |
| **DMEM** | Dulbecco's Modified Eagle Medium |
| **ECM** | Extracellular matrix |
| **EGF** | Epidermal growth factor |
| **ELISA** | Enzyme-linked immunosorbent assay |
| **FACS** | Fluorescence activated cell sorting |
| **FBS** | Foetal bovine serum |
| **FC** | Flow Cytometry |
| **FFPE** | Formalin-fixed Paraffin-embedded tissue |
| **FGF** | Fibroblast growth factor |
| **G-banding** | Giemsa banding |
| **GAG** | Glycosaminoglycans |
| **GF** | Growth factor |
| **GFP** | Green fluorescent protein |
| **GvHD** | Graft-versus-host disease |
| **HBSS** | Hank's Balanced Salt Solution |
| **HGF** | Hepatocyte growth factor |
| **HLA** | Human Leukocyte Antigen |
| **HRP** | Horseradish peroxidase |
| **HSC** | Haematopoietic stem cell |
| **IBMIR** | Instant Blood Mediated Inflammatory Reaction |
| **IDO** | Indoleamine 2,3-dioxygenase |
| **IFNγ** | Interferon-γ |
| **IGF** | Insulin-like growth factor |
| **IHC** | Immunohistochemistry |
| **IL** | Interleukin |
| **IMC** | Isotype matched control |
| **IMS** | Industrial methylated spirit |

| | |
|---|---|
| **iNOS** | Inducible nitric oxide synthase |
| **IP** | Intraperitoneal infusion |
| **ISCT** | International Society for Cellular Therapy |
| **IV** | Intravenous |
| **L-NMMA** | NG-Monomethyl-L-arginine |
| **LPS** | Lipopolysaccharide |
| **LVEF** | Left ventricular ejection fraction |
| **MACS** | Magnetic-activated cell sorting |
| **MELD** | Model for End Stage Liver Disease |
| **MHC** | Major histocompatibility antigens |
| **MI** | Myocardial infarction |
| **MLR** | Mixed lymphocyte reaction |
| **MMP** | Matrix metalloproteinase |
| **MSC** | Mesenchymal Stem Cell |
| **NIHSS** | National Institutes of Health Stroke Scale |
| **NK** | Natural killer |
| **NO** | Nitric oxide |
| **OA** | Osteoartharitis |
| **OD** | Optical density |
| **OI** | Osteogenesis Imperfecta |
| **OVA** | Ovalbumin |
| **P** | Passage number |
| **PBC** | Primary biliary cirrhosis |
| **PBS-T** | PBS+0.05% Tween |
| **PDGF-BB** | Platelet derived growth factor-BB |
| **PGA** | Polyglycolic acid |
| **$PGE_2$** | Prostaglandin E2 |
| **PI** | Propidium Iodide |
| **PSC** | Primary sclerosing cholangitis |
| **PSG** | Penicillin/Streptomycin/Glutamine |
| **PαS** | $PDGFR\alpha^{+}Sca\text{-}1^{+}$ MSCs |
| **QR** | Quadriradial |
| **RBC** | Red blood cell |
| **RCT** | Randomised controlled trial |
| **RPMI** | Roswell Park Memorial Institute medium |
| **SA-β-gal** | Senescence-associated β-galactosidase |
| **Sca-1** | Stem cell antigen 1 |
| **SCE** | Sister chromatid exchange |
| **SCF** | Stem cell factor |
| **SDF-1** | Stromal derived factor 1 |
| **SDS** | Sodium dodecyl sulphate |
| **SLE** | Systemic lupus erythematosus |
| **SLEDAI** | Systemic lupus erythematosus disease activity index |
| **TBS-T** | Tris-buffered saline + 0.1% Tween20 |
| **TCR** | T Cell Receptor |
| **TGF-β** | Transforming growth factor beta |
| **TLR** | Toll-like receptor |
| **TNFα** | Tumour necrosis factor alpha |
| **Treg** | Regulatory T cells |
| **VEGF** | Vascular endothelial growth factor |

# CHAPTER 1

# INTRODUCTION

## 1.1 Mesenchymal Stem Cells: A Historical Perspective

The term "Mesenchymal Stem Cell (MSC)" was first coined in 1991 by Arnold Caplan to describe a rare population of bone marrow (BM) cells with the ability to differentiate into a variety of skeletal tissues (Caplan, 1991). His work can be traced back to a series of seminal observations by Friedenstein and colleagues who showed that cells with osteogenic potential resided in the non-haematopoietic section of BM (Friedenstein et al., 1970). This stromal population was characterised by their spindle shaped morphology, ability to adhere onto tissue culture plastic, and their ability to form colonies. These cells were also capable of forming heterotrophic bone when transplanted in mice, demonstrating a degree of self-renewal and multipotency that are defining features of stem cells (Friedenstein et al., 1966). By combining the efforts of Friedenstein and other MSC biologists at the time, Caplan championed the idea that multiple mesenchymal tissues could arise from a single stem cell in a pathway termed 'The Mesengenic Process' (Figure 1.1; Caplan, 1994).

Although the early work in MSC biology was of limited interest to researchers outside the field, the potential of MSCs was demonstrated to a worldwide audience upon the publication of a landmark paper by Pittenger and colleagues (Pittenger et al., 1999a). They isolated MSCs from human BM and cultured them *in vitro* before inducing tri-lineage differentiation into bone, fat and cartilage. These findings laid the framework for future studies on MSC biology which revealed a broader differentiation potential ('plasticity') than originally thought (Krause, 2002), and a potent ability to suppress immune cell proliferation (Bartholomew et al., 2002). MSC-like cells have also been isolated from a variety of tissues,

suggesting a broad role for these cells in the maintenance of multiple organs (Murray et al., 2014). Their ease-of-isolation, growth characteristics, plasticity and immunosuppressive ability have made MSCs a desirable cell source for future stem cell therapies, with multiple human clinical trials already underway (Mendicino et al., 2014). However, very little is known about the *in vivo* location and function of these elusive cells due to the lack of specific markers to prospectively identify MSCs. This has drawn criticism from certain groups, who argue that the term "stem cell" should not be used to describe the heterogeneous populations of MSCs that have been isolated over the past 15 years (Bianco et al., 2008).

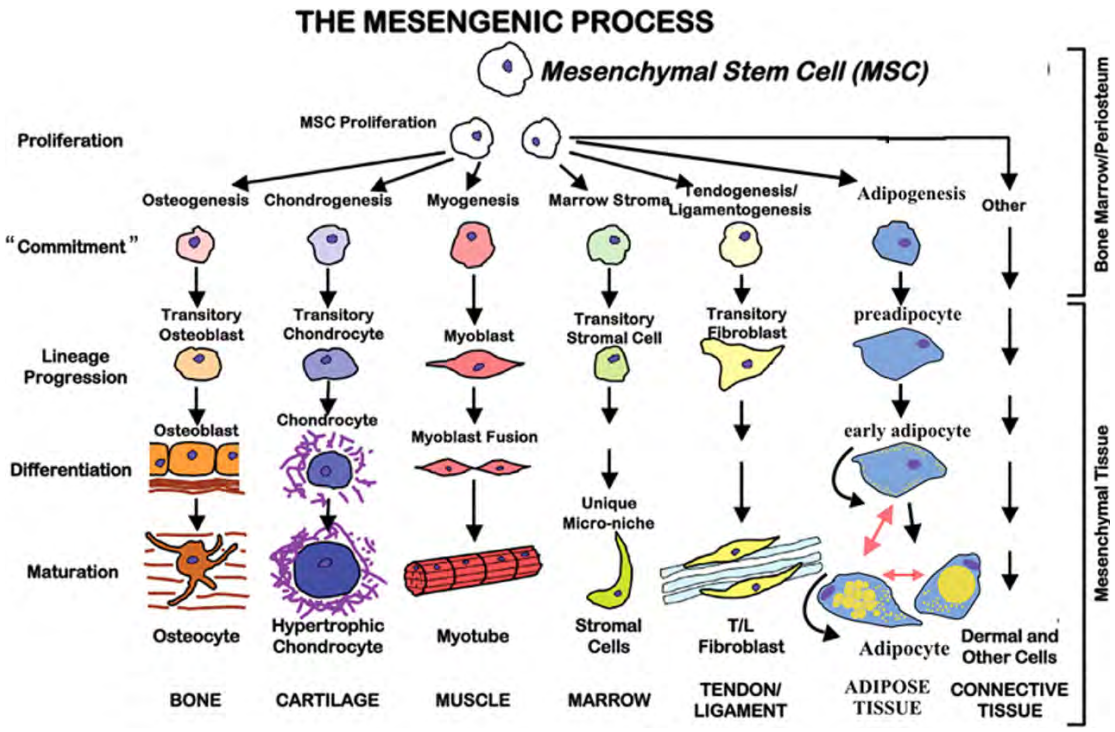


Figure 1.1 | **The Mesengenic Process**. This hypothetical pathway describes the ability of MSCs to differentiate into a variety of mature mesenchymal tissues, analogous to the proposed hierarchy of haematopoietic stem cells. Figure taken from Caplan, 1994.

## 1.2 What defines an MSC?

Traditionally, MSCs were defined by their ability to form spindle-shaped colonies (Colony forming unit-fibroblastic; CFU-F) on plastic and their ability to undergo *in vitro* tri-lineage differentiation towards bone, fat and cartilage. Over 40 years later, the same four tenets (combined with the expression of certain surface markers) are still viewed as the benchmark criteria to define putative MSCs (Dominici et al., 2006). This widely cited, but often criticised position paper by the International Society for Cellular Therapy (ISCT) was the first to try and standardise the heterogeneous populations of human BM cells used in past studies. Under their criteria, MSCs should fulfil the following three requirements: (1) plastic adherence; (2) express the surface markers CD105, CD73 and CD90 and lack expression of CD45, CD34, CD14, CD11b, CD19, CD79α and HLA-DR; and (3) tri-lineage differentiation (Figure 1.2).

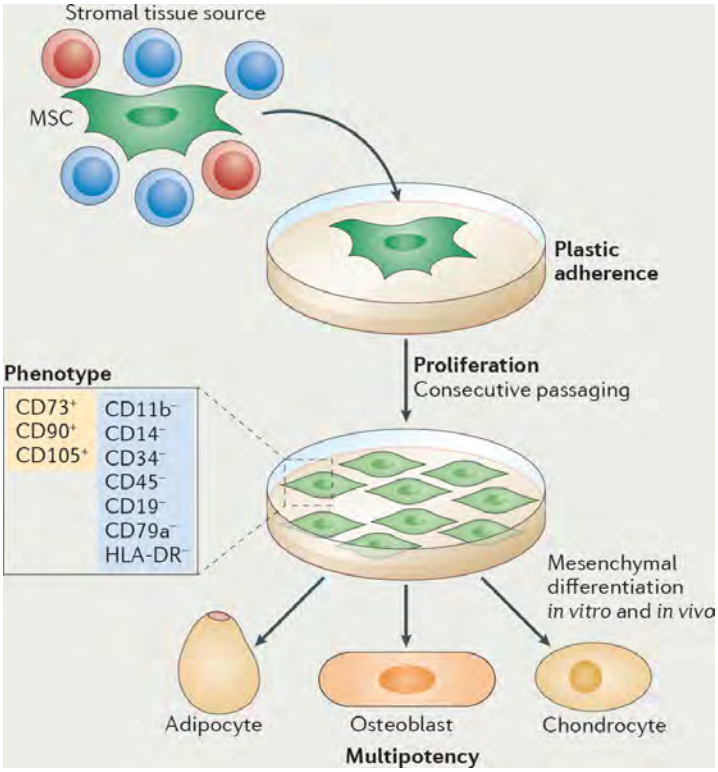


Figure 1.2 | **ISCT minimal criteria that define MSCs**. Human MSCs should be able to adhere to plastic and expand under normal culture conditions. They express certain phenotypic markers and lack expression of haematopoietic and immune cell markers. Finally, they are able to undergo tri-lineage differentiation *in vitro*. Figure taken from Le Blanc and Mougiakakos, 2012.

The main argument against the ISCT criteria revolves around whether MSCs could indeed be called “stem cells” (Bianco et al., 2013, Bianco et al., 2008). A single, prospectively isolated haematopoietic stem cell (HSC) has the capacity to serially recapitulate haematopoiesis in lethally irradiated mice (Krause et al., 2001). In doing so, HSCs meet the benchmark used to define stem cells: self-renewal and multipotency *in vivo*. By contrast, MSCs have, until recently, failed to meet these strict criteria since the biology of MSCs has been inferred from the study of *in vitro* cultured cells. Self-renewal is assumed after periods of *in vitro* expansion, and multipotency demonstrated by the generation of small amounts of extracellular matrix from non-clonal cultures. Fibroblasts share many features with MSC populations when assessed using these loose criteria, leading some to question whether MSCs are phenotypically distinct from fibroblasts (Haniffa et al., 2009). As such, there has been a shift in nomenclature towards “Multipotent mesenchymal stromal cells (MSCs)” due to the lack of evidence of self-renewal (Bianco et al., 2008). This evidence has only recently begun to emerge with the identification of markers that allow prospective isolation of mouse MSCs from BM (Pinho et al., 2013, Mendez-Ferrer et al., 2010, Morikawa et al., 2009).

Another disadvantage of the ISCT criteria is that it does not address the heterogeneity of starting MSC populations. In addition to BM, MSC-like cells have been isolated from adipose tissue (Zuk et al., 2002), dental pulp (Pierdomenico et al., 2005), umbilical cord (Lee et al., 2004) and placental tissue (Igura et al., 2004). When isolated using plastic adherence, these cultures yield heterogeneous populations of non-clonal cells that are all grouped together as “MSCs”. They have then been cultured on different surfaces, under different oxygen

concentrations and in diverse culture media (Figure 1.3; Wagner and Ho, 2007). However, all these cultures are able to form CFU-Fs, express the relevant markers and undergo tri-lineage differentiation, thereby meeting ISCT criteria. This heterogeneity has made it difficult to compare results between papers, and several different mechanisms of action have been reported. For example, a myriad of small molecules have been reported to mediate the therapeutic effects of MSCs in animal models (Caplan and Correa, 2011). These findings are rarely comparable and are usually redundant or contradictory, weakening the evidence base for translating promising pre-clinical work into humans (Krampera et al., 2013).

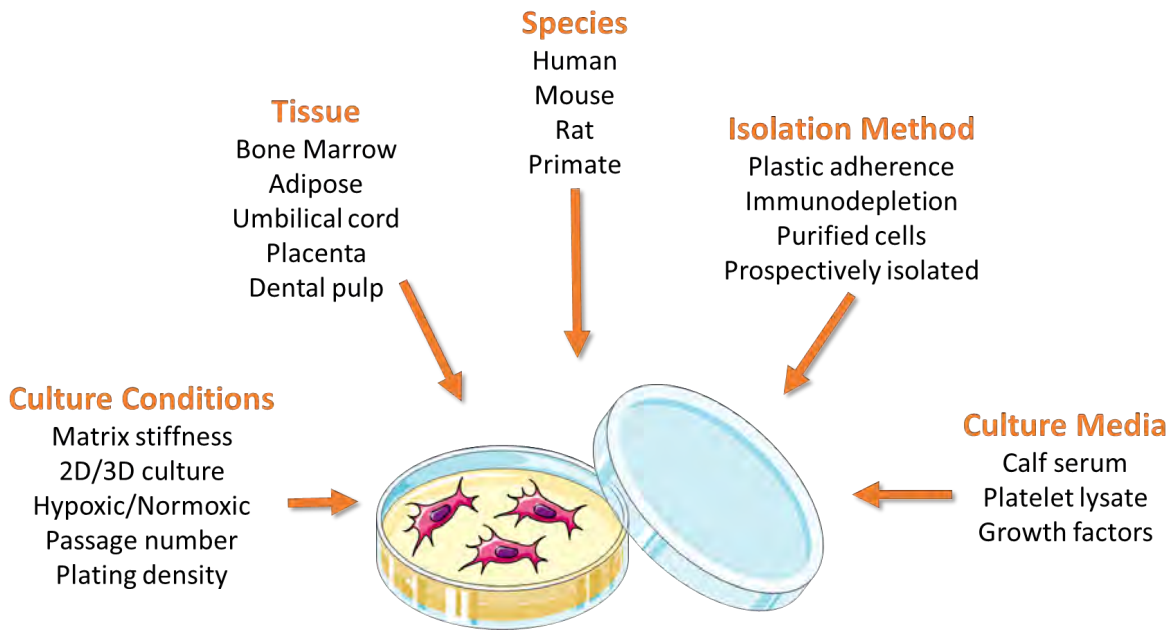


Figure 1.3| **Factors contributing to the heterogeneity of MSC populations**. Comparing results across studies is difficult due to differences between MSC isolation and culture protocols. All the factors listed above can impact on the efficacy of the resulting population of MSCs and needs to be taken into account when comparing studies.

## 1.3 Isolation of Murine MSCs

MSCs are an attractive source of cells for future therapies due to their potent trophic and immunomodulatory characteristics. However, the heterogeneous populations of MSC-like cells used in previous studies have hampered efforts to reach agreement over potential mechanisms of action. Additionally, the majority of studies have utilised human or rat MSCs due to difficulties in isolating and culturing a purified population of mouse MSCs (Frenette et al., 2013, Anjos-Afonso and Bonnet, 2011, Peister et al., 2004). Reasons behind this are unclear, but the relative rarity of stromal cells and the high percentage of haematopoietic cells found in mouse BM could play a part. It has also been argued that murine MSCs need some haematopoietic contaminants in culture to grow, and the stepwise purification of stromal cells described in newer isolation protocols could negatively impact MSC yields (Anjos-Afonso and Bonnet, 2011). As such, our current understanding of MSC biology is inferred from the study of *in vitro* cultured human cells. These issues have, until recently, prevented the field from studying the basic biology and *in vivo* functions of MSCs using the large number of transgenic mouse models available.

To overcome these limitations, researchers have developed new methods of MSC isolation that depends less on the plastic-adherence property of these cells. As this thesis investigates the effect of growth factors on a prospectively isolated population of mouse MSCs, I will be focusing here on the progress made in isolating mouse MSCs over their human counterparts (summarised in Table 1.1).

Table 1.1 | **Advantages and disadvantages of murine MSC isolation methods**.

| Isolation Method | Advantages | Disadvantages |
|---|---|---|
| **Plastic adherence** | ☑ Transferrable between mouse strains<br>☑ Low cost, easy to follow protocol | ☒ Heterogeneous populations of stromal cells isolated<br>☒ Persistence of haematopoietic and endothelial cells in culture<br>☒ Requires long-term *in vitro* culture which can lead to senescence |
| **Frequent media change** | ☑ Removal of haematopoietic cells allowing expansion of a purer MSC culture<br>☑ Transferrable between mouse strains<br>☑ Low cost | ☒ Haematopoietic cells still persist in culture<br>☒ Relies on plastic-adherence and extended *in vitro* culture for purification of stromal cells<br>☒ Labour intensive, cultures require attention every 8 hours |
| **Immuno-depletion** | ☑ Removes haematopoietic contamination from MSC cultures<br>☑ Transferrable between mouse strains | ☒ Significantly increased population doubling times<br>☒ Relies on plastic-adherence and extended *in vitro* culture for further purification<br>☒ Cost of magnetic beads and sorting equipment is high |
| **Positive selection** | ☑ Enriches for cells with MSC potential from BM<br>☑ No effect on population doubling times | ☒ Not suitable for all mouse strains<br>☒ Some markers are not detectable in uncultured BM cells<br>☒ Markers are not specific to MSCs<br>☒ Expensive |
| **Prospective isolation** | ☑ Pure populations of MSCs without the need for extended *in vitro* culture<br>☑ Allows for the study of MSC biology *in vivo*<br>☑ Self-renewal and multipotency clearly demonstrated at the single-cell level | ☒ Some methods require use of specialist transgenic mice<br>☒ Requires access to a cell sorter<br>☒ Labour-intensive and expensive |

### 1.3.1 Plastic Adherence

Initial attempts to isolate mouse MSCs mimicked those of their human counterparts by plating whole BM onto tissue culture plastic and expanding the plastic-adherent population. Differences in CFU-F ability and growth kinetics between mouse strains were immediately clear, with Balb/c BM yielding the most CFU-F (3 per $10^6$ cells) and C57BL/6 BM yielding nearly 10 fold lower numbers (Phinney et al., 1999). The plastic-adherent population was very heterogeneous, with 80% of cells expressing CD11b (marker of myeloid cells) and CD45 (leukocyte marker). These contaminating cells were able to survive for several weeks as the stromal fraction of mouse BM has been shown to support B-cell lymphopoiesis and granulopoiesis (Phinney, 2008).

Meirelles and Nadri demonstrated the importance of initial plating density on CFU-F ability (Meirelles Lda and Nardi, 2003). A density of $5x10^4$ BM cells/$cm^2$ showed the maximum number of non-overlapping colonies. They did detect the expression of CD11b in MSC cultures at passage (P) six, but this was lost by P10. Cells remaining at P10 onwards were homogenous in size and shape and were negative for the leukocytic markers CD45, CD11b and CD19. Interestingly, no differences in CFU-F ability were observed between Balb/c and C57BL/6 mice in this study, which contradicts the earlier report by Phinney *et al.* (1999).

Peister and colleagues published a similar protocol emphasising the importance of initial plating density on MSC isolation (Peister et al., 2004). Unlike Meirelles and Nadri (2003), they initially used high-density seeding of BM cells before swapping to a lower 50 cells/$cm^2$ from P2 onwards. Differences in growth kinetics, cell surface phenotype and tri-lineage differentiation were observed between the five mouse strains analysed. C57BL/6 and Balb/c strains showed the best growth characteristics, but failed to produce significant proteoglycan deposits after chondrogenic differentiation. By contrast, MSCs from FVB/N and DBA1 mice divided slower but produced better cartilage.

### 1.3.2 Frequent Media Change

Protocols involving frequent media change were employed to combat the adherence of haematopoietic cells in MSC cultures. Nadri and colleagues combined frequent media change with shortened trypsin incubation time to increase the percentage of MSCs in mouse BM preparations (Soleimani and Nadri, 2009, Nadri et al., 2007). Non-adherent BM cells were removed 3 hours after plating and replaced with fresh media, and this step was repeated every 8 hours for three days. Two minute trypsin incubation times was also used to selectively lift MSCs from tissue culture plastic while leaving behind firmly-adherent macrophages. However, between 5-10% cells that were re-plated still expressed CD11b and CD45, showing that some haematopoietic cells were still able to persist in culture.

### 1.3.3 Immunodepletion of non-MSCs

Baddoo and colleagues combined plastic adherence with immunodepletion to improve the purity of murine MSC cultures (Baddoo et al., 2003). Eight to ten day old plastic-adherent cells were subject to three rounds of immunodepletion with antibodies against CD11b, CD34, and CD45. The immunodepleted fraction (23% of plastic adherent cells in FVB/N mice, 7% in Balb/c mice) readily differentiated into bone, fat and cartilage and expressed typical markers of murine MSCs. However, immunodepleted cells displayed a prolonged doubling time of 5-7 days due to the downregulation of genes regulating cell cycle progression. Addition of fibroblast growth factor 2 (FGF2) increased the growth kinetics of immunodepleted MSC populations but inhibited their tri-lineage differentiation.

Tropel *et al*. used a single round of immunodepletion against CD11b to remove myeloid cells from mouse MSC cultures (Tropel et al., 2004). Despite this, $CD11b^+$ cells remained in culture for many weeks (until P10), which could be due to the single round of immunodepletion used in their study. Interestingly, Tropel *et al*. report a mean doubling time of 1.7 days, which compares favourably with the longer 5-7 days reported by Baddoo *et al*. (2003). Immunodepleted MSCs were able to undergo tri-lineage differentiation and prolonged growth *in vitro* for up to 30 passages with no evidence of karyotypic transformation.

### 1.3.4 Positive Enrichment of MSCs

A key disadvantage of the isolation methods listed above is the reliance on extended periods of *in vitro* culture for MSC-like cells to "outlive" any contaminating haematopoietic cells. Extended culture has been shown to induce replicative senescence in both mouse (Coutu et al., 2011) and human MSCs (Wagner et al., 2008). It can also predispose cells towards malignant transformation, a phenomenon that preferentially affects murine cells (Tolar et al., 2007, Miura et al., 2006). To overcome these limitations, researchers began to use markers that enriched for cells with CFU-F and tri-lineage potential from BM.

The cell surface glycoprotein CD34 has been used to enrich for MSCs in BM cultures. Although CD34 is primarily regarded as a marker of haematopoietic stem/progenitor cells, recent evidence suggests it may mark a whole host of stem/progenitors, including MSCs (Sidney et al., 2014, Lin et al., 2012). Nadri and Soleimani isolated $CD34^+$ cells from the BM of C57BL/6 mice using magnetic selection (Nadri and Soleimani, 2007). No expression of haematopoietic markers were observed in freshly-sorted and cultured cells, and they were able to undergo *in vitro* differentiation towards bone and fat. However, an increase in population doubling time was seen at each passage and attempts to repeat this isolation method on other strains of mice were unsuccessful.

Stem cell antigen 1 (Sca-1, or Ly-6A) can also be used to enrich MSCs from mouse BM (Boxall and Jones, 2012). Short *et al*. describe a protocol that uses fluorescence activated cell sorting (FACS) to isolate a pure population of $CD45^{-}CD31^{-}Sca\text{-}1^{+}$ MSCs with increased CFU-F potential from C57BL/6 mice (Short et al., 2009). $Sca\text{-}1^{+}$ MSCs also have increased neurogenic potential compared to plastic-adherent BM cells (Jamous et al., 2010). However, Sca-1 expression varies between mouse strains due to post-translational regulation, with mice expressing the *Ly6.2* allele (e.g. C57BL/6, FVB/N) having higher expression of Sca-1 than mice expressing the *Ly6.1* allele (e.g. Balb/c; Holmes and Stanford, 2007). This limits its use as a marker that can enrich MSCs across all mouse strains.

Other markers, such as CD105, CD73, CD90, CD44 and CD29 are also highly expressed by mouse MSCs (Boxall and Jones, 2012). However, most of these markers are not specific to stromal cells and are not detectable in fresh, uncultured BM (Anjos-Afonso and Bonnet, 2011). As mentioned above, there are also strain-specific differences in expression. Unlike human MSCs, which can be purified to a reasonable degree using CD146 (Sacchetti et al., 2007) or LNGFR (Mabuchi et al., 2013b), no one cell surface protein alone can be used for the prospective isolation of mouse MSCs.

### 1.3.5 Prospective isolation of MSCs

#### 1.3.5.1 PDGFRα$^{+}$Sca-1$^{+}$ MSCs

Morikawa and colleagues were the first to publish a method to prospectively identify and isolate murine MSCs (Morikawa et al., 2009). The authors used FACS to isolate non-haematopoietic (CD45-TER119-) BM cells that co-expressed platelet derived growth factor receptor alpha (PDGFRα) and Sca-1. They were able to isolate this double-positive (PαS) population from six inbred strains of mice, including C57BL/6, Balb/c, FVB/N and DBA1. PαS MSCs were able to undergo tri-lineage differentiation at the clonal level and showed 120,000-fold higher CFU-F frequency than unfractioned BM mononuclear cells. The reported population doubling time was 50.6 hours, with cultures yielding over $10^{7}$ cells from a starting population of 5000 cells. PαS MSCs expressed standard MSC markers (CD29, CD49e, CD105, CD133, CD34, CD90 and CD146) and did not express haematopoietic markers (CD45, CD150 or CD117). Interestingly, undifferentiated PαS MSCs also expressed markers of endothelial cells (Flk-1 and VEGFR3), with some clones being able to undergo angiogenic differentiation into CD31$^{+}$CD144$^{+}$ endothelial cells.

*In vivo* studies revealed that PαS MSCs resided in the perivascular space of cortical bone *in vivo* and expressed both angiopoietin-1 (Ang-1) and CXCL12, two necessary factors for haematopoiesis (Figure 1.4). Systemic co-transplantation of 10,000 green fluorescent protein positive (GFP$^{+}$) PαS cells alongside 100 CD34-KSL HSCs restored haematopoiesis in irradiated mice. Significant numbers of GFP$^{+}$ PαS cells were again found in the perivascular region expressing CXCL12 and Ang-1, while others were found to give rise to functioning

osteoblasts and adipocytes, demonstrating that PαS cells can reconstitute their *in vivo* niche. Furthermore, the authors were able to isolate secondary clonal $GFP^+$ CFU-Fs from recipient mice 16 weeks after transplantation and show they retained their tri-lineage differentiation potential. Thus, this paper was the first to convincingly show the *in vivo* self-renewal and multipotency of a specific cell type that displays many of the hypothesised functions of MSCs, and represents a major step forward for the field.

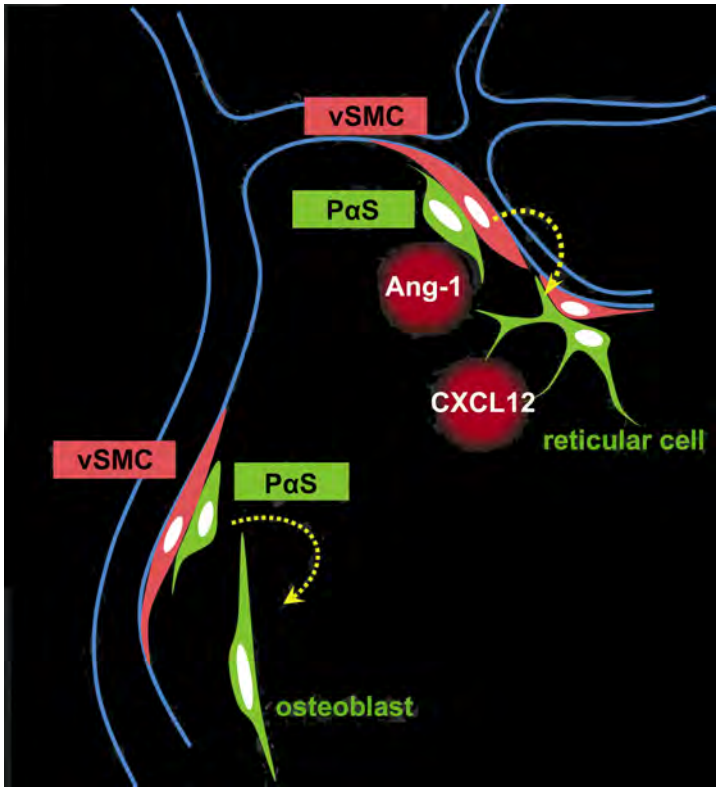


Figure 1.4 | **In vivo localisation of PαS MSCs in murine BM**. PαS MSCs were found in the perivascular space alongside vascular smooth muscle cells (vSMC). They can give rise to both osteoblasts and reticular cells that function as haematopoietic niche cells. Figure taken from Morikawa et al., 2009.

### 1.3.5.2 Nestin$^+$ MSCs

A comprehensive and elegant study by the Frenette group identified the intermediate filament protein Nestin as another marker for the prospective isolation of murine MSCs (Mendez-Ferrer et al., 2010). Nestin$^+$ MSCs represented 0.08% of total BM mononuclear cells, and 60% of Nestin$^+$ MSCs were located directly adjacent to HSCs. Expression of key HSC maintenance proteins were highest in the Nestin$^+$ population, and selective deletion of Nestin$^+$ cells resulted in a 50% reduction in BM HSC numbers. Deletion of Nestin$^+$ cells also decreased the homing of infused HSCs towards the BM of lethally irradiated mice by up to 90%, suggesting that Nestin$^+$ MSCs play a crucial role in maintaining the HSC niche.

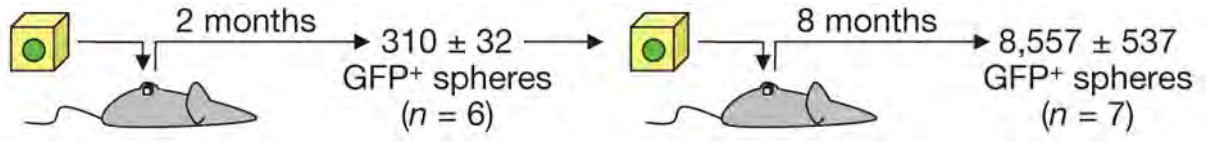


Figure 1.5 | **In vivo self-renewal of Nestin$^+$ MSCs**. Single clonal mesenspheres attached onto phosphate cubes were transplanted subcutaneously into recipient mice and left for two months. From these, 310 Nestin$^+$ mesenspheres were isolated, of which 38% showed multi-lineage differentiation. Single secondary spheres were transplanted into recipient mice and left for 8 months. A total of 8,557 Nestin+ tertiary mesenspheres could be isolated, demonstrating the remarkable self-renewal properties of these cells in serial transplantations. Figure taken from Mendez-Ferrer et al., 2010.

As Nestin is an intracellular protein, a transgenic Nestin-GFP mouse is required to isolate Nestin$^+$ MSCs using FACS. Nestin$^+$ cells can undergo tri-lineage differentiation and could be propagated as clonal 3D "mesenspheres" *in vitro*. The authors convincingly demonstrate *in vivo* self-renewal at the single cell level using a heterotrophic bone ossicle assay (Figure 1.5).

*In vivo* evidence of multi-lineage differentiation was demonstrated by lineage-tracing studies showing GFP$^+$ Nestin cells contributing to both the osteogenic and chondrogenic lineages under physiological conditions. This was the first study to demonstrate the *in* vivo contribution of MSCs in the maintenance and turnover of skeletal cells without injury, thereby confirming a long-hypothesised function of MSCs.

#### 1.3.5.3 PDGFRα$^+$CD51$^+$ MSCs

The intracellular expression of Nestin precludes the use of this marker to prospectively isolate MSCs from non-transgenic, wild-type mice. To address this issue, the Frenette group set out to identify cell surface markers that define the BM Nestin$^+$ population (Pinho et al., 2013). In another exhaustive study, they show that non-haematopoietic (CD45$^-$TER-119$^-$), non-endothelial (CD31$^-$) BM cells that express PDGFRα and CD51 (alpha V integrin) also express Nestin at high (≈75%) levels. This dual-positive population of stromal cells were able to recapitulate all the MSC activity reported in their earlier Nestin$^+$ MSC paper (Mendez-Ferrer et al., 2010). PDGFRα$^+$CD51$^+$ MSCs were enriched for HSC-maintenance factors and expressed them at similar levels to Nestin$^+$ MSCs. PDGFRα$^+$CD51$^+$ MSCs were also able to be propagated *in vitro* as self-renewing mesenspheres and clonally-expanded cells were able to undergo tri-lineage differentiation. The *in vivo* self-renewal and differentiation capacity of PDGFRα$^+$CD51$^+$ MSCs was proven by serial transplantation studies of bone ossicle formation. The authors then go on to isolate PDGFRα$^+$CD51$^+$ cells from human foetal BM, suggesting that the identity of MSCs in both species may be conserved through evolution.

### 1.3.5.4 Comparison of PαS, Nestin$^+$ and PDGFRα$^+$CD51$^+$ MSCs

These three studies were the first to comprehensively describe markers of murine MSCs. The authors tested the stemness of their populations using traditional stem cell assays to prove self-renewal and multipotency *in vivo* (Figure 1.6). Additionally, these papers have also described the essential role of MSCs in maintaining the HSC niche. As such, they represent major advances in the murine MSC field and should act as a platform for future research into the biology of these cells.

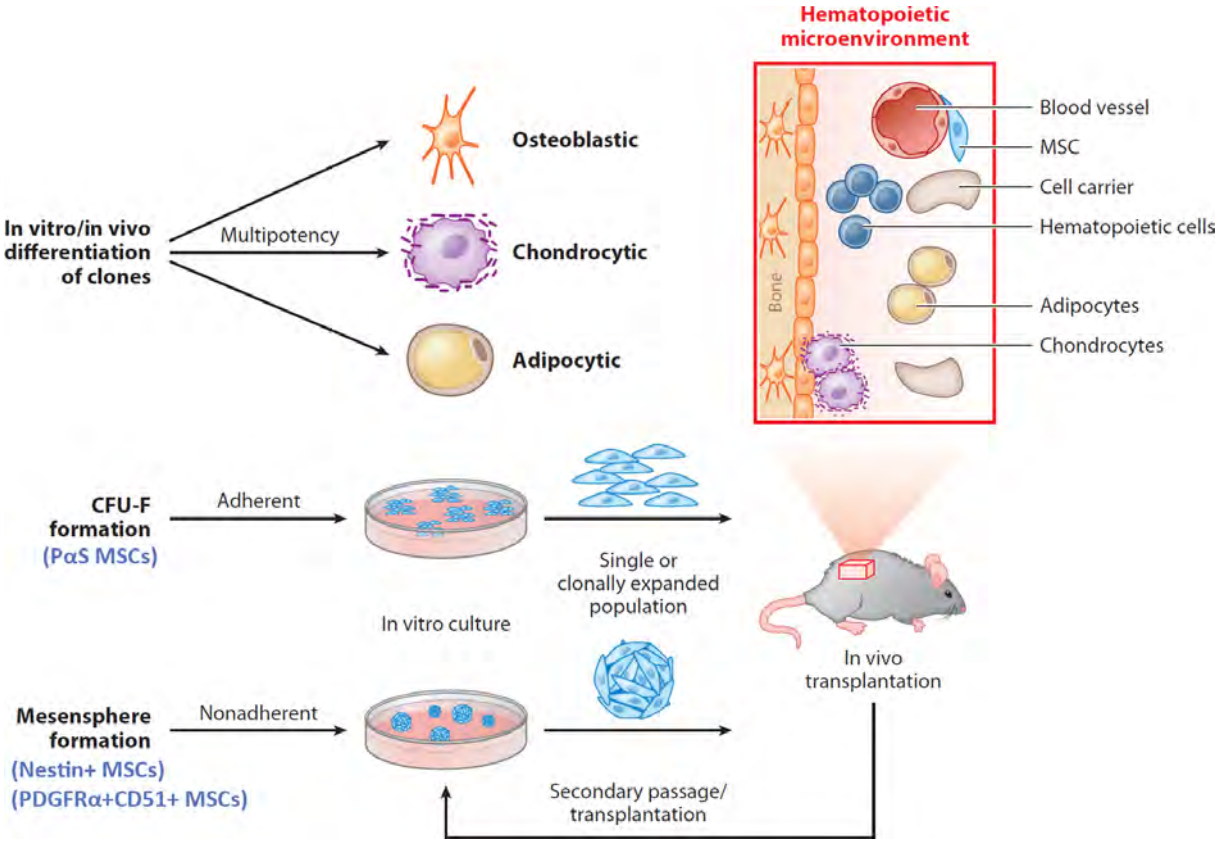


Figure 1.6 | **Methods used to test for stem cell characteristics in MSC populations.** All three marker combinations have demonstrated clonal tri-lineage differentiation *in vitro* and (to a degree) *in vivo*. CFU-F from PαS MSCs were shown to self-renew and re-populate the haematopoietic niche after intravenous infusion in irradiated mice. Mesenspheres from Nestin$^+$ and PDGFRα$^+$CD51$^+$ MSCs were shown to self-renew in bone ossicle formation assays after serial transplantation. Figure modified from Frenette *et al.*, 2013.

However, there are subtle differences between how the three MSC populations were isolated and tested that suggest that they mark independent, non-overlapping cells with an MSC phenotype (Table 1.2). Firstly, PαS MSCs are isolated from cortical bone with the BM discarded at the start of the protocol (Houlihan et al., 2012). The Nestin$^+$ and PDGFRα$^+$CD51$^+$ MSCs are isolated from collagenase-digested BM (Pinho et al., 2013, Mendez-Ferrer et al., 2010). As such, PαS enriches for cells with MSC potential from bone and not BM. Secondly, PαS MSC clones show differences in their differentiation ability, with some clones able to undergo angiogenic/endothelial differentiation. No vascular involvement has been reported for Nestin$^+$ and PDGFRα$^+$CD51$^+$ MSCs, and current evidence demonstrates contribution to the skeletal lineage only. Thirdly, while the Nestin$^+$ and PDGFRα$^+$CD51$^+$ MSCs have had their self-renewal proved using serial transplantation assays, the PαS MSCs have only been shown to reconstitute their BM niche in one round of transplantation.

The direct relationship between PαS MSCs and Nestin$^+$ MSCs was studied by Pinho *et al*. (2013). They show that only 6% of BM Nestin$^+$ MSCs express Sca-1. When they isolated Nestin$^+$ MSCs from compact bone, the percentage of Sca-1 expression increased to 23%. This suggests that both sets of markers identify distinct cell populations with MSC activity, although there is a degree of phenotypic overlap between the two. The functional differences and contribution to the HSC niche between bone-derived MSCs (PαS cells) and BM-derived MSCs (Nestin$^+$ and PDGFRα$^+$CD51$^+$ cells) still remain unexamined.

Table 1.2 | **Comparison between prospective isolation methods for murine MSCs.**

| MSC Type | Mouse strains | Clonal Growth | Clonal Potency | In vivo localisation | Contribution to *in vivo* tissue | Serial transplant | Reference |
|---|---|---|---|---|---|---|---|
| **PαS** | C57BL/6<br>Balb/c<br>FVB/N<br>DBA1<br>ICR<br>129 | ✓ | Bone<br>Fat<br>Cartilage<br>Endothelial | Perivascular | Bone and fat after lethal irradiation of BM | ✗<br>(Only one round) | Morikawa et al. (2009) |
| **Nestin$^+$** | Nes-GFP | ✓ | Bone<br>Fat<br>Cartilage | Perivascular (directly adjacent to HSCs) | Bone and cartilage under physiological conditions | ✓ | Mendez-Ferrer et al. (2010) |
| **PDGFRα$^+$ CD51$^+$** | C57BL/6 | ✓ | Bone<br>Fat<br>Cartilage | (nd) | (nd) | ✓ | Pinho et al. (2013) |

**Abbreviations**: (nd), not determined

## 1.4 Therapeutic Potential of MSCs in Regenerative Medicine

MSCs have a number of features that make them particularly suitable as a cellular therapy. Firstly, they can be isolated from a variety of adult tissues. Secondly, their immunosuppressive and immune privileged properties allow for allogeneic transplantation across major histocompatibility (MHC) antigens (Ankrum et al., 2014). Thirdly, their differentiation potential and plasticity can be exploited in a variety of clinical settings. Fourthly, MSCs can secrete a variety of bioactive molecules and trophic factors that promote healing and dampen inflammation (Ranganath et al., 2012). Finally, MSCs can also be cryopreserved and recovered as needed to form a bankable, "off-the-shelf" cell therapy product (Ginis et al., 2012). In this section, I will review the evidence for MSCs in regenerative medicine therapies, starting with traditional uses of MSCs to replace skeletal tissue before focusing on their non-mesenchymal potential.

### 1.4.1 MSCs in Bone Repair

There are numerous studies that have used MSCs to repair fractures due to osteogenesis being the best characterised and well understood pathways of MSC differentiation. An early study by Bruder *et al*. demonstrated that autologous MSCs seeded onto scaffolds could repair a critical-sized fracture in dogs (Bruder et al., 1998). By comparison, non-union fractures remained in animals treated with scaffolds alone. A follow up study by the same group established similar results using allogeneic MSCs transplanted without the use of immunosuppressive agents (Arinzeh et al., 2003).

The clinical translation of promising pre-clinical data was swift, with the first report being published in 2001 (Quarto et al., 2001). This study enrolled three patients with large bone defects that were treated with autologous MSCs seeded onto hydroxyapatite scaffolds and implanted at the lesion site. Over the 12-month follow up period, all patients regained limb function and there was radiographic evidence of new bone formation, vascular infiltration and integration with surrounding bone. A follow up study reported that all patients suffered no complications, pain, inflammation, or swelling at the implant site seven years after surgery (Marcacci et al., 2007). A larger, non-controlled study by Hernigou and colleagues reported successful fracture union in 43/60 patients treated with autologous MSC grafts (Hernigou et al., 2005). The authors also demonstrated a positive correlation between the number of CFU-F found in the grafts and the volume of mineralised matrix produced. In 7/17 patients who failed to reach fracture union, the number of CFU-F in their MSC grafts were significantly lower than that seen in successful patients.

MSCs have also been used in small-scale studies of patients with osteogenesis imperfecta (OI), a genetic condition resulting in impaired type I collagen synthesis by osteoblasts leaving patients susceptible to fractures. Horwitz *et al.* transplanted human leukocyte antigen (HLA)-matched BM into three children with severe OI (Horwitz et al., 1999). They hypothesised that “healthy” BM containing functional MSCs could incorporate into the host and function to increase bone mass. All three transplants engrafted well, and a 77% increase in total body bone mineral content (TBBMC) was seen in one patient 100 days post-transplant (range 45%-77%). However, the study design did not include a control group and the follow up

period was short. A later study by the same group addressed these limitations and looked at clinical responses in 3 patients receiving bone marrow transplants compared to age-matched controls (Horwitz et al., 2001). Short-term increases in height were observed, but this plateaued at 6 months post-transplant. A steady improvement in TBBMC was also observed, reaching the lower end of the normal range seen in healthy children. These findings have encouraged Horwitz and colleagues to start a phase I trial to evaluate the safety of repeated autologous MSC infusions in children with OI (ClinicalTrials.gov ID Number: NCT01061099).

### 1.4.2 MSCs in Cartilage Repair

Cartilage damage due to trauma or ageing affects an increasing number of people and places a large burden on the NHS. Current interventions range from drug therapy to autologous chondrocyte implantation (ACI) and total joint replacement (Jones and Peterson, 2006). ACI is a procedure where chondrocytes are biopsied from the patient at a non-load bearing site and cultured *in vitro* to expand cell numbers. Culture-expanded cells are then re-seeded onto the primary damage area in a second procedure (Brittberg et al., 1994). Although the short-to-medium term clinical benefits are good, the key disadvantage of ACI is the requirement for extracting healthy chondrocytes from the patient, which can lead to further injury (Shenaq et al., 2010). Additionally, large or systemic cartilage defects such as those seen in osteoarthritis (OA) would not be suitable for ACI as the cell numbers required for a successful graft would be too high. As such, MSCs hold great promise for the repair and regeneration of lost cartilage via differentiation into chondrocytes (Gupta et al., 2012).

Wakitani and colleagues were among the first to perform a clinical trial evaluating the safety and efficacy of autologous MSC transplantation in 24 patients with knee OA (Wakitani et al., 2002). Twelve patients were randomised to receive MSCs seeded onto a collagen gel, while the remaining 12 received cell-free gels as controls. Although the histology score for the MSC group was higher at the end of the study, no significant clinical improvements were seen. A subsequent study by the same group did identify clinical benefits over cell-free controls, but the number of enrolled patients (n=3) was low (Wakitani et al., 2007).

Although the above reports hint towards a clinical benefit when using MSCs to repair cartilage lost due to OA, none have compared MSC therapy to ACI, the current gold standard. To address this, Nejadnik *et al*. stratified 72 patients according to lesion site and age and treated them with ACI (n=36) or MSCs (n=36) in a non-randomised, non-blinded fashion (Nejadnik et al., 2010). Clinical improvements were measured at multiple time points using validated scoring systems. Improvements were seen in patients receiving ACI or MSC treatment compared to baseline values, but no significant differences were observed between groups except for the "physical role functioning" score (the ability to work and carry out other daily activities), in which MSC-treated patients scored higher.

Although larger studies have demonstrated the safety of autologous MSC transplantation for cartilage repair, the degree of clinical benefit varied. Several other single-patient case reports further validate these findings (reviewed in Koga et al., 2009). MSC-based therapy has several advantages over ACI, including the ability to expand cell numbers *in vitro* while

maintaining chondrogenic differentiation potential. This opens up the possibility of treating larger-size cartilage defects outside the scope of ACI procedures. As of June 2014, there are 17 registered human clinical trials testing MSCs in cartilage repair on the US Clinical Trials Database (www.clinicaltrials.gov). This list also includes commercial products such as CARTISTEM® (NCT01733186) looking to tap into the cell therapy market.

### 1.4.3 MSCs in Non-Mesenchymal Regenerative Therapies

Several groups have been able to differentiate MSCs down clinically relevant non-mesenchymal lineages *in vitro* and *in vivo*. Examples of MSC plasticity include differentiation towards hepatocytes (Sato et al., 2005, Pittenger et al., 1999b), neurons (Woodbury et al., 2000, Kopen et al., 1999), cardiomyocytes (Toma et al., 2002) and insulin-producing pancreatic β cells (Zanini et al., 2011). This trans-germ layer differentiation has led some groups to describe MSCs as pluripotent, with a differentiation potential to match that of embryonic stem cells (Jiang et al., 2002).

The topic of MSC plasticity has come under increasing scrutiny with recent reports linking cases of transdifferentiation with cell fusion or transient reprogramming of cells to adopt a new phenotype under strong chemical cues (Bianco et al., 2013). Cell fusion, in particular, remains a strongly debated subject. Data from the HSC field demonstrates that fused cells can display the phenotype of terminally differentiated somatic cells, leading to false claims of transdifferentiation potential (Wang et al., 2003, Terada et al., 2002). Up to 1% of MSCs

added to a co-culture of lung epithelial cells underwent cell fusion and begun to express genes characteristic of epithelial cells (Spees et al., 2003). Noiseux and colleagues report low levels of cell fusion after infusion of MSCs in a model of ischaemic heart injury (Noiseux et al., 2006). However, other groups have reported hepatic differentiation of human MSCs without any evidence of cell fusion in a liver injury model (Sato et al., 2005). Similar experiments also demonstrated the neurogenic (Tropel et al., 2006) and hepatic (Tao et al., 2009) potential of MSCs at the clonal level, demonstrating the plasticity of individual MSCs.

Nonetheless, as is commonly seen in the MSC field, this early pre-clinical work demonstrating transdifferentiation potential led to the creation of many human phase I/II trials testing the efficacy of MSC infusion in multiple clinical settings, such as cardiac and hepatic injury (Table 1.3). A recent meta-analysis of MSC clinical trials involving a total of 1012 patients reported MSC infusion to be safe, with the only significantly increased adverse event being transient fever following cell infusion (Lalu et al., 2012). However, the efficacy of MSCs has yet to be convincingly proven due to low numbers of enrolled patients and the lack of a comparator arm in many studies. Additionally, the mechanism behind any clinical improvements seen following MSC infusion *in vivo* remains to be elucidated, with recent studies reporting low levels of MSC engraftment and rapid clearance following infusion (von Bahr et al., 2012).

Table 1.3 | **Summary of selected clinical trials using MSCs in non-mesenchymal regenerative therapies**.

| Tissue | Disease | Study Design | Cell Type & Route | Outcomes | Reference |
|---|---|---|---|---|---|
| **Liver** | Cirrhosis (4 patients) | • Phase I study<br>• 12 month follow up<br>• Non-randomised<br>• No control group<br>• Unblinded | • Autologous BM MSCs<br>• Used P2-4 cells<br>• Systemic IV infusion | • Improvements in MELD scores seen in 2/4 patients<br>• QoL questionnaire scores improved in 4/4 patients<br>• No adverse events reported | Mohamadnejad et al. (2007) |
| | Cirrhosis (27 patients) | • Phase II study<br>• 12 month follow up<br>• RCT<br>• Single-blinded | • Autologous BM MSCs<br>• Used P3-4 cells<br>• Systemic IV infusion | • No differences in MELD, Child-Pugh, albumin and serum transaminase levels<br>• No difference in total liver volume<br>• No adverse events reported | Mohamadnejad et al. (2013) |
| | Liver failure Hepatitis B (158 patients) | • Phase II study<br>• 48 week follow up<br>• Non-randomised<br>• 105 matched controls<br>• Unblinded | • Autologous BM MSCs<br>• Used freshly isolated<br>• Hepatic artery infusion | • Significant improvements in MELD and albumin scores short term (4 weeks)<br>• No differences observed in liver function scores at end of study (48 weeks)<br>• No adverse events reported (192 weeks) | Peng et al. (2011) |
| **Neural** | Stroke (12 patients) | • Phase I study<br>• 12 month follow up<br>• Non-randomised<br>• No control group<br>• Unblinded | • Autologous BM MSCs<br>• Used <P3 cells<br>• Systemic IV infusion | • Improvements in NIHSS score in all patients for up to 12 months<br>• 7/12 patients displayed >15% reduction in lesion volume after MSC infusion<br>• One case of mild fever immediately following MSC infusion reported | Honmou et al. (2011) |
| | Traumatic brain injury (7 patients) | • Phase I study<br>• 6 month follow up<br>• Non-randomised<br>• No control group<br>• Unblinded | • Autologous BM MSCs<br>• Used P3 cells<br>• Direct infusion into damaged brain | • Significant improvements in neurologic function at 6 months compared to baseline<br>• No adverse events reported | Zhang et al. (2008b) |

Table 1.3 | **Summary of selected clinical trials using MSCs in non-mesenchymal regenerative therapies**. (Continued from previous page)

| Tissue | Disease (n) | Study Design | Cell Type & Route | Outcomes | Reference |
|---|---|---|---|---|---|
| **Neural** | Stroke (52 patients) | • Phase I/II study<br>• 5 year follow up<br>• RCT<br>• Single-blinded | • Autologous BM MSCs<br>• Culture expanded for 4 weeks<br>• Two doses via systemic IV infusion | • Significant increase in survival at 5 years in the MSC-treated group (75% compared to 42%)<br>• Significant increase in functional outcomes in the MSC-treated group.<br>• No major differences in adverse events between both groups | Lee et al. (2010a) |
| **Cardiac** | Acute MI (53 patients) | • Phase I study<br>• RCT<br>• 6 month follow up<br>• Double-blinded<br>• Multicentre study | • Allogeneic BM MSCs (PROCHYMAL®) from a single, unrelated donor<br>• Culture expanded<br>• Systemic IV infusion | • Significant (4-fold) reduction in arrhythmias in MSC treated group<br>• Significant (6.7%) increase in LVEF in MSC treated group<br>• No evidence of increased toxicity or adverse events in the MSC-treated group | Hare et al. (2009) |
| | Acute MI (16 patients) | • Phase I study<br>• 6 month follow up<br>• Non-randomised<br>• No control group<br>• Unblinded | • Autologous BM MSCs<br>• Culture expanded for 3 weeks<br>• Direct infusion into heart via coronary artery | • Significant improvements in LVEF at 6 months compared to baseline<br>• Significant increase in viable tissue at the infarct site at 6 months compared to baseline<br>• No adverse events relating to direct cardiac infusion or other symptoms were reported | Yang et al. (2010) |

**Abbreviations**: RCT, randomised controlled trial; MELD, Model for End Stage Liver Disease; IV, intravenous; QoL, Quality of Life; NIHSS, National Institutes of Health Stroke Scale; MI, myocardial infarction; LVEF, left ventricular ejection fraction.

## 1.5 Mechanisms behind MSC-mediated Tissue Repair

As described above, there is a growing body of evidence that proves MSC therapy to be safe in many different clinical settings. However, our understanding of the mechanisms behind any therapeutic benefit seen has changed over time and remains only partially understood. What was originally thought to be "direct" repair via differentiation into functional, mature cells to replace those lost due to injury has evolved to include a host of "indirect" mechanisms such as the release of trophic and immunomodulatory factors (Caplan and Correa, 2011). In this section, I will review current evidence for both the direct and indirect effect of MSCs in tissue repair. The immunosuppressive phenotype of MSCs will be discussed in detail in a later section.

### 1.5.1 Differentiation to replace lost cells

The conceptual idea of MSCs as a vehicle for cell "replacement" therapies for skeletal disorders is attractive and easily understood. In these cases, differentiation down an osteogenic or chondrogenic lineage is well documented, and MSCs grafted directly at sites of injury can generate mineralised matrix or immature chondrocytes which are maintained over the long-term (Nejadnik et al., 2010, Hernigou et al., 2005, Horwitz et al., 2001). Growth factors or bioactive scaffolds have been used to promote differentiation down a specific lineage and enhance repair (Marolt et al., 2010, Zhang et al., 2009). However, in all these cases, MSCs were transplanted directly at sites of injury and were usually immobilised in a gel or scaffold to promote successful engraftment with the host.

In conditions where implantation of MSCs directly at the site of injury is not feasible (e.g. neural, hepatic or cardiac injuries), evidence supporting long-term engraftment of MSCs and differentiation into functional cells is inconclusive. Tao *et al*. showed that human MSC-derived hepatocyte like cells could be detected in the livers of carbon tetrachloride ($CCL_4$) treated mice (Tao et al., 2009). However, the engraftment frequency was less than 0.25%, suggesting that successful homing and transdifferentiation of MSCs was a rare event. Kao and colleagues report a slightly higher engraftment frequency (4.2% at 4 weeks) in the same model of injury, but no engrafted cells remained three months after infusion (Kuo et al., 2008). Low levels of engraftment are also reported in papers testing MSC infusion in cardiac injury (Leiker et al., 2008). In these cases, a separate mechanism must be active as the low levels of engraftment and cell replacement cannot themselves be solely responsible for the clinical improvements seen in animal models and human patients.

### 1.5.2 Indirect Repair Mechanisms

In recent years, there has been a shift in thinking towards MSCs promoting tissue repair indirectly via the secretion of trophic factors which create a regenerative microenvironment at sites of injury (Caplan and Correa, 2011, Gnecchi et al., 2008). These factors can promote the expansion of tissue-resident progenitor cells, prevent further apoptosis of damaged cells, and promote tissue repair in the absence of engrafted MSCs. An elegant study by Iso and colleagues provides strong support for this theory in a mouse model of MI. They observed significant improvements in cardiac function following human MSC infusion, but no engraftment of human cells were detected in the hearts of each treated animal (Iso et al.,

2007). Several cardio-protective factors were identified in MSC conditioned media that were capable of preventing cardiomyocytes death *in vitro*. Furthermore, Gnecchi *et al*. showed that MSC conditioned medium alone was sufficient to reduce infarct size and improve LEVF in rats subject to MI (Gnecchi et al., 2006).

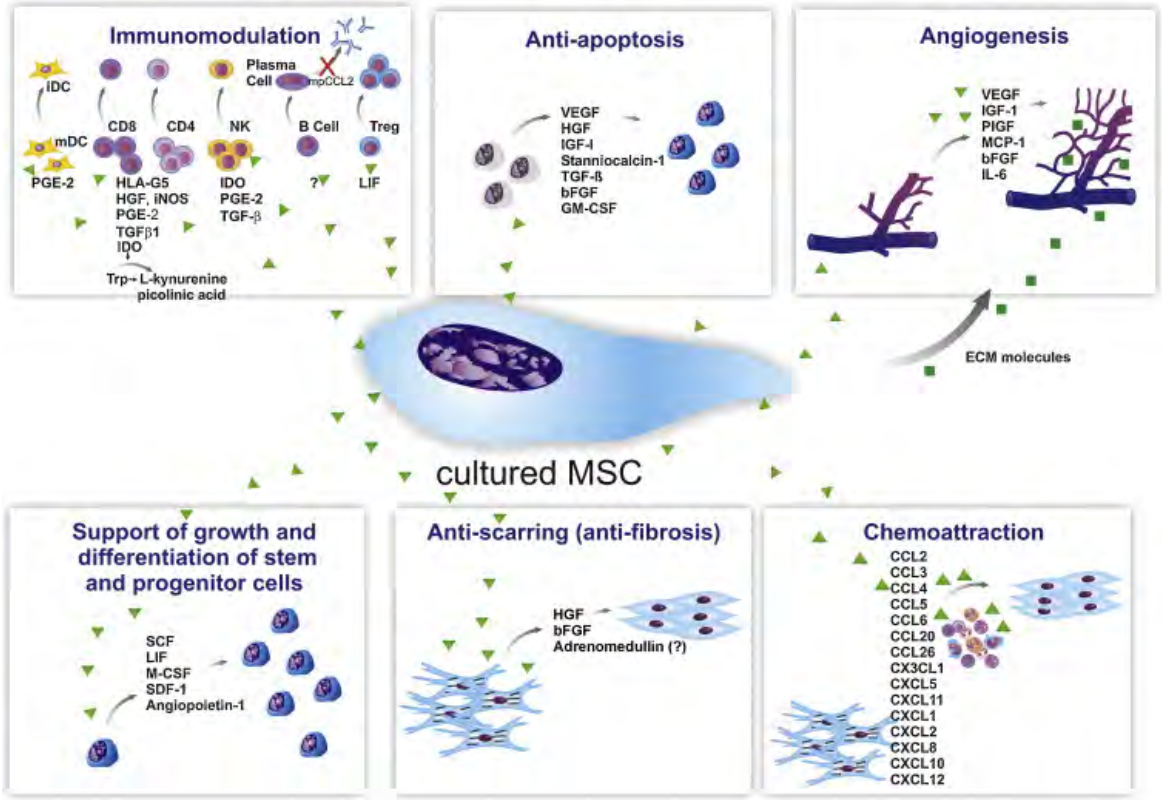


Figure 1.7 | **Paracrine factors secreted by MSCs**. This diagram lists the broad range of bioactive molecules secreted by MSCs that have been reported in past literature. Figure taken from Meirelles *et al*., 2009.

The variety of bioactive molecules secreted by MSCs can be broadly split into six different families (Figure 1.7; Meirelles et al., 2009) and has been referred to as the "MSC secretome" (Ranganath et al., 2012). Evidence for these groups are described below.

#### 1.5.2.1 Anti-apoptotic and Angiogenic factors

Anti-apoptotic factors secreted by MSCs prevent further cell death following injury, and angiogenic factors induce reinstallation of a blood supply for further repair of damaged tissues. Kim and colleagues reported the release of FGF2, transforming growth factor beta 1 (TGF-β1) and VEGF by MSCs protect lung fibroblasts from undergoing apoptosis due to cigarette smoke *in vitro* (Kim et al., 2012). An earlier study by the same group also demonstrated that MSC CM alone can increase the number of small pulmonary vessels in a rat model of emphysema (Huh et al., 2011). Further evidence of angiogenic activity is provided by Chen *et al*., who show that VEGF, insulin-like growth factor 1 (IGF1), and epidermal growth factor (EGF) secretion by mouse MSCs promotes vascularisation and faster wound healing *in vivo* (Chen et al., 2008).

#### 1.5.2.2 Factors that support local stem/progenitor cells

MSCs play a crucial role in maintaining the BM HSC niche under physiological conditions (Mendez-Ferrer et al., 2010). A population of perivascular BM cells (enriched for MSC markers) secrete stem cell factor (SCF) that is crucial for HSC maintenance (Ding et al., 2012). Deletion of these cells resulted in depletion of HSCs from their BM niche and reduced BM cellularity. Under pathological conditions, stromal derived factor 1 (SDF-1) and angiopoietin secretion by MSCs can actively recruit endothelial progenitor cells to promote wound healing and revascularisation (Chen et al., 2008). MSCs have also been shown to recruit Nestin+ neural progenitor cells that promote ocular regeneration in a murine glaucoma model (Manuguerra-Gagne et al., 2013).

### 1.5.2.3 Anti-fibrotic and Chemoattractive factors

Although reductions in fibrosis have been reported in both cardiac and hepatic injury models following MSC infusion, pinpointing the molecules responsible for this has proven difficult. One study reported that administration of chorionic plate-derived MSCs in a rat $CCL_4$ model resulted in increased levels of matrix metalloproteinase (MMP) 2 and 9 which reduced the degree of liver fibrosis seen (Lee et al., 2010b). Additionally, secretion of FGF2 by MSCs inhibited the delta-like 1 (Dlk1) dependent activation of hepatic stellate sells, resulting in significantly attenuated fibrosis in $CCL_4$ treated mice (Pan et al., 2011). Finally, MSCs also secrete a large number of chemokines to recruit other cell types at areas of injury, including immune cells and other stem/progenitor cells (Meirelles et al., 2008).

## 1.6 MSC-mediated Immunosuppression

One of the most exciting abilities of MSCs are their potent immunomodulatory functions (Le Blanc and Mougiakakos, 2012, Uccelli et al., 2008). Bartholomew and colleagues were first to identify that baboon MSCs could reduce the proliferation of activated T cells in mixed lymphocyte reactions (MLR) and prolong allogeneic skin graft survival in mismatched recipients (Bartholomew et al., 2002). A similar anti-proliferative effect was reported for human MSCs in MLRs soon after (Di Nicola et al., 2002). We now know MSCs exert their effect on both the innate and adaptive immune system through a variety of mechanisms (Figure 1.8; Uccelli et al., 2008). These studies have prompted rapidly growing interest in the use of MSCs as a cellular therapy for autoimmune conditions alongside the more "traditional" uses of MSCs in regenerative medicine.

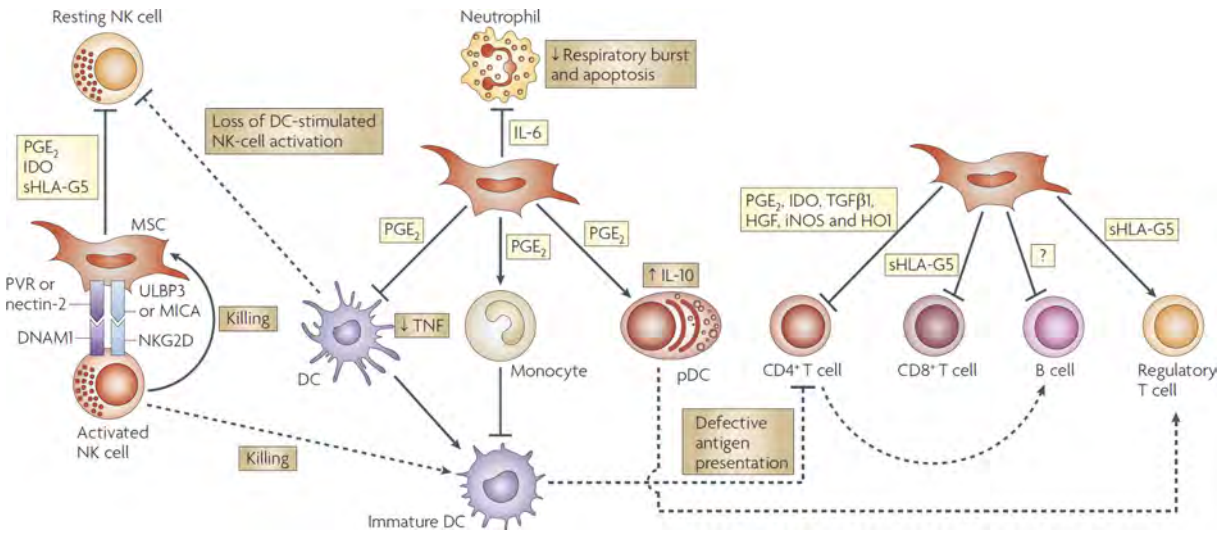


Figure 1.8 | **Immunosuppressive effects of MSCs on the innate and adaptive immune system**. This diagram summaries some of the known factors secreted by MSCs that can influence the activation, cytokine secretion and proliferation of various immune cells. Figure taken from Uccelli *et al.*, 2008.

### 1.6.1 Effect of MSCs on the Adaptive Immune System

#### 1.6.1.1 T Lymphocytes

The effect of MSCs on T lymphocytes has received the most research attention over the past decade due to the crucial role they play in maintaining immune homeostasis. CD4 T helper cells recognise antigens that have been processed and presented in a MHC class II context. After activation, these cells proliferate and secrete cytokines that attract other immune cells to areas of injury. CD8 cytotoxic T cells recognise antigen presented in a MHC class I context. After activation, these cells release granules containing perforin and granzyme B which induce apoptosis in target cells (Parkin and Cohen, 2001).

Both autologous and allogeneic MSCs can inhibit the proliferation of CD4 T cells that have been stimulated by mitogens (Di Nicola et al., 2002), alloantigen (Rasmusson et al., 2005), and activating (CD3/CD28) antibodies (Krampera et al., 2002). We know that MSCs need to be in an inflammatory environment to "switch on" certain immunomodulatory functions (Ryan et al., 2007, Krampera et al., 2006). Once activated, MSCs can secrete a plethora of soluble factors that mediate immunosuppression (summarised in Figure 1.8). Neutralisation of one or more of these factors does not result in a complete reversal of suppression, suggesting that there are other non-soluble, contact dependent factors in play (Ben-Ami et al., 2011). It is likely that there is a degree of redundancy in the immunosuppressive phenotype of MSCs, and several molecules may work in unison to create an anti-inflammatory microenvironment conducive to tissue repair.

Human MSCs suppress via the secretion of indoleamine 2,3-dioxygenase (IDO), an enzyme responsible for tryptophan catabolism (Meisel et al., 2004). Depletion of tryptophan from the local microenvironment removes an essential amino acid required for lymphocyte proliferation, resulting in lower numbers at sites of injury. Mouse MSCs secrete nitric oxide (NO) to inhibit CD4 T cell proliferation and causes cell cycle arrest at the $G_0/G_1$ phase (Ren et al., 2008, Glennie et al., 2005). Secretion of interleukin 10 (IL-10) by mouse (Yang et al., 2009) and human MSCs (Beyth et al., 2004) also exerts an anti-proliferative effect on lymphocytes. Secretion of prostaglandin E2 ($PGE_2$) has been shown to indirectly suppress T cell proliferation by promoting IL-10 secretion from nearby macrophages *in vivo* (Nemeth et al., 2009). Other molecules, such as TGF-β1, hepatocyte growth factor (HGF), and IL-6 have also been implicated in the suppression of CD4 T cell proliferation (Ma et al., 2014).

Studies reporting the effect of MSCs on cytotoxic CD8 T lymphocytes are rarer. Rasmusson *et al*. showed MSCs pulsed with viral peptides remained resistant to CD8 T cell lysis and failed to induce interferon-γ (IFNγ) or tumour necrosis factor alpha (TNFα) production (Rasmusson et al., 2007b). Human adipose-derived MSCs were able to reduce levels of activation markers CD28 and CD44 on CD8 T cells after co-culture (Hof-Nahor et al., 2012). Reductions in expression of the CD8 receptor and production of IFNγ and granzyme B were also observed, suggesting a loss in cytotoxicity. While MSC CM was sufficient to induce these changes, there was a requirement for CD14+ monocytes to be in direct contact with CD8 T cells for this to occur. The authors were unable to identify the soluble factor responsible for these changes, but they have ruled out TGF-β1 and $PGE_2$ in their analysis (Hof-Nahor et al., 2012).

#### 1.6.1.2 B Cells

B cells can function as antigen presenting cells (APCs) and can produce antigen-specific antibodies after differentiating into plasma cells. The effect of MSCs on B cell populations is less well understood than their T cell counterparts and cases of contradictory results have been published (Franquesa et al., 2012). The first study to examine the effect of MSC co-culture on B cells was published in 2005 by the Uccelli group (Corcione et al., 2005). They demonstrated that soluble factors secreted by human MSCs were able to inhibit the proliferation of CD19+ B cells and prevent their differentiation towards plasma cells. Similar anti-proliferative effects were described for mouse MSCs in a later study (Asari et al., 2009).

MSCs have also been shown to promote B cell proliferation and survival in some studies. Rasmusson *et al*. report that human MSCs could enhance antibody production via a contact-dependent mechanism when cultured at low (10 B cells:1 MSC) ratios (Rasmusson et al., 2007a). Tabera and colleagues show that MSCs can promote the viability and proliferation of B cells under “weak” stimulation, but cause cell cycle arrest when B cells are activated using a “strong” stimulus (Tabera et al., 2008). The reasons behind the disparity seen in these studies could be due to the B cell:MSC dose, stimulation method and MSC population (Franquesa et al., 2012).

#### 1.6.1.3 Regulatory T cells

Regulatory T cells (Treg) are a subset of T lymphocytes that express the transcription factor FOXP3 and function to maintain immune homeostasis (Vignali et al., 2008). Early experiments demonstrated that human MSCs could enhance the formation of CD4+CD25+ T cells in MLRs (Maccario et al., 2005). Further mechanistic insights were provided by English *et al*., who showed that cell-cell contact followed by TGF-β1 and $PGE_2$ secretion is required for the induction of FOXP3+ Tregs (English et al., 2009). Secretion of the soluble protein HLA-G5 has also been shown to have an effect on T cell proliferation and Treg formation *in vitro* (Selmani et al., 2008). Treating co-cultures with anti-HLA-G5 antibody restored T cell proliferation and caused a significant drop in FOXP3+ CD4 Treg cell numbers.

### 1.6.2 Effect of MSCs on the Innate Immune System

#### 1.6.2.1 Monocytes/Macrophages

Signals released from injured tissue rapidly recruit circulating monocytes, whereupon they migrate into the organ and become macrophages. Macrophages act directly to clear pathogens via phagocytosis and indirectly by instructing other immune cells to restore tissue homeostasis. Depending on environmental cues, macrophages can be polarised towards a pro-inflammatory M1 macrophage, or towards an anti-inflammatory M2 macrophage (Murray and Wynn, 2011). Current evidence suggests that MSCs interact closely with macrophages at sites of injury and factors secreted by both cell types work synergistically to create an anti-inflammatory environment suitable for tissue repair (Figure 1.9).

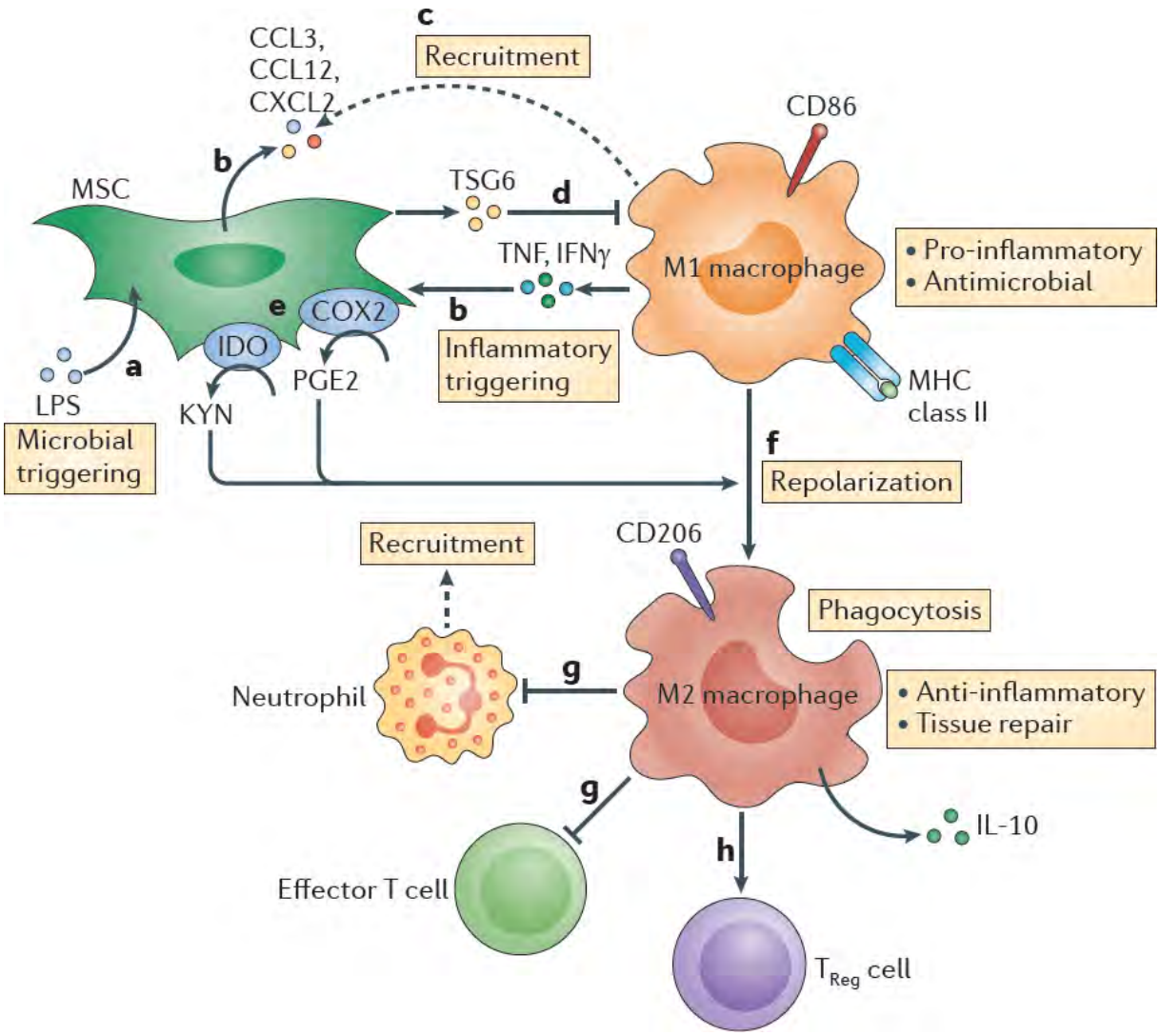


Figure 1.9 | **MSCs promote macrophage polarisation towards a M2 phenotype that further dampens the immune response**. Following activation by inflammatory stimuli (a), MSCs secrete a range of chemokines (b) that mediate the recruitment of monocytes/macrophages to sites of damage (c). The secretion of TSG-6, IDO and $PGE_2$ (d,e) keep the activity of macrophages in check, and they can induce the repolarisation of macrophages towards an M2 phenotype if needed (f). M2 macrophages can then further suppress T cell proliferation (g), neutrophil recruitment (g) and induce Treg formation via the secretion of IL-10 (h). Figure taken from Le Blanc and Mougiakakos, 2012.

Human and mouse MSCs can actively recruit monocytes to areas of injury via the secretion of monocyte chemoattractant proteins CCL2, CCL3, CXCL2 and CCL12 (Shi et al., 2011, Chen et al., 2008). Once recruited, MSCs can skew the differentiation of monocytes into M2 macrophages *in* vitro and *in vivo* (Cho et al., 2014). MSC-secreted proteins $PGE_2$, IDO, and TSG-6 have all been implicated in the preferential differentiation of macrophages towards an anti-inflammatory M2 phenotype (Francois et al., 2012, Choi et al., 2011, Maggini et al., 2010). M2 macrophages can then further suppress T cell proliferation via IL-10 secretion, prevent the ingress of neutrophils, and induce Treg formation (Murray and Wynn, 2011).

This synergistic interplay between MSCs, monocytes, macrophages and neutrophils is made clear in an elegant study by Nemeth and colleagues, who reported increased survival following MSC infusion in a mouse model of sepsis (Nemeth et al., 2009). Mechanistic studies revealed that circulating bacterial toxins bind to and activate MSCs, causing them to secrete $PGE_2$. This causes a reduction in the numbers of circulating monocytes and a subsequent increase in numbers of tissue macrophages. These macrophages are then reprogrammed towards an IL-10 secreting, M2 phenotype which dampen the immune response against host tissues. Furthermore, IL-10 secretion prevented neutrophils from entering organs to cause further damage and resulted in an increase in their total circulating numbers. These circulating neutrophils were then able to clear bacterial pathogens from the blood, preventing further immune-mediated damage from taking place.

#### 1.6.2.2 Neutrophils

Neutrophils form the majority of white blood cells and act as “first responders” at sites of injury. They function to clear foreign objects and bacteria via phagocytosis, secretion of antimicrobial proteins, the creation of NETs (neutrophil extracellular traps), and via the generation of reactive oxygen species ("respiratory burst"; Liaskou et al., 2012).

IL-6 release from human MSCs was able to significantly increase neutrophil survival and prevent activated neutrophils undergoing respiratory burst *in vitro* (Raffaghello et al., 2008). A later study reported similar pro-survival and anti-apoptotic effects of MSC co-culture on neutrophils which was mediated via the release of IL-6, IFN-β, and GM-CSF (Cassatella et al., 2011). Brandau *et al*. reported that lipopolysaccharide (LPS)-stimulated MSC secrete IL-8 and MIF (macrophage migration inhibitory factor) to enhance neutrophil migration across a transwell membrane (Brandau et al., 2010). Recruited neutrophils survived longer and displayed enhanced inflammatory activity over control cells. These studies suggest MSCs could play a crucial role in enhancing neutrophil recruitment at sites of injury to help clear pathogens, but additional work is needed to elucidate the functional relevance of this *in vivo*.

### 1.6.2.3 Natural Killer cells

Natural killer (NK) cells function in an analogous fashion to CD8 cytotoxic T lymphocytes, however they do not require antigen presentation (in an MHC context) to be activated, resulting in an expedited response against pathogens. NK cell activation is determined by the overall balance of signals from a range of 'activating' and 'inhibitory' receptors expressed on their surface. Activation results in the release of cytolytic granules against a target cell, causing apoptosis and cell death (Vivier et al., 2008).

MSCs were shown to inhibit the proliferation of NK cells stimulated with IL-2 or IL-15 (Spaggiari et al., 2006). However, these MSCs were susceptible to NK-mediated cell lysis due to the expression of ligands that bind to NK activating receptors. Following pre-stimulation with IFNγ, MSCs upregulated MHC class I molecules which allowed them to evade NK-mediated lysis, highlighting the importance of an inflammatory environment in switching on MSC immunosuppressive functions (Spaggiari et al., 2006). A follow-up study by the same group identified MSC-secreted IDO and $PGE_2$ as key molecules preventing the proliferation and cytokine production of NK cells *in vitro* (Spaggiari et al., 2008). Interestingly, they also observed down-regulation of activating NK receptors after MSC co-culture. Secreted HLA-G5, an inhibitory NK receptor ligand, has also been shown to inhibit IFNγ production and protect MSCs from NK-mediated lysis (Selmani et al., 2008).

#### 1.6.2.4 Dendritic cells

Dendritic cells (DCs) function as professional APCs to both CD4 and CD8 T cells. Compared to other APCs, DCs are the most potent at activating T cells and are the only cells able to present antigen to naïve T cells (Wieder, 2003). They can be broadly subdivided into myeloid DCs, which arise from CD34+ myeloid progenitor cells and monocytes, or plasmacytoid DCs, which arise from lymphoid progenitor cells.

Jiang *et al*. reported that human MSCs could inhibit the differentiation of monocytes towards myeloid DCs *in vitro* (Jiang et al., 2005). They also showed reduced IL-12 secretion and reduced expression of antigen presentation and costimulatory molecules in mature DCs after MSC co-culture. MSCs could also inhibit the differentiation of CD34+ myeloid progenitor cells into DCs (Nauta et al., 2006). Any DCs that were formed after co-culture struggled to induce T cell activation. Mouse MSCs were able to induce the generation of a 'regulatory' DC population via the upregulation of the notch signalling ligand Jagged-2 in DCs (Zhang et al., 2008a, Li et al., 2008). This regulatory DC population could inhibit the proliferation and cytokine secretion of alloantigen-stimulated lymphocytes. The Uccelli group were able to demonstrate an impaired ability of DCs to prime CD4 T cells *in vivo* (Chiesa et al., 2011). They also showed significantly reduced numbers of DCs in the lymph nodes of animals after treatment, suggesting a reduction in their migratory capacity as well.

The effect of MSCs on plasmacytoid DCs is less well understood, but there is some evidence that suggests human MSCs can alter the cytokine secretion profile of plasmacytoid DCs towards more anti-inflammatory (IL-10 secreting) phenotype (Aggarwal and Pittenger, 2005). These data suggest that MSCs can affect DCs across all stages of their development, from the initial differentiation of progenitor cells to antigen presentation, lymph node homing and stimulation of T cells (Figure 1.10).

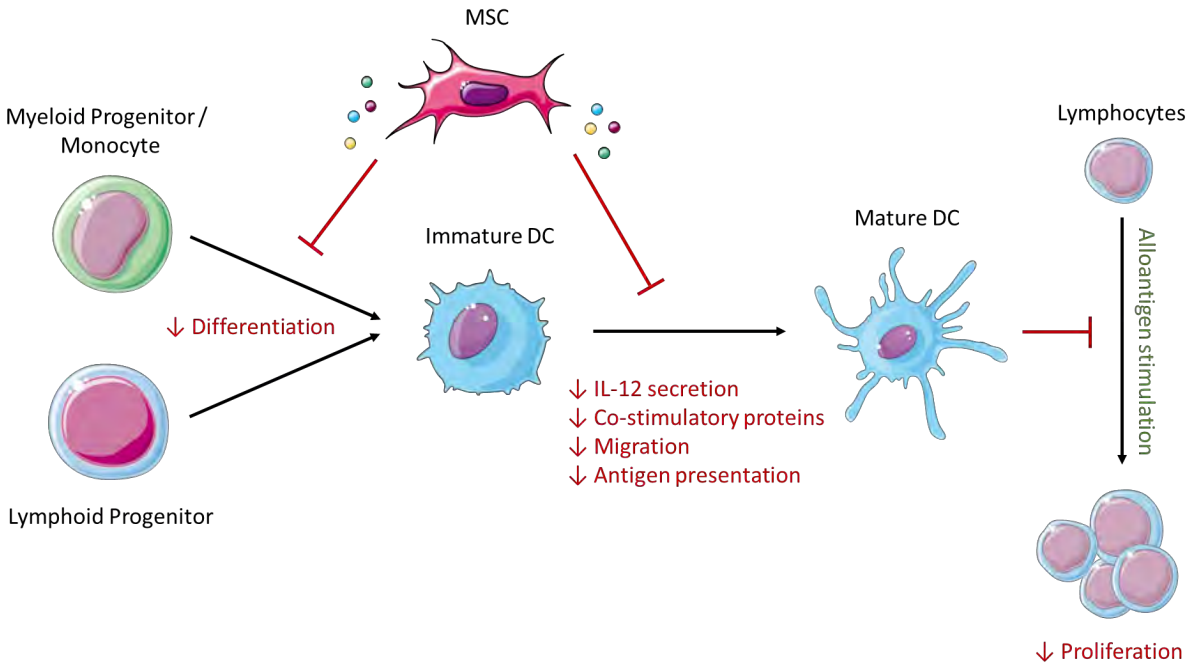


Figure 1.10 | **Modulation of DC differentiation and function by MSCs**. MSCs can inhibit the differentiation and maturation of DCs using a combination of secreted factors and cell-cell contact. DCs co-cultured with MSCs typically show reduced IL-12 secretion and an impaired ability to present antigen and migrate to nearby lymph nodes. 'Regulatory' DCs are also able to inhibit the proliferation and cytokine secretion of alloantigen-stimulated T lymphocytes *in vitro*.

### 1.6.3 Clinical Evidence for Immunosuppression

MSCs have shown efficacy in modulating the immune response in pre-clinical animal models of sepsis (Nemeth et al., 2009), graft-versus-host disease (GvHD; Ren et al., 2008), experimental autoimmune encephalomyelitis (Zappia et al., 2005), skin grafts (Bartholomew et al., 2002), and type 1 diabetes (Urban et al., 2008). These promising results have encouraged the translation of pre-clinical work into human diseases with immune-mediated pathogenesis. As seen with MSC-based regenerative therapies, early-phase clinical results have demonstrated MSC infusion to be safe in immune-mediated disorders, although the degree of clinical benefit varied (summarised in Table 1.4).

#### 1.6.3.1 MSCs in GvHD

Of the various immune-mediated disorders studied, the effect of MSCs on patients suffering from GvHD is the most striking. GvHD is a complication of allogeneic transplantation (particularly bone marrow transplants) where donor T cells in the graft recognise host antigens as foreign and initiate an immune reaction against the host (Ferrara et al., 2009). GvHD affects many organs, including the skin, liver and lower gastrointestinal tract resulting in high morbidity and mortality. Current therapy is inadequate and involves treatment with immunosuppressive agents which further increases their risk of infections. Additionally, a subset of patients do not respond to initial therapy ("treatment-resistant GvHD"), resulting in a bleak prognosis (Deeg, 2007). As the pathophysiology of GvHD involves the activation and proliferation of a variety of immune cell subsets, it was believed MSCs could play a crucial role in regulating this process and preventing further damage.

Table 1.4 | **Summary of selected clinical trials using MSCs in immune-mediated conditions**.

| Disease | Study Design | Cell Type & Route | Outcomes | Reference |
|---|---|---|---|---|
| **GvHD** | • Case study<br>• 1 patient<br>• 12 month follow up | • HLA-matched MSCs<br>• Culture expanded for 3 weeks<br>• Systemic IV Infusion (2 doses) | • Rapid restoration of liver and gut function<br>• Symptom free for up to 1 year post-transplant<br>• No adverse events reported | Le Blanc et al. (2004b) |
| | • Phase I trial<br>• 8 Patients<br>• Up to 16 month follow up<br>• No control group<br>• Non-randomised, Unblinded | • Mixture of HLA-matched and mismatched donor MSCs.<br>• P1 to P4 cells used<br>• Systemic IV infusion (1-2 doses) | • Resolution of GvHD seen in 6/8 patients<br>• No difference in efficacy between HLA-matched and mismatched MSCs<br>• No adverse events reported | Ringdén et al. (2006) |
| | • Phase II trial<br>• 55 patients<br>• Median 16 month follow up<br>• No control group<br>• Non-randomised, Unblinded | • Mixture of HLA-matched and mismatched donor MSCs<br>• P1 to P4 cells used<br>• Systemic IV infusion (1-5 doses) | • Complete resolution seen in 30/55 patients, partial response seen in 9/55<br>• Children (21/39) showed a greater response<br>• Response seen in 27/55 after one MSC infusion<br>• 8/30 patients with complete resolution had discontinued all immunosuppressive drugs | Le Blanc et al. (2008) |
| | • Phase III trial<br>• 244 patients<br>• RCT<br>• Double-blinded | • PROCHYMAL® allogeneic MSCs<br>• Unknown passage<br>• Systemic IV infusion (8 doses) | • No difference in complete response for >28 days (response rate: 35% MSCs vs. 30% placebo, p=0.3)<br>• Significant improvements in response in patients with GvHD affecting liver, skin and gut (rate: 63% MSCs vs. 0% placebo, p<0.05) | Martin et al. (2010) |
| | • Phase II trial<br>• 75 paediatric patients<br>• 100 day follow up<br>• No control group<br>• Non-randomised, Unblinded | • PROCHYMAL® allogeneic MSCs<br>• Unknown passage<br>• Systemic IV infusion (8 doses) | • Complete response seen in 46/75 patients 28 days after last MSC infusion<br>• Complete responders had significantly increased survival compared to non-responders at day 100 | Kurtzberg et al. (2014) |

Table 1.4 | **Summary of selected clinical trials using MSCs in immune-mediated conditions**. (Continued from previous page)

| Disease | Study Design | Cell Type & Route | Outcomes | Reference |
|---|---|---|---|---|
| **SLE** | • Phase I trial<br>• 15 patients<br>• 17 month follow up<br>• No control group<br>• Non-randomised, Unblinded | • HLA mismatched donor MSCs<br>• P3 to P5 cells used<br>• Systemic IV infusion (1 dose) | • Significant reductions in SLEDAI score at 12 months compared to baseline<br>• Significant reductions in proteinuria at 12 months compared to baseline<br>• Significant increases in CD4+FOXP3+ cells at 1, 3 and 6 weeks post-MSC transplant | Liang et al. (2010) |
| **Crohn's Disease** | • Phase I trial<br>• 9 patients<br>• 6 month follow up<br>• No control group<br>• Non-randomised, Unblinded | • Autologous MSCs<br>• Up to P3 cells used<br>• Systemic IV infusion (2 doses) | • CDAI scores improved in 5/9 patients, with 3/9 showing a reduction >70 units<br>• No patients achieved complete remission<br>• 7/9 patients showed no endoscopic improvement<br>• No adverse events due to MSC infusions reported | Duijvestein et al. (2010) |
| **Ulcerative Colitis** | • 3 patient case series<br>• 19 month follow up | • Allogeneic MSCs isolated from BM or umbilical cord<br>• Unknown passage<br>• Systemic IV infusion (1 dose) | • Significant reductions in CAI scores in 3/3 patients<br>• One patient showed significant endoscopic improvement<br>• One patient had transient fever for 2 days following MSC infusion | Liang et al. (2012) |
| **Solid Organ Transplant** | • Two patient case series<br>• Kidney transplantation<br>• 12 month follow up | • Autologous MSCs<br>• Used at P2 or less<br>• Systemic IV infusion (1 dose) 7 days post kidney transplant | • Transient increase in serum creatinine 7-14 days after MSC infusion which improved over time<br>• Both patients showed no signs of graft rejection up to 1 year post-transplant with no background immunosuppression | Perico et al. (2011) |

**Abbreviations**: SLE, systemic lupus erythematosus; SLEDAI, systemic lupus erythematosus disease activity index; CDAI, Chron's disease activity index; CAI, clinical activity index

Studies on the effects of MSC infusion in patients with GvHD mainly originate from Katarina Le Blanc's group at the Karolinska Institute, Stockholm. Her initial case report showed that matched MSC infusion caused a rapid improvement in gut and liver function in a young patient who was unresponsive to steroid therapy (Le Blanc et al., 2004b). A later study by the same group expanded the numbers of MSC-treated patients with steroid-resistant GvHD to eight (Ringdén et al., 2006). They showed resolution of acute GvHD in 6/8 patients, with the remaining two patients showing no response to MSC treatment. Survival rates for patients receiving MSC treatment were significantly improved compared to control patients. Importantly, no side effects were noted in the four patients who received unrelated, HLA-mismatched MSC transplants.

A phase II, multicentre trial involving 55 patients was performed on the back of these promising case reports. Over 50% (30/55) of patients showed a complete response to MSC therapy, with a further 16% (9/55) showing a partial response (Le Blanc et al., 2008). Over half (27/55) showed a complete response after a single infusion of MSCs. An increase in 2-year survival was observed in patients responding to MSC treatment compared to controls (52% vs. 10%). No side effects were noted and allogeneic MSCs were shown to be as effective as autologous cells in this study. However, a later retrospective cohort study of 60 patients who died of pneumonia-related death after BM transplants at the Karolinska Institute identified MSC infusion being a significant risk factor (Forslöw et al., 2012). This study highlights the urgent need for larger, longer RCTs to assess both the safety and efficacy of MSC infusion in patients with GvHD.

To date, there has only been one published phase III RCT (NCT00366145) looking at MSCs in GvHD. This trial, funded and performed by Osiris Therapeutics Inc. (Columbia, USA) enrolled 244 patients, with 163 receiving PROCHYMAL® (generic name remestemcel-L) and 81 patients receiving placebo (Martin et al., 2010). No significant differences were observed in the primary endpoint of overall complete response rate between PROCHYMAL®-treated patients and controls (p=0.3). However, significant differences were observed in some secondary endpoints, with patients suffering from severe GvHD affecting the skin, liver and gut showing a 63% complete or partial response to PROCHYMAL® treatment compared to 0% in the placebo arm. Although this result represents a major setback for Osiris, they have recently gained Canadian marketing approval for PROCHYMAL® in the treatment of GvHD in children on the back smaller studies focusing on paediatric patients (Kurtzberg et al., 2014, Prasad et al., 2011). The Canadian Health Authority have stated that although there is currently limited evidence indicating a therapeutic benefit with PROCHYMAL®, the safety profile of the therapy warrants further investigation in the treatment of paediatric GvHD (Health Canada, 2012).

## 1.7 Enhancing the Regenerative and Immunosuppressive Potential of MSCs

Although clinical evidence has proven MSC therapy to be safe, the degree of clinical benefit observed was modest. The recent failure of PROCHYMAL® in phase III clinical trials highlights the need to better understand ways to improve the efficacy of MSC therapy. In this final part of the introduction, I will summarise the different methods used to enhance the regenerative and immunosuppressive potential of these cells.

### 1.7.1 Prospective Isolation and the use of Lower-Passage Cells

Markers for the prospective isolation of mouse (Mendez-Ferrer et al., 2010, Morikawa et al., 2009) and human MSCs (Pinho et al., 2013, Mabuchi et al., 2013b) represent major advancements for the study of MSC biology and for future therapeutic applications. Unlike plastic-adherent cells, prospectively isolated MSCs are highly enriched for CFU-F ability and have been shown to self-renew and undergo multi-lineage differentiation *in vivo*. No publications to date have compared the efficacy of prospectively isolated MSCs against classically isolated plastic-adherent cells, although one would expect the purified population to perform better. Additionally, by starting off with a pure population of stem cells, the MSC field can reach agreement over potential mechanisms of action and generate more reproducible results. This could lead to more effective uses of MSCs in the clinic, and therefore lead to facilitated regulatory approval.

Another benefit of prospective isolation is the ability to study MSC function without the prerequisite of *ex vivo* expansion, allowing us to use lower passage cells *in vivo* (Mabuchi et al., 2013a). Previous studies have shown that MSCs are susceptible to replicative senescence as early as P7, resulting in reduced growth kinetics and differentiation ability (Wagner et al., 2008, Kretlow et al., 2008). Prolonged *in vitro* culture can also increase the risk of karyotypic abnormalities in murine MSCs, leading to transformation and tumour formation (Tolar et al., 2007, Miura et al., 2006). *In vitro* expansion can also impair the ability of murine MSCs to migrate back to BM due to decreased expression of chemotactic receptors (Karp and Teol, 2009, Rombouts and Ploemacher, 2003).

The consequences of passage number on clinical efficacy are made clear in two publications from the Le Blanc group. A retrospective analysis of patients receiving MSCs for GvHD showed that the 1-year survival rate of patients receiving P1-P2 MSCs was significantly higher than those receiving P3-P4 MSCs (75% vs 21%; von Bahr et al., 2012). A complete response was detected in 86% of patients receiving young cells compared to only 36% receiving older MSCs. Interestingly, the authors did not detect any differences in the *in vitro* immunomodulatory properties of P2 and P7 MSCs. Another study has shown that higher passage (>P5) MSCs are more rapidly cleared by the host compared to lower passage cells (Moll et al., 2012). Culture expanded MSCs were at higher risk of IBMIR (Instant Blood Mediated Inflammatory Reaction) due to increased expression of pro-thrombotic proteins on their cell surface resulting in quicker activation of the coagulation cascade.

### 1.7.2 Augmenting MSC function using Growth Factors

Growth factors (GFs) have been used to augment MSC growth and differentiation in previous publications (Rodrigues et al., 2010). Selected factors include FGF2 (Ito et al., 2008), TGF-β1 (Mimura et al., 2011), platelet-derived growth factor-BB (PDGF-BB; Betsholtz, 2004), hepatocyte growth factor (HGF; Neuss et al., 2004), VEGF (Pons et al., 2008), EGF (Tamama et al., 2006), and IGF1 (Huang et al., 2012).

Of these GFs, FGF2 is possibly the most commonly used cytokine in MSC literature. FGF2 has a potent mitogenic effect, thereby reducing the *in vitro* expansion time required to reach cell numbers for therapeutic infusions (Lai et al., 2011). Human MSCs cultured with FGF2 underwent 25 population doublings over a 100 day period while control cells underwent <10 doublings over the same time course (Gharibi and Hughes, 2012). It can also delay the onset of senescence in mouse MSCs by promoting the hyper-phosphorylation of Mdm2, resulting in enhanced degradation of p53 tumour suppressor gene and increased cell growth (Coutu et al., 2011). Finally, FGF2 can also promote the tri-lineage differentiation of MSCs towards bone (Ito et al., 2008), fat (Song et al., 2014) and cartilage (Handorf and Li, 2011).

Recent work has concentrated on moving towards serum-free media for the culture of MSCs, thereby avoiding the undefined nature of foetal bovine serum (FBS; Jung et al., 2012). Chase and colleagues show that serum-free basal media supplemented with FGF2, TGF-β1 and PDGF-BB was able to expand human MSC populations while maintaining their tri-lineage

differentiation potential (Chase et al., 2010). However, Jung *et al*. show that PDGF-BB has a negative effect on MSC growth, and a combination of FGF2 and TGF-β1 was optimal for the serum-free isolation and expansion of human MSCs (Jung et al., 2010). The reason behind these contradictory findings could be due to heterogeneity in the plastic-adherent human MSC populations used in both studies.

### 1.7.3 Hypoxia

MSCs, like most cultured cells, are frequently maintained at atmospheric oxygen tensions (20% $O_2$). Hypoxic culture conditions (<5% O2) more closely match the oxygen tension found in BM and confers several positive effects on MSC function (Das et al., 2010). Firstly, hypoxia exhibits a pro-proliferative effect on MSCs. Ren and colleagues show that hypoxia significantly increased murine MSC numbers due to a higher percentage of cells entering the G2-M phase of the cell cycle (Ren et al., 2006). Similar mitogenic effects have also been described for human MSCs (Grayson et al., 2007). The effect of hypoxia on MSC tri-lineage differentiation is mixed, with some studies reporting enhanced differentiation (Lennon et al., 2001) and others reporting an unaltered or decreased potential (Salim et al., 2004).

Hypoxic pre-conditioning can also increase the survival of *in vivo* infused cells and enhance repair in models of injury. Pre-conditioned rat MSCs (1% $O_2$ for 24h) increased overall survival and serum albumin levels in a rat hepatectomy model (Yu et al., 2013). Similar results were not observed with MSCs grown at atmospheric oxygen tension. This was due to

increased VEGF secretion by hypoxic pre-conditioned MSCs, suggesting that hypoxia can also alter the gene and protein expression of MSC populations. Human MSCs have also been shown to increase production of trophic factors including VEGF, IL-6 and MCP-1 after hypoxic culture (Hung et al., 2007).

Finally, hypoxic culture can also increase the migratory capacity of MSCs by increasing expression of chemokine receptors. Increased expression of CXCR4 in rat MSCs enhanced their migration towards injured tissue in a rat brain injury model (Kuo et al., 2008). Hypoxic pre-conditioning of human MSCs also improved their migration in a hind limb ischemia model, resulting in significantly improved blood flow to the injured limb compared to normoxic-MSCs (Rosová et al., 2008).

### 1.7.4 Matrix Stiffness

The culture matrix has an important role to play in directing stem cell behaviour, with traditional culture protocols using uncoated tissue culture plastic for the expansion and differentiation of MSCs *in vitro*. However, newer studies have demonstrated the importance of the culture matrix in directing MSC differentiation down specific lineages. McBeath and colleagues were able to control the differentiation of human MSCs down osteogenic or adipogenic lineages solely by controlling the shape of the cell (McBeath et al., 2004). MSCs that were cultured as small, round cells underwent adipogenic differentiation, while MSCs that were able to adhere and spread underwent osteogenic differentiation. Oh and

colleagues were able to differentiate MSCs towards bone irrespective of any osteogenic-inducing media by culturing cells on nanotubes that promoted adhesion and spreading (Oh et al., 2009).

The importance of surface rigidity has been demonstrated in a well-cited study by Engler *et al*., who observed profound gene and protein expression changes in human MSCs cultured on polyacrylamide gels of varying stiffness (Engler et al., 2006). MSCs cultured on "soft" gels expressed proteins found in neurons, while MSCs that were cultured on "medium" and "hard" gels expressed myogenic and osteogenic markers respectively. A similar finding was reported when human MSCs were cultured in 3D on gels of varying stiffness (Pek et al., 2010a). These studies demonstrate how the culture matrix can work in synergy with inductive signals from culture media to enhance MSC differentiation down a specific lineage.

### 1.7.5 MSC "Licensing" and TLR signalling

MSCs, although regarded primarily as immunosuppressive cells, can have proinflammatory functions by acting as APCs (Chan et al., 2006) and by supporting the survival and function of B cells (Rasmusson et al., 2007a) and neutrophils (Raffaghello et al., 2008). As such, we now know that the immunosuppressive functions of MSCs are not constitutively active, but tightly regulated by the inflammatory microenvironment it encounters. This balance centres on the number of 'immunosuppressive signals' provided by proinflammatory cytokines compared to 'immunosupportive signals' mediated by toll-like receptor (TLR) signalling. The

stepwise process resulting in the eventual activation of MSC immunosuppressive machinery has been termed MSC "licensing", and the importance of this process is increasingly becoming clear (Krampera, 2011).

The proinflammatory cytokine IFNγ plays a crucial role in the licensing process. Binding of IFNγ to its receptor on MSCs is required for MSC-mediated immunosuppression (Krampera et al., 2006). Addition of an IFNγ antibody neutralised this suppressive activity. IFNγ receptor knockout MSCs failed to prevent T cell proliferation *in vitro* and also failed to prevent GvHD in experimental animals. Other pro-inflammatory cytokines TNFα, IL-1α and IL-1β have also been shown to work synergistically with IFNγ to induce immunosuppression (Ren et al., 2008). Finally, MSCs that were pre-stimulated with IFNγ could prevent GvHD more efficiently (5x less cell number required) than unstimulated control cells. However, MSCs failed to prevent the proliferation of $IFN\gamma^{-/-}$ T cells, highlighting the importance of IFNγ in the initiation of MSC-derived immunosuppression (Polchert et al., 2008).

TLR signalling can counterbalance the immunosuppressive signals provided by IFNγ and other inflammatory cytokines (Keating, 2012). TLRs are expressed on innate immune cells and recognise a variety of "danger signals" such as bacterial proteins or viral RNA (Patten and Collett, 2013). Both human and mouse MSCs express TLRs 1-6, with TLR3 and TLR4 being particularly important in regulating immunosuppressive functions (DelaRosa and Lombardo, 2010). Priming of MSCs using TLR3 ligands (double stranded RNA, a hallmark of viral infection) resulted in the production of anti-inflammatory cytokines and the inhibition of T

cell proliferation. Conversely, TLR4 priming (using LPS, a hallmark of bacterial infection) results in the production of proinflammatory cytokines and enhanced T cell proliferation (Waterman et al., 2010, Tomchuck et al., 2008).

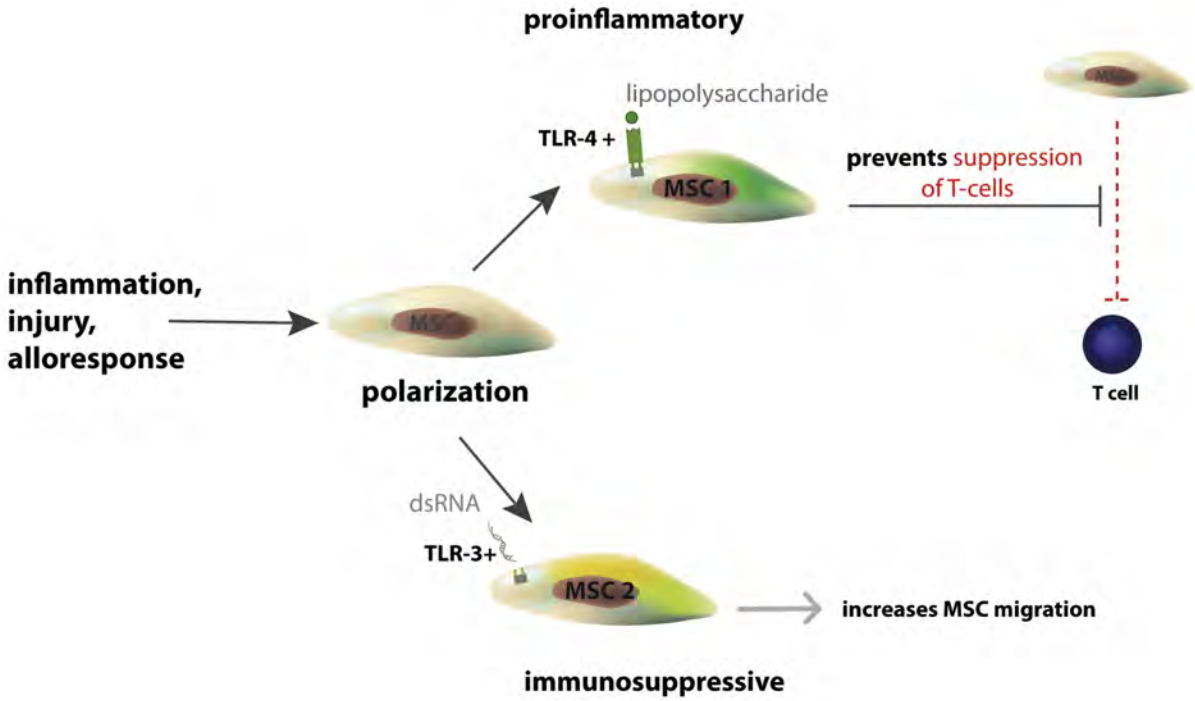


Figure 1.11 | **TLR signalling in MSCs**. TLR4 activation polarises MSCs towards a proinflammatory cell that enhances the proliferation of activated T cells. TLR3 activation polarises MSCs towards a more immunosuppressive phenotype. Figure modified from Keating, 2012.

The current hypothesis is that MSCs can respond to signals in the inflammatory microenvironment to both promote (TLR4 primed) or suppress (TLR3 primed) the immune system at different stages of tissue injury (Figure 1.11; Keating, 2012). Future studies should examine the effect of TLR3 priming and IFNγ licensing on the therapeutic properties of MSCs *in vivo* to see if this hypothesis remains true.

## 1.8 Aims and Objectives

MSCs hold great promise in future uses as a regenerative or immunosuppressive therapy. However, previous work in the murine MSC field has been confounded by the heterogeneous population of plastic-adherent cells used in most studies. Three recent publications detailing the prospective isolation of murine MSCs have the potential to revolutionise this field, but the uptake of these techniques by the wider scientific community has been slow. If the claims made by these groups are reproducible, we would venture that all further studies on murine MSCs utilise these cells exclusively.

In this study, I set out to prospectively isolate murine PαS MSCs based on the expression of PDGFRα and Sca-1 (Morikawa et al., 2009). PαS MSCs formed the substrate for my *in vitro* and *in vivo* studies on MSC biology, and the specific aims for my project were to:

1. Isolate PαS MSCs and characterise their growth, CFU-F, differentiation and immunosuppressive properties
2. Examine the effect of extended culture on PαS MSC function
3. Examine the effect of FGF2, PDGF-BB and TGF-β1 supplementation for the enhancement of PαS MSC function and the reduction of senescence
4. Examine the effect of GF-stimulated PαS MSCs in a mouse model of alloimmune liver injury

# CHAPTER 2

# MATERIALS AND METHODS

## 2.1 Prospective Isolation of Murine PαS MSCs

The prospective isolation of PαS MSCs was performed as described by Morikawa *et al*. (2009). We typically processed 10 mice per isolation and the sample preparation took approximately five hours until it was ready for cell sorting. The majority of experiments were performed using PαS MSCs isolated from C57BL/6 mice, with some *in vitro* immunosuppression assays performed using Balb/c-derived PαS MSCs. Instances where Balb/c-derived cells were used have clearly been indicated in text.

### 2.1.1 Cell isolation from Compact Bone

Male 8-12 week old C57BL/6 (Harlan, Bicester, UK) or Balb/c mice (Jackson Laboratory, ME, USA) were sacrificed by cervical dislocation. The femur and tibia were dissected out of the lower limbs and all soft tissue removed using tissue paper. Cleaned bones were stored in ice-cold PBS while the remaining animals were processed.

Cleaned bones were washed three times in sterile PBS to remove any non-adherent tissue. They were then placed in a sterile pestle and mortar and gently crushed to achieve one fracture per bone. Bone fragments were then further cut using sterile scissors until a homogenous paste was formed. The resulting paste was washed once in 5ml PBS and the bone marrow was discarded. Compact bone fragments were then incubated in 20ml DMEM (Dulbecco's Modified Eagle Medium; Gibco, Paisley, UK) supplemented with 0.2% (40mg) collagenase (Wako Chemicals, Neuss, DE) and 1x penicillin/streptomycin/glutamine (PSG; Gibco) for 60 minutes in a temperature-regulated shaker set at 37°C and 125rpm.

Following incubation, the cell suspension was filtered through a sterile 70µm strainer (Corning, Amsterdam, NL) and the larger bone fragments placed back in the mortar. The fragments were then placed in 2.5ml ice-cold HBSS (Hank's Balanced Salt Solution; Gibco) supplemented with 2% FBS (Gibco), 10mM HEPES (Sigma-Aldrich, Dorset, UK) and 1x PSG. Resuspended bone fragments were gently tapped 50 times with the pestle before a further 2.5mls of supplemented-HBSS was added. This solution was pipetted up and down several times to liberate cells from the bone fragments. The liquid supernatant was carefully aspirated and passed through a sterile 70µm strainer into the same falcon tube containing the filtrate from earlier. This tapping and re-suspending step was repeated a further six times to end up with a final cell suspension of 50ml.

The resulting cell suspension was pelleted by centrifugation at 1500 rpm for 7 minutes at 4°C. The supernatant was discarded and the pellet was resuspended in the residual volume by vigorous tapping. Red blood cell (RBC) lysis was performed by adding 1ml ice-cold sterile water (Sigma-Aldrich) to the resuspended pellet for 5 seconds. The reaction was quickly quenched by the addition of 1ml 2x (double-strength) PBS supplemented with 4% FBS followed by 20ml of supplemented HBSS-solution. The sample was filtered before centrifugation at 2000 rpm for 5 minutes at 4°C. The resulting pellet was resuspended in 1ml of supplemented-HBSS solution prior to antibody staining.

### 2.1.2 Antibody Staining of BM cells

Single-cell suspensions of BM were labelled with conjugated antibodies to CD45 (PE; 1µl/mouse), Ter-119 (PE; 1µl/mouse), Sca-1 (FITC; 1µl/mouse) and PDGFRα (APC; 2µl/mouse) for 30 minutes on ice. All antibodies were purchased from eBioscience (Hatfield, UK). Relevant control tubes were prepared by adding 1µl BM cell suspension to 100µl supplemented-HBSS containing 1µl each of PE-CD45, FITC-Sca-1 and APC-PDGFRα and incubated for 30 minutes on ice.

After incubation, the main sample was washed in 20ml of supplemented-HBSS while the control tubes were washed in 1ml each of supplemented-HBSS. Samples were spun at 2000 rpm for 5 minutes at 4˚C prior to re-suspension in supplemented-HBSS containing 2µg/ml propidium iodide (PI; Sigma-Aldrich). All sample tubes were filtered through a sterile 50µl filter (Partec, Görlitz, DE) and stored on ice prior to cell sorting.

### 2.1.3 Purification of MSCs via Cell Sorting

Samples were sorted on a MoFlo XDP cell sorter (Beckman Coulter, CA, USA). Stream setup, laser alignment and drop delay were calibrated before each sort. Single colour tubes were run and appropriate compensation applied. Relevant gates were added to select the PI-negative live cell population, exclude PE-CD45$^{+}$/PE-Ter119$^{+}$ haematopoietic cells and purify APC-PDGFRα$^{+}$/FITC-Sca-1$^{+}$ cells of interest. Samples were run at approximately 20,000 events per second for sorting.

## 2.2 PαS Cell Culture

### 2.2.1 Maintenance and Expansion

Sorted PαS cells were cultured in standard media (SM) consisting of αMEM (α-modified Minimum Essential Medium, Gibco) supplemented with 10% FBS and 1xPSG. Initial seeding density was 5000 cells/$cm^2$ in 6-well plates. Cultures were maintained at 37˚C, 5% $CO_2$ in humidified incubators. To test the effect of GF stimulation, SM was supplemented with 10ng/ml of murine PDGF-BB (Peprotech, London, UK), FGF2 (Peprotech) or TGF-β1 (New England Biolabs, Hitchin, UK).

### 2.2.2 Passaging

PαS cultures were passaged when they reached 90% confluency. Spent media was removed and cultures were washed once in PBS. Pre-warmed (37˚C) TrypLE Express (Gibco) was added and incubated at 37˚C for 3 minutes or until cells became fully detached. An equal volume of SM was added to neutralise the TrypLE and cells were pelleted by centrifugation at 2000 rpm for 5 minutes. Cultures were usually expanded at 1:2 or 1:3 ratios into bigger culture dishes.

## 2.3 CFU-F Assay

CFU-F assay was performed on freshly isolated cells by seeding 2000 PαS MSCs in a 10cm$^2$ tissue culture petri dish. Cultures were maintained for 14 days before being fixed in 10% formal saline solution (Adams Healthcare, Northwich, UK) for 5 minutes. Fixed cultures were washed once in PBS and then stained using 0.5% crystal violet solution (Sigma-Aldrich) for 60 minutes at room temperature. Excess stain was removed with two further washes in tap water and dishes were allowed to air dry before imaging.

## 2.4 Growth Curves

PαS MSCs were seeded at a density of 4000 cells per well of a 48-well plate in the presence of SM or GF-supplemented medium. Once confluent, cells were passaged into larger wells at a 1:2 ratio. After 50 days an aliquot was taken to estimate final cell number and the samples fixed for senescence staining.

## 2.5 Beta-galactosidase staining

The expression of beta-galactosidase (β-gal) was used to estimate the level of senescence in PαS MSC cultures. A senescence detection kit (Biovision, CA, USA) was used for this purpose and the manufacturer's instructions were followed. Briefly, this involved fixing PαS MSC cultures and incubating them overnight in X-Gal (a chromogenic substrate for β-gal). Senescent cells develop a blue-green colour, which was then imaged and quantified from 12 randomly selected fields of view per sample.

## 2.6 Differentiation Cultures

To induce differentiation, SM was swapped over to commercially available differentiation medium and GF treatment was stopped. Thus, the changes we saw in differentiation ability were due to the 'priming' effect of GFs used during the expansion stage only (Figure 2.1).

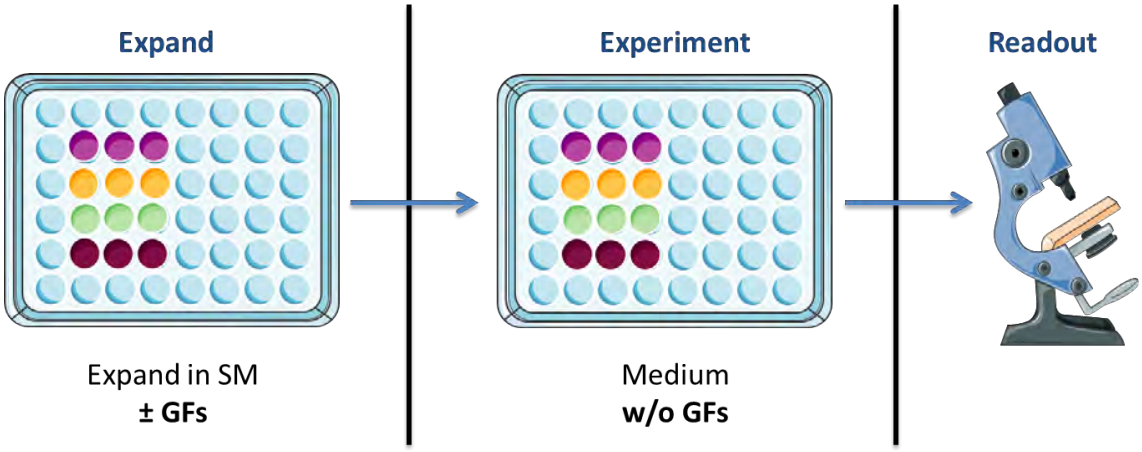


Figure 2.1 | **Effect of GF priming on PαS MSCs**. GFs were added during the expansion stage of PαS MSC culture only. Cells were washed thoroughly with PBS to remove GFs before conducting any experiments.

### 2.6.1 Osteogenic Differentiation & Alizarin Red Staining

To induce osteogenic differentiation, subconfluent MSCs were cultured in osteogenic basal medium (Lonza, Cologne, DE) for 16 days, with the media swapped every 4 days. Cultures were fixed in 10% formal saline solution for 15 minutes and washed three times in distilled water ($dH_20$) prior to staining with an Osteogenesis Assay Kit (Millipore, Watford, UK) according to manufacturer's instructions. Briefly, this involved staining the fixed cultures with alizarin red staining solution to mark any calcium deposits. Samples were imaged at this point for visual analysis.

Quantitative analysis of alizarin red staining was performed by measuring the optical density (OD) values of our samples compared to a set of known calcium standards. Alizarin red was extracted from fixed cultures by incubating them in 10% acetic acid for 30 minutes. The supernatant was then transferred into a 1.5ml eppendorf tube and vortexed vigorously for 30 seconds before being heated to 85˚C for 10 minutes. Samples were allowed to cool for 5 minutes on ice and then centrifuged at 20,000g for 15 minutes. The supernatant was carefully transferred into a new eppendorf tube and neutralised with 10% ammonium hydroxide. 150µl of samples and alizarin red standards were transferred into a flat-bottomed 96 well plate and $OD_{405}$ measured on a plate reader (Synergy HT, BioTek, Potton, UK).

### 2.6.2 Adipogenic Differentiation & Oil Red O Staining

To induce adipogenic differentiation, confluent PαS MSCs were cultured for four days in adipogenic induction medium (Lonza), followed by four days in adipogenic maintenance medium (Lonza). Differentiated cultures were fixed in 10% formal saline solution for 10 minutes before being incubated in 60% isopropanol for 5 minutes. Oil Red O stock solution was made by dissolving 0.25g Oil Red O (Sigma-Aldrich) in 50ml 100% isopropanol. This stock was then diluted in water at a ratio 1.5:1 (Oil Red O:$H_2O$). Freshly made Oil Red O working solution was added to cultures and left for 60 minutes at room temperature. After incubation, cultures were incubated in 60% isopropanol for 5 minutes followed by two washes in $dH_2O$. Cultures were counterstained with Mayer's haematoxylin for 1 minute followed by two further washes in tap water before imaging.

### 2.6.3 Chondrogenic Differentiation & Toluidine Blue Staining

To induce chondrogenic differentiation, 250,000 PαS MSCs were re-suspended in chondrogenic differentiation medium (Lonza) supplemented with 10ng/ml TGF-β3 (Peprotech) in 15ml polypropylene tubes. Samples were centrifuged at 150g for 5 minutes to pellet cells. The tube was transferred into a cell culture incubator and the cap loosened to allow gas exchange. The pellets were left undisturbed for 48 hours before being flicked to release them into suspension. Samples were incubated for 21 days with the media carefully replaced every 3 days.

After 21 days of differentiation, cartilage pellets were carefully aspirated onto a flat-bottomed foil boat and excess media was removed. Three drops of OCT embedding compound (Sakura Tissue-Tek, Thatcham, UK) was added to the foil boat and slowly frozen in the vapour phase of liquid nitrogen to cryoembed the cartilage pellet. 7µm sections of cartilage pellets were cut on a cryostat and acetone-fixed onto microscope slides (Superfrost Plus, Thermo Scientific, MA, USA) and stored at -20˚C until needed.

Toluidine blue staining was used to visualise proteoglycan deposits in cartilage pellets. Slides were allowed to defrost for 10 minutes and a wax ring was drawn around sections. 200µl of 0.1% Toluidine blue (dissolved in a pH 4.0 acetic acid/sodium acetate buffer; Sigma-Aldrich) was added to each slide and incubated at room temperature for one minute. Slides were then rinsed three times in tap water for 2 minutes each. Slides were then dehydrated by

passing through industrial methylated spirit (IMS; PFM Medical, Cheshire, UK) twice, and Xylene solvent (PFM Medical) three times before mounting coverslips using DPX (Leica, Wetzlar, DE). DPX was allowed to set overnight before imaging on a conventional light microscope (Carl Zeiss AG, Oberkochen, DE).

### 2.6.4 Pathway Analysis of PαS MSC Differentiation

Preliminary studies on downstream signalling pathways were performed to identify how GFs were exerting their effects on PαS cells. In a subset of experiments, PαS cell were cultured in SM containing one of the following small-molecule inhibitors: 25nM dasatinib (gift from Prof. Heath, University of Birmingham), 20µM SU5402 (Tocris, Abingdon, UK), and 10ng/ml PDGF-AA (Peprotech). The growth curves and adipogenic differentiation of PαS cells were then examined as described previously.

## 2.7 Biochemical analysis of Chondrogenic Differentiation

Further quantitative analysis of chondrogenic differentiation was performed in collaboration with Dr Shang Zhang and Prof. Anthony Hollander at Bristol University, Bristol, UK.

### 2.7.1 Micromass Pellet Cartilage Differentiation

$5x10^5$ PαS MSCs were pelleted in 15ml polypropylene tubes and resuspended in chondrogenic differentiation media (Bristol formulation). Chondrogenic differentiation media (Bristol formulation) consisted of DMEM (Gibco) supplemented with 1x PSG (Gibco), 1mM sodium pyruvate (Sigma-Aldrich), 1x insulin-transferrin-selenium (Gibco), 50 µg/ml ascorbic acid-2-phosphate (Sigma-Aldrich), 100nM dexamethasone (Sigma-Aldrich) and 10ng/ml TGF-β3 (Peprotech). Fresh media was added every three days and an additional 50µg/ml insulin (Sigma-Aldrich) was added at day seven to all cultures. Cartilage pellets were harvested for biochemical analysis after 21 days culture.

### 2.7.2 Cartilage Tissue Engineering

Cartilage scaffolds were produced as described by Kafienah *et al*. (2007), with a few modifications. Biofelt® polyglycolic acid (PGA) scaffolds (5mm diameter, 2mm thickness; Biomedical Structures, Warwick, UK) were sterilised in absolute ethanol (Sigma-Aldrich) for 5 minutes. Excess ethanol was removed and scaffolds were washed in PBS three times. Sterile PGA scaffolds were coated in 100µg/ml fibronectin (Sigma-Aldrich) for 30 minutes and allowed to air-dry overnight.

A 1% solution of agarose was used to coat empty wells of a 24-well plate and left to solidify. One fibronectin-coated PGA scaffold was added to each agarose-coated well of a 24-well plate. The agarose coating ensures PαS cells do not adhere onto the tissue-culture plastic after being seeded onto PGA scaffolds. PGA scaffolds were then rehydrated for 30 minutes in SM. After incubation, SM is removed and the scaffolds were ready for seeding.

PαS MSCs at P7 were used for tissue engineering studies. $6x10^5$ PαS MSCs were harvested as described previously and placed in separate polypropylene tubes. Samples were centrifuged at 1500rpm for 5 minutes and resuspended in 30µl of SM. This concentrated cell suspension was slowly added to the PGA scaffolds and left to incubate overnight. Scaffolds were turned over the next day to promote even seeding. 1ml of chondrogenic differentiation media (Bristol formulation) was then added to each well containing scaffolds and the plates were placed on a rotating platform (50rpm) inside a 37˚C, 5% $CO_2$ humidified incubator. Fresh differentiation media was then added every three days. Additional 50µg/ml insulin was again added to the differentiation media at day seven. Scaffolds were maintained on a rotating platform for a total of 35 days before analysis.

### 2.7.3 Sample digestion and solubilisation

Micromass pellets or tissue-engineered scaffolds were weighed after overnight freeze-drying in a Modulyo Freeze Drier (Thermo Scientific) prior to protease digestion. Samples were digested in 125µl digestion solution containing 2mg/ml bovine pancreatic trypsin

supplemented with 1mM iodoacetamide, 1mM EDTA and 10µg/ml pepstatin A (all from Sigma-Aldrich) for 15 hours at 37˚C. Afterwards, a further 125µl digestion solution was added and samples heated to 65˚C for 2 hours. Protease digestion was then stopped by boiling samples for 15 minutes to inactivate trypsin.

Digested samples were centrifuged at 14,000rpm for 5 minutes and the solubilised supernatant was collected and transferred into a new eppendorf tube. Any remaining undigested sample was vortexed in 500µl water and centrifuged at 14,000rpm for 5 minutes. The supernatant was discarded and the undigested material was again freeze-dried overnight and weighed. The weight of undigested sample was removed from the weight of the freeze-dried pellets/scaffolds taken at the start of this protocol to give the total weight of the solubilised sample.

### 2.7.4 Quantification of Collagen Type I using Competition ELISA

The quantification of collagen type I (Col1) was performed using a competition ELISA assay (Figure 2.2) developed by the Hollander group using peptides and antibodies made in-house (Dickinson et al., 2005). Col1 peptide (AH23; sequence: SFLPQPPQ) was dissolved in sodium carbonate buffer (pH 9.2) to give a final concentration of 40µg/ml. 50µl of this solution was added to each well of a 96 well plate (Immulon-2HB, Thermo Scientific) and left to incubate at 4˚C for three days. Coated plates were washed three times with PBS+0.05% (v/v) Tween-20 (PBS-T; Sigma-Aldrich). Each well was then blocked with PBS+1% (v/v) BSA (Sigma-Aldrich) for 30 minutes at room temperature before being washed with PBS-T and kept at 4˚C.

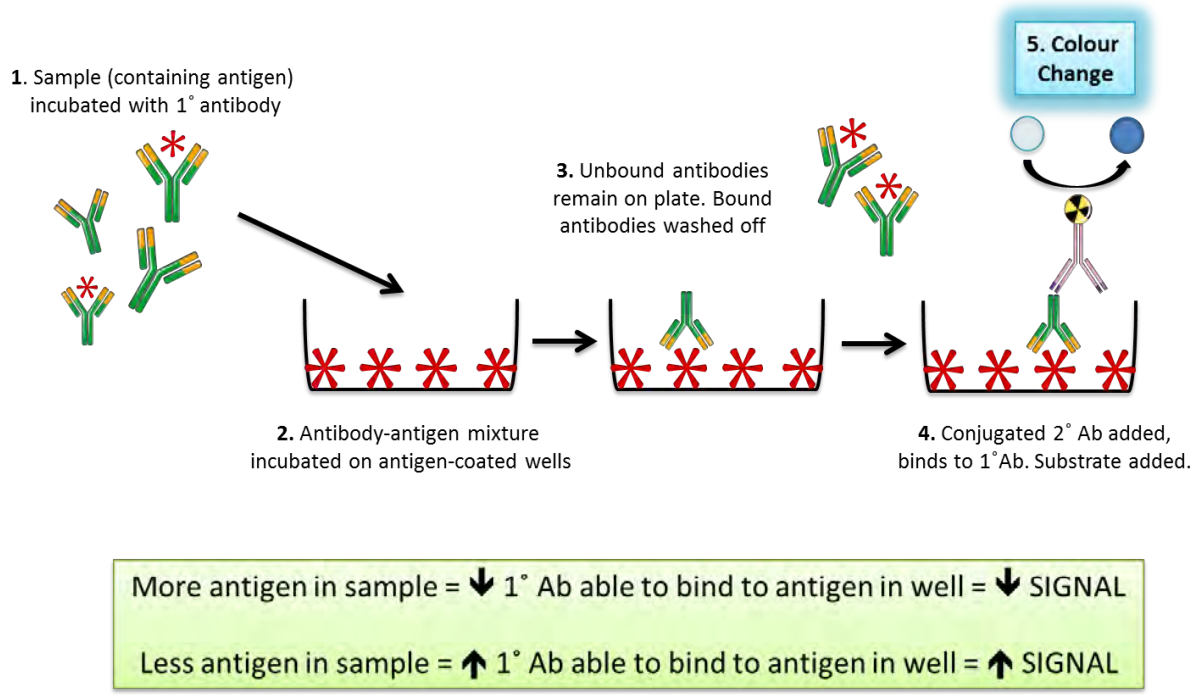


Figure 2.2 | **Principles of competition ELISA**. The amount of antigen found in your samples directly competes for the antibody with the antigen found in the pre-coated wells, hence the name "Competition" ELISA. Note the inverse relationship between the signal (colour change) and the amount of antigen found in the sample.

AH23 Col1 peptide was used as the standards for this assay (sensitivity range 4-1000ng/ml). Standards and solubilised samples were diluted in 0.8% sodium dodecyl sulphate (SDS)-Tris solution. A proprietary rabbit anti-AH23 IgG antibody (diluted 1:1000 in Tris buffer+4% Triton-X100) was used to bind to the AH23 peptide sequence on collagen 1 (Dickinson et al., 2005). This mixture of antibody and samples (50µl samples/standards to 50µl primary antibody) were left to incubate overnight in uncoated 96-well plates at 37˚C.

Following overnight incubation, 50µl of the antibody/sample mixture was transferred into empty wells of the AH23-coated 96-well plates prepared earlier. This was left to incubate for

30 minutes at room temperature before being washed three times with PBS-T. Alkaline phosphatase (ALP)-conjugated goat anti rabbit (Southern Biotech, Cambridge, UK) secondary antibody was diluted 1:1000 in PBS-T and added to each well of the AH23-coated plate containing samples. This was left to incubate for 2 hours at 37˚C. After incubation, plates were washed 2x in PBS-T and 0.5mg/ml p-nitrophenyl phosphate (substrate for AP; Sigma-Aldrich) was added to each well and left to incubate for 20 minutes for the colour to develop. The absorbance was read at $OD_{405}$ on an Ascent plate reader (MTX Lab Systems, VA, USA).

### 2.7.5 Quantification of Collagen Type II using Competition ELISA

A similar competition ELISA-based system was used for the measurement of type II collagen (Col2; Dickinson et al., 2005). 384-well high-binding ELISA plates (Corning) were coated with 40µg/ml bovine tracheal Col2 (Sigma-Aldrich) for 3 days at 4˚C. Coated plates were washed three times with PBS-T and each well was then blocked with PBS+1% BSA for 30 minutes at room temperature. Plates were then washed once with PBS-T and kept at 4˚C until needed.

CB11B peptide (sequence: CGKVGPSGAP[OH]GEDGRP[OH]GPP[OH]GPQY) was used as Col2 standards in this assay (Hollander et al., 1994). The sensitivity range was between 2-10µg/ml. A proprietary mouse IgG monoclonal antibody against Col2 (diluted 1:600 in 50mM Tris-HCL, pH 7.6) was used as the primary antibody in this assay. An equal mixture of sample and antibody (10µl samples to 10µl diluted antibody) were incubated in triplicate in sealed 384-well plates overnight at 37˚C.

Following overnight incubation, 10µl of the antibody/sample mixture was transferred into empty wells of the bovine Col2-coated 384-well plates prepared earlier. This was left to incubate for 30 minutes at room temperature before being washed three times with PBS-T. AP-conjugated goat anti mouse (Southern Biotech) secondary antibody was diluted 1:1000 in PBS-T and added to each well of the plate containing samples. This was left to incubate for 2 hours at 37˚C. After incubation, plates were washed 2x in PBS-T and 0.5mg/ml p-nitrophenyl phosphate was added to each well and left to incubate for 20 minutes for the colour to develop. The absorbance was then read at $OD_{405}$ on an Ascent plate reader.

### 2.7.6 Quantification of Glycosaminoglycans

The quantification of glycosaminoglycans (GAG) was done colourimetrically using a system established by Handley and Buttle (1995). This assay is based around the ability of the metachromatic dye dimethylmethylene blue (DMB) to form a complex with sulphated GAGs under acidic pH conditions. Binding of DMB to GAGs causes a shift in their absorption spectrum that can be read at $OD_{525}$. This shift is proportional to the amount of sulphated GAGs found in the sample and can be quantified via the use of known standards. Bovine tracheal chondroitin sulphate (Sigma-Aldrich) was used as standards (sensitivity range 5-50µg/ml) in our experiments. 250µl DMB solution (Sigma-Aldrich) was added to 20µl samples in 96-well round-bottomed plates. Samples were mixed and the absorbance read immediately at 525nm on an Ascent plate reader.

## 2.8 *In vitro* Immunosuppression Assay

This purified assay used magnetic-activated cell sorting (MACS) to isolate naive T cells that were stimulated with anti-CD3 antibody and purified CD19 B cells. Graded numbers of PαS MSCs isolated from Balb/c mice were added in a subset of experiments and cultures were maintained for 3 days before analysis. A pictorial representation of this experiment can be found in Figure 2.3. For immunosuppression using PαS MSCs isolated from C57BL/6 mice, see "Splenocyte reaction" (section 2.9).

### 2.8.1 Preparation of Buffers and Culture Medium

P2 wash buffer consisted of PBS supplemented with 2% FBS. MACS buffer consisted of PBS + 0.5% FBS + 2mM EDTA. C10 culture medium consisted of Roswell Park Memorial Institute (RPMI) basal media (Gibco) supplemented with 10% FBS, 50mM β-mercaptoethanol (Sigma-Aldrich) and 1x PSG.

### 2.8.2 Magnetic separation of $CD19^+$ B cells

8-12 week old Balb/c mice were sacrificed by cervical dislocation. The spleen was dissected free and stored in cold P2 buffer. A single cell suspension was made by gently pushing the spleen through a 70µm cell strainer (Corning) in RBC lysis buffer (Sigma-Aldrich). Dissociated tissue was pipetted up and down to ensure efficient RBC lysis for 2 minutes. Samples were washed in excess P2 buffer and centrifuged at 1400rpm for 7 minutes at 4°C. An aliquot containing approximately $40x10^6$ splenocytes was removed for the magnetic bead

purification stage. The cell pellet was resuspended in 90µl cold MACS buffer per $10^7$ cells. CD19 microbeads (Miltenyi Biotec, Cologne, DE) was added according to manufactures instructions and left to incubate in the dark at 4°C for 15 minutes. Following incubation, samples were washed in excess P2 buffer to remove unbound microbeads and centrifuged at 1400 rpm for 7 minutes. The pellet was resuspended in 500µl MACS buffer prior to MACS.

MACS separators and LS columns (both Miltenyi Biotec) were set up according to manufacturer's instructions. Columns were prepared by running 3ml warm MACS buffer through it, followed by 500µl of cell suspension and 3x washes with 3ml warm MACS buffer. The flow through was discarded and the LS column removed from the MACS separator. 4ml of MACS buffer was flushed through the column using a plunger to 'flush out' all magnetically labelled $CD19^+$ cells from the LS column. Samples were spun again at 1400rpm for 7 minutes and resuspended in C10 medium and stored on ice until needed.

### 2.8.3 Magnetic separation of $CD4^+CD25^-$ T cells

MACS was used to negatively isolate naive T cells using a $CD4^+CD25^-$ T cell isolation kit (Miltenyi Biotec). 8-12 week old Balb/c mice were sacrificed and their lymph nodes removed. Lymph nodes were forced through a 70µm cell strainer in 1ml P2 buffer to produce a single cell suspension. Samples were washed in excess P2 buffer and an aliquot taken for counting. The cell pellet was resuspended in 40µl MACS buffer and 15µl of biotinylated antibody cocktail (containing antibodies for CD8, CD11b, CD45, CD49 and Ter-119) per $10^7$ cells. Samples were left to incubate in the dark at 4°C for 15 minutes. After incubation, 30µl of

MACS buffer, 20µl of anti-Biotin microbeads and 10µl of CD25-PE antibody was added per $10^7$ cells and left to incubate for a further 15 minutes at 4°C. Samples were then quenched in excess MACS buffer to remove unbound antibodies and centrifuged at 1400 rpm for 7 minutes. Cell pellets were resuspended in 500µl MACS buffer prior to separation.

MACS separators and LD columns (Miltenyi Biotec) were set up according to manufacturer's instructions. Columns were prepared by running 2x 1ml warm MACS buffer through, with the flow-through discarded. The cell suspension was then run followed by 2x 1ml washes in warm MACS buffer to collect any remaining unlabelled cells. This flow-through contains the $CD4^+$ enriched population of cells. This population was washed in excess P2 buffer and pellets were resuspended in 90µl MACS buffer and 10µl anti-PE microbeads per $10^7$ cells and incubated at 4°C for 15 minutes. The samples were then washed in excess MACS buffer and centrifuged at 1400rpm for 7 minutes. Cell pellets were again resuspended in 500µl MACS buffer prior to the last round of magnetic separation.

MACS separators and MS columns (Miltenyi Biotec) were set up according to manufacturer's instructions. The MS column was prepared by running a single wash of 500µl warm MACS buffer with the flow-through discarded. The cell suspension was then run followed by 3x 500µl washes in warm MACS buffer to collect any remaining unlabelled cells. This flow-through contains the $CD4^+CD25^-$ naive T cell population, which was resuspended in C10 medium and stored on ice until needed.

### 2.8.4 *In vitro* proliferation assay

Purified $CD4^+CD25^-$ naive T cells were cultured in C10 media at a density of 25,000 cells per well of a 96-well, round bottomed plate (Sarstedt, Nümbrecht, DE). Purified $CD19^+$ B cells were added at a density of 50,000 cells per well (2:1 ratio) to provide the co-stimulatory signal to T cells via CD28-CD86 interaction. The primary stimulus was provided by 0.8µg/ml anti-mouse CD3e (BD Bioscience). A titrated dose of PαS MSCs was added in a subset of experiments. Cultures were maintained for 72 hours at 37°C, 5% $CO_2$ in a humidified incubator prior to flow cytometric analysis of T cell proliferation (Figure 2.3).

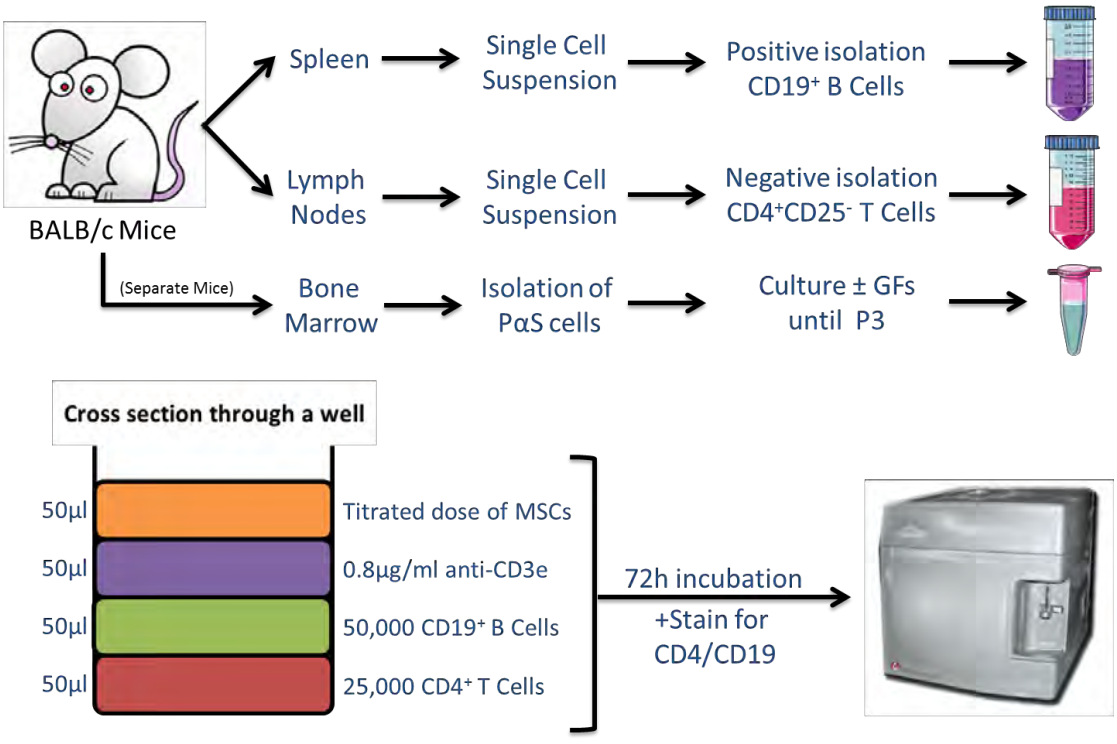


Figure 2.3 | **Overview of *in vitro* T cell proliferation assay**. This diagram summaries the stages involved in setting up this assay. See text for further details.

### 2.8.5 Flow Cytometric analysis of T cell proliferation

Cultures were pipetted up and down to remove the non-adherent lymphocyte population while leaving behind the adherent MSCs. Triplicate samples were merged together in one FACS tube and washed in FACS buffer (PBS+2% FCS). Samples were resuspended in 100µl FACS buffer and conjugated antibodies to CD4 (PerCP, 1:100 dilution; BD Bioscience) and CD19 (APC, 1:100 dilution; BD bioscience) were added and incubated at 4°C for 30 minutes. Unbound antibodies were removed in excess FACS buffer and the samples resuspended in 250µl FACS buffer prior to running on a Cyan ADP flow cytometer (Beckman Coulter).

### 2.8.6 Mechanistic studies on MSC-mediated Immunosuppression

In a subset of experiments, small molecule inhibitors of previously reported mechanisms were added to the *in vitro* T cell suppression assay. They were used at the concentrations listed in Table 2.1 below.

Table 2.1 | **Details of inhibitors used to test mechanisms of immunosuppression**.

| Reagent | Inhibits | Solvent | Final concentration | Reference |
|---|---|---|---|---|
| **Indomethacin** | $PGE_2$ release | DMSO | 5µM | Nemeth et al. (2009) |
| **SB-3CT** | MMP2/9 | DMSO | 6µM | Ding et al. (2009) |
| **1-Methyltryptophan** | IDO | Culture Media | 1MM | Meisel et al. (2004) |
| **L-NMMA** | NO release | $dH_2O$ | 1MM | Ren et al. (2008) |

### 2.8.7 Griess Assay of NO production

NO release from PαS MSCs was indirectly quantified using the Griess Assay kit (Promega, WI, USA). This kit measures the total amount of nitrite ($NO_2$-) in cell culture supernatants, which is a stable breakdown product of NO. PαS MSCs were cultured in 96-well plates (15,000 cells/well) in C10 media supplemented with 20ng/ml murine IFNγ and TNFα (both from Peprotech) to recreate an inflammatory microenvironment *in vitro*. After overnight incubation, supernatants were collected and processed according to manufacturer's instructions. The absorbance was read at 520nm and nitrite values determined against known standards that were run at the same time.

## 2.9 MSC-mediated immunosuppression in the "Splenocyte reaction"

Strain-specific differences in the immunosuppressive mechanism between Balb/c and C57BL/6 mice required the immunosuppression assay to be modified. When studying the effects of PαS MSCs isolated from C57BL/6 mice, un-purified 'bulk' splenocytes were used that contained a mixture of lymphocytes, B cells, APCs and other immune and stromal cell subsets. The lymphocytes were induced to proliferate using a variety of molecules including plant lectins, CD3/CD28 beads and T cell receptor (TCR)-specific peptide sequences.

### 2.9.1 Isolation and staining of Splenocytes

8-12 week old C57BL/6 or OT-1 mice (Jackson Laboratories) were sacrificed and their spleens removed and stored in cold C10 medium. A single cell suspension was made by gently pushing the spleen through a 70µm cell strainer in cold RBC lysis buffer. Dissociated tissue was pipetted up and down to resuspended all cells and ensure efficient RBC lysis. This reaction was stopped in excess C10 media and samples were centrifuged at 1400rpm for 7 minutes at 4˚C. An appropriate aliquot of cells was removed for staining with the remainder kept for use later on as single-colour controls.

Splenocytes were stained using the membrane dye cell trace violet (CTV; Molecular Probes, Paisley, UK) to track their proliferation in this assay. Pellets were resuspended in PBS at a concentration of $1x10^6$ cells/ml and 5µM CTV was added to each sample and incubated in the dark at 37˚C in a shaking incubator (50rpm). Samples were then quenched by adding 5x

the staining volume of C10 media and incubating for a further 5 minutes at 37˚C before centrifugation at 1400rpm for 7 minutes. Pellets were then resuspended in C10 medium and kept on ice until required.

### 2.9.2 Setting up the Splenocyte Reaction

CTV-stained splenocytes were cultured in C10 media supplemented with 50U/ml murine IL-2 (eBioscience) at a density of $1x10^5$ splenocytes per well of a 96-well, round bottomed plate. A variety of stimulatory signals were tested to induce T cell proliferation in the splenocyte mixture (Table 2.2). Cultures were then left to incubate overnight at 37˚C, 5% $CO_2$. Graded numbers of PαS MSCs from C57BL/6 mice were then added the following day. The total volume per well was made up to 200µl with fresh C10 media and cultures were left to incubate for a further 72 hours before flow cytometric analysis of lymphocyte proliferation.

Table 2.2 | **Details of the molecules used to stimulate T cell proliferation.**

| Reagent | Concentrations used | Supplier |
|---|---|---|
| **Concanavalin A (ConA)** | 1µg/ml to 100µg/ml | Sigma-Aldrich |
| **CD3/CD28 Dynabeads®** | 2000 to 500,000 beads per well | Gibco |
| **OVA (257-264) [SIINFEKL]** | 10µg/µl, 50µg/ml | AnaSpec |

### 2.9.3 Intracellular staining and Flow Cytometric analysis

In a subset of experiments, final day (day 4) samples were treated with 1µg/ml brefeldin A (BD Biosciences) to inhibit the extracellular secretion of cytokines. They were then re-stimulated with 50ng/ml phorbol myristate acetate (PMA; Sigma-Aldrich) and 1µM ionomycin (INO; Sigma-Aldrich) for 4 hours to induce cytokine production. Samples were then collected into FACS tubes by gentle pipetting to remove the non-adherent immune cells and leave behind PαS MSCs. Following one wash step in FACS buffer, all samples were resuspended in PBS and stained using a Live/Dead marker (1µl/ml; eBioscience) for 30 minutes at 4˚C. Unbound dye was washed in an excess of FACS buffer and samples were resuspended in 100µl FACS buffer for surface staining.

Surface staining was performed using a range of antibodies including CD3, CD4 and CD8. Details on the dilution factor, fluorophore and supplier information can be found in Table 2.6. Samples were incubated for 30 minutes at 4˚C before being washed once in FACS buffer. Samples were then permeabilised by incubating in Fix/Perm solution (BD Bioscience) for 20 minutes at 4˚C followed by one wash in Perm wash buffer (BD Bioscience). Samples were then resuspended in 50µl Perm wash buffer for intracellular staining. Samples were stained for 30 minutes at 4˚C followed by two washes in FACS buffer. All samples were filtered through a 50µm filter before analysis on a Cyan ADP flow cytometer. Compensation beads (BD Bioscience) were used to minimize fluorescence spillover and data was analysed offline using FlowJo v8.7 software (TreeStar Inc, OR, USA).

## 2.10 RNA Isolation and Microarray Analysis

PαS MSCs from C57BL/6 mice were cultured in SM±GFs as described previously. Confluent cultures at P1 were used for RNA isolation using an RNeasy mini kit (Qiagen, MD, USA) according to manufacturer's instructions. All samples underwent DNase I digestion (Qiagen) to remove genomic DNA contamination. Good quality RNA isolates (OD260/280≈2.0 and OD260/230 between 2.0 and 2.2) from three independent PαS MSC isolations per condition were used for downstream analysis.

Samples were then hybridised onto individual whole-genome GeneChip Mouse Exon 1.0 ST Arrays (Affymetrix, High Wycombe, UK) for transcriptional profiling. Sample preparation and hybridisation was performed by technical staff working for Affymetrix Microarray Service at the University of Birmingham. Bioinformatics and heatmap generation was performed by Dr Wenbin Wei, School of Cancer Sciences, University of Birmingham.

## 2.11 Karyotype Analysis

Chromosomes of C57BL/6 PαS MSCs at P3 and P5 were analysed for the presence of any culture-induced abnormalities. The same culture was maintained between both time points, allowing us to identify whether any clonal growth of abnormal cells took place (Figure 2.4). This work was done in collaboration with Ms Mary Strachan, Dr Sara Dyer and Prof. Mike Griffiths at the West Midlands Regional Genetics Laboratory, Birmingham Women's Hospital.

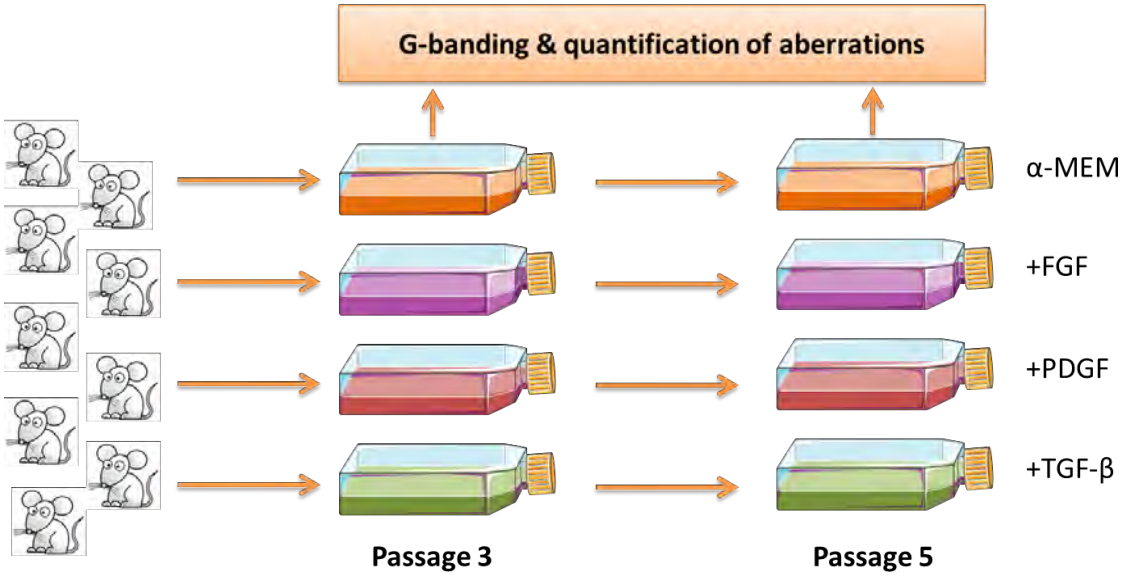


Figure 2.4 | **Overview of PαS MSC karyotyping**. PαS MSCs were grown in SM ± GFs. An aliquot of cells was taken for G-banding analysis at P3 and the same culture was maintained until P5 when another aliquot was taken. This allows us to detect any clonal expansion that could have taken place.

### 2.11.1 PαS MSC Harvesting

PαS MSCs were expanded as described previously in SM±GFs. When cultures reached 70% confluency, a 1:50 dilution of B-ONC (BRDU-overnight colcemid) was added and incubated overnight. Colcemid prevents spindle fibre formation and arrests dividing cells in metaphase.

Fresh colcemid was added the morning after to each flask and incubated for an hour. Samples were washed in PBS and harvested using TrypLE to yield a single cell suspension. Cell pellets were slowly resuspended in a hypotonic 0.025M KCL solution and incubated at 37˚C for 20 minutes. This solution causes the cell nuclei to swell in size to prevent the chromosomes from overlapping each other. After incubation, samples were spun at 1500rpm for 5 minutes and the supernatant discarded. The pellet was resuspended in the residual volume that remained and flicked gently to ensure a single-cell suspension. Samples were then slowly fixed in Carnoy's fixative (1 part glacial acetic acid to 3 parts methanol). Samples were then spun at 1500rpm for 5 minutes and further fixative added in a drop-by-drop basis. The supernatant was discarded after centrifugation and sample tubes stored at 4°C until slide making and Giemsa banding (G-banding).

### 2.11.2 Chromosome Spreads

The fixed cell suspensions were used to make slides for cytogenetic examination. Fixed cell samples were aspirated in a pipette and held over the middle of each slide from a height of approximately 50cm. One drop was allowed to fall and hit the slide, whereupon the nuclei would burst and the chromosomes would spread across the slide. Slides were checked to ensure minimal overlapping chromosomes and the cell density altered if necessary by adding more fixative. Slides were then 'aged' overnight at 60°C prior to G-banding.

### 2.11.3 Giemsa Banding, Imaging and Analysis

Leishman's stain (belonging to the same family of stains as Giemsa) was used in this study to mark chromosomes for cytogenetic analysis. The banding pattern observed with Leishman's stain is virtually identical to Giemsa (Moore and Best, 2001). As such, both stains can be interchangeably used for analysis.

'Aged' slides were allowed to cool to room temperature and rinsed gently in tap water. Slides were then incubated in 0.25% trypsin for 90 seconds and then rinsed in saline solution. Slides were incubated in Leishman's stain for 2 minutes before being rinsed in excess saline. Excess saline was removed using blotting paper and the slides were left on a hot plate at 60°C to air-dry before coverslipping.

Each slide was examined using a standard light microscope and images taken when a metaphase spread contains all 40 non-overlapping mouse chromosomes in the same optical field was observed. Individual chromosomes were electronically cut and arranged to produce a karyogram where sister chromatids are arranged in order. A total of 60 metaphase spreads per culture condition at P3 and P5 were analysed by Ms Mary Strachan for the presence of any karyotypic abnormalities. These findings were independently verified by Dr Sara Dyer before the final karyotype was reported.

## 2.12 Immunohistochemistry

### 2.12.1 Formalin-fixed Paraffin-embedded (FFPE) Tissue

FFPE tissue blocks were cut at 5µM thickness and fixed onto microscope slides (X-tra Adhesive, Leica). Slides were dewaxed and rehydrated by passing through xylene (3x 2 minutes each), IMS (2x 2 minutes each) and water (1x 2 minute wash). Antigen retrieval was performed using a high pH buffer (Vector Laboratories, Peterborough, UK). The buffer was pre-warmed in a microwave for 5 minutes at high power before slides were added. It was then heated for a further 15 minutes before being left to stand for 10 minutes. The buffer was cooled by the gentle addition of cold tap water until it reached room temperature.

Slides were then dried and sections were encircled using a wax pen. Endogenous peroxidase activity was blocked by incubating sections in a pre-diluted peroxidase blocking solution (Dako, Ely, UK) for 40 minutes. Slides were then washed in Tris-buffered saline + 0.1% Tween20 (TBS-T; 2x 5 minutes each) before blocking in 1x casein buffer (Vector Laboratories) for 60 minutes. Primary antibodies were diluted in TBS at the appropriate dilutions (Table 2.6) and added directly the after casein blocking stage. Slides were incubated with primary antibody at room temperature for 60 minutes with gentle rocking. Unbound antibody was removed by two further TBS-T washes (5 minutes each). Sections were then incubated with pre-diluted horseradish peroxidase (HRP)-conjugated secondary antibody (Vector Laboratories) for 30 minutes at room temperature with gentle rocking. Unbound secondary antibody was removed in three TBS-T washes (5 minutes each) before chromogenic visualisation.

3,3'-Diaminobenzidine (DAB; AbD Serotec, Kidlington, UK) was prepared according to manufacturer's instructions and incubated with sections until brown staining was visible (typically around 30-120 seconds). Sections with an isotype-matched control (IMC) primary antibody were run at the same time to check for non-specific binding. Excess substrate was washed off in tap water for 5 minutes to stop the chromogenic reaction. Sections were then counterstained in Mayer's haematoxylin and "blued" for 150 seconds in tap water. Slides were then dehydrated by passing through IMS twice and xylene three times before mounting coverslips using DPX. DPX was allowed to set overnight before imaging on a conventional light microscope (Carl Zeiss AG).

### 2.12.2 Snap-Frozen Tissue

In some cases, tissue was snap-frozen in liquid nitrogen and embedded in OCT compound (Sakura Tissue-Tek). 7µm sections were cut, mounted on pre-coated glass slides (Thermo Scientific), and fixed in acetone for 10 minutes. Excess acetone was removed in two washes of TBS-T (5 minutes each). Endogenous peroxidases were blocked by incubating slides for 15 minutes in a pre-diluted peroxidase blocking solution (Dako). Sections were then blocked in 1x casein buffer (Vector Laboratories) for 30 minutes before primary antibody (Table 2.6) was added. Sections were left to incubate at room temperature for 60 minutes with gentle rocking. Unbound primary antibody was removed in two washes of TBS-T (5 minutes each) and HRP-conjugated secondary antibody (Vector Laboratories) was added for 30 minutes at room temperature with gentle rocking. Sections were then washed, stained with DAB, dehydrated and mounted in DPX as described above.

## 2.13 OVA-Bil model of Alloimmune Liver Injury

### 2.13.1 Animal Husbandry

OT-1 and OT-2 T cell receptor transgenic mice were purchased from Jackson Laboratories (Table 2.5). OVA-Bil mice were maintained as heterozygotes on a C57BL/6 background (Buxbaum et al., 2006). All animals were housed in accordance with established care protocols at the University of Birmingham. All procedures using mice underwent ethical review and were performed in accordance with the Animals (Scientific Procedures) Act of 1986 under Home Office Project License 70/7707.

### 2.13.2 Genotyping

Polymerase chain reaction (PCR) was used to confirm the genotype of transgenic animals. Ear clippings were heated to 95°C in 50mM NaOH for 20 minutes to extract genomic DNA. Samples were then cooled on ice for 10 minutes and neutralised in a 1:10 dilution of 1M Trizma base (Sigma-Aldrich). PCR was performed using a Fast-cycling PCR Kit (Qiagen) containing a Hot-start *Taq* DNA polymerase according to manufacturer's instructions. Samples were made up in a final volume of 20µl containing 2µl of genomic DNA and 1µl of each primer. Primer sequences and amplicon lengths can be seen in Table 2.3. Samples were then run on a G-storm PCR thermal cycler (Somerton, UK) and the cycling conditions can be found in Table 2.4. PCR products were run in a 2% agarose gel for 60 minutes at 125mV prior to imaging on a UV transilluminator. Band size was determined by comparison against a 100bp molecular weight ladder (Bioline, Hemel Hempstead, UK).

Table 2.3 | **List of PCR primers used to genotype mice**

| **Primer** | **OVA-Bil** |
|---|---|
| Forward | 5'-GGC GTG TTG AAA GTA AGC-3' |
| Reverse | 5'-CCA GAC AGA TTG GCT GAA GAG CTA-3' |
| Amplicon length | 994bp |
| **Primer** | **OT-1** |
| Forward | 5'-CAG CAG GTG AGA CAA AGT-3' |
| Reverse | 5'-GGC TTT ATA ATT AGC TTG GTC C-3' |
| Amplicon length | 250bp |
| **Primer** | **iNOS-/-** |
| Common | 5'-ACA TGC AGA ATG AGT ACC GG-3' |
| Wild-type | 5'-TCA ACA TCT CCT GGT GGA AC-3' |
| Mutant | 5'-AAT ATG CGA AGT GGA CCT CG-3' |
| Amplicon length | Mutant=275bp, Heterozygote=275bp and 108bp, Wild-type=108bp |

Table 2.4 | **Thermal cycler settings for gene amplification**

| **OVA-Bil** | | | |
|---|---|---|---|
| **Stage** | **Temperature (°C)** | **Duration (min)** | **Cycles** |
| Hot-start | 95 | 05:00 | 35 Cycles |
| Denaturation | 96 | 00:05 | |
| Annealing | 55 | 00:05 | |
| Extension | 68 | 00:30 | |
| Final Extension | 72 | 01:00 | |
| **OT-1** | | | |
| **Stage** | **Temperature (°C)** | **Duration (min)** | **Cycles** |
| Hot-start | 95 | 05:00 | 32 Cycles |
| Denaturation | 96 | 00:05 | |
| Annealing | 53 | 00:05 | |
| Extension | 68 | 00:30 | |
| Final Extension | 72 | 01:00 | |
| **iNOS-/-** | | | |
| **Stage** | **Temperature (°C)** | **Duration (min)** | **Cycles** |
| Hot-start | 95 | 05:00 | 35 cycles |
| Denaturation | 94 | 00:15 | |
| Annealing | 59 | 00:15 | |
| Extension | 72 | 01:00 | |
| Final Extension | 72 | 02:00 | |

### 2.13.3 Induction of Liver Inflammation

8-12 week old male OT-1 and OT-2 mice were sacrificed by cervical dislocation and their spleens removed and stored in cold C10 media. Single cell suspensions were made by gently pushing the spleens through a 70µm mesh in RBC lysis buffer. Dissociated tissue was pipetted up and down to resuspended all cells and ensure efficient RBC lysis for 2 minutes. Samples were washed in excess C10 buffer and centrifuged at 1400rpm for 7 minutes at 4°C. Cell pellets were resuspended in PBS and an aliquot of cells containing $10x10^6$ OT-1 splenocytes and $4x10^6$ OT-2 splenocytes was removed and merged together. Cells were made up in a final volume of 200µl for infusion and adoptively transferred via a single intraperitoneal (IP) infusion into male OVA-Bil mice between 8-12 weeks of age to initiate inflammatory liver injury. Mice were sacrificed at different time points thereafter to assess the degree of liver injury occurring.

### 2.13.4 Treatment of OVA-Bil mice with PαS MSCs

PαS MSCs were cultured in SM±GFs as described previously. On the day of infusion, cells were lifted off tissue culture plastic using TrypLE and resuspended in PBS. $1x10^6$ PαS MSCs were given at days 3 and 7 after the onset of injury via IP infusions (Figure 2.5).

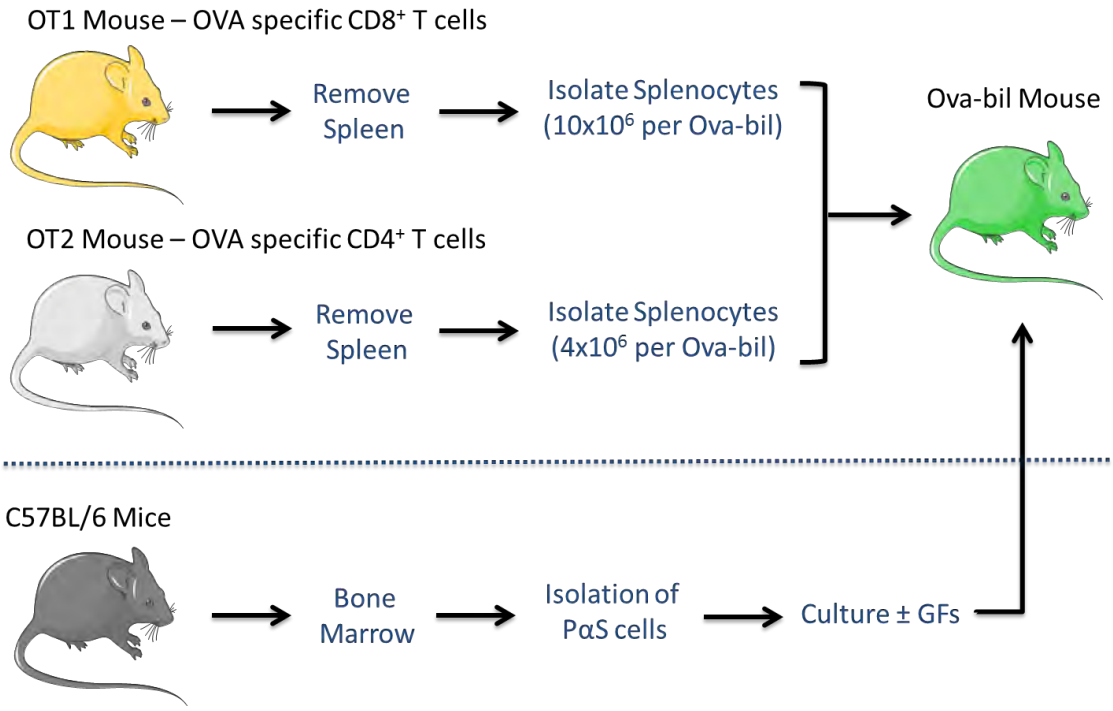


Figure 2.5 | **Overview of the OVA-Bil model.** Adoptive transfer of OVA-specific CD4 and CD8 T cells into OVA-Bil mice results in their migration to the liver where they induce necro-inflammatory damage. PαS MSCs were infused after injury to see whether they could attenuate the immune response.

### 2.13.5 Blood and Tissue Collection

OVA-Bil mice were anaesthetised in 4% isoflurane in 4 litres/minute oxygen and blood was collected via cardiac puncture through a 25g needle. Approximately 700µl to 900µl blood per mouse was aspirated before the mice were sacrificed via cervical dislocation. The livers were then removed from each animal and placed inside a sterile petri dish. The largest liver lobe was dissected out, weighed, and placed in C10 media for cell isolation. The remaining lobes were split evenly between formalin pots and snap-freezing in liquid nitrogen. These lobes were then processed accordingly and sections stained for markers of interest using immunohistochemistry (IHC).

### 2.13.6 Liver Function Tests

Whole blood was centrifuged at 10,000 rpm for 5 minutes to isolate serum. Approximately 100-150µl serum was carefully removed and placed in 13mm false-bottomed sample tubes (Sarstedt) and any remaining serum was stored at -80˚C for future use. Serum was assayed for alanine transaminase (ALT) and alkaline phosphatase (ALP) as markers of hepatocytic and biliary damage respectively. Liver function tests (LFTs) were performed by the Clinical Biochemistry team at Birmingham Women's Hospital.

### 2.13.7 Isolation of Liver Lymphocytes

Liver lobes were placed in gentleMACS 'C' Tubes (Miltenyi) with 10ml of plain RPMI. The tubes were then processed using the "Mouse spleen 1.01" program to produce a single-cell suspension. Samples were then forced through a 60µm mesh and washed with 40ml RPMI. Samples were then spun at 50g for 10 minutes to remove hepatocytes from downstream analysis. Supernatants were collected and washed three times in an excess of cold RPMI until it appears clear and less fatty. At this stage, the cell pellets were resuspended in 7ml RPMI and passed through a 50µm filter prior to density gradient separation.

Lympholyte®-Mouse cell separation media (Cedarlane, Burlington, CA) was used for the isolation of viable lymphocytes from murine cell suspensions. 7ml of room temperature Lympholyte® was carefully added to a 15ml polypropylene tube. An equal volume of cell suspension was layered on top of the Lympholyte® with extra care taken to ensure a distinct

interphase is formed between solutions. Samples were then centrifuged at 2000rpm for 30 minutes with the brake set to zero. Successful separation results in a distinctive "cloudy" layer of lymphocytes appearing at the interphase between the Lympholyte® and RPMI. This was carefully aspirated with a Pasteur pipette and transferred into a new tube before being washed twice in FACS buffer to remove residual Lympholyte® from the sample.

Samples were then resuspended in PBS and stained using a Live/Dead dye as described previously. Following one wash in FACS buffer, samples were resuspended in 100µl FACS buffer for staining with fluorescently conjugated antibodies (Table 2.6) for 60 minutes at 4˚C. Samples were then washed once in an excess of FACS buffer to remove any unbound antibodies. All samples were filtered through a 50µm filter before analysis on a Cyan ADP flow cytometer (FC). Compensation beads were used to minimize fluorescence spillover. Results were then normalised back to the starting weight of each liver lobe to allow comparison between mice.

## 2.14 Statistical Analysis

Statistical analysis was performed using Prism 5.0 (GraphPad Software, CA, USA). Normality tests were performed before deciding which analysis to perform. Generally, values were analysed using unpaired Student's t-test when comparing two groups, and one-way ANOVA with Bonferroni's post-hoc test when comparing three or more groups. Significance was represented as: *≤0.05; **≤0.01; ***≤0.001.

## 2.15 Supplier Information and Catalogue Numbers

### 2.15.1 Details of Mice used in this Study

Table 2.5 | **Details of mice used in this study.**

| Strain | Background | Supplier | Catalogue Number |
|---|---|---|---|
| **C57BL/6** | n/a | Harlan | 057 |
| **Balb/c** | n/a | Jackson Laboratory | 000651 |
| **OT-1** | C57BL/6 | Jackson Laboratory | 003831 |
| **OT-2** | C57BL/6 | Jackson Laboratory | 004194 |
| **OVA-Bil** | C57BL/6 | Gift (Liver Laboratories) | n/a |
| **iNOS-/-** | C57BL/6 | Jackson Laboratory | 007072 |

### 2.15.2 Details of Antibodies used in this Study

Table 2.6 | **List of primary and secondary antibodies used in this study.**

| Antibody | Fluorophore | Final Concentration | Intended use | Supplier | Catalogue Number |
|---|---|---|---|---|---|
| **CD3** | PE | 5µg/ml | FC | eBioscience | 12-0031 |
| **CD3** | APC | 2.5µg/ml | FC | eBioscience | 17-0031 |
| **CD3** | PE-Cy7 | 10µg/ml | FC | eBioscience | 25-0031 |
| **CD3** | BV510 | 5µl/test | FC | Biolegend | 100233 |
| **CD3e** | Purified | 0.8µg/ml | Functional | BD Bioscience | 553057 |
| **CD4** | BV421 | 5µl/test | FC | Biolegend | 100544 |
| **CD4** | FITC | 2.5µg/ml | FC | eBioscience | 11-0042 |
| **CD4** | PerCP | 1:100 | FC | BD Bioscience | 561090 |
| **CD8** | PE-Cy7 | 5µg/ml | FC | eBioscience | 25-0081 |
| **CD8** | APC | 1.25µg/ml | FC | eBioscience | 17-0081 |
| **CD8** | APC-Cy7 | 1:100 | FC | BD Bioscience | 561967 |
| **CD19** | APC | 1:100 | FC | BD Bioscience | 561738 |
| **CD25** | PE | 1.25µg/ml | FC | eBioscience | 12-0251 |
| **CD25** | APC | 1.25µg/ml | FC | eBioscience | 17-0251 |
| **CD29** | PE | 10µg/ml | FC | eBioscience | 12-0291 |
| **CD34** | FITC | 10µg/ml | FC | eBioscience | 11-0341 |
| **CD44** | FITC | 5µg/ml | FC | eBioscience | 11-0441 |
| **CD45** | PE | 1µl/mouse | FACS | eBioscience | 12-0451 |
| **CD45** | Purified | 1:200 | IHC | eBioscience | 14-0451 |

| Antibody | Fluorophore | Final Concentration | Intended use | Supplier | Catalogue Number |
|---|---|---|---|---|---|
| **CD49e** | PE | 5µg/ml | FC | eBioscience | 12-0493 |
| **CD62L** | APC | 0.6µg/ml | FC | eBioscience | 17-0621 |
| **CD69** | FITC | 5µg/ml | FC | eBioscience | 11-0691 |
| **CD69** | Pacific Blue | 2.5µg/ml | FC | Invitrogen | HM4028 |
| **CD90** | PE | 0.3µg/ml | FC | eBioscience | 12-0902 |
| **CD105** | FITC | 5µg/ml | FC | eBioscience | 12-1051 |
| **F4/80** | FITC | 5µg/ml | FC | eBioscience | 11-4801 |
| **F4/80** | Purified | 1:00 | IHC | AbD Serotec | MCA497R |
| **Ter-119** | PE | 1µl/mouse | FACS | eBioscience | 12-5921 |
| **Sca-1** | FITC | 1µl/mouse | FACS | eBioscience | 11-5981 |
| **PDGFRα** | APC | 1µl/mouse | FACS | eBioscience | 17-1401 |
| **FoxP3** | PE | 10µg/ml | FC | eBioscience | 12-5773 |
| **Vα2** | PE | 5µg/ml | FC | eBioscience | 12-5812 |
| **IFNγ** | FITC | 5µg/ml | FC | eBioscience | 11-7311 |
| **TNFα** | PE | 2.5µg/ml | FC | eBioscience | 12-7321 |
| **Live/Dead Marker** | eFluor®780 | 1µl/ml | FC/FACS | eBioscience | 65-0865 |
| **HRP-conjugated anti rabbit Ig** | N/A | Pre-diluted | IHC | Vector Laboratories | MP-7401 |
| **HRP-conjugated anti rat Ig** | N/A | Pre-diluted | IHC | Vector Laboratories | MP-7444 |
| **AP-conjugated anti rabbit Ig** | N/A | 1:1000 | IHC | Southern Biotech | 4010-04 |
| **AP-conjugated anti mouse Ig** | N/A | 1:1000 | IHC | Southern Biotech | 1030-04 |

### 2.15.3 Details of General Reagents used in this Study

Table 2.7 | **List of general laboratory reagents used in this study.**

| Item | Supplier | Catalogue Number |
|---|---|---|
| **DAB substrate** | AbD Serotec | BUF022 |
| **10% formal saline solution** | Adams Healthcare | 416479 |
| **OVA (257-264) peptide** | AnaSpec | 60193-5 |
| **Anti-rat/hamster compensation beads** | BD Bioscience | 552845 |
| **Brefeldin A** | BD Bioscience | 555029 |
| **Fix/Perm Solution** | BD Bioscience | 554722 |
| **Perm wash buffer** | BD Bioscience | 554723 |
| **PCR Hyperladder 100bp** | Bioline | 33029 |

| Item | Supplier | Catalogue Number |
|---|---|---|
| **Senescence Detection Kit** | Biovision | K320-250 |
| **Lympholyte®-Mouse** | Cedarlane | CL5035 |
| **Peroxidase blocking solution** | Dako | 52023 |
| **IL-2** | eBioscience | 16-7022 |
| **CD3/CD28 Dynabeads®** | Gibco | 11452 |
| **DMEM** | Gibco | 41965-039 |
| **FBS** | Gibco | 10500 |
| **HBSS** | Gibco | 14170-088 |
| **Insulin-transferrin-selenium** | Gibco | 41400-045 |
| **Penicillin/Streptomycin/Glutamine** | Gibco | 10378-016 |
| **RPMI** | Gibco | 31870-025 |
| **TrypLE Express** | Gibco | 12605010 |
| **αMEM** | Gibco | 32561-029 |
| **Dasatinib** | Gift | N/A |
| **DPX Mounting Medium** | Leica | 08600E |
| **Adipogenic Differentiation Media** | Lonza | PT-3004 |
| **Chondrogenic Differentiation Media** | Lonza | PT-3003 |
| **Osteogenic Differentiation Media** | Lonza | PT-3002 |
| **Osteogenesis Assay Kit** | Millipore | ECM815 |
| **CD19 microbeads** | Miltenyi Biotec | 130-052-201 |
| **$CD4^+CD25^-$ T Cell Isolation Kit** | Miltenyi Biotec | 130-091-041 |
| **Cell Trace Violet Proliferation Kit** | Molecular Probes | C34557 |
| **Murine recombinant TGF-β1** | New England Biolabs | 5231LC |
| **Human recombinant TGF-β3** | Peprotech | 100-36E |
| **Murine recombinant FGF2** | Peprotech | 450-33 |
| **Murine recombinant IFNγ** | Peprotech | 315-05 |
| **Murine recombinant PDGF-AA** | Peprotech | 315-17 |
| **Murine recombinant PDGF-BB** | Peprotech | 315-18 |
| **Murine recombinant TNFα** | Peprotech | 315-01 |
| **Industrial Methylated Spirit** | PFM Medical | PRC/R/101 |
| **Xylene** | PFM Medical | PRC/R/201 |
| **Griess Assay Kit** | Promega | G2930 |
| **DNase I** | Qiagen | 79254 |
| **Fast-cycling PCR Kit** | Qiagen | 203745 |
| **OCT Embedding Compound** | Sakura Tissue-Tek | 4583 |
| **1-methyl tryptophan** | Sigma-Aldrich | 447439 |
| **Absolute ethanol** | Sigma-Aldrich | 459844 |
| **Ascorbic acid-2-phosphate** | Sigma-Aldrich | A8960 |
| **Bovine pancreatic trypsin** | Sigma-Aldrich | T1426 |
| **Bovine tracheal chondroitin sulphate** | Sigma-Aldrich | C9819 |
| **Bovine tracheal type II collagen** | Sigma-Aldrich | C1188 |
| **Concanavalin A** | Sigma-Aldrich | C5275 |

| Item | Supplier | Catalogue Number |
|---|---|---|
| **Crystal Violet** | Sigma-Aldrich | C3886 |
| **Dexamethasone** | Sigma-Aldrich | D4902 |
| **Dimethylmethylene blue (DMB)** | Sigma-Aldrich | 341088 |
| **EDTA** | Sigma-Aldrich | E6758 |
| **Fast Green Dye** | Sigma-Aldrich | F7252 |
| **Fibronectin** | Sigma-Aldrich | F0895 |
| **HEPES** | Sigma-Aldrich | H0887 |
| **Indomethacin** | Sigma-Aldrich | IL378 |
| **Insulin** | Sigma-Aldrich | I5500 |
| **Iodoacetamide** | Sigma-Aldrich | L1149 |
| **Ionomycin** | Sigma-Aldrich | I3909 |
| **L-NMMA** | Sigma-Aldrich | M7033 |
| **Oil Red O** | Sigma-Aldrich | O0625 |
| **p-nitrophenyl phosphate** | Sigma-Aldrich | 71768 |
| **Pepstatin A** | Sigma-Aldrich | P5318 |
| **Phorbol myristate acetate** | Sigma-Aldrich | P8139 |
| **Propidium Iodide** | Sigma-Aldrich | P4170 |
| **RBC lysis buffer** | Sigma-Aldrich | R7757 |
| **Safranin O solution** | Sigma-Aldrich | S2255 |
| **SB-3CT** | Sigma-Aldrich | S1326 |
| **SB431542** | Sigma-Aldrich | S4317 |
| **Sodium carbonate buffer** | Sigma-Aldrich | S7795 |
| **Sodium pyruvate** | Sigma-Aldrich | S8636 |
| **Toluidine blue** | Sigma-Aldrich | 89640 |
| **Trizma** | Sigma-Aldrich | T1503 |
| **Tween-20** | Sigma-Aldrich | P2287 |
| **Water** | Sigma-Aldrich | W3500 |
| **β-mercaptoethanol** | Sigma-Aldrich | M6250 |
| **SU5402** | Tocris | 3300 |
| **Antigen retrieval high pH buffer** | Vector Laboratories | H-3301 |
| **Caesin buffer** | Vector Laboratories | SP-5020 |
| **Collagenase** | Wako | 034-10533 |

### 2.15.4 Details of Consumables used in this Study

Table 2.8 | **List of general laboratory consumables used in this study.**

| Item | Supplier | Catalogue Number |
|---|---|---|
| **70µm cell strainer** | Corning | 352350 |
| **50µm cell strainer** | Partec | 04-004-2327 |
| **X-tra Adhesive Slides** | Leica | 38002032 |
| **Superfrost Slides** | Thermo Scientific | 4951PLUS4 |
| **Sterile FACS tubes** | BD Biosciences | 352063 |
| **FACS tubes** | BD Biosciences | 352002 |
| **Biofelt® PGA Scaffolds** | Biomedical Structures | http://www.bmsri.com/biofelt/ |
| **Immulon-2HB ELISA Plate** | Thermo Scientific | 10795026 |
| **384-well HB ELISA Plate** | Corning | 3700 |
| **MACS Separators** | Miltenyi Biotec | 130-042-302 |
| **LS Columns** | Miltenyi Biotec | 130-042-401 |
| **LD Columns** | Miltenyi Biotec | 130-042-901 |
| **MS Columns** | Miltenyi Biotec | 130-042-201 |
| **gentleMACS 'C' tubes** | Miltenyi Biotec | 130-096-334 |
| **RNeasy Mini Kit** | Qiagen | 74104 |
| **13mm false-bottom tubes** | Sarstedt | 60.617.010 |
| **96-well U-bottom plate** | Sarstedt | 83.18357.500 |
| **96-well flat-bottom plate** | Corning | 353072 |
| **48-well plate** | Corning | 3548 |
| **24-well plate** | Corning | 3526 |
| **12-well plate** | Corning | 3513 |
| **6-well plate** | Corning | 3516 |
| **T25 Culture flask** | Corning | 430639 |
| **T75 Culture flask** | Corning | 430641 |
| **T150 Culture flask** | Corning | 875823 |
| **T175 Culture flask** | Corning | 353112 |
| **15ml polypropylene tubes** | Corning | 430791 |
| **50ml polypropylene tubes** | Corning | 430829 |

# CHAPTER 3

# PHENOTYPE AND IMMUNOMODULATORY PROPERTIES OF PαS MSCs

## 3.1 Chapter Rationale and Aims

MSCs hold great promise for future use as a cellular therapy for regenerative or immunosuppressive indications. However, the heterogeneous populations of MSCs used in past studies have hampered efforts to reach agreement over potential mechanisms of action. Difficulties in isolating a purified population of mouse MSCs has prevented the field from studying the function of these cells in the absence of any contaminants (Anjos-Afonso and Bonnet, 2011). This has also prevented us from studying the biology of these cells using the large number of transgenic mouse models currently available. Thus, our current understanding of MSC biology and function is inferred from the study of *in vitro*-cultured human MSCs as they can easily be isolated using plastic-adherence. Despite the lack of comprehensive murine data, MSCs have been used in small-scale clinical trials in which many report marginal clinical improvements after infusion. There is a pressing need to fully understand the biology and function of these cells in the murine system to better design culture conditions to optimise the therapeutic potential of MSCs. These findings can then be translated towards the clinic to improve the efficacy of MSCs in patients.

Mouse MSC isolation methods have traditionally been hampered by persistence of contaminating cells (Phinney et al., 1999), slow-growing cells (Baddoo et al., 2003) and the lack of specific markers (Boxall and Jones, 2012). The recent publication of three prospective isolation methods (Pinho et al., 2013, Mendez-Ferrer et al., 2010, Morikawa et al., 2009) were the first to comprehensively describe markers of murine MSCs and test their function *in vivo* using traditional assays of stem cell function. However, the uptake of these new

methods by the wider scientific community has been slow. Reasons for this could be due to lack of access to a cell sorter and the more challenging nature of the protocols compared to the plastic-adherence approach. Importantly, the regenerative and immunomodulatory potential of prospectively-isolated mouse MSCs has not been studied previously, and it remains to be seen whether purified MSCs are as effective as their non-purified counterparts.

To meet these needs, I set out to prospectively isolate PDGFRα$^{+}$Sca-1$^{+}$ (PαS) MSCs and use these purified cells as a substrate for *in vitro* and *in vivo* studies on MSC biology in my thesis. PαS MSCs were chosen over their Nestin$^{+}$ counterparts because their isolation does not necessitate the use of a Nestin-GFP transgenic mouse, allowing isolation from a variety of mouse strains. This chapter focuses on the isolation, culture and phenotype of PαS MSCs. The specific aims for this chapter were to:

1. Reproducibly isolate PαS MSCs and successfully culture them *in vitro*
2. Characterise their grown, surface marker phenotype and tri-lineage differentiation in accordance with the ISCT criteria
3. Describe the immunosuppressive potential of PαS MSCs and depict the mechanism behind this effect
4. Examine the immunosuppressive potential of PαS MSCs from different mouse strains

## 3.2 Results

### 3.2.1 Isolation of PαS MSCs

Collagenase-digested compact bone was processed and stained with conjugated antibodies against CD45, Ter-119, PDGFRα and Sca-1 (Houlihan et al., 2012, Morikawa et al., 2009). PI was used to exclude non-viable cells from downstream analysis and increase the purity of our MSC cultures. $PI^{low}$ cells typically represented 80-85% of the total population (Figure 3.1A). Next, the haematopoietic cells ($CD45^{+}Ter\text{-}119^{+}$) were excluded by gating on PE-negative cells (<1% of viable cells; Figure 3.1B). This PE-negative fraction was then analysed for PDGFRα and Sca-1 expression, and the double-positive population was isolated using FACS (Figure 3.1C). PαS MSCs typically represented 10-15% of non-haematopoietic cells, or 0.05% of all BM cells. The isolation was successful on all occasions and I routinely achieved a purity of >95% and a yield approaching 5,000-8,000 PαS MSCs/mouse.

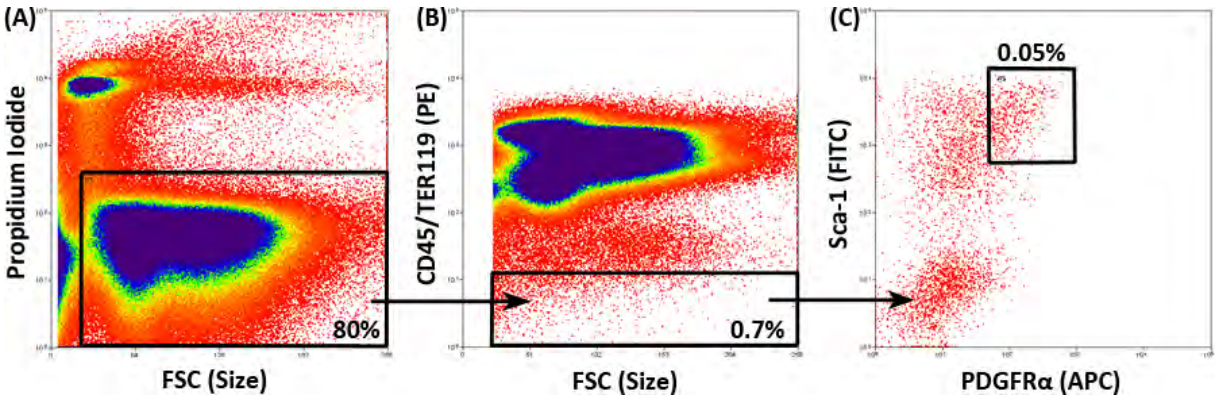


Figure 3.1 | **Representative FACS plots for PαS MSC isolation from C57BL/6 mice**. (A) A live cell gate is applied around $PI^{low}$ BM cells. (B) The non-haematopoietic fraction is then selected and (C) analysed for PDGFRα/Sca-1 expression. This double-positive population is then collected in SM for *in vitro* culture.

### 3.2.2 Morphology and CFU-F potential

Freshly isolated PαS MSCs were cultured in standard media (SM; α-MEM+10% FBS) on un-coated tissue culture plastic. They were able to adhere within 2 hours and displayed spindle-shaped morphology characteristic of stromal cells (Figure 3.2A). The media was replaced 24 hours after plating to remove any dead cells (due to the cell sorting procedure) from the culture. Thereafter, fresh media was added every 3 days to expand PαS MSCs.

To examine CFU-F potential, 2000 freshly isolated PαS MSCs were cultured in a 10cm$^2$ petri dish for 14 days. Samples were then fixed and stained with crystal violet to visualise separate colonies (Figure 3.2B). Colonies of MSCs with >50 cells were counted as CFU-Fs, which revealed approximately 30 colonies per dish, a CFU-F efficiency of 1 in every 66 PαS MSCs (Figure 3.2C).

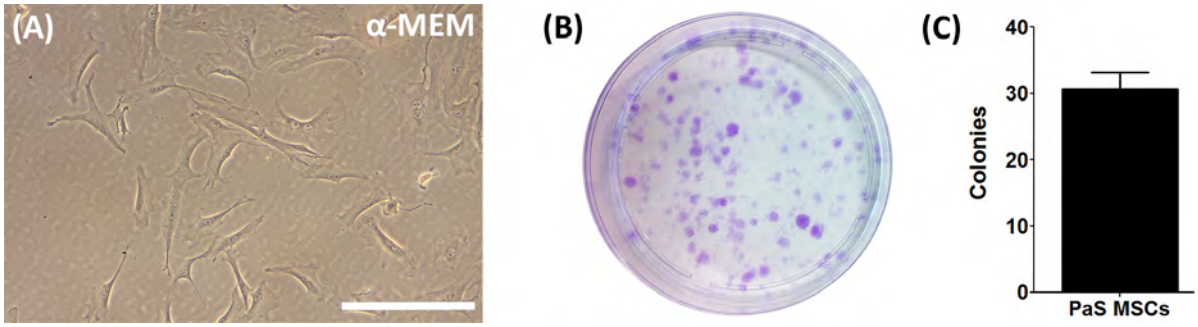


Figure 3.2 | **Morphology and CFU-F of PαS MSCs.** (A) PαS MSCs adopt a spindle-shaped morphology on tissue-culture plastic. Image taken at 100x magnification. Bar, 25µm. (B) Representative image of CFU-F potential of PαS MSCs. 10cm$^2$ petri dish stained with crystal violet showing colony formation. Image taken without magnification. (C) Quantification of total colony number (clusters >50 cells). Data shown as mean±SD, n=3 technical repeats.

### 3.2.3 Growth of PαS MSCs *in vitro*

The ability of MSCs to undergo serial passaging *in vitro* under standard culture conditions is one of the criteria used to define MSC populations (Dominici et al., 2006). 4000 freshly-isolated PαS MSCs were seeded in a 96-well plate and expanded at a 1:2 ratio over a 50 day period. The number of population doublings (PD; Figure 3.3A) and total cell number (Figure 3.3B) was recorded at different time points. A robust growth rate was observed, with an initial doubling time of 2-3 days. However, this increased to nearly 12-14 days near the end of the experiment as the growth rate of the cells slowed. Significant increases in cell number were also observed at days 30 and 50 compared to baseline (Day 0, $p \leq 0.001$). However, the rate of increase did slow down, suggesting a drop in proliferative capacity of PαS MSCs after extended *in vitro* culture.

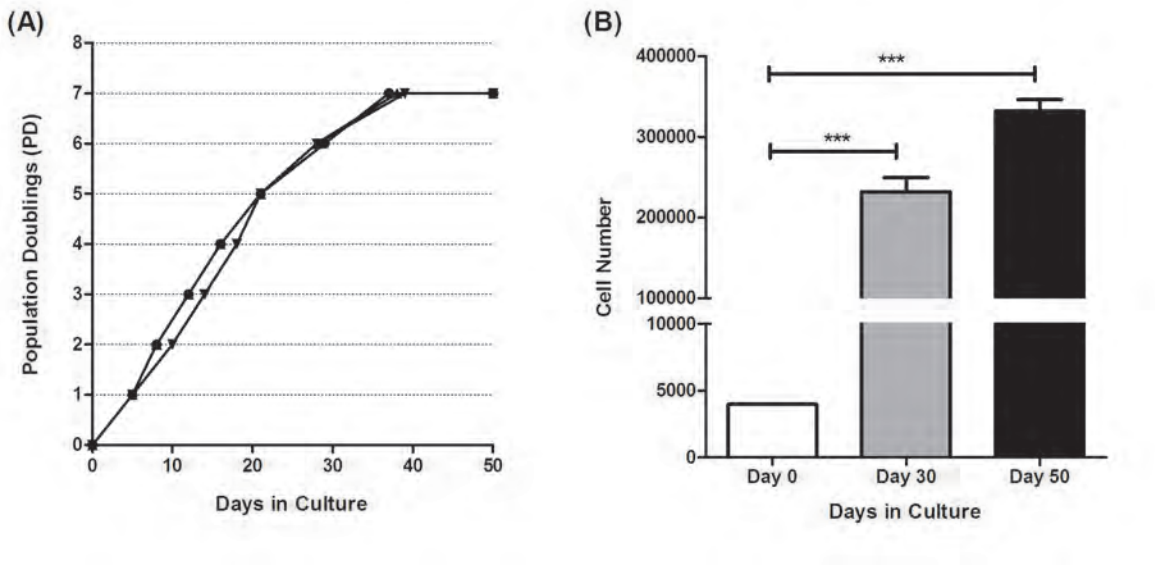


Figure 3.3 | **Growth of PαS MSCs over 50 days culture**. (A) Population doublings over 50 days. Each line represents an independent experiment on different cultures of PαS MSCs (n=3 biological repeats). (B) Cell counts at day 30 and 50 post seeding. Data shown as mean±SD, n=3 biological repeats. Statistical analysis performed using One-way ANOVA with Bonferroni's Correction.

### 3.2.4 Surface Marker Profile of PαS MSCs

The surface marker expression of P1 PαS MSCs was examined using flow cytometry. Propidium iodide was used to exclude dead cells were from analysis and the expression of characteristic MSC markers were examined alongside IMCs and unstained cells as controls. PαS MSCs were negative for haematopoietic and leukocytic markers CD45, Ter-119 and CD34. High levels of expression (>85% positive) were seen for the 'MSC markers' CD29, CD90, CD49e, Sca-1, CD44, CD105 and CD140a (Figure 3.4).

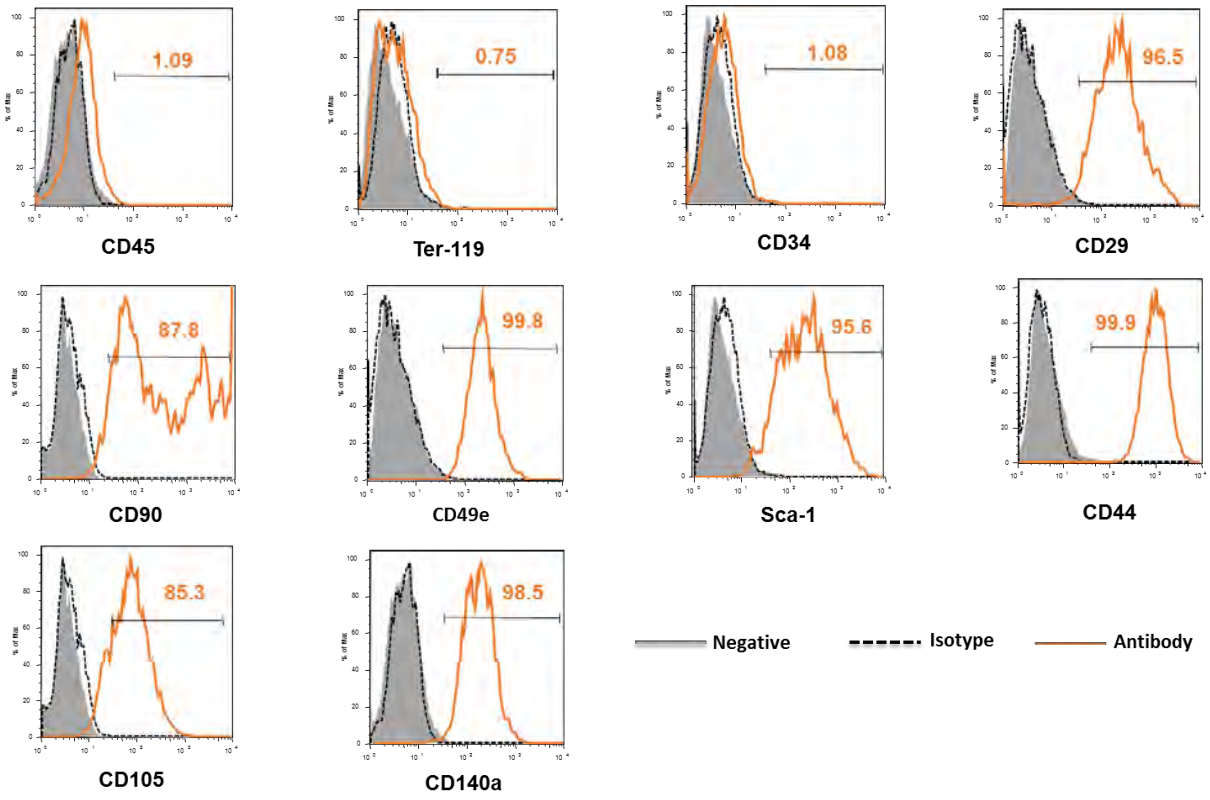


Figure 3.4 | **Cell surface phenotype of PαS MSCs**. Representative fluorescence histograms showing the surface marker expression of P1 PαS MSCs. PI was used to exclude dead cells from analysis. Unstained cells (grey bars) and IMC controls (hatched lines) are included for comparison.

### 3.2.5 Tri-lineage differentiation of PαS MSCs

Osteogenic differentiation samples were fixed and stained using Alizarin red, an organic dye that stains calcium deposits. PαS MSCs readily underwent osteogenic differentiation (Figure 3.5A) and produced approximately 600µM calcium (Figure 3.5B). Adipogenic differentiation was visualised with oil red O, which stains lipids in a red colour. Patches of oil red O-positive adipocytes could be found in samples after staining (Figure 3.5C). Chondrogenic differentiation was induced by micromass pellet culture in serum-free differentiation medium. Cartilage pellets were embedded, sectioned and stained with toluidine blue, which stains proteoglycan deposits in a purple colour (Figure 3.5D).

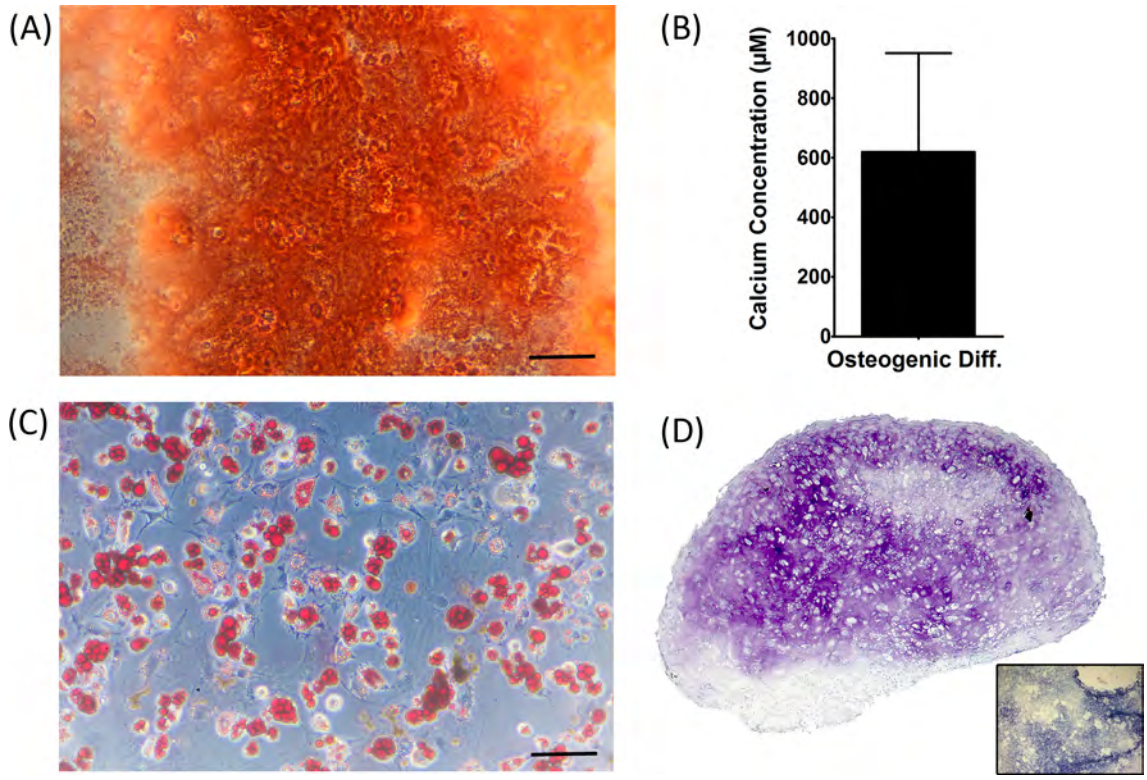


Figure 3.5 | **Tri-lineage differentiation of PαS MSCs.** (A) Osteogenic differentiation visualised by alizarin red stain. (B) Quantification of calcium deposition. Data shown as mean±SD, n=6 technical repeats. (C) Adipogenic differentiation visualised by oil red O staining. Bar, 25µm. (D) Chondrogenic differentiation visualised by toluidine blue stain. Insert shows negative control.

### 3.2.6 Modulation of T cell proliferation

The immunosuppressive phenotype of PαS MSCs has not been reported in literature. To examine the effect of MSC co-culture on T cell proliferation, graded numbers of P3 PαS MSCs were cultured alongside $CD4^{+}CD25^{-}$ naïve T lymphocytes that were stimulated with anti-CD3e antibody (binds to T cell receptor [TCR], provides primary signal) and $CD19^{+}$ B cells (co-stimulation via CD86-CD28 interaction). After 72 hours' co-culture, the total number of $CD4^{+}$ cells was quantified using flow cytometry (Figure 3.6). The results are expressed as a percentage±SD to the no-MSC control, which have been normalised to 100%. Significant ($p<0.001$) reductions in T cell proliferation can be seen across all MSC ratio's tested, achieving 80% suppression at the 1:16 ratio. The immunosuppressive effect plateaus thereafter, with increasing numbers of MSCs producing smaller reductions in T cell numbers.

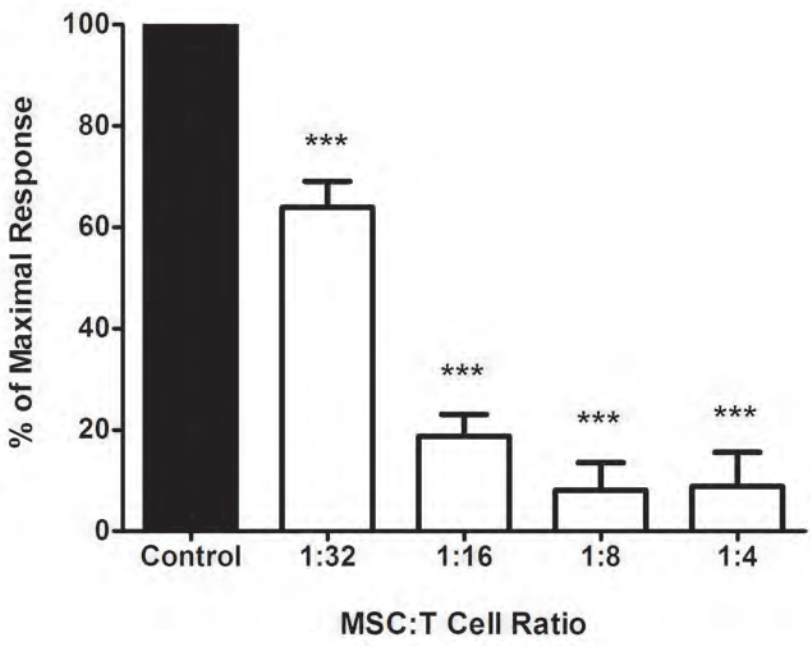


Figure 3.6 | **Immunosuppression by Balb/c PαS MSCs**. PαS cells at P3 (n=3 biological repeats) were co-cultured with activated CD4 T cells for 72 hours. Samples were then analysed by flow cytometry and total CD4 numbers counted and expressed as a percentage to the no-MSC control. Data shown as mean±SD. Statistical analysis performed using One-way ANOVA with Bonferroni's Correction. P-values calculated vs. no-MSC controls.

### 3.2.7 Mechanistic studies of Balb/c PαS MSC Immunosuppression

A variety of small molecule inhibitors of previously reported mechanisms were tested in the T cell proliferation assay to determine how Balb/c PαS MSCs were exerting their immunosuppressive effect. Cultures were maintained for 72 hours and analysed using flow cytometry to see whether reversal of the suppressive phenotype could be observed (summarised in Table 3.1).

Table 3.1 | **Details of inhibitors used to study immunosuppressive mechanisms.**

| Mechanism | Inhibitor/Method | Reference | Reversal of suppression seen? |
|---|---|---|---|
| **Prostaglandin E2** | Indomethacin | Nemeth et al. (2009) | × |
| **MMP2/MMP9** | SB-3CT | Ding et al. (2009) | × |
| **IDO** | 1-MT | Ren et al. (2009) | × |
| **'Indirect' effects** | Removal of B cells | n/a | × |
| **Nitric Oxide** | L-NMMA | Ren et al. (2008) | ✓ |

Indomethacin is a non-steroidal anti-inflammatory that works by inhibiting the cyclooxygenase enzymes responsible for prostaglandin E2 synthesis (Mitchell et al., 1993). Inhibition of $PGE_2$ release has been shown to reverse the suppressive phenotype of MSC cultures (Nemeth et al., 2009, Spaggiari et al., 2008, Rasmusson et al., 2005). The addition of indomethacin failed to prevent PαS MSC-mediated immunosuppression (Figure 3.7A). Significant drops in T cell numbers were seen across all ratios tested, although some variation was seen in the 1:32 and 1:16 samples. This suggests that $PGE_2$ secretion is not responsible for the immunosuppressive effect seen in this assay.

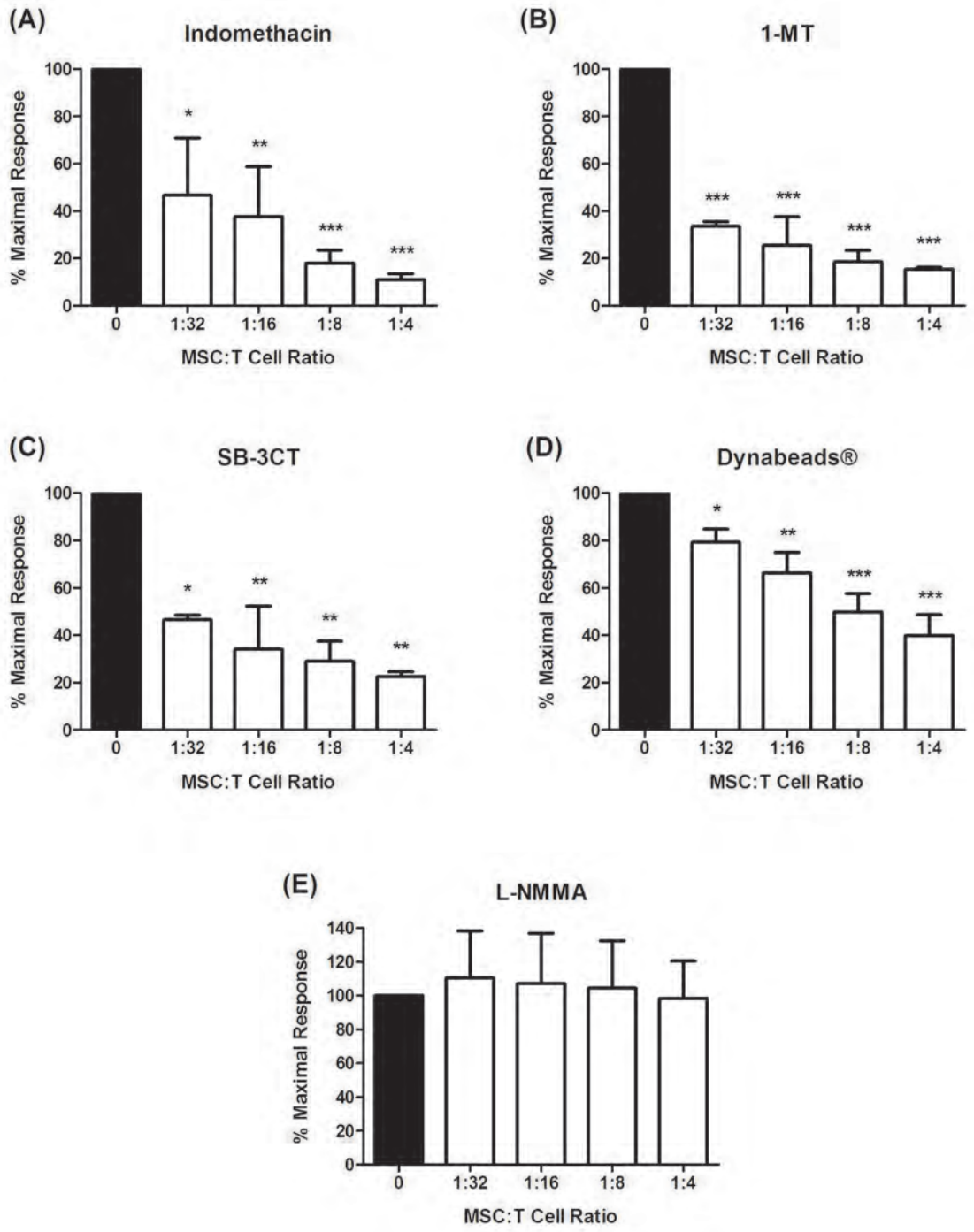


Figure 3.7 | **Mechanism behind Balb/c PαS MSC Immunosuppression**. Graded numbers of P3 PαS MSCs isolated from Balb/c mice were co-cultured with activated T cells in the presence of (A) Indomethacin (n=3), (B) 1-MT (n=2), (C) SB-3CT (n=2), (D) Dynabeads® (n=3) and (E) L-NMMA (n=3). Total CD4 T cell numbers were quantified and expressed as a percentage to the no-MSC control. Data shown as mean±SD. Statistical analysis performed using One-way ANOVA with Bonferroni's Multiple Comparison Test. P-values calculated vs. no-MSC controls. In all experiments, n is indicative of biological repeats using different cultures of PαS MSCs.

IDO, the rate limiting enzyme responsible for tryptophan catabolism, has also been cited as a potential mechanism of action (Meisel et al., 2004). 1-methyl tryptophan (1-MT) is a competitive inhibitor of IDO and prevents the breakdown of tryptophan from the local microenvironment. Reversal of immunosuppression was not seen when 1-MT was added to the T cell proliferation assay (Figure 3.7B). This fits the current hypothesis that human MSCs, not murine, primarily mediate immunosuppression via IDO secretion (Ren et al., 2009).

SB-3CT is a small molecule competitive inhibitor of metalloproteinases (MMP) 2 and 9 (Kleifeld et al., 2001). MMP2/MMP9 secretion by Balb/c MSCs has previously been shown to prevent CD4 T cell activation by cleavage of CD25 from its surface (Ding et al., 2009). In our hands, SB-3CT had no effect, and PαS MSCs were still able to elicit significant reductions in T cell number across all ratios tested (Figure 3.7C).

Removal of B cells from the proliferation assay was also examined to identify any potential indirect effects of PαS MSCs on T cell proliferation. CD3/CD28 Dynabeads® were used in place of B cells to provide the signals necessary for T cell activation. Dynabeads® were added at a 1:1 ratio to T cells and graded numbers of MSCs were added as before. A weaker immunosuppressive response was seen with Dynabeads® stimulation, however PαS MSCs were still able to cause significant reductions across all ratio's tested (Figure 3.7D). This reduced response could be due to the 'artificially-enhanced' activating signals provided by Dynabeads® over the more physiological signals produced by B cells.

The final mechanism examined was the inhibition of NO release using $N^G$-Monomethyl-L-arginine (L-NMMA), a competitive inhibitor of the inducible NO synthase (iNOS) enzymes. A profound reversal of suppression was seen when L-NMMA was added to the co-culture (Figure 3.7E). Lymphocyte proliferation returned to normal levels, and there was no difference in T cell numbers in the MSC-treated samples compared to the no-MSC control. This suggests that PαS MSCs primarily use NO release to prevent T cell suppression, backing up previous findings by Ren et al. (2008) and Sato et al. (2007).

### 3.2.8 Effect of iNOS-/- PαS MSCs on T cell proliferation

To test the effect of NO release in greater detail, I isolated MSCs from iNOS knockout mice that were bred on a Balb/c background. These mice have a targeted mutation on the Nos2 gene (iNOS) preventing them from synthesising NO in response to inflammatory stimuli. The genotype of iNOS-/- mice was confirmed using conventional PCR, with homozygotes producing a band approximately 275bp in length (Figure 3.8A). Overnight stimulation in IFNγ and TNFα did not cause iNOS-/- PαS MSCs to secrete any NO, as measured by the Griess Assay (0.2±0.09µM nitrite; Figure 3.8B). By comparison, WT MSCs isolated from Balb/c mice secreted 71.2±3.8µM nitrite over the same time period. iNOS-/- PαS MSCs also failed to prevent T cell proliferation in the *in vitro* suppression assay (Figure 3.8C). Significantly higher T cell counts were recorded in iNOS-/- samples compared to WT samples across all ratios. These findings provide further evidence for NO secretion as the exclusive mechanism behind the immunosuppressive phenotype of Balb/c-derived PαS MSCs on $CD4^+$ T cell populations.

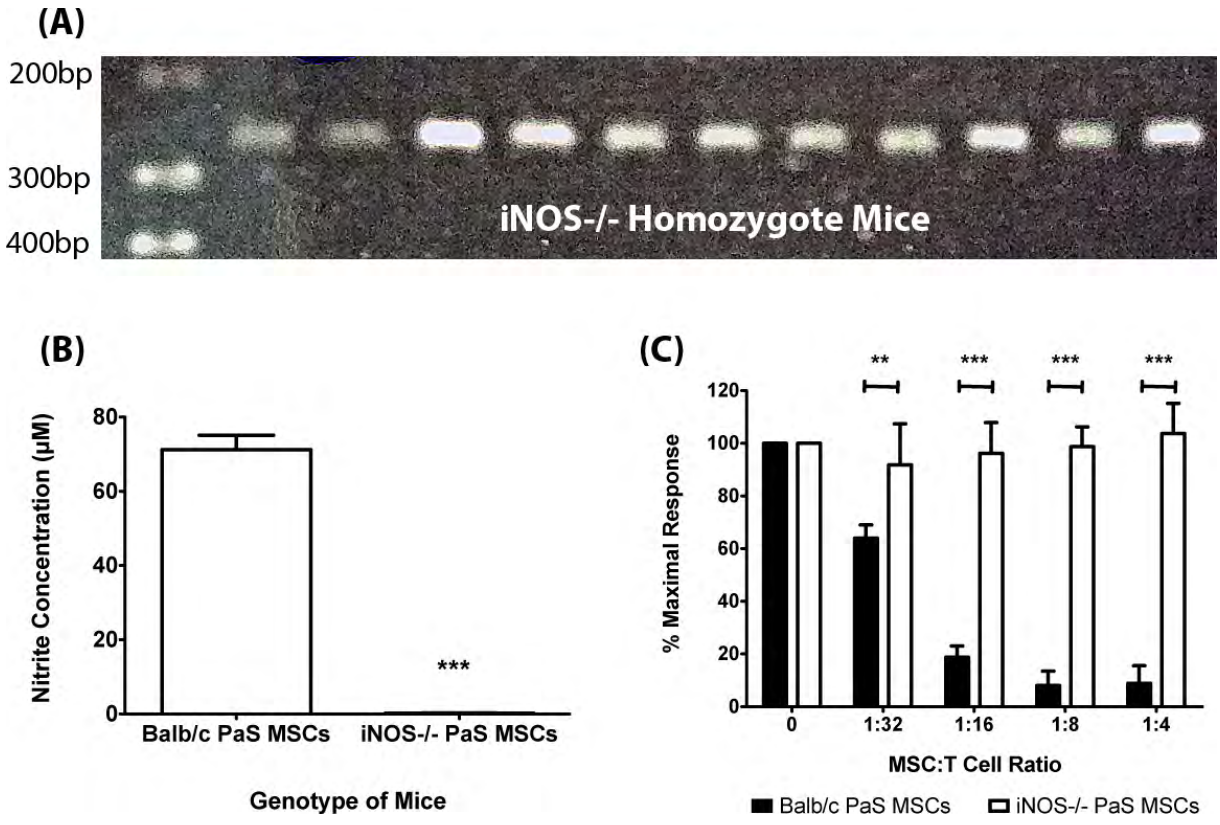


Figure 3.8 | **iNOS-/- PαS MSCs fail to suppress T cell proliferation**. (A) The genotype of iNOS-/- mice was confirmed using conventional PCR. Homozygotes produced a band 275bp in length. (B) Total levels of Nitrite was quantified using the Griess Assay. iNOS-/- PαS MSCs failed to produce NO after overnight stimulation in TNFα & IFNγ (n=3 per condition, $p<0.001$, Student's T test). (C) Graded numbers of iNOS-/- PαS MSCs (n=3) or Balb/c PαS MSCs (n=3) were co-cultured with CD4 T cells for 72 hours. iNOS-/- MSCs failed to prevent T cell proliferation and significantly higher CD4 T cell number was recorded across all ratios. Data shown as mean±SD. Statistical analysis performed using One-way ANOVA with Bonferroni's Multiple Comparison Test. In all experiments, n is indicative of technical repeats using the same culture of PαS MSCs.

### 3.2.9 C57BL/6-derived PαS MSCs fail to suppress T cell proliferation

The work presented above used MSCs isolated from wild-type Balb/c mice. To study possible strain-specific differences in immunosuppression, we then examined the potential of PαS MSCs derived from C57BL/6 mice, the most commonly used wild-type strain in biomedical research (Yoshiki and Moriwaki, 2006). Graded numbers of PαS MSCs from C57BL/6 mice were added to the T cell proliferation assay and cultured as before for 72 hours. However, C57BL/6-derived MSCs failed to suppress T cell proliferation across all ratios tested (Figure 3.9). A pro-proliferative effect was seen at higher MSC doses compared to no-MSC controls (118%±12% at 1:4 ratio). This experiment was repeated several times (n=6) with the same result, suggesting that this 'purified' assay of T cell proliferation was not ideal to study the immunosuppressive phenotype of C57BL/6-derived PαS MSCs.

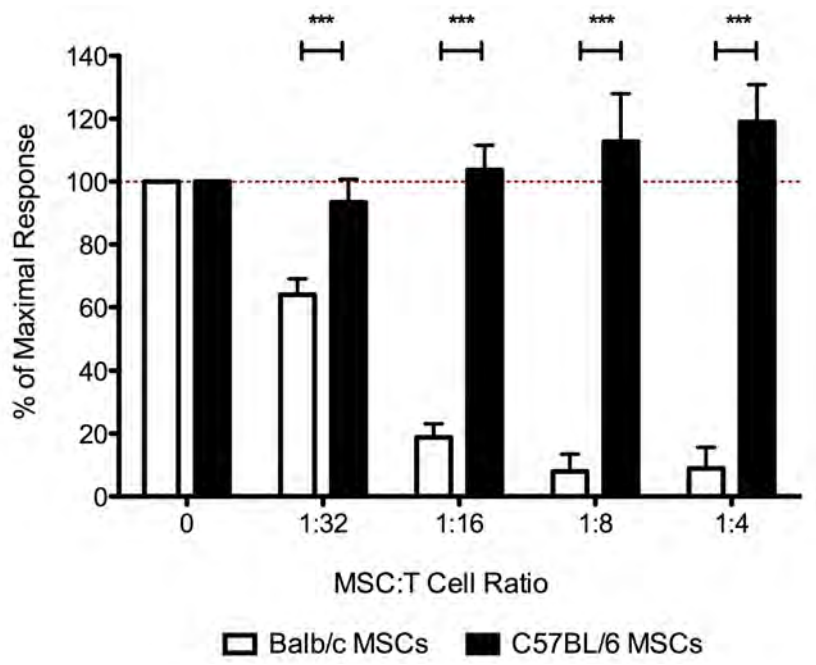


Figure 3.9 | **C57BL/6-derived MSCs fail to prevent T cell proliferation.** Graded numbers of Balb/c (n=3) or C57BL/6 MSCs (n=3) were co-cultured with activated T cells for 72 hours. Balb/c PαS MSCs were able to suppress T cell proliferation, while C57BL/6 MSCs failed in this assay. Data shown as mean±SD. Statistical analysis performed using One-way ANOVA with Bonferroni's Multiple Comparison Test. In all experiments, n is indicative of biological repeats using different cultures of PαS MSCs.

### 3.2.10 Optimising the 'Splenocyte reaction'

Previous mouse literature has identified differences in the biology of MSCs isolated from different mouse strains, although their investigations were limited to the growth and differentiation of these cells (Cunha et al., 2013, Peister et al., 2004, Phinney et al., 1999). One study looked at the immunosuppressive properties of adipose-derived MSC conditioned media from C57BL/6 and Balb/c mice and identified Balb/c mice to be more suppressive (Hashemi et al., 2013). However, no study has performed a comparative analysis of the immunosuppressive mechanism of Balb/c and C57BL/6 strains using a purified population of BM-derived MSCs.

We hypothesised that C57BL/6 MSCs may indirectly suppress lymphocyte proliferation by acting at the antigen presentation stage or on another cell (e.g. monocyte/macrophage). Our current T cell proliferation assay bypassed the antigen presentation stage via the use of antibodies or beads that bind directly to the TCR. Additionally, no supporting cells (except B cells) were present in the mixture. To test this hypothesis, I developed a new assay that used 'bulk' splenocytes instead of purified T and B cells (termed the '*Splenocyte reaction*'). Mouse spleen contains a variety of cell types, including T cells, B cells, dendritic cells, monocytes/macrophages and stromal cells (Hey and O'Neill, 2012). I then tested the effect of various stimulatory reagents in the splenocyte reaction to achieve a strong and reproducible proliferative effect on the T cell population.

### 3.2.10.1 Concanavalin A Stimulation

The plant lectin Concanavalin A (ConA) is used to trigger T cell proliferation by binding directly to the TCR (Palacios, 1982). A range of ConA concentrations (1µg/ml to 100µg/ml) was used in splenocyte cultures and incubated for 72 hours. Cultures were stained with the membrane dye cell trace violet (CTV) to assess proliferation and total numbers of CD4 and CD8 T lymphocytes was then quantified using flow cytometry. Surprisingly, all ConA concentrations tested failed to induce CD4 T cell proliferation in this assay (Figure 3.10A). Some cell division was seen with 5µg/ml ConA in the CD8 T cell samples (Figure 3.10B), but the majority of cells remained undivided. Higher doses of ConA (>20µg/ml) could not be tested on CD8 T cell samples due to cell death at higher concentrations.

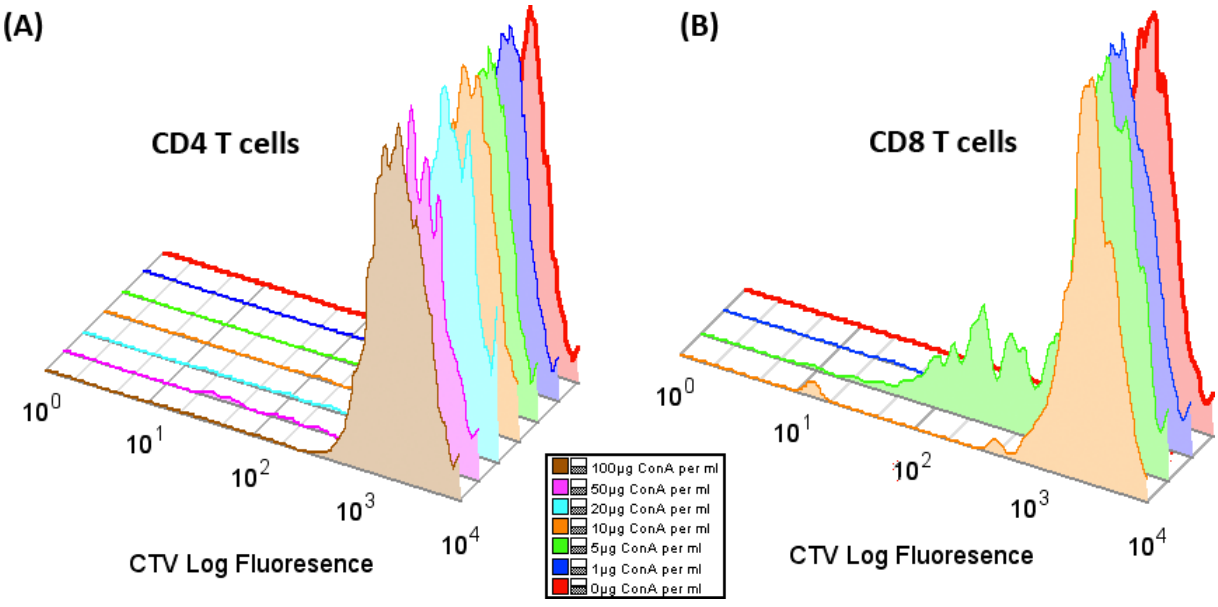


Figure 3.10 | **Stimulation of splenocyte cultures with ConA**. Proliferation of CD4 (A) and CD8 T cells (B) in splenocyte cultures after incubation with different concentrations of ConA. Representative fluorescence histograms of two independent repeats shown.

### 3.2.10.2 CD3/CD28 Dynabeads® Stimulation

CD3/CD28 Dynabeads® bind directly to the TCR and CD28 to provide both the primary and secondary signals required for T cell proliferation. A range of concentrations was used to induce proliferation in our splenocyte cultures (Table 3.2). Low doses of Dynabeads® (<15,000 beads per well) failed to elicit a proliferative response in both the CD4 and CD8 populations (Figure 3.11A and B). Medium doses of Dynabeads® (100,000 to 300,000 beads per well) were able to induce a strong CD8 response (≈80% proliferated) but less than half the CD4 population responded. High doses of beads (>400,000 beads per well) were required to generate a strong response in both lymphocyte populations (Figure 3.11C and D). As such, Dynabeads® stimulation was, in our hands, a cost-ineffective method of inducing T cell proliferation in the splenocyte reaction and alternative approaches involving TCR-specific peptide sequences were tested.

Table 3.2 | **Percentage of T cell proliferation after Dynabeads® stimulation.**

| Number of Beads/well | Percentage of $CD4^+$ T Cells that proliferated (% ) | Percentage of $CD8^+$ T Cells that proliferated (% ) |
|---|---|---|
| **0** | 0.18 | 0.67 |
| **1875** | 0.69 | 1.00 |
| **3750** | 0.67 | 1.81 |
| **7500** | 0.92 | 1.79 |
| **15,000** | 0.54 | 1.83 |
| **30,000** | 2.55 | 35.4 |
| **60,000** | 11.9 | 77.5 |
| **100,000** | 24.2 | 51.5 |
| **200,000** | 39.2 | 73.2 |
| **300,000** | 49.9 | 81.1 |
| **400,000** | 54.4 | 85.1 |
| **500,000** | 60.3 | 89.5 |

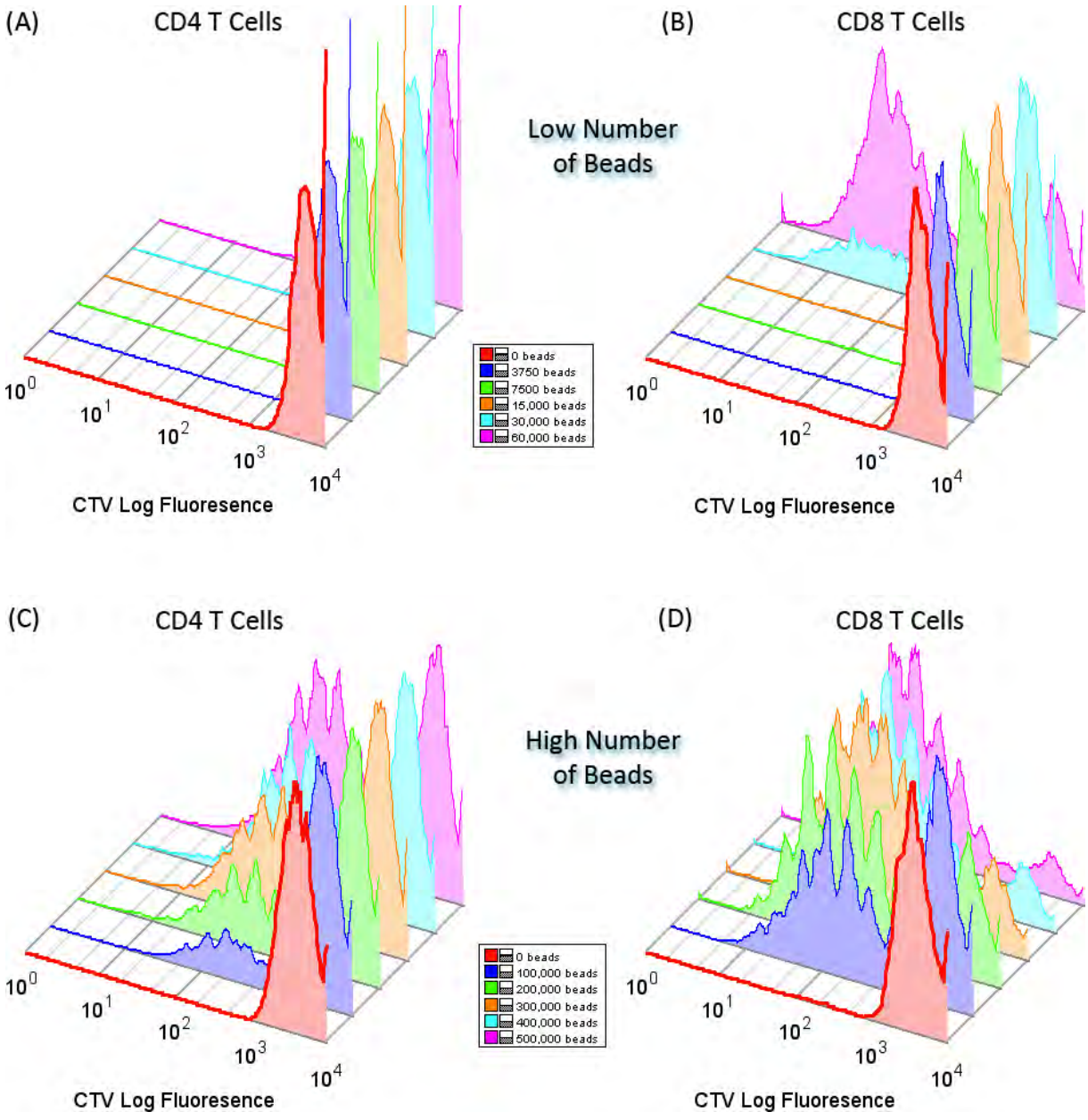


Figure 3.11 | **Stimulation of splenocyte cultures with Dynabeads®**. Proliferation of CD4 (A and C) and CD8 (B and D) T cell populations with low (upper row) and high (lower row) numbers of Dynabeads® per well. Cultures were maintained for 72 hours before analysis. N=1 biological repeat per condition.

### 3.2.10.3 Ovalbumin peptide stimulation

CD8 T cells from OT-1 transgenic mice have a TCR that is specific for the ovalbumin (OVA) peptide sequence SIINFEKL when presented in a MHC class I context (Wright et al., 2005, Clarke et al., 2000). The addition of OVA peptide to OT-1 splenocyte cultures causes expansion of antigen-specific CD8 T cells in a physiological manner. Unlike ConA and CD3/CD28 Dynabeads®, which can bind directly to T cells to cause activation, OVA peptide needs to be processed and presented alongside a co-stimulatory signal to cause activation and proliferation of CD8 lymphocytes. Additionally, stimulating OT-1 splenocytes with OVA peptide is a good *in vitro* correlate of the OVA-Bil mouse model (Chapter 6) in which adoptive transfer of OT-1 cells causes their migration to the liver (where OVA is expressed) and induction of inflammatory liver injury (Buxbaum et al., 2006).

The dose of OVA peptide was first optimised for this reaction. Past literature recommends concentrations ranging from 10µg/ml (Li et al., 2009, Rafiq et al., 2002) to 50µg/ml (Huang et al., 2010, Bedoret et al., 2009). Both doses of OVA peptide were incubated with OT-1 splenocytes for 72 hours and the percentage of proliferated CD8 T cells was quantified using flow cytometry. Unstimulated cultures failed to proliferate (Figure 3.12A), with 0.32±0.1% of CD8 cells losing CTV fluorescence (Figure 3.12D). Cultures stimulated with 10µg/ml and 50µg/ml had significantly more CD8 T cell proliferation compared to controls, but there was no significant difference between the doses (32.3±2.1% vs. 32.0±3%; Figure 3.12B, C, D). Therefore, 10µg/ml OVA peptide dose was chosen for future experiments.

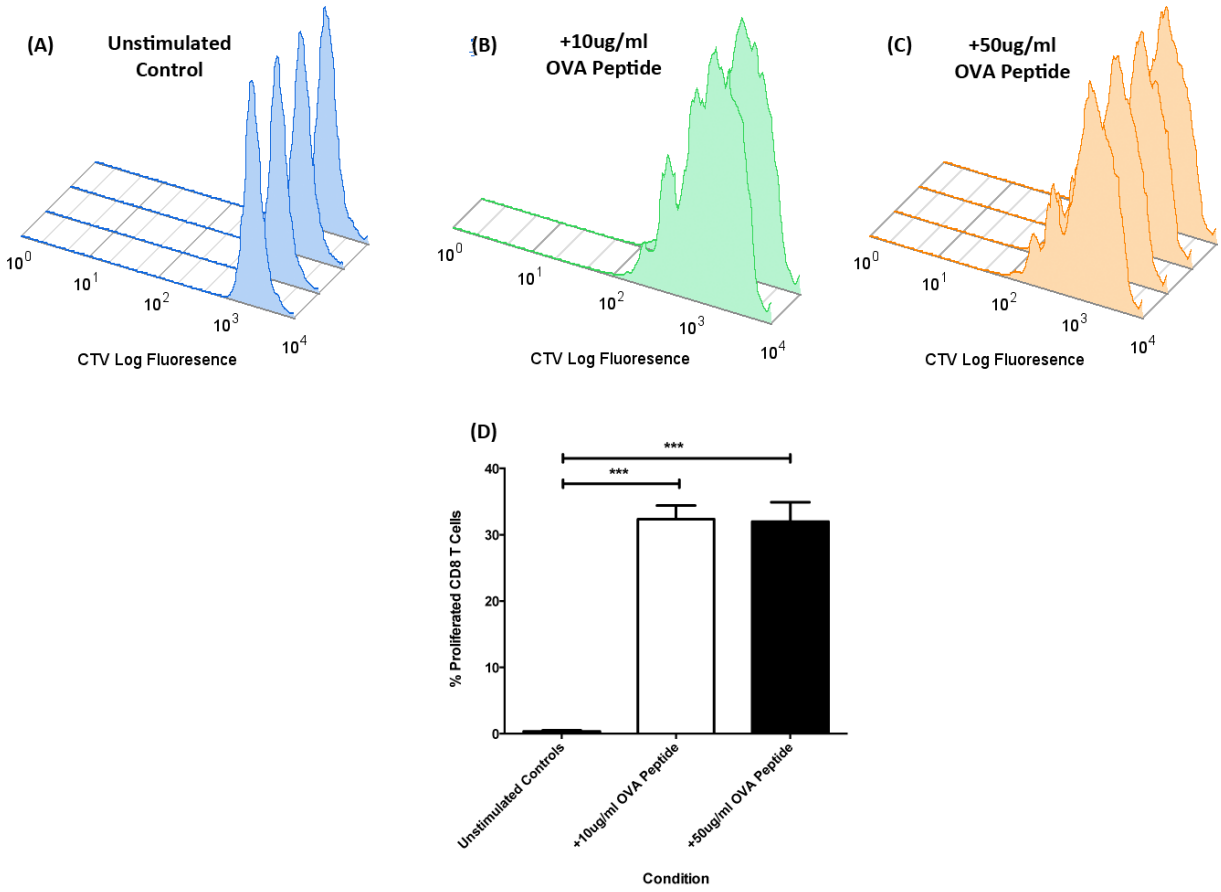


Figure 3.12 | **Optimisation of OVA peptide dose with OT-1 splenocytes**. CTV fluorescence histograms of CD8 T cells in OT-1 splenocyte cultures supplemented with (A) no OVA peptide (n=4), (B) 10µg/ml OVA peptide (n=2), and (C) 50µg/ml OVA peptide (n=4). (D) Quantification of CD8 T cell proliferation. Data shown as mean±SD. Statistical analysis performed using One-way ANOVA with Bonferroni's Multiple Comparison Test. In all experiments, n is indicative of technical repeats using the same culture of PαS MSCs.

I then optimised the culture time to achieve maximal CD8 T cell proliferation. As the OVA peptide needs to be processed and presented, there will be a lag phase before T cell proliferation. For example, co-culture with Dynabeads® for 72 hours caused a proliferative response in >90% of CD8 T cells (Figure 3.11D), while <35% divided when co-cultured with OVA peptide for the same time period (Figure 3.12D). The effect of 10µg/ml OVA peptide stimulation for 3, 4 and 6 days culture was examined. Significant increases in CD8 T cell proliferation were observed at days 4 and 6 compared to day 3 cultures (Figure 3.13).

However, there was no significant difference between the CD8 T cell proliferation seen at day 4 (93.6±0.7%) compared to day 6 (94.4±1.1%). Flow cytometry histograms for all time-points alongside their matched controls are displayed in Figure 3.14. As such, 4-day cultures supplemented with 10µg/ml OVA peptide was used to stimulate OT-1 CD8 T cell proliferation and to examine the effect of C57BL/6-derived PαS MSC co-culture.

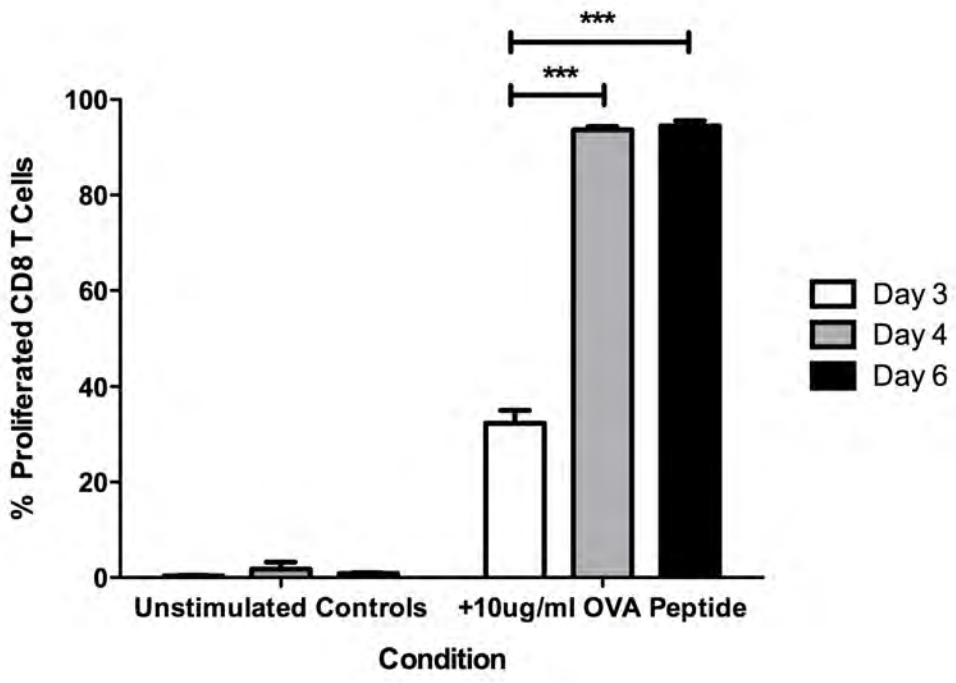


Figure 3.13 | **Optimisation of overall culture period with OT-1 splenocytes**. OT-1 cells were cultured unstimulated or stimulated with 10µg/ml OVA peptide for three (n=5), four (n=5), or six (n=6) days. The percentage of proliferated CD8 T cells was then quantified using flow cytometry based on CTV fluorescence. Data shown as mean±SD. Statistical analysis performed using One-way ANOVA with Bonferroni's Multiple Comparison Test. In all experiments, n is indicative of technical repeats using the same culture of PαS MSCs.

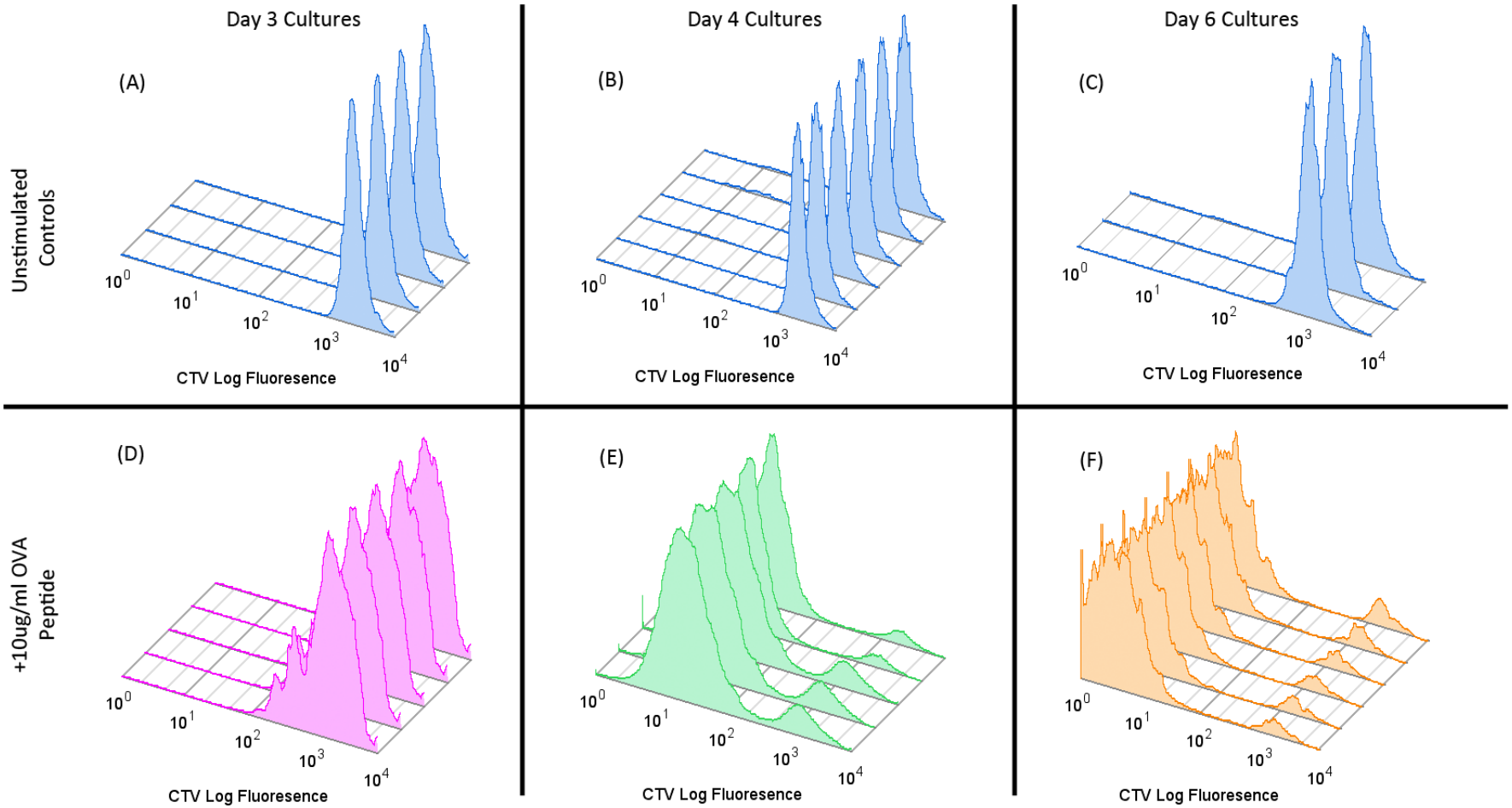


Figure 3.14 | **CTV fluorescence histograms of OT-1 CD8 T cells cultured for different periods of time**. No proliferation was observed in unstimulated control cultures at days three (A; n=4), four (B; n=6), and six (C; n=3). Limited cell division was seen in stimulated cultures at day three (D; n=5), but over 90% CD8 T cell proliferation was seen at day 4 (E; n=5) and 6 (F; n=6). In all experiments, n is indicative of technical repeats using the same culture of PαS MSCs.

### 3.2.11 C57BL/6-derived PαS MSCs in the 'Splenocyte Reaction'

The immunosuppressive properties of C57BL/6-derived PαS MSCs were tested in the newly optimised splenocyte reaction. P4 MSCs were added 24 hours after seeding OT-1 splenocytes with OVA peptide to ensure an inflammatory microenvironment (Figure 3.15A). Graded numbers of MSCs were added and cultured for a further 72 hours before quantification of total CD8 T cell number by flow cytometry. Preliminary findings (n=1) indicate that there was a dose-dependent reduction in the total numbers of viable CD8 lymphocytes after MSC co-culture (Figure 3.15B). Intracellular straining also revealed reductions in IFNγ production of CD8 T cells after re-stimulation with PMA and INO (Figure 3.15C). Although there was a reduction in total CD8 T cell numbers after PαS MSC co-culture, the cells that remained alive were still proliferating (Figure 3.15D). CTV fluorescence histograms showing CD8 T cell proliferation can be seen in Figure 3.15E, F and G. These results suggest that C57BL/6-derived PαS MSCs can prevent T cell proliferation, but work via a distinct mechanism to Balb/c-derived MSCs. Future work should repeat this experiment to ensure reproducibility and then attempt to elucidate the mechanism via the use of inhibitors.

Figure 3.15 (following page) | **C57BL/6-derived PαS MSCs in the splenocyte reaction**. (A) Time course of experiment. P4 PαS MSCs were added 24 hours after OT-1 splenocytes and OVA peptide were seeded. Cultures were maintained for an additional 72 hours before analysis. (B) Total viable CD8+ T cell number was quantified using flow cytometry. (C) Cultures were re-stimulated with PMA and INO for 4 hours before intracellular staining and quantification of total numbers of IFNγ+ CD8 cells using flow cytometry. (D) The percentage of proliferated CD8 T cells was quantified using flow cytometry based on CTV fluorescence. All data shown as mean±SD. (E,F,G) CTV histograms of CD8 T cells from unstimulated (E; n=3), 10μg/ml OVA peptide stimulated (F; n=3) and PαS MSC-supplemented cultures (G; n=1 per dose).

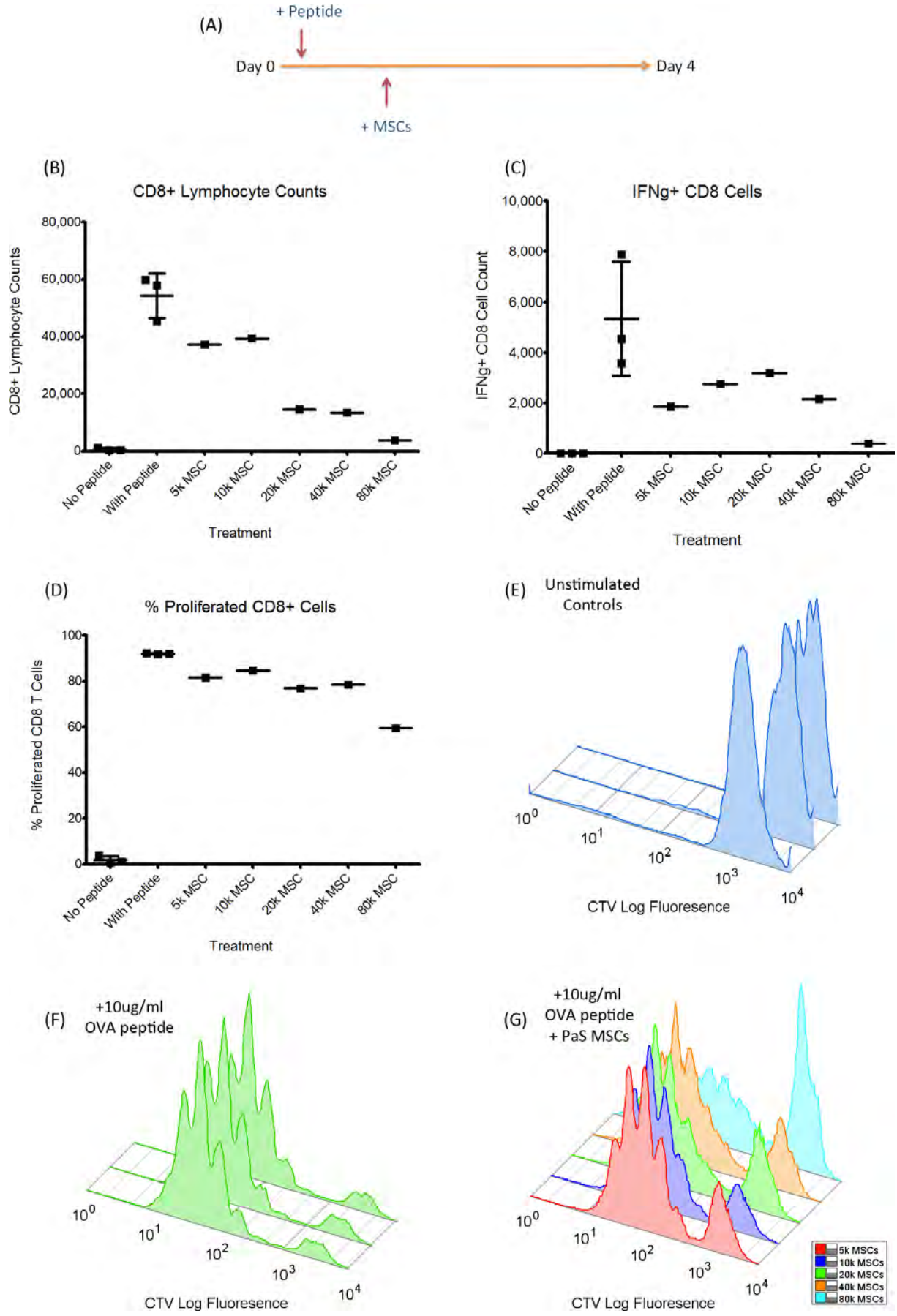
(A)
+ Peptide
Day 0
Day 4
+ MSCs
(B)
CD8+ Lymphocyte Counts
CD8+ Lymphocyte Counts
80,000
60,000
40,000
20,000
0
No Peptide
With Peptide
5k MSC
10k MSC
20k MSC
40k MSC
80k MSC
Treatment
(C)
IFNg+ CD8 Cells
IFNg+ CD8 Cell Count
10,000
8,000
6,000
4,000
2,000
0
No Peptide
With Peptide
5k MSC
10k MSC
20k MSC
40k MSC
80k MSC
Treatment
(D)
% Proliferated CD8+ Cells
% Proliferated CD8 T Cells
100
80
60
40
20
0
No Peptide
With Peptide
5k MSC
10k MSC
20k MSC
40k MSC
80k MSC
Treatment
(E)
Unstimulated
Controls
$10^0$
$10^1$
$10^2$
$10^3$
$10^4$
CTV Log Fluoresence
(F)
+10ug/ml
OVA peptide
$10^0$
$10^1$
$10^2$
$10^3$
$10^4$
CTV Log Fluoresence
(G)
+10ug/ml
OVA peptide
+ PaS MSCs
$10^0$
$10^1$
$10^2$
$10^3$
$10^4$
CTV Log Fluoresence
5k MSCs
10k MSCs
20k MSCs
40k MSCs
80k MSCs

## 3.3 Discussion

### 3.3.1 Chapter Summary

PαS MSCs were successfully isolated and cultured according to previously published protocols (Houlihan et al., 2012). These cells had characteristic spindle-shaped morphology, were able to form CFU-F and undergo tri-lineage differentiation into bone, fat and cartilage. PαS MSCs were also able to be expanded in standard culture conditions and expressed characteristic MSC markers, thereby meeting the ISCT criteria for MSCs (Dominici et al., 2006). The immunosuppressive phenotype of PαS MSCs have also been described for the first time, with different wild type mouse strains utilising distinct mechanisms to suppress T cell proliferation. Balb/c-derived PαS MSCs secreted NO to inhibit CD4 lymphocytes that were stimulated with anti-CD3e antibody and CD19 B cells. C57BL/6-derived PαS MSCs failed to suppress in the same assay, and required the development of a more complex *in vitro* system involving the use of TCR transgenic OT-1 mice. Preliminary results show reduction in CD8 T cell numbers after co-culture with C57BL/6-PαS MSCs in the splenocyte reaction, although more work is required to elucidate the mechanism behind this.

### 3.3.2 Phenotype of PαS MSCs

Protocols for the prospective isolation of murine MSCs represent a major advance in the field. PαS MSC yields achieved from C57BL/6 and Balb/c mice were similar in number to the ones reported by Morikawa et al. (2009). Approximately 5000 to 8000 PαS MSCs were isolated per mouse, and the flow cytometry plots looked similar to the original study. All

cells were fibroblastic in morphology, and cell surface staining revealed <1% positivity for haematopoietic or leukocytic markers in PαS cultures after one passage. This compares favourably with older protocols in which leukocytic cells persisted in culture for several weeks, even after serial passaging (Meirelles Lda and Nardi, 2003, Phinney et al., 1999). Population doubling times for PαS cells at early passage was approximately 55 hours, which is similar to the 50.6 hours reported by Morikawa and colleagues. Interestingly, we only observed a CFU-F forming efficiency of 1 in every 66 PαS MSCs, which is lower than the 1 in 50 reported by Morikawa et al. (2009). As CFU-F was performed on freshly-sorted PαS MSCs, cell death due to the sorting procedure may have negatively affected the CFU-F efficiency. Pinho et al. (2013) report similar CFU-F forming efficiency in PDGFRα$^{+}$CD51$^{+}$ MSCs, and suggest that the "harsh" sorting procedure adversely affects their cell viability. I did observe some dead, floating cells in PαS MSC cultures 24 hours after cell sorting, which gives further evidence for this theory. As such, PDGFRα and Sca-1 *enriches* for cells with MSC-like phenotype from mouse BM, but not every PαS MSC can perform all the functions expected of MSCs. However, the CFU-F efficiency of PαS MSCs is significantly higher than those reported in plastic-adherent studies, which range from 1 in every 9000 BM cells (Meirelles Lda and Nardi, 2003) to 1 in 3.3x10$^{6}$ BM cells (Phinney et al., 1999).

The tri-lineage differentiation of PαS MSCs was demonstrated using well-established *in vitro* techniques. PαS MSCs readily underwent osteogenic and chondrogenic differentiation, although adipogenic differentiation was less impressive. Clonal PαS MSC differentiation studies by Morikawa *et al.* revealed all clones (6/6) could differentiate towards bone and

cartilage, but less than half (2/6) could differentiate towards fat (Morikawa et al., 2009). Poor adipogenic differentiation (relative to osteogenic differentiation) was also observed in previous studies of mouse (Cunha et al., 2013), sheep (Heidari et al., 2013), and rat (Peng et al., 2008) MSC populations. The reasons behind this disparity are unclear and could be due to heterogeneity in the PDGFRα$^{+}$Sca-1$^{+}$ population or the fact that BM MSCs are naturally primed towards bone and cartilage (skeletal tissue) over fat (connective tissue). Additionally, culture on a stiff surface has also been shown to enhance osteogenic differentiation in MSC populations (Engler et al., 2006).

### 3.2.3 Immunosuppressive phenotype of PαS MSCs

*In vitro* T cell suppression assays demonstrated that Balb/c-derived PαS MSCs suppressed CD4 T cell proliferation in a dose-dependent manner. Blocking studies revealed that local release of NO by PαS MSCs was responsible for immunosuppression. Additional experiments using PαS MSCs isolated from transgenic iNOS-/- mice provided further proof for this finding. A comparative study by Ren et al. (2009) identified that mouse MSCs exclusively use NO secretion to immunosuppress while human MSCs secrete IDO. Our findings back up this hypothesis, as we did not see any effect when using an IDO inhibitor. It is interesting to note that inhibition of NO secretion caused a complete reversal in the immunosuppressive phenotype of PαS MSCs. Past studies have noted that neutralisation of one factor secreted by mouse or human MSCs does not result in a complete reversal of suppression, suggesting that there are other factors in play (Ben-Ami et al., 2011). This degree of redundancy could be due to the heterogeneous stromal populations used in past studies, with each having a

different mechanism of immunosuppression. The purified population of PαS MSCs used in this study displayed a 'unified' response to the compounds tested and demonstrates nicely how prospective isolation could help reduce diversity in the MSC field.

NO is a potent signalling molecule with a short half-life that is involved in many physiological processes ranging from vasodilation to immune regulation (Bogdan, 2001). NO production by macrophages has been shown to suppress T cell proliferation via the inhibition of STAT5 phosphorylation, resulting in cell cycle arrest (Mazzoni et al., 2002, Bingisser et al., 1998). Interestingly, Sato et al. (2007) identified the same mechanism at play with murine MSCs, highlighting the importance of the NO-STAT5 axis. Future work could include western blotting for phosphorylated STAT5 in CD4 T cells to identify whether the same mechanism occurs with PαS MSC co-culture.

Recent studies have identified MSCs as key players in the HSC niche, as they are the precursors of multiple niche components and can secrete factors that are crucial for HSC maintenance (Frenette et al., 2013). However, the physiological role for MSC-mediated immunosuppression and NO release in the BM niche is unclear. Some authors have suggested that MSCs may function to protect HSCs from immune mediated damage by creating an 'immunoprivileged zone' around these cells (Hsu and Fuchs, 2012). However, an elegant imaging study by Fujisaki et al. (2011) demonstrates that Tregs co-localise with HSCs *in vivo* to create an immunoprivileged site that enabled allogeneic-HSCs to avoid rejection for up to 30 days. A similar function has not been convincingly attributed to MSCs, and it

remains to be seen whether they do play an immunosuppressive role in the BM niche. Data from the Matsuzaki group suggest that mismatched naïve PαS MSCs can trigger the onset of GvHD in a mouse model of BM transplantation (Ogawa et al., 2012). The selective depletion of PαS MSCs from BM grafts reduced fibrosis across all organs. From these findings, it can be speculated that naïve PαS MSCs directly isolated from their niche are not suppressive and that immunosuppression is a property acquired through *in vitro* culture. This hypothesis is further backed up by the various human phase I/II trials using *in vitro* cultured MSCs in the treatment of GvHD that report favourable outcomes (Le Blanc et al., 2008, Le Blanc et al., 2004b). Future studies using freshly-isolated PαS cells in immunosuppression assays would be required to test this hypothesis.

### 3.2.4 Strain-specific differences in Immunosuppression

PαS MSCs isolated from C57BL/6 mice failed to suppress T cell proliferation in our standard assay, leading us to hypothesise that there might be strain-specific differences in the immunosuppressive mechanism of MSCs isolated from Balb/c and C57BL/6 mice. Hashemi et al. (2013) compared the immunosuppressive properties of conditioned media (CM) isolated from adipose-derived MSCs of Balb/c and C57BL/6 mice. They report that Balb/c MSC CM is more suppressive than C57BL/6-derived CM, partly due to higher levels of IDO, TGF-β and NO in Balb/C MSC supernatants. Although a comparative study of immunosuppression from BM-derived MSCs has not yet been performed, one can assume with the differences observed in CFU-F and differentiation from different mouse strains that immunosuppression may vary as well.

We hypothesised that C57BL/6-derived PαS MSCs were exerting an indirect effect on T cell proliferation by inhibiting antigen presentation or polarising macrophages towards a regulatory phenotype. To test this hypothesis, we moved away from a 'purified' system where no antigen presentation was required to a more complex splenocyte culture containing several different immune cell subsets. After unsuccessful attempts to stimulate splenocyte cultures with ConA or Dynabeads®, the OT-1 transgenic mouse was chosen as our model system. CD8 T cells from OT-1 mice have a TCR specific for the ovalbumin protein (Wright et al., 2005). Exogenous addition of OVA peptide into OT-1 splenocyte cultures causes antigen-specific proliferation of CD8 lymphocytes (Clarke et al., 2000). OVA peptide needs to be processed and presented in a MHC class I context to CD8 lymphocytes to cause activation, thereby making this system more physiologically relevant than the use of TCR-binding antibodies or beads. It is also a good *in vitro* representation of the OVA-Bil mouse model, where ectopic expression of OVA on the biliary epithelium of the liver results in an OT-1 mediated immune reaction and inflammation (Buxbaum et al., 2006).

Our preliminary findings show that C57BL/6-derived PαS MSCs can suppress CD8 lymphocyte proliferation in a dose-dependent manner. We also saw reductions in the IFNγ production of CD8 cells after MSC co-culture, a finding that has been shown before by Hof-Nahor and colleagues for human MSCs (Hof-Nahor et al., 2012). Interestingly, although there were large drops in total numbers of CD8 T cells after PαS MSC co-culture, we only observed minor differences in the proliferation status of CD8 cells that remained viable. This suggests that MSCs could induce CD8 lymphocyte apoptosis and that any lymphocytes which escaped

MSC-mediated immunosuppression were still proliferating in response to OVA antigen. The induction of CD8 T cell apoptosis has been reported previously for human MSC populations due to IDO-mediated depletion of tryptophan from the local microenvironment (Plumas et al., 2005). Further experiments are needed to see whether a similar mechanism is in play for PαS MSCs. Further repeats are also needed to increase the sample size and to understand the significance of these findings. Small molecule inhibitors of known immunosuppressive pathways can be added to the splenocyte reaction to try and identify a mechanism of action. Additionally, individual immune cell subsets (e.g. monocytes/macrophages, B cells, DCs) can be selectively removed from the splenocyte mixture to study indirect effects on T cell proliferation.

# CHAPTER 4

# LOSS OF FUNCTION IN PαS MSCs

## 4.1 Chapter Rationale and Aims

PDGFRα$^{+}$Sca-1$^{+}$ marks cells in BM enriched for an MSC phenotype. However, the frequency of these cells in BM is very rare, resulting in yields of approximately 5000 to 8000 PαS MSCs per mouse. A degree of *in vitro* expansion is therefore required to reach the cell numbers we need for experimentation or therapeutic infusions. Previous publications have injected single doses of murine MSCs ranging from 0.4x10$^{5}$ (Ding et al., 2009) to 1x10$^{6}$ MSCs per mouse in acute models of injury (Nemeth et al., 2009). More chronic models of graft rejection have necessitated multiple infusions of 1x10$^{6}$ cells given before, during and after transplantation (Casiraghi et al., 2008). Human clinical trials have used cell doses ranging from a single dose of 2x10$^{6}$ MSCs/kg body weight (Le Blanc et al., 2004b) to multiple doses of 2x10$^{6}$ MSCs/kg given twice weekly for one month (Kurtzberg et al., 2014). In all these cases, MSCs were expanded *in vitro* before infusion.

Although murine MSCs can be expanded *in vitro*, they are eventually susceptible to replication-induced senescence and loss of function (Coutu et al., 2011, Kretlow et al., 2008). Senescence typically manifests as an increase in the expression of senescence-associated β-galactosidase (SA-β-gal), an enzyme specifically expressed in senescent cells (Gary and Kindell, 2005). Senescent MSCs lose their spindle-shaped morphology and display a wider, more spread out morphology (Sethe et al., 2006). Their population doubling times increase and their tri-lineage differentiation ability is lost (Wagner et al., 2008). An impaired capacity to migrate towards pro-inflammatory signals has also been described for senescent human MSCs, making them less effective in a mouse model of endotoxemia (Sepulveda et al., 2014).

A retrospective analysis of GvHD clinical trials has revealed that patients receiving older MSCs (P3-P4) had worse 1-year survival rates than patients receiving P1-P2 cells (von Bahr et al., 2012). Passage five human MSCs were also shown to be cleared by the host much quicker than younger cells (Moll et al., 2012). Finally, prolonged *in vitro* expansion can also increase the risk of karyotypic abnormalities in murine MSCs, leading to transformation and tumour formation (Tolar et al., 2007, Miura et al., 2006).

The effect of prolonged *in vitro* expansion on PαS MSC function and immunosuppression has not been described previously. This results chapter describes how PαS MSCs are vulnerable to replication-induced senescence and how this negatively impacts the functionality of these cells. The specific aims for this chapter were to:

1. Describe the effect of extended *in vitro* culture on PαS MSC senescence
2. Assess the ability of late-passage PαS MSCs to undergo tri-lineage differentiation
3. Examine the immunosuppressive potential of late-passage PαS MSCs

## 4.2 Results

### 4.2.1 PαS MSCs undergo Senescence

PαS MSC growth curves shown in the previous chapter demonstrated linear growth during the first 30 days that 'plateaued' thereafter (Figure 3.3A). Concordant increases in population doubling times were also observed with extended culture, rising from approximately 55 hours between day 0-30 to >10 days by day 50. These are characteristic traits observed in cultures undergoing senescence (Wagner et al., 2008). To examine whether PαS MSCs were becoming increasingly senescent, I first examined the morphology of freshly isolated and culture-expanded cells (Figure 4.1). Older cells had an enlarged and irregular morphology (Figure 4.1B arrowheads) compared to freshly isolated PαS MSCs (Figure 4.1A). Older MSCs were also more 'spread out' and flatter with decreased nuclear to cytoplasm ratios, another trademark of more mature cells (Wlodkowic et al., 2011).

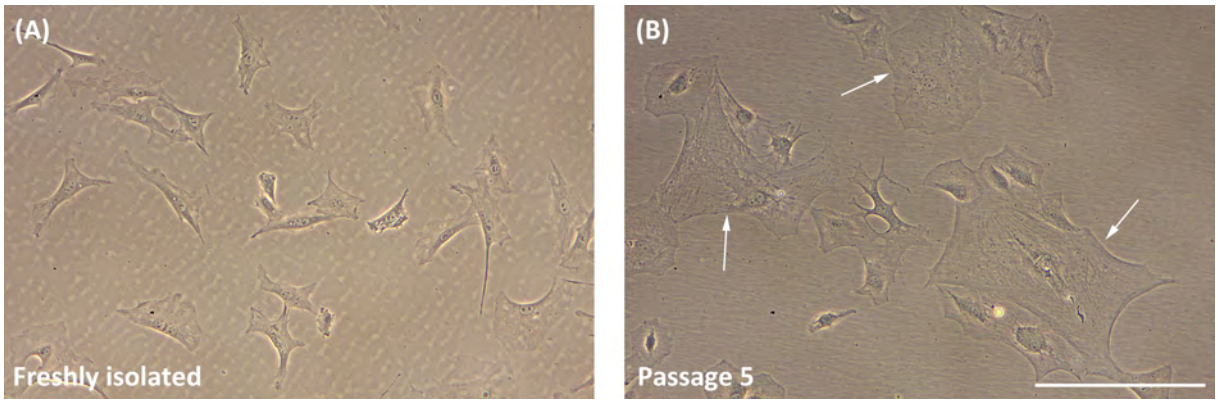


Figure 4.1 | **Morphology of freshly isolated and culture-expanded PαS MSCs**. (A) Freshly isolated PαS MSCs display a characteristic spindle-shaped, fibroblastic morphology. All cells are roughly similar in size and shape. (B) Culture-expanded PαS MSCs are heterogeneous in size and shape, with some cells appearing much larger than others (arrowheads). Images taken at 100x magnification. Scale bar, 25µm.

To examine this in greater detail, PαS MSCs at different passages were stained for the expression of the senescence marker β-gal. The chromogenic substrate X-gal was added to fixed cultures to visualise β-gal$^+$ cells in a blue/green colour (Figure 4.2A-C). The percentage of β-gal$^+$ MSCs was then quantified (Figure 4.2D). PαS MSCs at P3 were 2.3±0.9% β-gal$^+$, while P5 had a non-significant increase to 11.5±1.7%. Passage 7 MSCs had significantly more β-gal$^+$ cells than P3 cultures samples (40.2±20.7%). These findings show that PαS MSCs are susceptible to replicative senescence, which can limit the therapeutic potential of these cells.

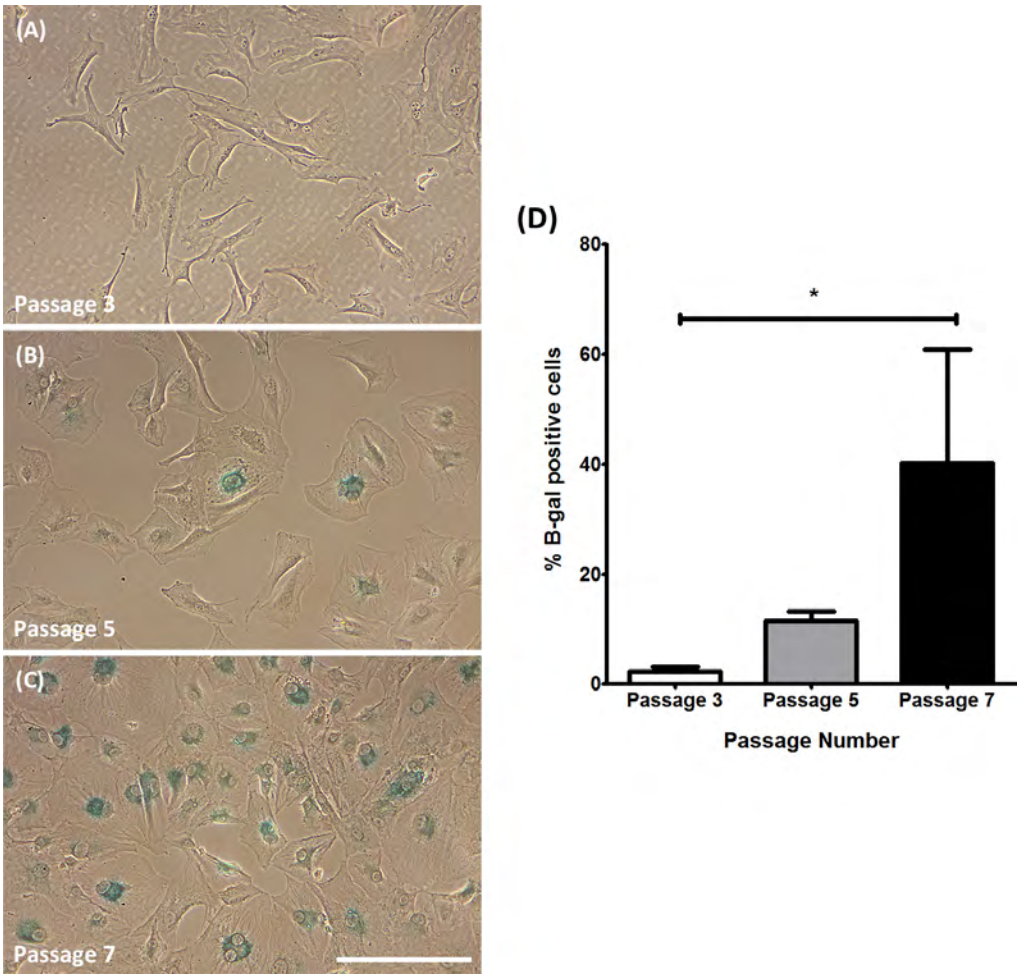


Figure 4.2 | **SA-β-gal expression in PαS MSCs**. Representative images of SA-β-gal staining at (A) P3, (B) P5 and (C) P7. Images taken at 100x magnification. Bar, 25µm. (D) Quantification of SA-β-gal staining from 12 fields of view per sample, 3 samples per condition. Data represented as mean±SD. Statistical analysis performed using One-way ANOVA with Bonferroni's Multiple Comparison Test.

### 4.2.2 Effect of Senescence on PαS MSC Tri-lineage Differentiation

#### 4.2.2.1 Osteogenic Differentiation

The effect of extended culture on the tri-lineage differentiation of PαS MSCs was examined. Osteogenic differentiation was induced as before and cultures stained with alizarin red to visualise calcium deposition (Figure 4.3A). After imaging, the dye was extracted from the stained monolayer and quantified against known calcium standards (Figure 4.3B). PαS MSCs exhibited robust osteogenic differentiation across all passages tested. Interestingly, significant increases in calcium concentration were observed at P5 compared to all earlier passages. Similar findings have been reported previously (Wagner et al., 2008). It would seem that tissue culture plastic is an independent promoter of osteogenic differentiation, as the propensity for osteogenesis increased at later passages in growth factor-supplemented cultures as well (Chapter 5).

#### 4.2.2.2 Adipogenic Differentiation

Adipogenic differentiation was visualised using oil red O, which stains lipids in a red colour. PαS MSCs underwent sporadic adipogenic differentiation at earlier passages, but this ability was lost at P3 onwards (Figure 4.4). Loss of adipogenic potential is observed upon senescence in mouse (Kretlow et al., 2008) and human MSCs (Welter et al., 2013), and the authors of the original PαS MSC isolation paper also had difficulty pushing freshly-isolated PαS cells down the adipogenic lineage as well (Morikawa et al., 2009). In our hands, adipogenesis was the first property to be lost as PαS MSCs became increasingly senescent.

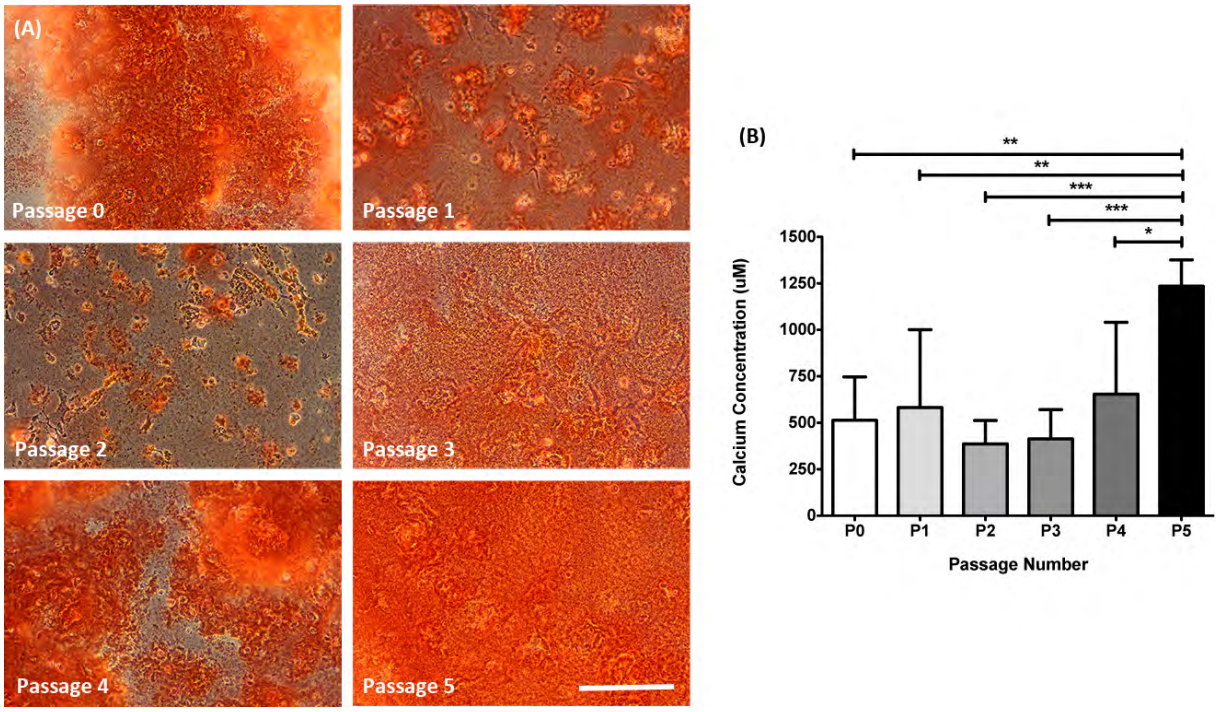


Figure 4.3 | **Effect of extended culture on PαS MSC osteogenesis**. (A) Representative images of alizarin red stained differentiation cultures at various passages. Images taken at 100x magnification. Bar, 25µm. (B) Quantification of calcium concentration in differentiation samples (n≥5 technical repeats per passage). Data shown mean±SD. Statistical analysis performed using One-way ANOVA with Bonferroni's Correction.

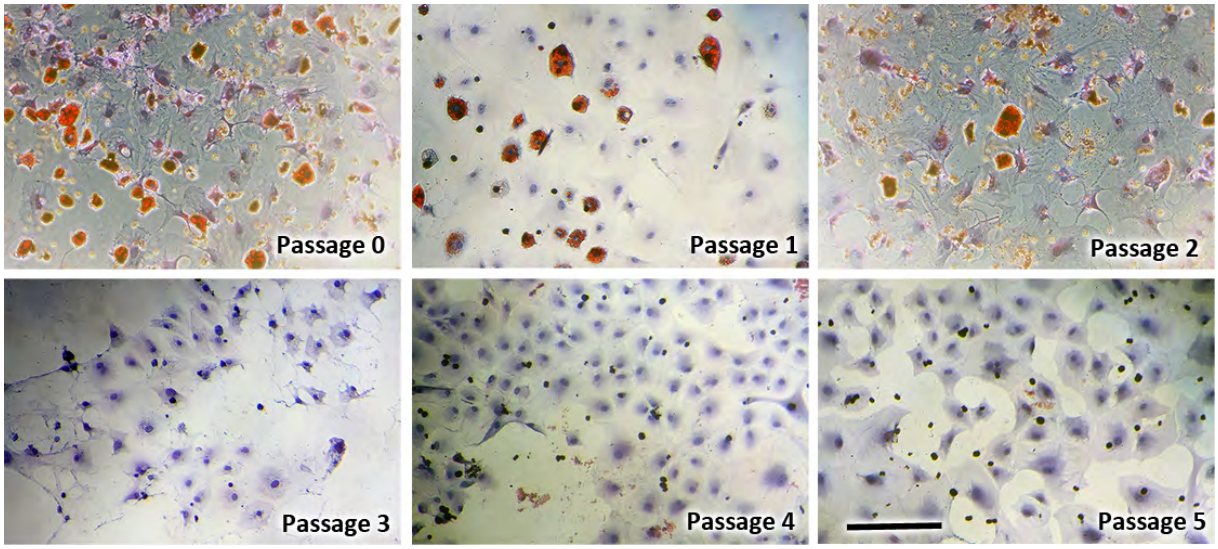


Figure 4.4 | **Effect of extended culture on PαS MSC adipogenesis**. Representative images of adipogenic differentiation cultures stained with oil red O and counterstained with haematoxylin. Loss of adipogenic potential can be seen from P3 onwards. Images taken at 100x magnification, n≥3 per condition. Bar, 25µm.

#### 4.2.2.3 Chondrogenic Differentiation

Chondrogenic differentiation of PαS MSCs was studied using micromass pellet cultures in collaboration with Dr Zhang and Professor Hollander at Bristol University. Using their proprietary methods, we were able to quantify the amount and quality of cartilage produced in PαS MSC-derived micromass pellets. Fixed numbers of PαS MSCs at P5 and P9 underwent chondrogenic differentiation. Pellets were then freeze-dried and weighed prior to enzymatic digestion. Older P9 PαS MSCs produced significantly smaller and lighter pellets than their younger P5 counterparts ($p=0.0004$; Figure 4.5A).

Cartilage pellets were then digested in trypsin to solubilise extracellular matrix (ECM) components. The major ECM components of cartilage are water (65-80%), collagen fibres (10-20%) and proteoglycans (5-10%; Poole et al., 2001). Of the collagen fibres, type I collagen (Col1) is synthesised by immature or de-differentiated chondrocytes (Yang et al., 2006). Col1 is found in fibrocartilage, an inferior cartilage that is produced as a wound healing response (Punwar and Khan, 2011). Type II collagen is synthesised by fully differentiated chondrocytes and predominates in hyaline cartilage. Col1 and Col2 were detected, but there was no difference between groups (Figure 4.5B-C). The amount of Col2 produced was higher than Col1 (approximately 1.5µg Col2 compared to <1ng Col1), suggesting that PαS MSC-derived chondrocytes are healthy and functional. The ratio of Col2:Col1 is also used to assess the quality of MSC-generated cartilage, with higher values representing better cartilage differentiation (Marlovits et al., 2004). No significant differences were observed in the Col2:Col1 ratio between P5 and P9 PαS MSCs (Figure 4.5D).

Aside from collagen fibres, the other major ECM components of cartilage are proteoglycans. Proteoglycans consist of a 'core' protein onto which several glycosaminoglycan (GAG) chains are covalently attached (Esko et al., 2009). Proteoglycans provide load bearing and compression resistance properties to healthy cartilage and is an important marker of chondrocyte function (Knudson and Knudson, 2001). The total GAG content of PαS MSC-derived cartilage was quantified using a colourimetric assay. Passage 5 cells had significantly more GAG compared to older, P9 cells (2.3±1.2µg vs. 0.8±0.04µg, p=0.049). These results demonstrate that senescence has a negative effect on the size and GAG content of PαS MSC-derived cartilage, although their collagen content remained quite similar.

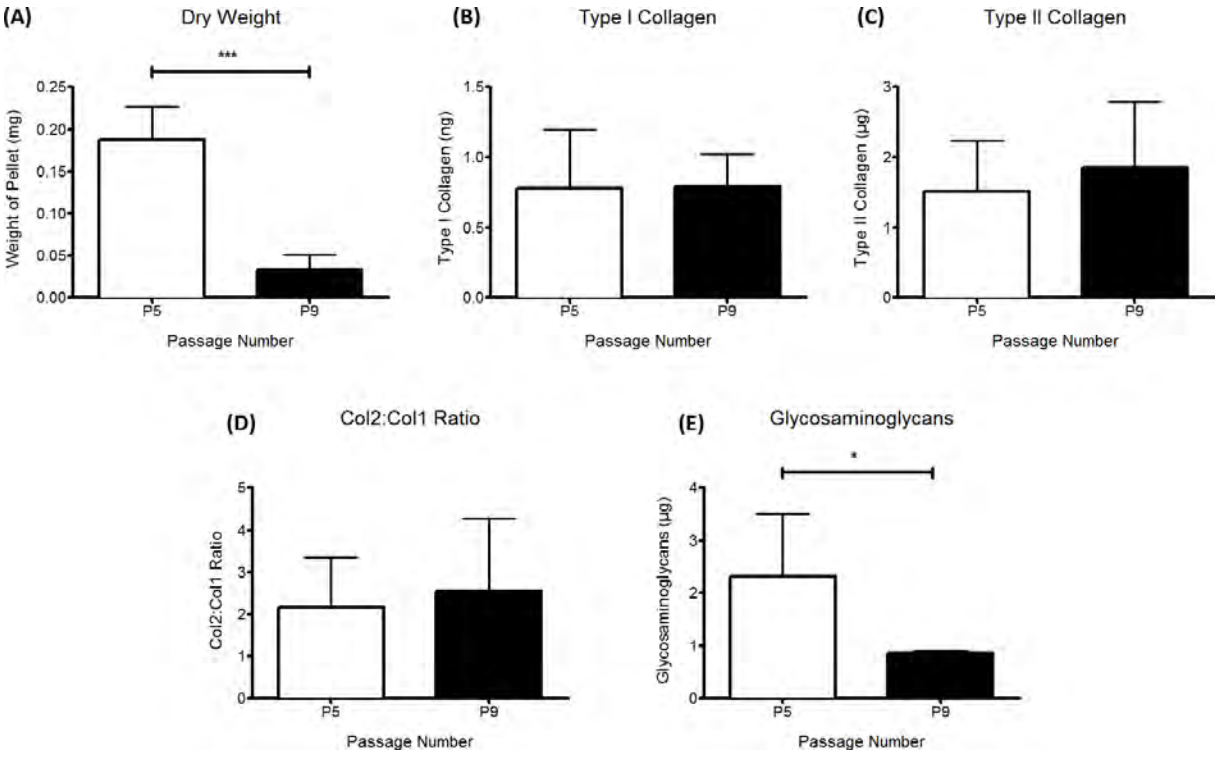


Figure 4.5 | **Effect of extended culture on PαS MSC chondrogenesis**. (A) Dry weight of MSC-derived cartilage after freeze drying. (B) Total amount of type I and (C) type II collagens in cartilage samples. (D) Ratio of Col2:Col1 as a marker of cartilage quality. (D) Total amount of GAGs present in MSC-derived cartilage. Data shown as mean±SD, n≥4 biological repeats per passage. Statistical analysis performed using unpaired Student's T test.

### 4.2.3 Effect of Senescence on PαS MSC Immunosuppression

The effect of extended culture on Balb/c-derived PαS MSCs was examined using the 'purified' *in vitro* T cell proliferation assay. Early-passage (P3) MSCs were able to suppress in a dose-dependent fashion as before, but P5 MSCs fared slightly worse (Figure 4.6A). Significant increases in CD4 T cell numbers (compared to P3) were seen at the 1:32, 1:16 and 1:8 ratios, with P5 MSCs only being able to suppress equally well as P3 cells at the highest 1:4 dose. Late-passage (P7) MSCs failed to suppress T cell proliferation across all ratios tested. Significant increases in CD4 T cell numbers (compared to P5) were seen at 1:8 and 1:4 ratios, and across all ratios when compared to P3 cells. Additionally, P7 MSCs also failed to cause significant drops in T cell number when compared to their no-MSC control, demonstrating that senescence completely eliminates the immunosuppressive phenotype of PαS MSCs.

As NO secretion was the mechanism behind Balb/c-derived PαS MSC immunosuppression, we repeated the Griess assay using supernatants from late-passage cells. A significant decrease in the nitrite concentration of P7 cells was observed after overnight incubation with TNFα and IFNγ stimulation (71.1±2.5μM vs 22.2±0.9μM nitrite, $p<0.0001$; Figure 4.5B). These findings demonstrate a profound reduction in the immunomodulatory function of PαS MSCs after extended *in vitro* culture due to impaired production of NO in older cells.

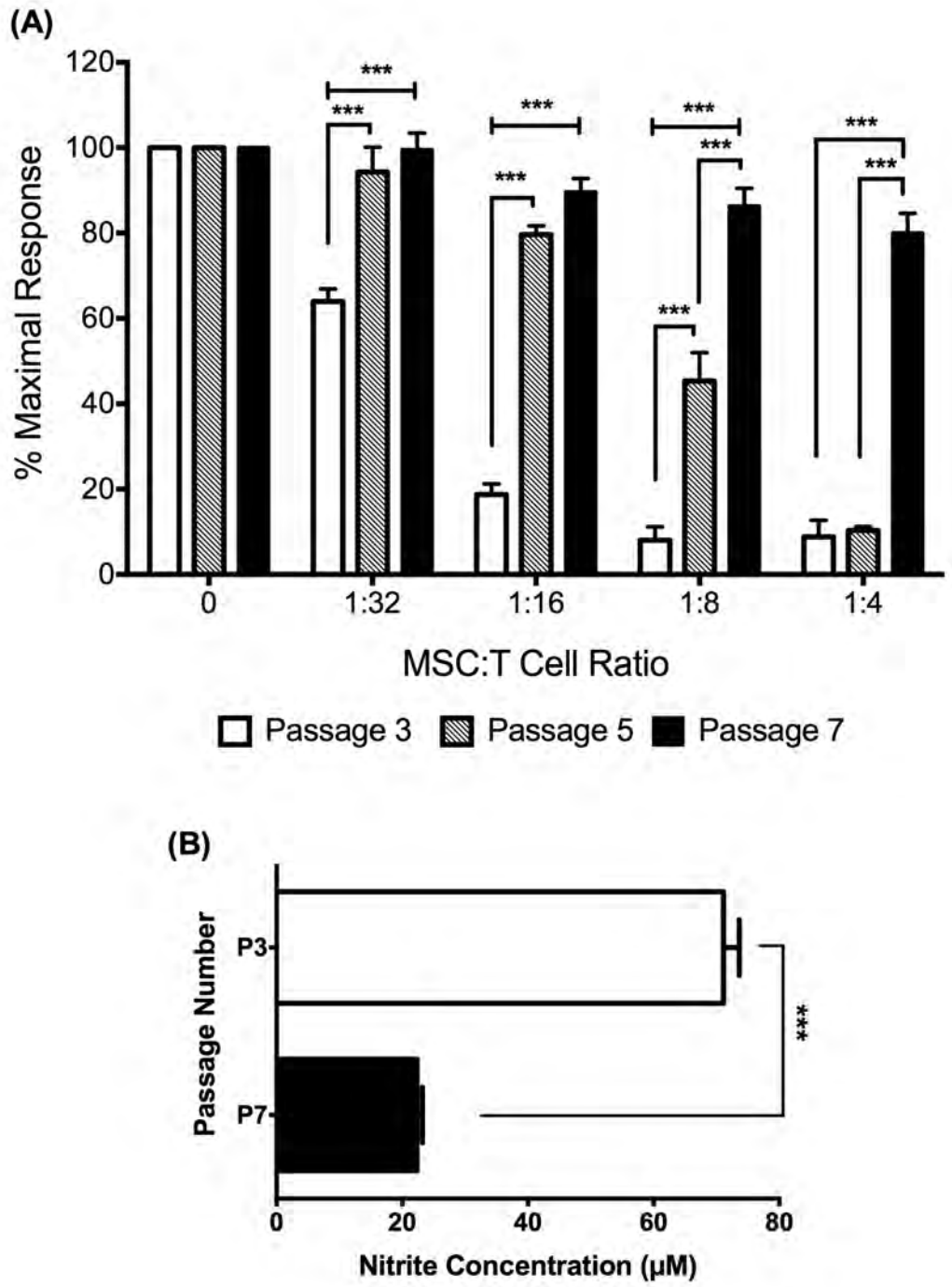


Figure 4.6 | **Effect of extended culture on Balb/c-derived PαS MSC immunosuppression**. (A) Balb/c-derived PαS MSCs (n=3 biological repeats for each passage) were co-cultured for 72 hours with activated $CD4^+$ T cells. Samples were then analysed by flow cytometry and total CD4 numbers counted and expressed as a percentage to the no-MSC control. Data shown as mean±SD. Statistical analysis performed using Two-way ANOVA with Bonferroni's Multiple Comparison Test. (B) Total levels of nitrite from P3 and P7 PαS MSCs was quantified using the Griess assay (n=3 technical repeats). Data shown as mean±SD. Statistical analysis performed using unpaired Student's T test.

## 4.3 Discussion

### 4.3.1 Chapter Summary

The rarity of PαS MSCs in BM mandates a period of *in vitro* expansion to reach cell numbers required for experiments. The findings of this chapter demonstrate that PαS MSCs are susceptible to replication-induced senescence, characterised by a reduction in proliferative capacity, an increase in cell size and increased expression of SA-β-gal. Increased senescence has implications for the therapeutic application of PαS MSCs, as we saw reductions in adipogenic and chondrogenic differentiation potential in aged cells. Interestingly, we observed an increase in osteogenic differentiation at later passages, suggesting that aged MSCs lose their multipotency and become lineage-restricted towards bone. We also observed a progressive loss of immunomodulatory function in P5 and P7 PαS MSCs, due to decreased secretion of NO.

### 4.3.2 PαS MSCs undergo Senescence

Cellular senescence was first described by Leonard Hayflick in a seminal study that showed human somatic cells have a limited capacity to divide *in vitro*, known as the “Hayflick limit” (Hayflick, 1965). Senescence is believed to be tumour-suppressive mechanism as it prevents mitotic cells from replicating indefinitely. Studies have shown that exposing a cell to oncogenic or mitogenic stimuli can induce the onset of premature senescence as a way to avoid transformation (Dimri, 2005). The trademark characteristic of senescence is growth arrest, but the senescent cells remain viable, metabolically active, and more resistant to

apoptosis (Hampel et al., 2004, Di Leonardo et al., 1994). Senescence also induces increased expression of cell cycle inhibitors such as p21 and p16 in MSCs (Yu and Kang, 2013, Campisi and Fagagna, 2007). Senescent human MSCs downregulate expression of genes involved in mitosis and proliferation at later passages (Tsai et al., 2010, Schallmoser et al., 2010, Lee et al., 2009a). Similar findings have also been reported for murine MSCs (Himeno et al., 2013). Future work should examine the expression of senescence-related genes in PαS MSCs to confirm their senescent status after extended culture.

The expression of senescence-associated β-galactosidase was used as a marker of senescent cells in this study. SA-β-gal is defined as β-gal activity detectable at pH 6.0 in cultured cells that have undergone replicative senescence (Lee et al., 2006). We observed a significant increase in SA-β-gal expression in PαS MSCs at P7, corresponding to approximately 50 days culture. Senescent PαS MSCs appear larger, with a decreased nucleus to cytoplasm ratio ("fried egg" morphology) that has been described before for MSCs and other stromal cell populations (Wagner et al., 2010). Aside from the loss of function, the systemic infusion of larger MSCs carries a risk of them being trapped in small capillaries in mouse models which can lead to tissue ischemia and further injury (Furlani et al., 2009, Toma et al., 2009).

In our studies, PαS MSCs cultured in SM displayed increased population doubling times after 50 days in culture. This was a lot earlier than reported by Morikawa and colleagues, who were able to expand PαS MSC for up to 100 days, yielding approximately $10^7$ cells (Morikawa et al., 2009). However, the number of population doublings was not reported in the original

paper, which makes it difficult to compare results. The reason behind this discrepancy in proliferative capacity is unclear, and it remains to be seen whether PαS MSCs could have been expanded past the 50-day limit used in this study. One potential reason could be that our *in vitro* culture conditions are not optimised for PαS MSC expansion. Culture in 3D, under hypoxic conditions and supplemented with growth factors have been shown to promote MSC growth and differentiation (Gharibi and Hughes, 2012, Das et al., 2010). Additionally, the prospectively-isolated Nestin$^{+}$ and PDGFRα$^{+}$CD51$^{+}$ murine MSCs required 3D culture as "mesenspheres" as they were not able to be expanded as 2D monolayers (Pinho et al., 2013, Mendez-Ferrer et al., 2010). Identification of optimal culture conditions for PαS MSCs should delay the onset of senescence and improve the therapeutic potential of these cells.

PαS MSCs also have a reduced proliferative capacity when compared to traditionally isolated, plastic-adherent murine MSCs that can be expanded to reach $10^7$ cells within fourteen days (Zhu et al., 2010). However, the contribution of contaminating and transformed cells in MSC cultures could have had an impact in previous studies. Miura et al. (2006) showed that mouse MSCs displayed signs of senescence at P5, but they overcame this "crisis phase" and re-acquired proliferative capacity through transformation. Transformed cells could be expanded for >500 PDs over a 400 day period and formed tumours after *in vivo* infusion. The onset of senescence in PαS MSCs suggests that these cells are not prone to malignant transformation, however future karyotypic studies must be performed to check the genetic stability of these cells after extended culture.

### 4.3.3 Effect of Senescence on PαS MSC Differentiation

The osteogenic differentiation potential of PαS MSCs increased at later passages, producing significantly more calcium at P5. This finding goes against previous published literature, which reports a loss in osteogenic potential with increasing passage number for murine (Despars et al., 2013, Moerman et al., 2004) and human MSCs (Bajada et al., 2009, Sethe et al., 2006). Only Wagner and colleagues report an increase in the amount of alizarin red staining at later passages using human MSCs (Wagner et al., 2008). One possible reason for this discrepancy could be due to prolonged culture on tissue culture plastic, a relatively 'stiff' culture matrix. The importance of matrix elasticity has been elegantly demonstrated by Engler et al. (2006) and Oh et al. (2009), who were able to induce osteogenic differentiation by culturing human MSCs on 'stiff' culture matrices alone. To test this theory, it would be interesting to see whether PαS MSCs cultured on softer hydrogels lose their osteogenic potential and gain adipogenic potential at later passages.

PαS MSCs lost their adipogenic and chondrogenic potential at later passages, suggesting that senescent PαS cells become lineage-restricted towards bone after *in vitro* expansion. Loss of fat and cartilage differentiation has been described previously for aged MSCs (Sethe et al., 2006). Loss of chondrogenesis has implications for future therapeutic uses. There is increasing demand for alternative therapies for cartilage repair, and MSC-derived chondrocytes are one option currently being researched (Solchaga et al., 2011, Zhang et al., 2009, Chen and Tuan, 2008). Pre-clinical studies have demonstrated the safety of MSC infusion in patients with cartilage defects, but the degree of clinical benefit varied (Koga et

al., 2009). This reflects the relative technical complexity involved in differentiating MSCs into chondrocytes compared to the other main lineages (Vinatier et al., 2009). In collaboration with Bristol University, we were able to quantify collagen and proteoglycan deposits in PαS MSC-derived cartilage to fully assess the quality of cartilage produced. Passage 5 PαS MSCs were able to produce large cartilage pellets rich in collagen type II and glycosaminoglycans. Therefore, PαS MSCs can be used as a model system for future tissue engineering approaches to make cartilage, with a view to translating any promising findings to the clinic. Although the collagen content between P5 and P9 cells were similar, their size and proteoglycan deposits were significantly different. Further work is necessary to identify culture conditions that maintain the chondrogenic potential of PαS over extended culture.

### 4.3.4 Effect of Senescence on PαS MSC Immunosuppression

The effect of *in vitro* culture on MSC-mediated immunosuppression has not been studied in detail, and the limited literature on this topic describes the effect of senescence on human MSC populations and not their murine equivalents (Asumda, 2013). We have demonstrated that PαS MSCs display a progressive loss of immunosuppressive function, with P7 cells having completely lost the ability to prevent CD4 T cell proliferation due to an impaired ability to secrete NO. In a similar study, Li and colleagues show that human MSCs cultured for 7 passages *in vitro* lost their ability to suppress CD4 T cell proliferation due to increased senescence and downregulaton of IL-10 secretion (Li et al., 2012). Sepulveda et al. (2014) also report loss of immunosuppression in senescent human MSCs after *in vivo* infusion in a lethal endotoxaemia model. Interestingly, they did not see any difference in the *in vitro*

immunosuppressive capacity of senescent MSCs. Another interesting study demonstrated that the onset of senescence in human fibroblasts triggered a complex 'senescence-associated secretory phenotype' during which elevated levels of pro-inflammatory cytokines IL-6 and IL-8 were produced (Rodier et al., 2009, Fumagalli and Fagagna, 2009). Although the similarities observed between MSCs and fibroblasts make this an attractive mechanism to explain loss in immunosuppression at later passages, a similar finding has not yet been reported for purified MSC cultures.

Finally, clinical evidence for a loss in immunosuppression is reported by Moll et al. (2014) and von Bahr et al. (2012), who show that culture expanded MSCs perform worse in patients with GvHD due to rapid clearance of infused cells from the host. The recent failed phase III RCT (NCT00366145) investigating the potential of MSCs (PROCHYMAL®) in patients with GvHD used MSCs that had been expanded using a proprietary method to yield 10,000 doses ($20x10^9$ cells) from a single BM donor (Galipeau, 2013). PROCHYMAL® MSCs expressed all markers defined by the ISCT criteria, but functional analysis of differentiation and immunosuppression were not performed on the cells infused into patients. Given what we now know about MSC senescence, it is likely that the majority of infused MSCs could have undergone senescence that would explain the apparent lack of efficacy in patients. These studies corroborate the urgent need to identify methods to maintain MSC function during *in vitro* expansion.

# CHAPTER 5

# GROWTH FACTOR PRIMING OF PαS MSCS

## 5.1 Chapter Rationale and Aims

Replicative senescence affects both human and mouse MSCs, leading to reductions in growth and function (Sethe et al., 2006). Our data shows that PαS MSCs are also susceptible to replication-induced senescence, which limits their use as a pre-clinical model population of MSCs. To overcome these issues, several groups have examined the effect of hypoxia (Das et al., 2010), 3D culture (Pek et al., 2010b), matrix stiffness (Engler et al., 2006) and growth factors (Rodrigues et al., 2010) as a way of improving MSC function. In this study, we examined the effect of GF stimulation as a way of overcoming PαS MSC senescence and augmenting their growth, differentiation and immunosuppressive characteristics.

### 5.1.1 Overcoming senescence using GFs

A wide variety of GFs have been studied previously to augment MSC growth and function (reviewed in Introduction section 1.7.2). Commonly used factors include FGF2, PDGF-BB and TGF-β1 (Jung et al., 2012, Coutu et al., 2011, Rodrigues et al., 2010). These three factors have a potent mitogenic effect on MSCs, thereby reducing the *in vitro* expansion time required to reach cell numbers for therapeutic infusions. They are also able to promote the tri-lineage differentiation of MSCs (Song et al., 2014, Ito et al., 2008, Jung et al., 2012). Commercially available MSC culture media are frequently supplemented with undisclosed "factors" that maintain MSC growth and tri-lineage differentiation (Inamdar and Inamdar, 2013, Jung et al., 2012). These undisclosed "factors" are likely to be combinations of GFs that have been described in previous literature.

However, there are many contradictory findings on the effects of GF-supplementation on MSC cultures. FGF2 has been shown to inhibit the differentiation of mouse MSCs (Lai et al., 2011, Osathanon et al., 2011, Baddoo et al., 2003) while other studies have described its ability to enhance differentiation (Rodrigues et al., 2010). TGF-β1 has been reported to be pro-osteogenic in some studies (Roelen and Dijke, 2003) and pro-chondrogenic in others (Xu et al., 2008). Similarly, PDGF-BB can both inhibit (Gharibi and Hughes, 2012) and promote (Kratchmarova et al., 2005) adipogenic differentiation. The heterogeneous populations of MSCs used in previous studies may be one reason for the contradictory findings; however, it is also likely that the duration of GF-exposure may also have an effect. Most studies have examined the short-term, transient effect of GF-stimulation on MSC biology but the effect of long-term culture in GF-supplemented medium is less well understood. It is likely that GF supplementation can "prime" MSCs down specific lineages, which could have significant implications for downstream therapeutic uses. Additionally, the effect of long-term GF-supplementation on the immunosuppressive phenotype of MSCs has not been studied previously and could be of major translational interest.

### 5.1.2 Lineage Priming of MSCs

Lineage priming can be defined as a model of stem cell differentiation in which a given stem cell expresses a subset of genes related to the lineage they are already committed to differentiate into. This model has been extensively studied and proven in the HSC field (Månsson et al., 2007), but there is only one paper that has applied this concept to MSCs (Delorme et al., 2009). In this study, Delorme and colleagues show that clonal populations of

undifferentiated human and mouse MSCs are primed towards the osteogenic, adipogenic and chondrogenic lineages irrespective of any differentiation-inducing stimuli. The importance of this finding is that MSC differentiation into non-primed lineages (e.g. hepatocytes) would require extensive epigenetic reprogramming to turn off the "core program" and switch on novel pathways (Delorme et al., 2009).

The concept of lineage-primed MSCs is also important when looking at future therapeutic uses of these cells. For example, a surgeon would ideally want MSCs primed towards the osteogenic lineage to treat patients with skeletal defects, while chondrocyte-primed MSCs would be ideal in patients with cartilage disorders. When transplanted, these lineage-primed MSCs would readily differentiate into bone and cartilage respectively, allowing us to infuse lower numbers of MSCs to reach the same beneficial outcome.

To this end, Ng *et al*. used a broad transcriptomics approach to identify PDGF, TGF-β and FGF as key signalling pathways regulating human MSC proliferation and differentiation (Ng et al., 2008). PDGF signalling was active during adipogenesis and chondrogenesis; TGF-β signalling was active during chondrogenesis; and FGF signalling was active during osteogenesis, adipogenesis and chondrogenesis (Figure 5.1). Inhibition of any of these signalling pathways resulted in an altered differentiation potential, cell death and increased population doubling times. However, the exogenous addition of their respective ligands was sufficient to maintain MSCs in serum-free media (Ng et al., 2008).

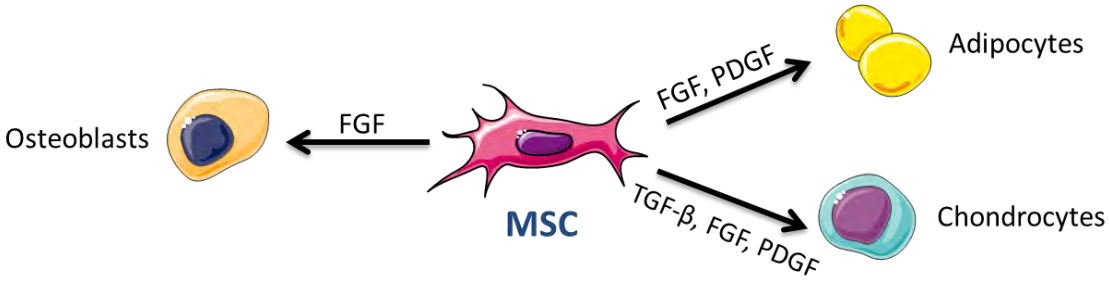


Figure 5.1 | **Active signalling pathways during MSC differentiation**. The findings of Ng et al. (2008) show that the FGF pathway was active during osteogenic, adipogenic and chondrogenic differentiation of MSCs. The PDGF signalling pathway was active during adipogenesis and chondrogenesis. The TGF-β pathway was active during chondrogenesis only.

### 5.1.3 Chapter Aims

GFs are commonly used to overcome senescence and augment MSC function in previous literature. However, little is known about the effect of long-term GF-supplementation on purified MSC cultures. Although GFs increase the proliferation and differentiation of MSCs in the short term, they may also prime MSCs towards specific lineages after extended culture. Defining culture conditions that prime MSCs towards pre-determined fates is of significant interest for future medical uses as it would allow culture conditions to be tailor-made for the clinical indication. Additionally, defining conditions that prolong the suppressive phenotype of MSCs would also be beneficial for use in immune-mediated disorders.

The findings of Ng and colleagues have identified the FGF, PDGF and TGF-β signalling pathways to be active during MSC growth and differentiation down specific fates. We hypothesised that the exogenous addition of their respective ligands (FGF2, PDGF-BB and

TGF-β1) may enhance MSC growth and prime MSCs down specific lineages. One key strength of this study is that we were able to observe the effects of the aforementioned GFs on a pure population of MSCs directly after isolation, thereby avoiding any bias associated with a culture-manipulated starting population. The specific aims of this chapter were to:

1. Describe the effect of FGF2, PDGF-BB and TGF-β1 on PαS MSC growth and senescence.
2. Perform karyotype analysis on PαS MSCs to see whether GF-treatment has a detrimental effect on their genetic stability.
3. Examine whether GF-treatment primes PαS MSCs down specific lineages at the genetic and phenotypic level.
4. Examine the effect of GF-treatment on PαS MSC immunosuppression.

## 5.2 Results

### 5.2.1 Effect of PDGF-BB, FGF2 and TGF-β1 on PαS MSC Growth

To investigate the effects of GF-supplementation on PαS MSCs, freshly isolated cells were cultured in SM ± each individual GF at a concentration of 10ng/ml. PαS MSCs cultured in SM adopted a spindle-shaped morphology as before (Figure 5.2A), but the addition of PDGF or FGF caused the cells to adopt a smaller, more 'spindly' morphology (Figure 5.2B,C). The addition of TGF-β caused PαS MSCs to grow in discrete colonies that were tightly packed with cells, although the overall morphology was similar to the SM controls (Figure 5.2D). No obvious cell death or spontaneous differentiation was observed with the addition of GFs.

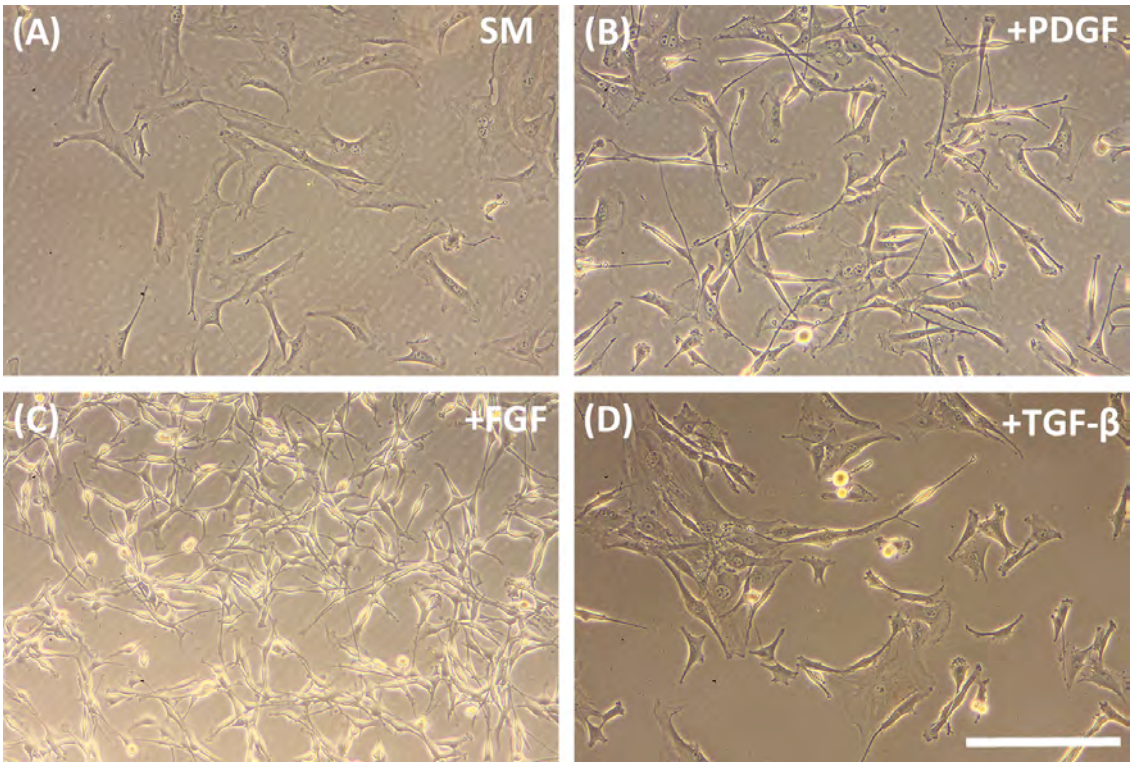


Figure 5.2 | **Morphologies of freshly isolated PαS MSCs with GFs**. Representative images of P0 PαS MSCs cultured in (A) SM, (B) SM+10ng/ml PDGB-BB, (C) SM+10ng/ml FGF2 and (D) SM+10ng/ml TGF-β1. All images taken at 100x magnification. Bar, 25µm.

CFU-F assays were performed to examine whether GF-supplementation affected the colony forming ability of PαS MSCs. Low numbers of PαS MSCs (2000 per 10cm$^2$ dish) were seeded to ensure a clonal density and cultured for 14 days prior to staining with crystal violet to visualise colony formation (Figure 5.3). Addition of FGF or PDGF had the most pronounced effect on CFU-F ability, with increases in both the size and number of colonies formed. TGF-β supplementation had a more modest effect, with total colony number and size similar to that of SM cultures.

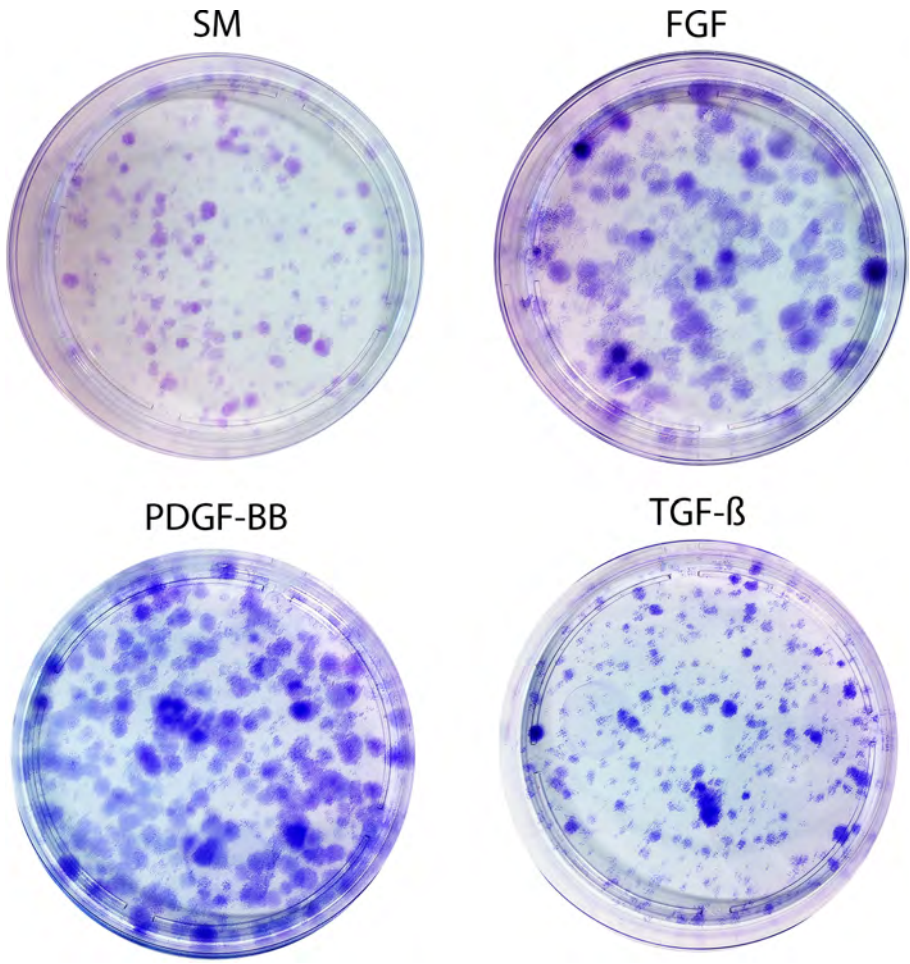


Figure 5.3 | **Effect of GF-supplementation on CFU-F**. Whole-dish image of 10cm$^2$ petri dishes stained with crystal violet to visualise colony formation. Representative images taken without magnification (n=2 biological repeats per condition).

A smaller cell size and improved CFU-F efficiency are indicative of increased growth potential in MSCs (Sethe et al., 2006). Growth curves over a 50-day period were performed to test the effect of GF-supplementation on PαS MSC proliferation. As expected, GF-supplementation had a mitogenic effect on PαS MSCs (Figure 5.4A). MSCs grown in SM underwent 7 PDs over a 50-day period compared to approximately 10 PDs in TGF-β1 supplemented media, 11 PDs in PDGF-BB supplemented media, and 13 PDs in the presence of FGF2. Growth curves for GF-supplemented MSCs were still in their lineage phase of growth at day 50 compared to cells in SM that began to plateau after 40 days. This suggests that GF-supplemented MSCs could have been expanded further past the 50 days used in this study without slowing down and undergoing senescence.

Due to the differences in cell size and morphology seen with the addition of GFs (in particular FGF2; Figure 5.2), the total number of PDs does not fully portray the mitogenic effect of these cytokines. To address this issue, cell counts were taken at day 30 to quantify the total number of viable cells present (Figure 5.4B). PαS MSCs in SM grew from 4000 cells seeded at day 0 to reach 205,000±53,000 cells by day 30. Increases in cell number were seen following TGF-β1 (950,000±570,000 cells) and PDGF-BB ($1.9x10^6$±680,000 cells) supplementation, although this failed to reach statistical significance. By contrast, FGF2-supplemented PαS MSCs increased in number significantly over the 30-day period, yielding cultures containing $9.8x10^6$±$1.25x10^6$ viable MSCs.

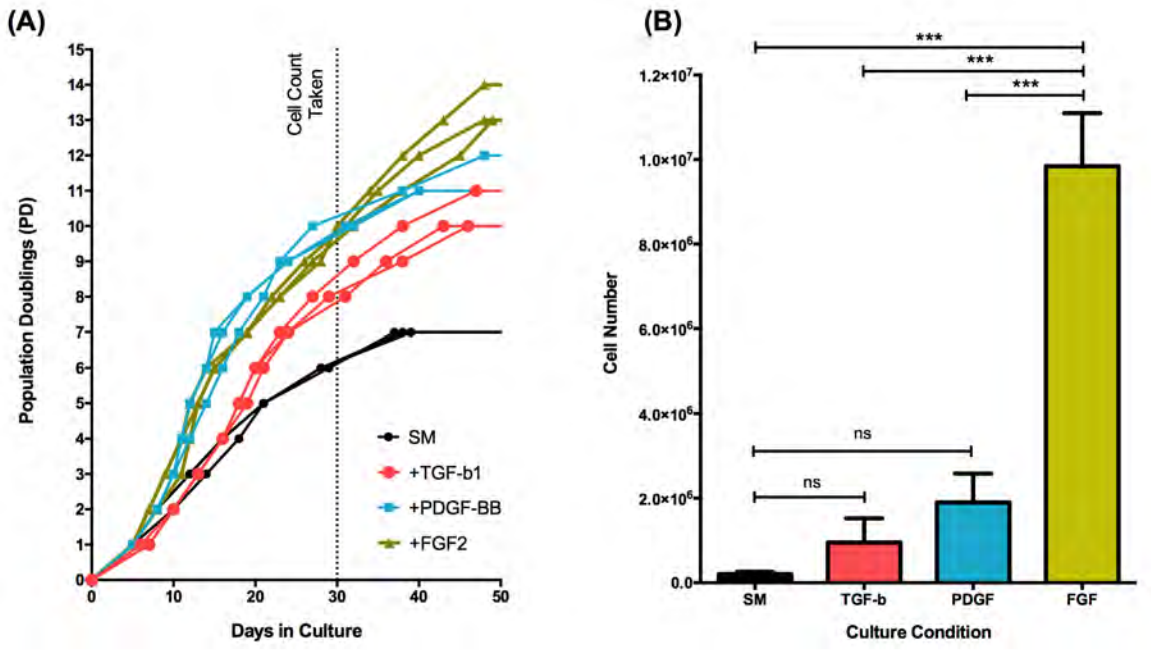


Figure 5.4 | **Effect of GF-supplementation on PαS MSC growth**. (A) Population doublings over 50 days. Each line represents an independent culture of cells, n=3 biological repeats per condition. (B) Cell counts taken at day 30 post seeding. Data shown as mean±SD, n=3 biological repeats per condition. Statistical analysis performed using One-way ANOVA with Bonferroni's Multiple Comparison Test.

### 5.2.2 Effect of GF-supplementation on PαS MSC Senescence

SA-β-gal staining was performed on days 30 and 50 to identify whether increased proliferation was due to a reduction in senescence. Aged cells in SM, PDGF-BB and TGF-β1 groups displayed a shift in morphology towards larger, flatter cells (Figure 5.5A arrowheads). In contrast, FGF supplemented MSCs remained small and retained a spindle-shaped morphology. The percentage of SA-β-gal$^{+}$ MSCs were then quantified at both time points (Figure 5.5B). At day 30, significant drops in the number of SA-β-gal$^{+}$ MSCs were observed in FGF2 and TGF-β1 supplemented cultures compared to SM, and a non-significant reduction was also seen in PDGF-supplemented cells. An increase in the number of senescent cells was

seen across all groups at day 50, but GF-supplemented cultures had significantly lower numbers of SA-β-gal$^{+}$ MSCs compared to SM alone. These findings show that GF-treatment can delay the onset of senescence in PαS MSCs during *in vitro* expansion and could explain the improved proliferation seen in GF-supplemented cultures during growth curve analysis.

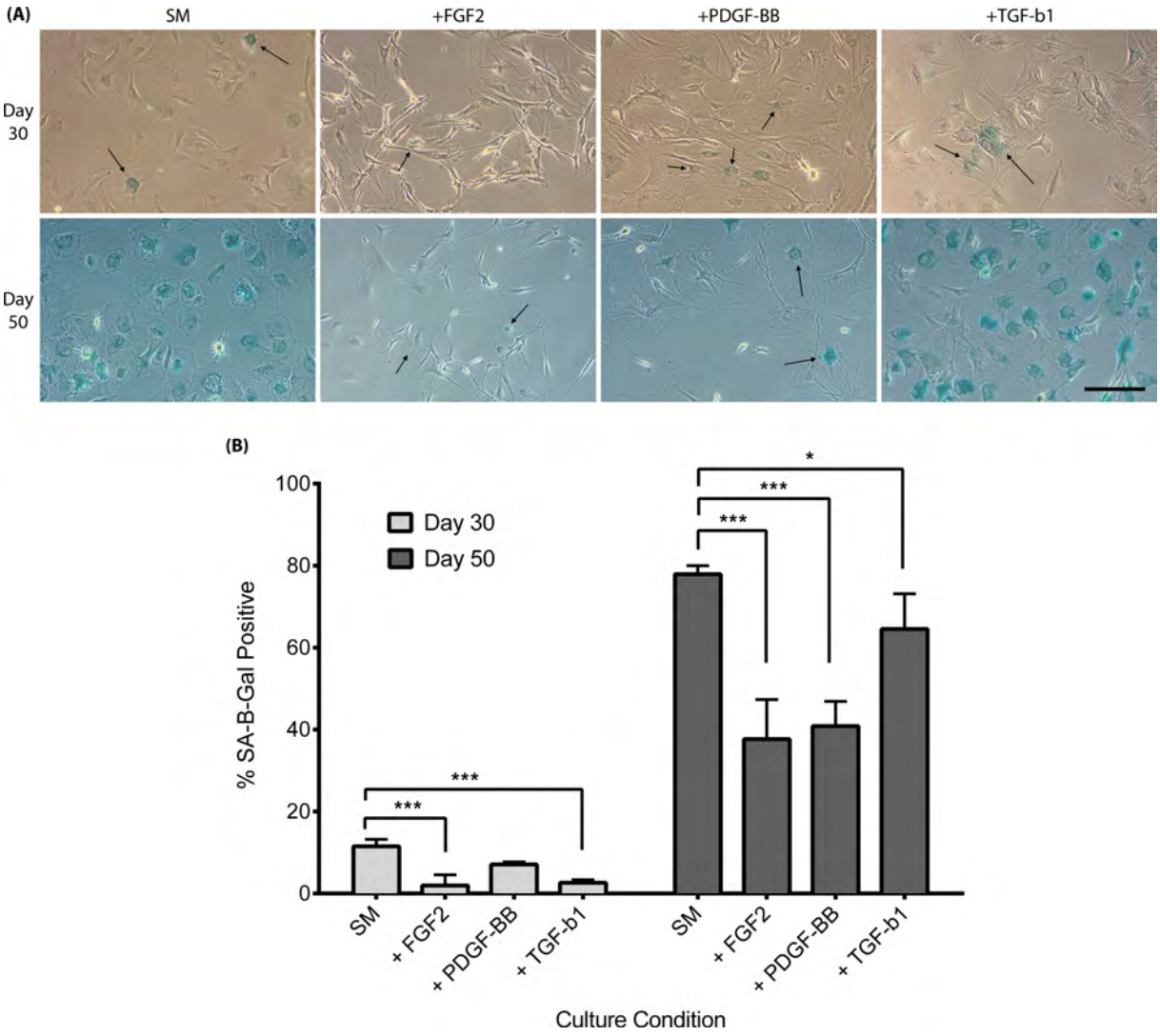


Figure 5.5 | **Effect of GF-supplementation on PαS MSC senescence**. (A) Representative images of SA-β-gal staining. Arrowheads pick out cells of interest/senescent cells. Images taken at 100x magnification. Bar, 20µm. (B) Quantification of SA-β-gal staining from 10 fields of view per sample, 3 to 6 samples per condition. Data represented as mean±SD. Statistical analysis performed using One-way ANOVA with Bonferroni's Multiple Comparison Test.

### 5.2.3 Karyotypic Stability of PαS MSCs

Prolonged *in vitro* expansion can predispose MSCs towards malignant transformation, a phenomenon that preferentially affects murine cells (Rangarajan et al., 2004). The karyotypic stability of PαS MSCs has not been reported previously. Our data demonstrates that GF-supplementation increases the proliferation (Figure 5.4A) and lowers the senescence (Figure 5.5B) of PαS MSCs, which could be possible signs of immortalisation (Miura et al., 2006). Chromosome analysis was therefore performed on P3 and P5 PαS MSC cultures to observe whether GF-treatment had a detrimental effect on the chromosomal stability of these cells (Methods Figure 2.4).

Giemsa-banding (G-banding) chromosome analysis and chromosome breakage studies were performed in collaboration with Mary Strachan, Dr Sara Dyer and Prof. Mike Griffiths at the West Midlands Regional Genetics Laboratory, Birmingham. A total of 60 metaphase spreads each of P3 and P5 MSCs cultured in SM±GFs were analysed. The number of gross chromosomal abnormalities (changes in the total number of chromosomes) was quantified (Figure 5.6A). Representative examples of PαS MSC karyograms can be seen in Figure 5.7. 93% (56/60 metaphase spreads) of PαS MSCs grown in SM at P3 had a normal mouse karyotype of 40, XY. Data for P5 cells in SM are still under analysis. PDGF-supplemented PαS MSCs had slightly higher numbers of karyotypically normal metaphase spreads at P3 (95%; 57/60) and P5 (92%; 55/60). FGF-supplemented cultures were 100% normal at both P3 and P5 for all 60 metaphase spreads analysed. By comparison, TGF-β1 supplemented PαS MSCs had a slightly reduced number of karyotypically normal metaphase spreads at P3 (85%;

51/60) compared to all other culture conditions. By P5, this percentage had dropped even lower to reach 61% (37/60). Interestingly, all samples with abnormal chromosomal numbers were cases of tetraploidy (80, XXYY; Figure 5.7D). Tetraploidy is frequently observed in non-neoplastic tissues (e.g. heart and liver) as part of terminal differentiation and it has been estimated that tetraploid cells can be found at a frequency between 0.5-20% in humans (Storchova and Kuffer, 2008). Conversely, tetraploidisation is also part of the neoplastic process as changes in chromosome number are a hallmark of cancer (Albertson et al., 2003). Surprisingly, Shoshani et al. (2012) report that tetraploidisation acts as a protective mechanism against tumourigenesis in murine MSC cultures, but it remains to be seen whether this applies to PαS MSCs, particularly TGF-β1 supplemented cells. Importantly, there was no cytogenetic evidence of neoplastic transformation in SM or GF-supplemented cultures at P3 and P5, suggesting that these cells are more genetically stable than plastic-adherent murine MSCs.

Chromosome breakage analysis was also performed to examine DNA damage events that manifest as chromosome gaps or breaks in PαS MSCs (Figure 5.7E). P3 PαS MSCs grown in SM were 77% (46/60 metaphase spreads) normal (Figure 5.6B). The frequency of damaged cells was lower in all GF-supplemented groups at P3 and P5 compared to SM. Interestingly, damaged cells in PDGF-supplemented cultures exhibited quadriradial (QR) chromosome formation at P3 and P5 (Figure 5.7F). As these involved homologous chromosomes, QR chromosome formation may be indicative of an elevated level of sister chromatid exchanges. QR chromosomes are formed when chromatid breaks in two separate chromosomes are

misrepaired and joined together (Joenje and Patel, 2001). The presence of QR chromosomes is elevated in genetic instability diseases such as Bloom's syndrome (Singh et al., 2010) and Fanconi's anaemia (Joenje and Patel, 2001). Further studies are required to fully understand why the presence of QR chromosomes is found PDGF-supplemented cultures only.

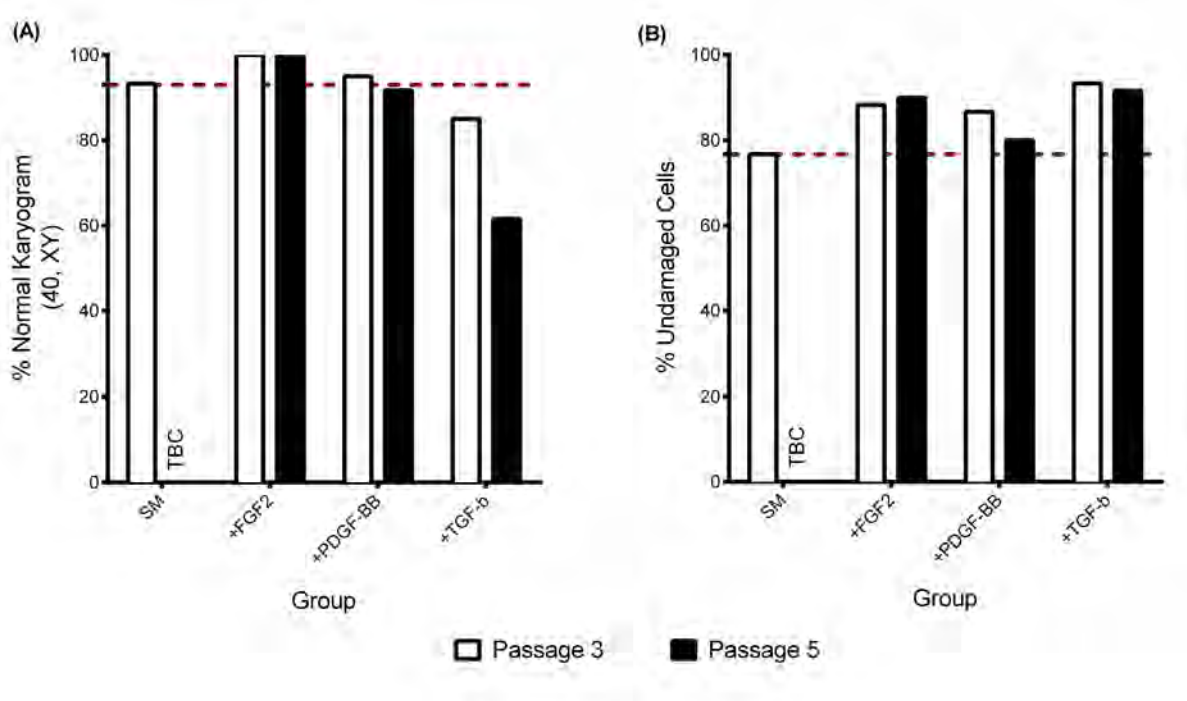


Figure 5.6 | **Quantification of chromosomal abnormalities in PαS MSCs**. 60 metaphase spreads were analysed per culture conditions at each time point. (A) The number of metaphase spreads containing the normal mouse male karyogram of 40, XY was quantified and expressed as a percentage. (B) The number of metaphase spreads displaying structural abnormalities was quantified and expressed as a percentage. TBC, to be confirmed.

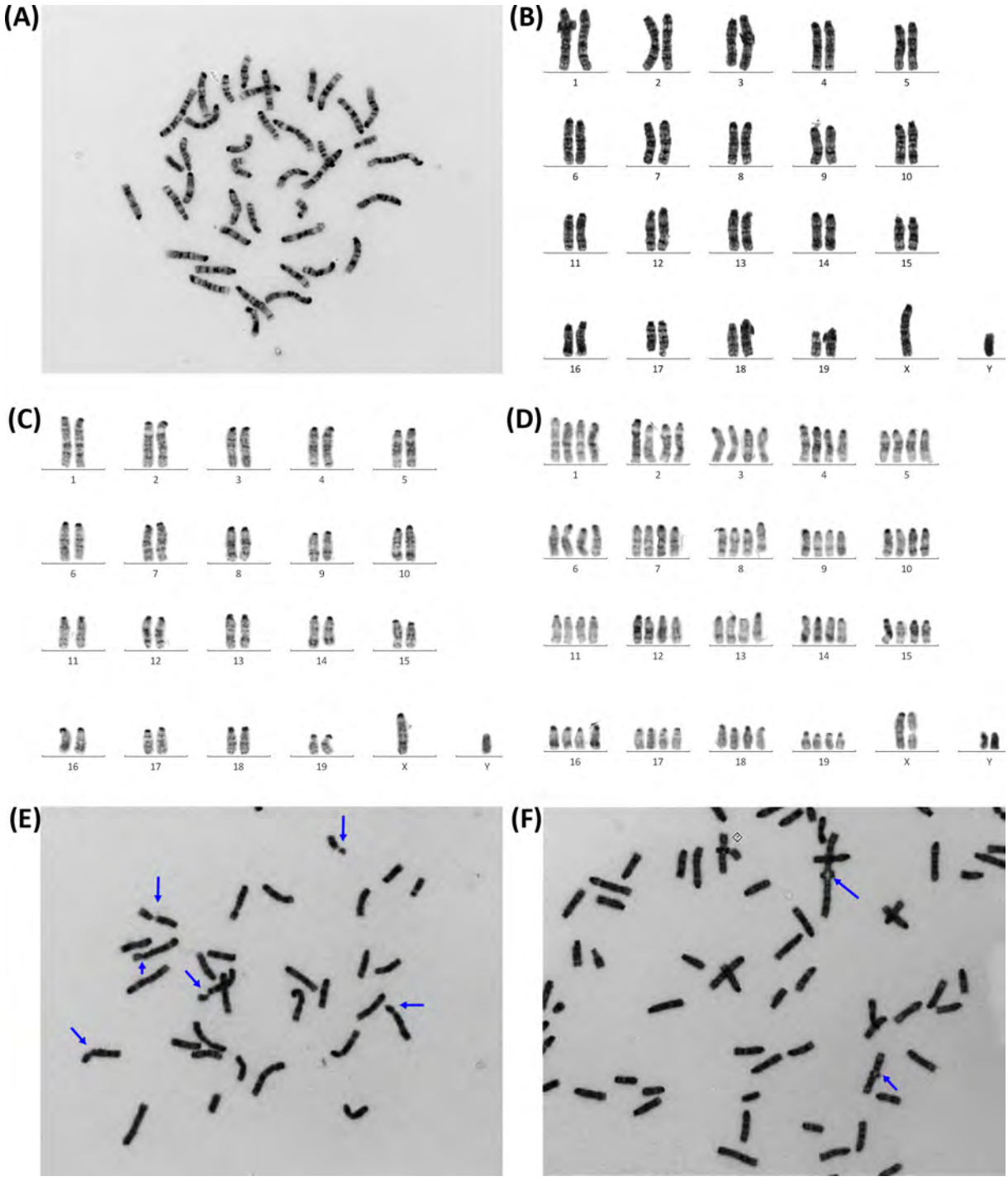


Figure 5.7 | **Representative images of PαS MSC karyotype analysis**. (A) Giemsa stained metaphase spread from P3 PDGF supplemented PαS MSCs. (B) Ordering of homologous chromosomes from a P3 PDGF culture to form a karyogram with a normal karyotype of 40, XY. (C) Representative karyogram from P5 FGF-supplemented cells with a normal karyotype of 40, XY. (D) Image showing a tetraploid (80, XXYY) metaphase spread form a P5 TGF-b supplemented cell. (E) Image showing locations of chromosome breaks and gaps (arrowheads) in a P5 PDGF-supplemented cell. (F) Image showing quadriradial chromosome formation (arrowheads) in a P5 PDGF-supplemented cell.

### 5.2.4 Genomic Analysis of 'Lineage Priming'

#### 5.2.4.1 Summary of Differentially-expressed Genes

Delorme and colleagues identified that MSCs express a subset of genes related to the osteogenic, adipogenic and chondrogenic lineages irrespective of any differentiation-inducing stimuli, suggesting that MSCs are naturally 'primed' towards these lineages (Delorme et al., 2009). The findings of Ng et al. (2008) demonstrate that the FGF, PDGF and TGF-β signalling pathways are active during human MSC differentiation down certain lineages (Figure 5.1). We hypothesised that the addition of their respective ligands could prime PαS MSCs down a specific lineage while maintaining them in a proliferative, undifferentiated state. Thus, when any differentiation inducing stimuli is introduced, PαS MSCs would readily differentiate towards the lineage they have been 'primed' towards.

Whole-genome murine microarrays were performed to examine whether lineage priming occurred in PαS MSCs following culture in GF-supplemented medium compared to SM controls. RNA was isolated from undifferentiated, P1 cultures (Table 5.1) and hybridised onto Affymetrix mouse genome arrays containing a total of 21,156 genes. Twelve independent PαS MSC cultures from C57BL/6 mice were used to isolate RNA samples. They were then hybridised onto separate microarrays for analysis. RNA workup and hybridisation was performed by the Affymetrix Array Service at the University of Birmingham.

Table 5.1 | **Properties of RNA samples used for whole-genome microarray analysis.**

| Culture Condition | Sample | Total RNA (µg) | OD260/280 | OD260/230 |
|---|---|---|---|---|
| **SM** | 1 | 3.88 | 2.11 | 2.01 |
| | 2 | 2.27 | 2.15 | 1.71 |
| | 3 | 1.87 | 2.22 | 1.80 |
| **+FGF2** | 1 | 4.49 | 2.13 | 2.12 |
| | 2 | 5.94 | 2.11 | 2.17 |
| | 3 | 4.77 | 2.11 | 2.26 |
| **+PDGF-BB** | 1 | 2.73 | 2.09 | 1.84 |
| | 2 | 5.03 | 2.07 | 2.13 |
| | 3 | 5.21 | 2.09 | 2.09 |
| **+TGF-β1** | 1 | 3.70 | 2.09 | 1.86 |
| | 2 | 11.64 | 2.03 | 2.17 |
| | 3 | 5.94 | 2.10 | 2.14 |

Scanned images of microarrays were analysed using Affymetrix software. Genes with a fold change >1.0 and P<0.001 were classed as 'significantly differentially expressed' in accordance with Smyth (2004). In FGF-supplemented PαS MSCs, 14.5% (3060/21,156) genes were differentially expressed compared to SM controls, with 1567 genes upregulated and 1493 genes downregulated (Figure 5.8). PDGF-supplemented PαS had differential expression in 8.1% (1707/21,156) genes compared to SM controls, with 748 genes upregulated and 959 downregulated. TGF-β-supplemented PαS MSCs also had differential expression in 8.1% (1711/21,156) genes compared to SM controls, with 597 genes upregulated and 1114 genes downregulated.

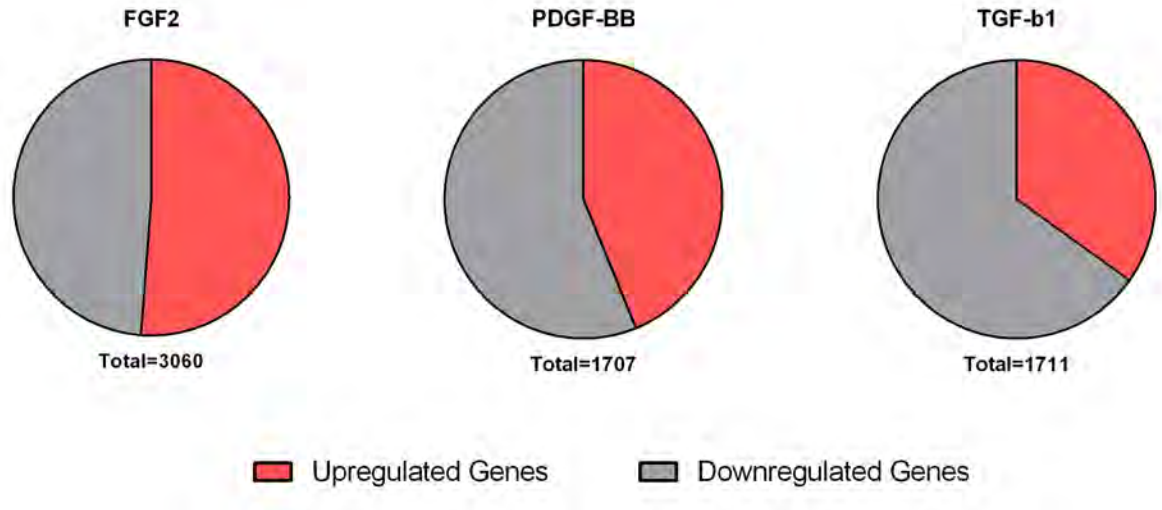


Figure 5.8 | **Summary of up- and down-regulated genes in GF-supplemented PαS MSCs**. Genes with a fold change of >1.5 and a p-value <0.001 compared to SM cultures were quantified and expressed as a percentage. The total number of differentially regulated genes can be found below the pie chart.

Gene ontology analysis was performed to gain a better understanding of the biological relevance of differentially regulated genes in PαS MSC cultures. The Gene Ontology Consortium database (www.geneontology.org) was queried using the "PANTHER" classification system (www.pantherdb.org) to produce a list of annotated biological processes (Mi et al., 2013). The top five up and down-regulated biological processes for each culture condition can be found in Table 5.2. Interestingly, we observed similar biological processes (e.g. signal transduction, cell adhesion, cell communication) being upregulated in all GF-supplemented cultures compared to SM. Similarly, genes related to DNA and RNA processing were downregulated in all GF-supplemented cultures compared to SM.

Table 5.2 | **PANTHER Gene Ontology Analysis.** Top 5 upregulated and downregulated biological processes shown.

| Sample | Biological Process (Upregulated) | Differentially expressed genes | P value | Biological process (Downregulated) | Differentially expressed genes | P value |
|---|---|---|---|---|---|---|
| **FGF2 vs. SM** | Signal transduction | 916 | $1.71e^{-27}$ | Response to pheromone | 3 | $1.19e^{-11}$ |
| | Cell communication | 946 | $1.25e^{-26}$ | RNA metabolic process | 43 | $1.10e^{-08}$ |
| | Cell adhesion | 356 | $2.44e^{-25}$ | mRNA processing | 23 | $1.61e^{-08}$ |
| | Immune system process | 605 | $1.82e^{-23}$ | Nucleoside, nucleotide and nucleic acid metabolic process | 444 | $5.68e^{-08}$ |
| | Cell-cell adhesion | 236 | $6.22e^{-21}$ | Nuclear mRNA splicing, via spliceosome | 20 | $1.28e^{-06}$ |
| **PDGF-BB vs. SM** | Signal transduction | 607 | $3.64e^{-39}$ | Nucleoside, nucleotide and nucleic acid metabolic process | 224 | $3.96e^{-09}$ |
| | Cell communication | 623 | $7.37e^{-38}$ | Translation | 10 | $3.14e^{-07}$ |
| | Cellular process | 758 | $9.29e^{-30}$ | RNA metabolic process | 21 | $1.03e^{-06}$ |
| | Immune system process | 399 | $8.95e^{-29}$ | mRNA processing | 11 | $2.60e^{-06}$ |
| | Cell adhesion | 241 | $3.49e^{-28}$ | Nuclear mRNA splicing, via spliceosome | 10 | $7.25e^{-05}$ |
| **TGF-β vs. SM** | Cell communication | 624 | $1.35e^{-36}$ | Nucleoside, nucleotide and nucleic acid metabolic process | 226 | $2.87e^{-09}$ |
| | Signal transduction | 603 | $1.97e^{-36}$ | RNA metabolic process | 19 | $1.05e^{-07}$ |
| | Immune system process | 402 | $1.05e^{-28}$ | mRNA processing | 12 | $6.19e^{-06}$ |
| | Cell adhesion | 236 | $1.00e^{-25}$ | DNA metabolic process | 17 | $2.71e^{-05}$ |
| | Cellular process | 738 | $2.21e^{-23}$ | Response to pheromone | 4 | $2.77e^{-05}$ |

### 5.2.4.2 Selection of lineage specific genes

To examine whether 'lineage priming' of PαS MSCs occurred, the expression of key genes related to osteogenic, adipogenic and chondrogenic lineages were examined in GF-supplemented PαS MSCs prior to the induction of differentiation. Candidate genes for all three lineages were prospectively chosen from previous literature (Delorme et al., 2009, Ng et al., 2008, Gesta et al., 2007, Engler et al., 2006, Goldring et al., 2006, Komori, 2006a). Selected genes were then split into two groups to identify the master regulators that have a fundamental role in the differentiation process and downstream effectors that have a less crucial role in the pathway (Table 5.3).

Table 5.3 | **List of lineage specific candidate genes chosen for analysis.**

| Lineage | Master Regulators | Downstream Effectors |
|---|---|---|
| **Bone** | *Runx2*<br>*Sp7 (Osterix)* | *Alpl, Atf4, Bgn, Bmp4, Bmp6, Bmp6, Bmpr1a, Cbfb, Cebpb, Col1a1, Col1a2, Comp, Csf1, Dcn, Dkk2, Dlx5, Dlx6, Egr2, Esr1, Ets1, Gata1, Gata2, Gata3, Ibsp, Igf1, Il18, Jun, Kitl, Lifr, Men1, Msx1, Msx2, Ogn, Opg, Opn, Pthr1, Smad1, SP3, Thy1, Tnfsf11, Wisp1,Wisp2, Znf145.* |
| **Fat** | *Cebpa*<br>*Pparg* | *Adfp, Adipoq, Angptl4, Aoc3, Apoe, Apol6, Aqp7, CD24, Col6a2, Cspg4, Dlk1, Fabp4, Fgf1, Fgf10, Fgf16, Fgf19, Flrt3, Gata3, Gli3, Gpc4, Gpd1, Hoxa10, Hoxa5, Hoxc8, Hoxc9, Lpl, Mrap, Nodal, Nr2f1, Pdgfrb, Plin1, Rxra, Sfrp2, Slco2a1, Smo, Srebf1, Twist1.* |
| **Cartilage** | *Sox5*<br>*Sox9* | *Agc1, Bmp2, Bmp4, CDRAP, Cebpb, Col10a1, Comp, Ctnnb1, Fgf10, Fgfr3, Gli3, Hapln1, HoxA, HoxD, Hoxd11, Hoxd13, Mapk1, Mapk14, Mapk3, Mef2c, Nkx3.2, Plzf, Ptch1, Pthr1, Rankl, Runx3, Smad1, Smad5, Smad8, Smo, Sox6, Tfap2a, Wnt2, Wnt2c.* |

### 5.2.4.3 Expression of Osteogenic Candidate Genes

Raw expression values for osteogenic lineage genes were converted into heatmaps for visual analysis (Figure 5.9). Heatmap generation was performed by Dr Wenbin Wei, University of Birmingham. Microarray analysis revealed that major transcripts of the osteogenic program were highly expressed in undifferentiated PαS MSCs cultured in SM in the absence of any differentiation-inducing stimuli (Figure 5.9A). This included the master regulators of osteogenesis, *Runx2* and *Sp7* (*Osterix*). FGF and PDGF-supplemented PαS MSCs expressed significantly less *Runx2* (FGF 1.31 fold decrease, PDGF 1.30 fold decrease, $p<0.01$) and all three GFs expressed less *Sp7* (FGF 1.7 fold decrease, PDGF 1.68 fold decrease, TGF-β 2.25 fold decrease, $p<0.01$) compared to control SM cells. This suggests that culture in SM primes MSCs down the osteogenic lineage, and could explain why we saw increased bone differentiation of PαS MSCs at later passages (Chapter 4, Figure 4.3).

Further proof of osteogenic priming in SM cultures can be observed when examining the expression of downstream effector genes. A large group of genes including *Alpl* (alkaline phosphatase), *Ogn* (osteoglycin), *Comp* (cartilage oligomeric matrix protein), *Bmp4* (bone morphogenetic protein 4) and *Dlx5* (distal-less homeobox 5) were significantly upregulated in SM cultures compared to GF-supplemented PαS cells. However, not all candidate genes were highly expressed by SM cells, as some may require osteogenic induction prior to expression. Furthermore, they may also have other roles in maintaining cellular homeostasis in addition to their roles during bone formation and maturation.

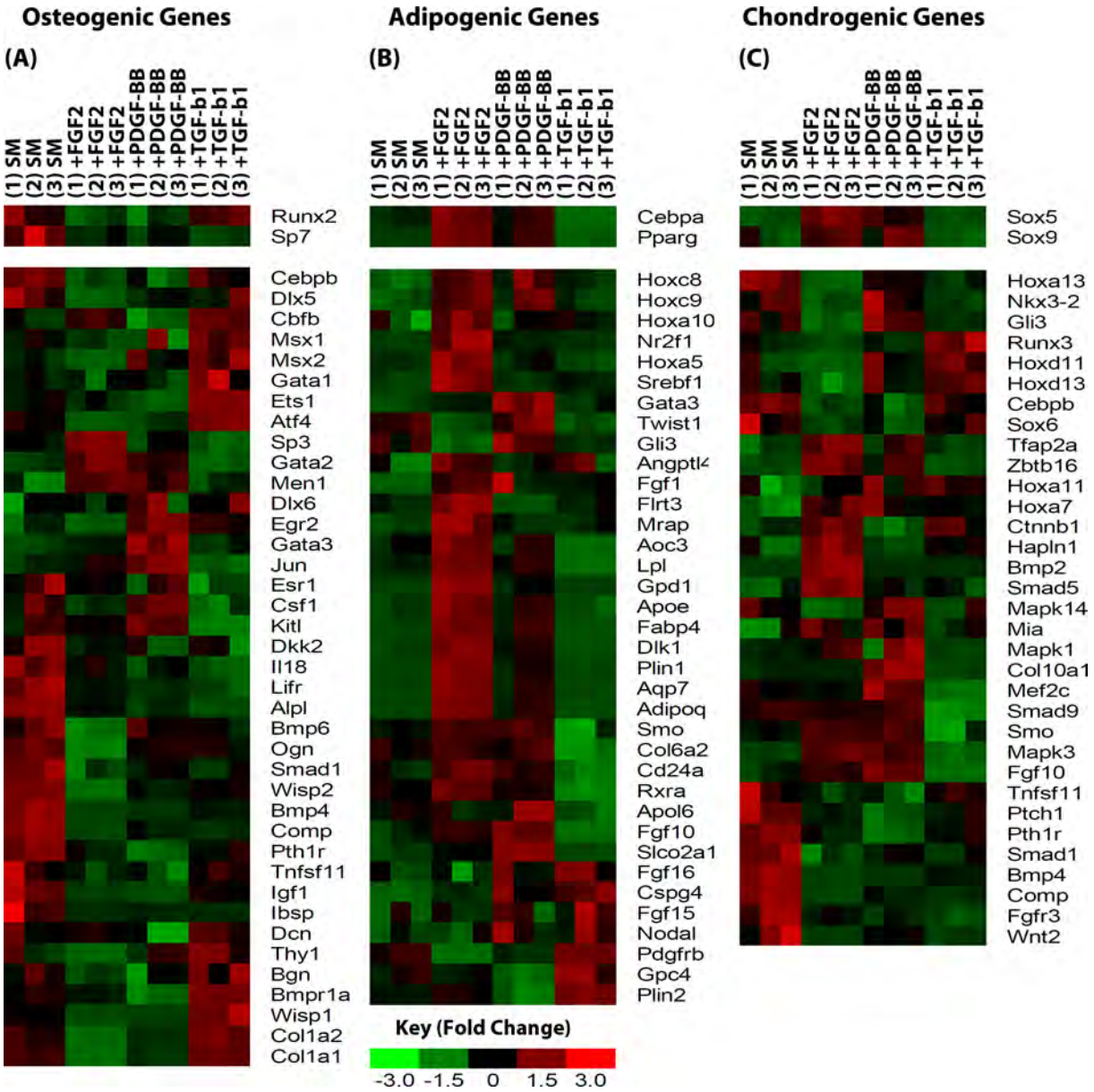


Figure 5.9 | **Microarray heatmap of lineage priming in PαS MSCs.** RNA isolated from undifferentiated, P1 PαS MSCs grown in SM±GFs were hybridised onto separate Affymetrix whole genome microarrays (n=3 per condition). The expression of key (A) osteogenic, (B) adipogenic, and (C) chondrogenic genes were examined. The mean expression value for each gene across all samples was set as 0 (black box). A relative fold decrease in gene expression (compared to the mean) is represented by a green square, and a relative fold increase is represented by a red square.

### 5.2.4.4 Expression of Adipogenic Candidate Genes

Analysis of adipogenic lineage genes revealed that key transcripts of this pathway were highly expressed in undifferentiated FGF and PDGF-supplemented PαS MSCs (Figure 5.9B). These included master regulators *Cebpa* (FGF 2.55 fold increase, PDGF 1.70 fold increase, $p<0.01$) and *Pparg* (FGF 4.53 fold increase, PDGF 2.97 fold increase, $p<0.0001$), which were highly significantly upregulated compared to SM cultures. In contrast, TGF-β supplemented PαS MSCs expressed *Cebpa* (3.33 fold decrease, $p<0.0001$) and *Pparg* (3.24 fold decrease, $p<0.0001$) at much lower levels than SM cultures, suggesting that culture in TGF-β may inhibit the adipogenic differentiation of MSCs.

Analysis of downstream effector genes provides further proof of adipogenic priming in FGF and PDGF-supplemented PαS MSC cultures. These include the homeobox genes *Hoxc8*, *Hoxc9* and *Hoxa10*, which are all involved in the development of adipose tissue (Cantile et al., 2003). Interestingly, a subset of mature adipocyte genes such as *Adipoq* (adiponectin), *Lpl* (lipoprotein lipase), *Plin1* (perilipin 1) and *Apoe* (apolipoprotein E) are further enriched in FGF-supplemented samples compared to PDGF-supplemented cultures. We did not observe any spontaneous differentiation towards fat in FGF-supplemented cultures, and further work is required to understand the significance of mature adipocyte gene expression in undifferentiated PαS MSCs in the presence of FGF. Taken together, this data suggests that PαS MSCs expanded in FGF- and, to a lesser extent, PDGF-containing medium are primed towards the adipogenic lineage.

### 5.2.4.5 Expression of Chondrogenic Candidate Genes

Analysis of chondrogenic lineage genes revealed higher expression of key transcripts in FGF and PDGF-supplemented PαS MSCs (Figure 5.9C). Undifferentiated FGF and PDGF-supplemented cultures had higher expression of the master regulators of chondrogenesis, *Sox9* (FGF 1.42 fold increase, PDGF 1.38 fold increase, $p<0.05$) and *Sox5* (FGF 4.56 fold increase, PDGF 3.28 fold increase, $p<0.0001$), compared to un-supplemented SM cultures. They also had significantly upregulated expression of downstream effectors including *Hoxa11*, *Hoxa7*, *Bmp2* and *Hapln1* (hyaluronan and proteoglycan link protein 1) compared to SM cultures, suggesting potential priming towards the chondrogenic lineage.

Analysis of other downstream effector genes gave mixed results, with different culture conditions highly expressing different clusters of chondrogenic genes. For example, PαS MSCs cultured in SM expressed high levels of *Hoxa13* and *Nkx3-2* compared to all other samples, but had low expression of master regulators *Sox9* and *Sox5*. TGF-β supplemented cultures also expressed low levels of *Sox9* and *Sox5*, but had high expression of chondrocyte maturation genes *Hoxd11*, *Hoxd13* and *Runx3* (Soung do et al., 2007). These mixed findings suggest that it is relatively more difficult to prime MSCs down the chondrogenic lineage, and this could be one reason behind why differentiating MSCs down the chondrogenic lineage has always been more technically demanding than the osteogenic or adipogenic lineages (Vinatier et al., 2009).

### 5.2.5 Phenotypic Analysis of 'Lineage Priming'

#### 5.2.5.1 Effect of GFs on Osteogenic Differentiation

Genomic analysis of lineage-specific genes revealed that culture conditions could have a profound effect on MSC gene expression. PαS MSCs grown in SM highly expressed master regulators of osteogenic differentiation compared to GF-supplemented cells (Figure 5.10). FGF and PDGF-supplemented PαS MSCs expressed significantly higher levels of adipogenic and chondrogenic master regulators compared to SM and TGF-β supplemented cultures. Interestingly, TGF-β supplemented PαS MSCs did not display evidence of priming towards any lineage, suggesting that addition of TGF-β may inhibit their differentiation.

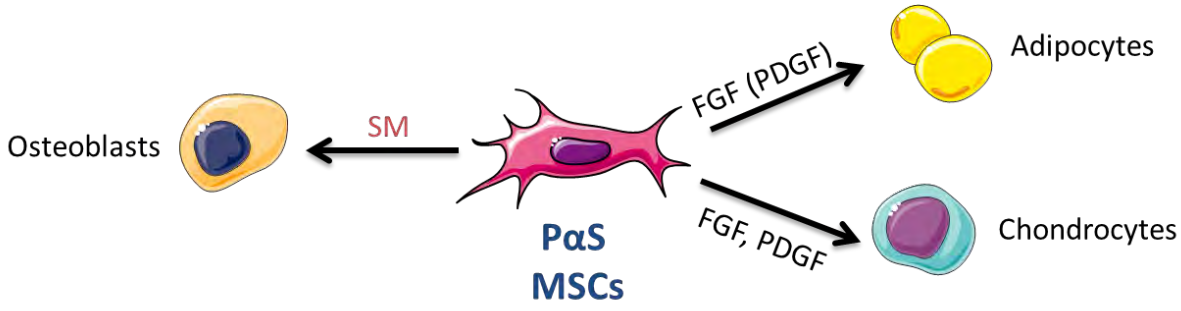


Figure 5.10 | **Summary of microarray analysis of lineage priming in PαS MSCs**. Undifferentiated, P1 PαS MSCs expressed more osteogenic transcripts when grown in SM. FGF2 and, to a lesser extent, PDGF-BB supplemented cells expressed more adipogenic genes. Master regulators of chondrogenesis were equally upregulated in FGF2 or PDGF-BB supplemented cells.

To test our hypothesis of lineage priming and to provide phenotypic evidence to back up our microarray data, PαS MSCs were grown ± GFs and induced to differentiate towards bone, fat and cartilage. GF treatment was stopped and cells were thoroughly washed before differentiation to ensure any changes between groups were due to the 'priming' effect of GFs during the PαS MSC expansion stage only (Methods Figure 2.1).

Osteogenic differentiation was induced for 16 days before being stained using alizarin red. Visual inspection showed reduced alizarin red staining in GF-primed MSCs compared to SM (Figure 5.11). In particular, TGF-β1 primed MSCs had substantially less calcium deposition compared to all other culture conditions. After imaging, the dye was extracted from the stained monolayer and quantified against known calcium standards (Figure 5.12). PαS MSCs expanded in SM produced significantly more calcium than GF-supplemented cultures at P0, P1, P3, P4 and P5, with the mean difference increasing at later passages. Interestingly, there seems to be an overall trend for increased osteogenic differentiation at later passages across all culture conditions, which suggests that extended culture on plastic is an independent promoter of bone differentiation.

These findings strongly support the concept of osteogenic lineage priming in PαS MSCs. Our microarray data showed increased expression of key osteogenic transcripts in undifferentiated MSCs grown in SM. When induced to undergo differentiation, PαS MSCs expanded in SM readily underwent osteogenic differentiation and produced significantly more calcium than their GF-supplemented counterparts.

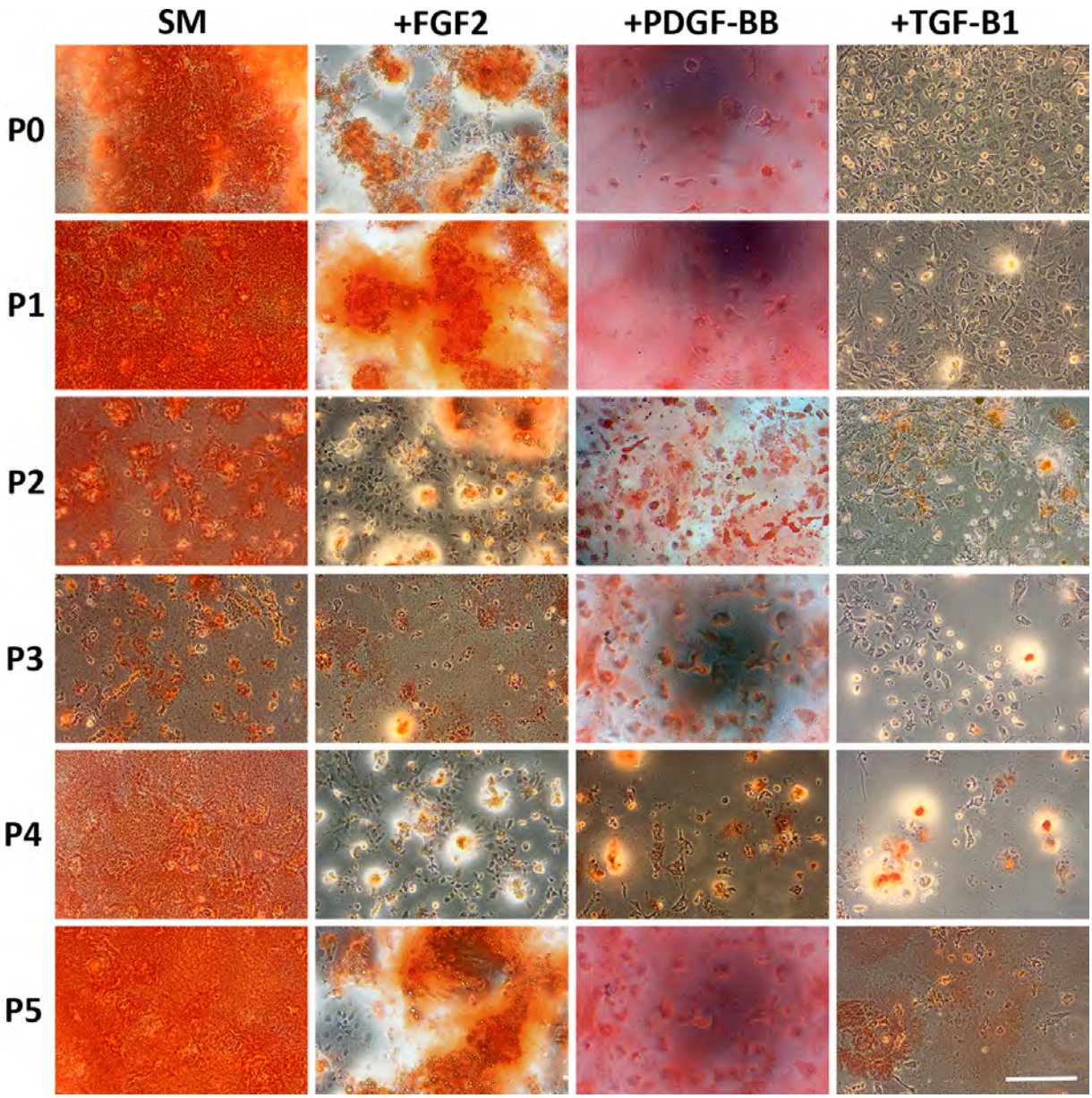


Figure 5.11 | **Osteogenic priming of PαS MSCs expanded in SM**. Representative images of alizarin red staining of PαS MSCs grown in SM±GFs at different passage numbers (n≥4 technical repeats per condition at each passage). All images taken at 100x magnification. Bar, 25µm.

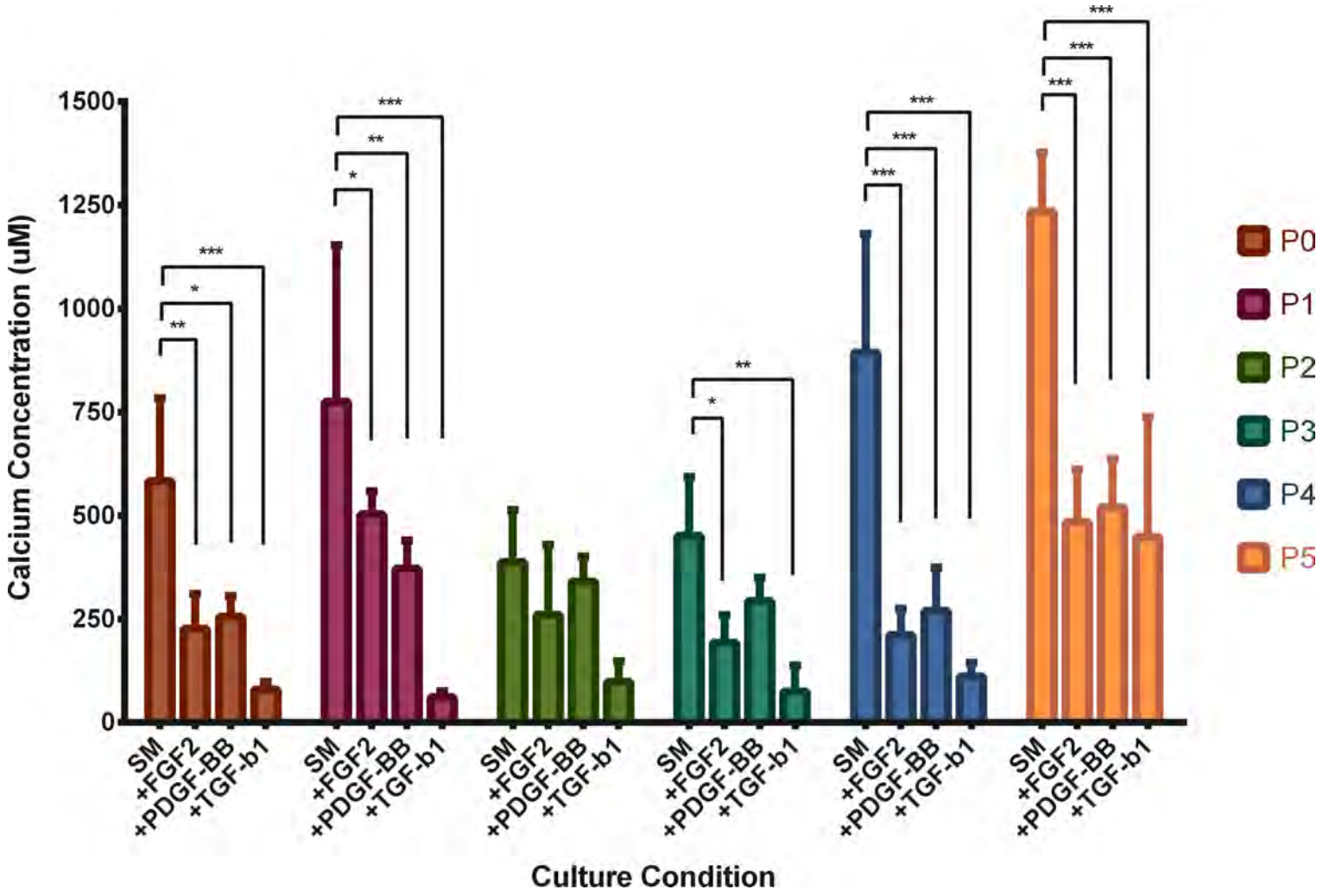


Figure 5.12 | **Quantification of calcium in PαS MSC osteogenic differentiation cultures**. Alizarin red dye was removed from all samples after imaging and quantified against known calcium standards. Data shown as mean±SD, n≥4 technical repeats per culture condition at each passage number. Statistical analysis performed using Two-way ANOVA with Bonferroni's Multiple Comparison Test.

#### 5.2.5.2 Effect of GFs on Adipogenic Differentiation

Microarray analysis revealed that undifferentiated PαS MSCs expanded in FGF-2 and, to a lesser extent, PDGF-BB supplemented medium had significantly higher expression of master regulators and downstream effectors of adipogenesis. To test priming towards the adipogenic lineage, fat differentiation was induced in one cycle of commercially available 'induction' and 'maintenance' differentiation medium. This was shorter than the manufacturer's recommendation of three cycles as the addition of GFs had a profound impact on fat formation and cultures were undergoing necrosis due to excessive lipid droplet formation. After differentiation, cultures were fixed and stained using oil red O.

As was observed earlier, PαS MSCs expanded in SM underwent sporadic adipogenic differentiation at earlier passages, but this ability was lost from P3 onwards (Figure 5.13). However, the addition of FGF or PDGF profoundly increased the number of adipocytes formed, and this ability was maintained until P5. FGF supplementation in particular caused almost 100% differentiation into adipocytes at earlier passages. By comparison, TGF-β1 supplemented PαS MSCs again failed to undergo differentiation across all passages tested.

These findings demonstrate that FGF and PDGF supplementation were able to strongly induce and maintain adipogenic potential over several passages, even with a shortened protocol. Taken together with the gene expression data from the microarray, this differentiation data strongly supports the idea of adipogenic lineage priming in PαS MSCs.

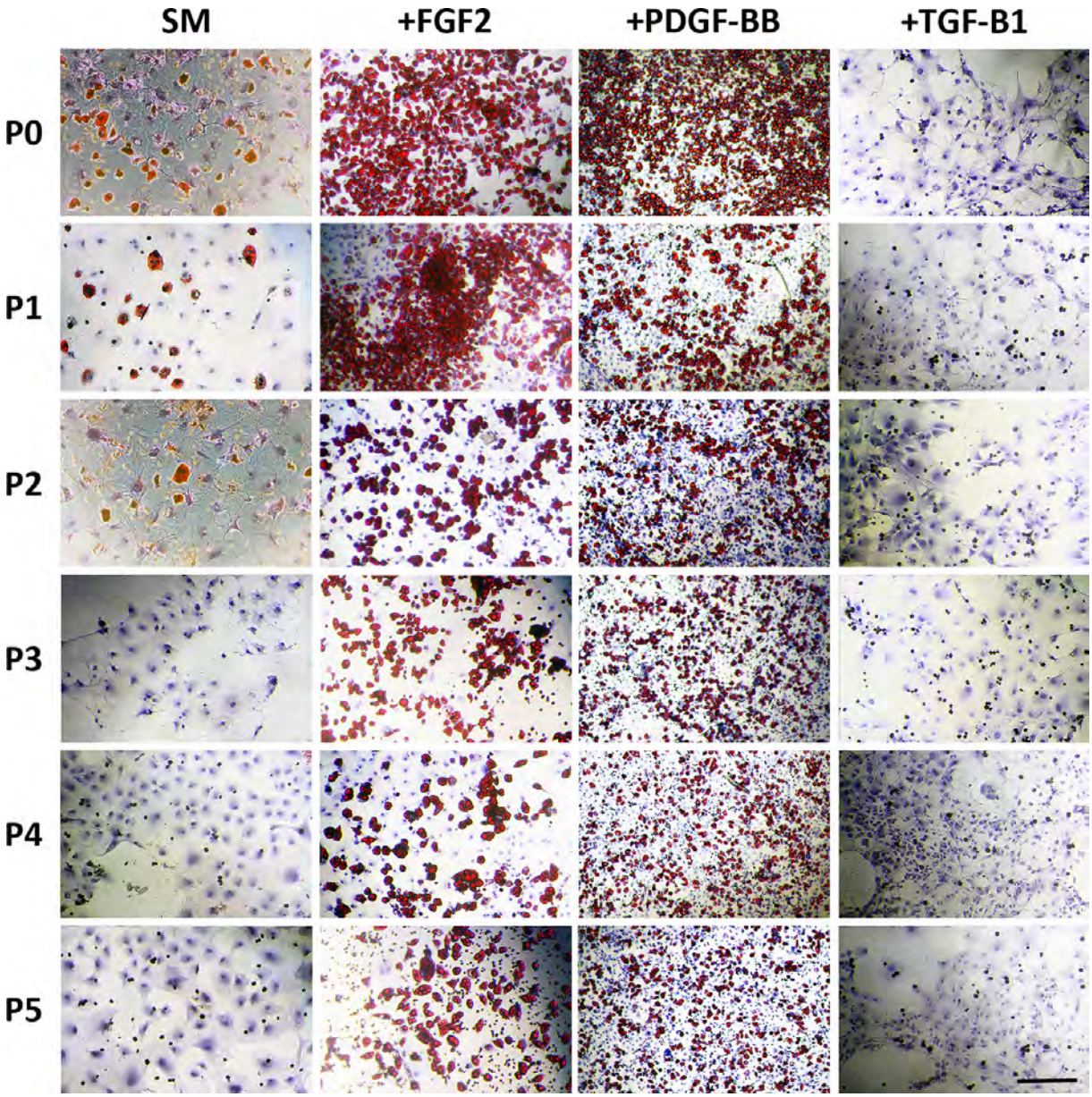


Figure 5.13 | **Adipogenic priming of PαS MSCs expanded in FGF or PDGF-supplemented medium**. Representative images of oil red O stained cultures showing lipid droplet formation in MSC cultures at different passage numbers (n≥3 technical repeats per condition at each passage). Samples were counterstained with haematoxylin to identify undifferentiated MSCs. Images taken at 100x magnification. Bar, 25µm.

### 5.2.5.3 Effect of GFs on Chondrogenic Differentiation

Genomic analysis of chondrogenic priming was less clear than the other two lineages, with different culture conditions highly expressing different clusters of genes. However, the master regulators *Sox9* and *Sox5* were significantly upregulated in undifferentiated FGF and PDGF-supplemented PαS MSCs. To examine the effect of GFs on chondrogenesis, micromass pellet systems were used in collaboration with the Hollander group at Bristol University.

Fixed numbers ($5x10^5$ MSCs/pellet) of P5 PαS MSCs expanded in SM±GFs underwent differentiation to form cartilage-like pellets. Significant increases in pellet weight could be observed in MSCs expanded in FGF or PDGF-containing medium compared to SM or TGF-β supplemented cells (Figure 5.14A). TGF-β primed MSCs made the smallest cartilage pellets by weight. Examination of total Col1 content, a marker of immature chondrocytes, in PαS MSC-derived cartilage pellets failed to show significant differences between groups (Figure 5.14B). Similarly, total levels of Col2, a marker of mature, healthy chondrocytes was similar between SM, FGF, and PDGF-supplemented MSCs (Figure 5.14C). TGF-β primed MSCs had the lowest Col2 content, but stopped short of reaching statistical significance. Examination of Col2:Col1 ratio, a marker of overall cartilage quality, showed similar readings in SM cultures compared to FGF and PDGF primed MSCs, but reached significance compared to TGF-β1 supplemented cells (Figure 5.14D). Analysis of GAG content showed FGF-primed cells produced the largest proteoglycan deposits across all four culture conditions, although this only reached statistical significance compared to TGF-β primed cells (Figure 5.14E).

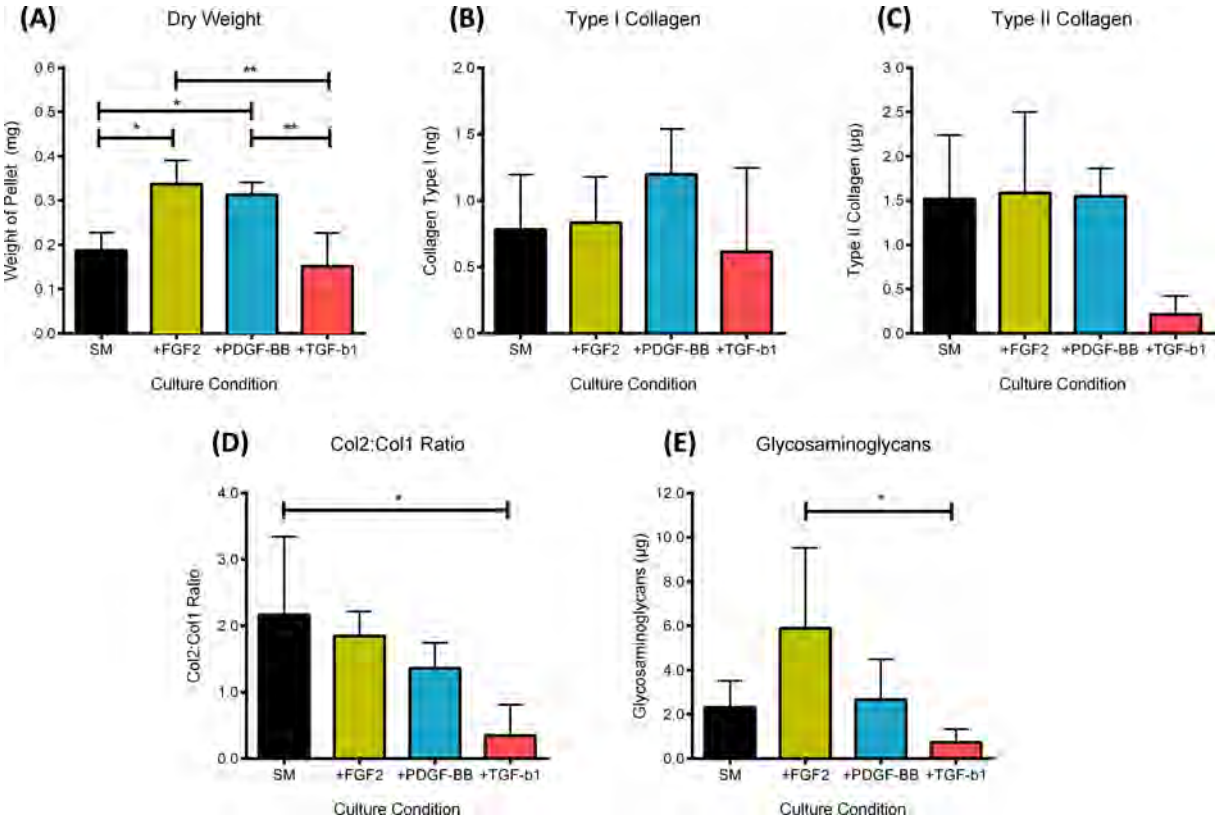


Figure 5.14 | **Effect of GFs on chondrogenic differentiation of PαS MSCs**. 5x10$^5$ PαS MSCs expanded in SM±GFs at P5 were induced to undergo chondrogenic differentiation in micromass pellet cultures. (A) The weight of MSC-derived cartilage pellets were recorded after freeze drying. (B) Total amount of type I and (C) type II collagen in MSC-derived cartilage pellets. (D) Ratio of Col2:Col1 as a marker of cartilage quality. (E) Total amount of GAGs present in MSC-derived cartilage pellets. Data shown as mean±SD, n≥3 independent samples per culture condition. Statistical analysis performed using One-way ANOVA with Bonferroni's Correction.

The lack of major differences between groups suggests that it is difficult to prime PαS MSCs down the chondrogenic lineage. In summary, MSCs expanded in TGF-β1 supplemented medium made the smallest pellets with a low Col2:Col1 ratio and GAG content. SM-expanded cells made cartilage pellets of similar quality to FGF and PDGF-supplemented cells, but their cartilage pellets were significantly smaller in size. MSCs expanded in FGF or PDGF-supplemented medium made pellets of equal size and collagen content, but FGF-primed MSCs had a greater GAG content.

#### 5.2.5.3.1 Tissue Engineered Cartilage from PαS MSCs

Injection of MSC-derived chondrocytes in suspension is feasible for the treatment of focal lesions, however, the treatment of larger injuries would necessitate the use of scaffolds to retain cells at the injury site for extended periods of time (Zhang et al., 2009). Immobilisation of MSCs on biodegradable scaffolds would ensure that cells are retained by the host long enough to produce enough ECM that bridges large, unconfined lesions. Additionally, the size of MSC-derived cartilage pellets made using micromass pellet cultures are suitable for *in vitro* studies, but are too small to be of practical value in animal models. To address this issue, cartilage tissue engineering experiments using PαS MSCs seeded onto fibronectin-coated biodegradable PGA scaffolds was performed as described by Kafienah et al. (2007). FGF-supplemented PαS MSCs were chosen for analysis as they had the greatest growth potential (Figure 5.4) and demonstrated robust chondrogenic differentiation in micromass pellet cultures (Figure 5.14). SM-expanded cells were used as controls.

Fixed numbers ($6x10^5$ cells) of PαS MSCs at P7 were used for tissue engineering studies. Seeded scaffolds were incubated in chondrogenic differentiation media on a rotating platform for 35 days during which the scaffold would dissolve, leaving behind MSC-derived ECM proteins. Macroscopic analysis after 35 days revealed the formation of shiny pink/white tissue that resembled hyaline cartilage (Figure 5.15A). Clear differences in size between SM-primed MSCs and FGF-primed MSCs could be seen. Samples were then freeze-dried, weighed, and digested in trypsin to solubilise ECM proteins prior to analysis. As suggested by its macroscopic appearance, significant increases in dry weight were observed between SM

and FGF-primed MSC samples (0.2±0.1mg vs. 1.0±0.4mg, p=0.002; Figure 5.15B). No significant differences were observed in the collagen content of tissue-engineered cartilage, although FGF-primed cells had a higher Col2:Col1 ratio than SM cells (0.8±0.3 vs. 5.4±7.0; p=0.1; Figure 5.15C-E). Finally, the proteoglycan content of FGF-primed cells was significantly higher than SM cultures (1.1±1.1µg vs. 9.3±2.7µg, p<0.0001; Figure 5.15F).

These studies demonstrate the value of PαS cells as a model MSC population for pre-clinical studies on cartilage repair. Compared to micromass pellet cultures (Figure 5.14), FGF-primed MSC tissue engineered cartilage was up to 4-fold heavier in size and had a 2-fold increase in collagen and proteoglycan content. These improvements were achieved with a small increase in MSC number, from $5x10^5$ cells per micromass pellet to $6x10^5$ cells per scaffold. Murine PαS MSC-derived cartilage can be tested in transgenic mouse models to fully understand and optimise conditions that promote optimal repair using MSCs (Chu et al., 2010). These findings could then be translated to produce novel tissue engineered cartilage therapies that improve on current methods used in human clinical trials (Delaere, 2013).

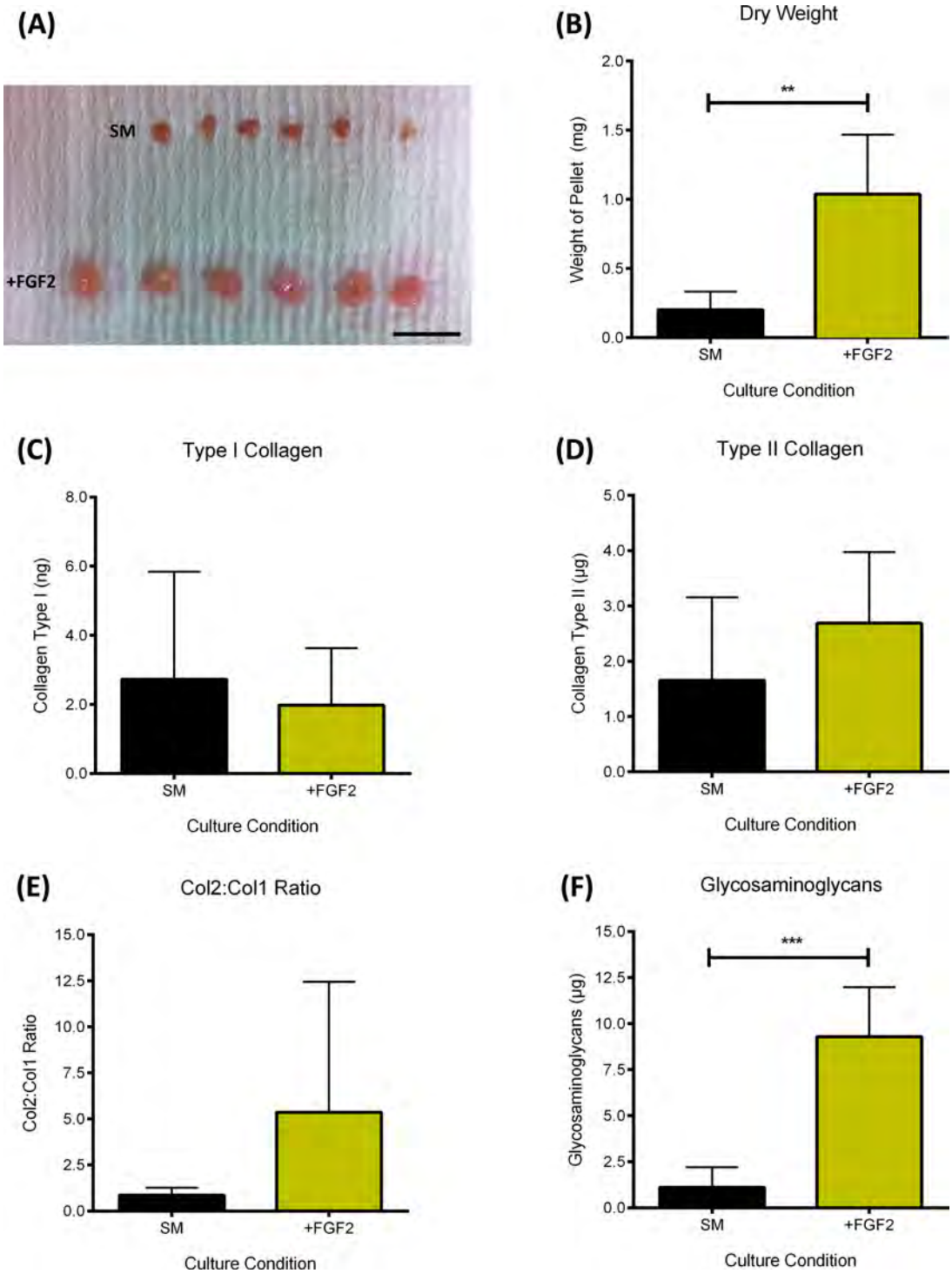


Figure 5.15 **| Tissue engineered cartilage using PαS MSCs**. Biodegradable PGA scaffolds were seeded with $6x10^5$ PαS MSCs expanded in SM±FGF2 at P7. (A) Macroscopic analysis of tissue engineered scaffolds after differentiation. Bar, 1cm. (B) The weight of tissue engineered cartilage was recorded after freeze drying. (C) Total amount of type I and (D) type II collagen in tissue engineered cartilage. (E) Ratio of Col2:Col1 as a marker of cartilage quality. (F) Total amount of GAGs present in tissue engineered cartilage. Data shown as mean±SD, n=5 for SM and n=8 for FGF2 samples. Statistical analysis performed using unpaired Student's T test.

### 5.2.6 Mechanism of GF Action

#### 5.2.6.1 Adipogenic priming by FGF2

Preliminary analysis of the signalling pathways involved in GF priming was performed using small molecule inhibitors. The FGF family contains 22 different FGF ligands which bind to 4 receptor tyrosine kinases (Ornitz and Itoh, 2001). The downstream signalling pathway after receptor dimerisation and activation are complex and involve recruitment of intracellular signalling proteins to the activated receptor complex (summarised in Figure 5.16). Activation of the receptor can lead to the activation of Src family kinases and further downstream signalling events (Cunningham et al., 2010). It can also lead to phosphorylation of the receptor associated docking protein Frs2. Frs2 can in turn recruit further downstream effectors, the two most prominent being the recruitment of Gab1 and activation of Akt kinase, or the recruitment of Grb2 and activation of Erk kinase (Eswarakumar et al., 2005).

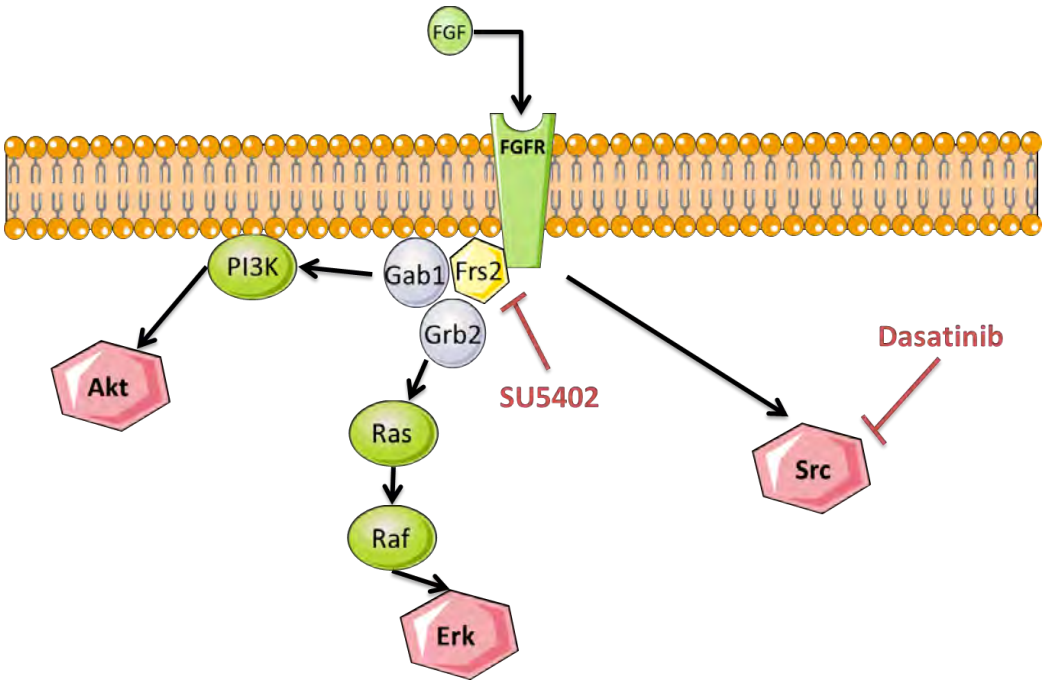


Figure 5.16 | **FGF signalling pathway**. Cartoon summarising the signalling pathways downstream of the FGF receptor and the proteins inhibited by the small molecule compounds used in this study.

Previously reported small molecule inhibitors of FGF signalling proteins were used to elucidate the downstream signalling pathways responsible for the adipogenic priming seen with FGF supplementation. The Src-family kinase pathway was inhibited using dasatinib, a compound currently used as a treatment for chronic myeloid leukaemia and under investigation for various other cancers (Montero et al., 2011, Buettner et al., 2008, Nam et al., 2005). The Frs2-dependent activation of Akt or Erk family kinases was inhibited using SU5402, a FGF receptor tyrosine kinase blocker (Vallier et al., 2005, Gotoh et al., 2004, Mohammadi et al., 1997).

Freshly-isolated PαS MSCs were expanded in FGF-supplemented medium alongside dasatinib or SU5402. MSC cultures were thoroughly washed and both FGF and inhibitor treatment was stopped before adipogenic differentiation was induced. Visual inspection of oil red O stained cultures revealed potent inhibition of fat differentiation in PαS MSCs that had been expanded in FGF2+SU5402 (Figure 5.17A). Quantification of the total oil red O positive area using Image J backed up this finding, with significant reductions in the SU5402 samples compared to all other groups at each passage tested (Figure 5.17B). Significant drops were also observed in fat differentiation following dasatinib treatment at P0 and P2. These results indicate that the adipogenic priming seen with FGF treatment is primarily mediated downstream of the receptor docking protein Frs2 and may involve the Akt or Erk kinases. However, Src kinase could also have a minor role to play as we did see drops in fat differentiation when cultures were expanded in medium containing dasatinib.

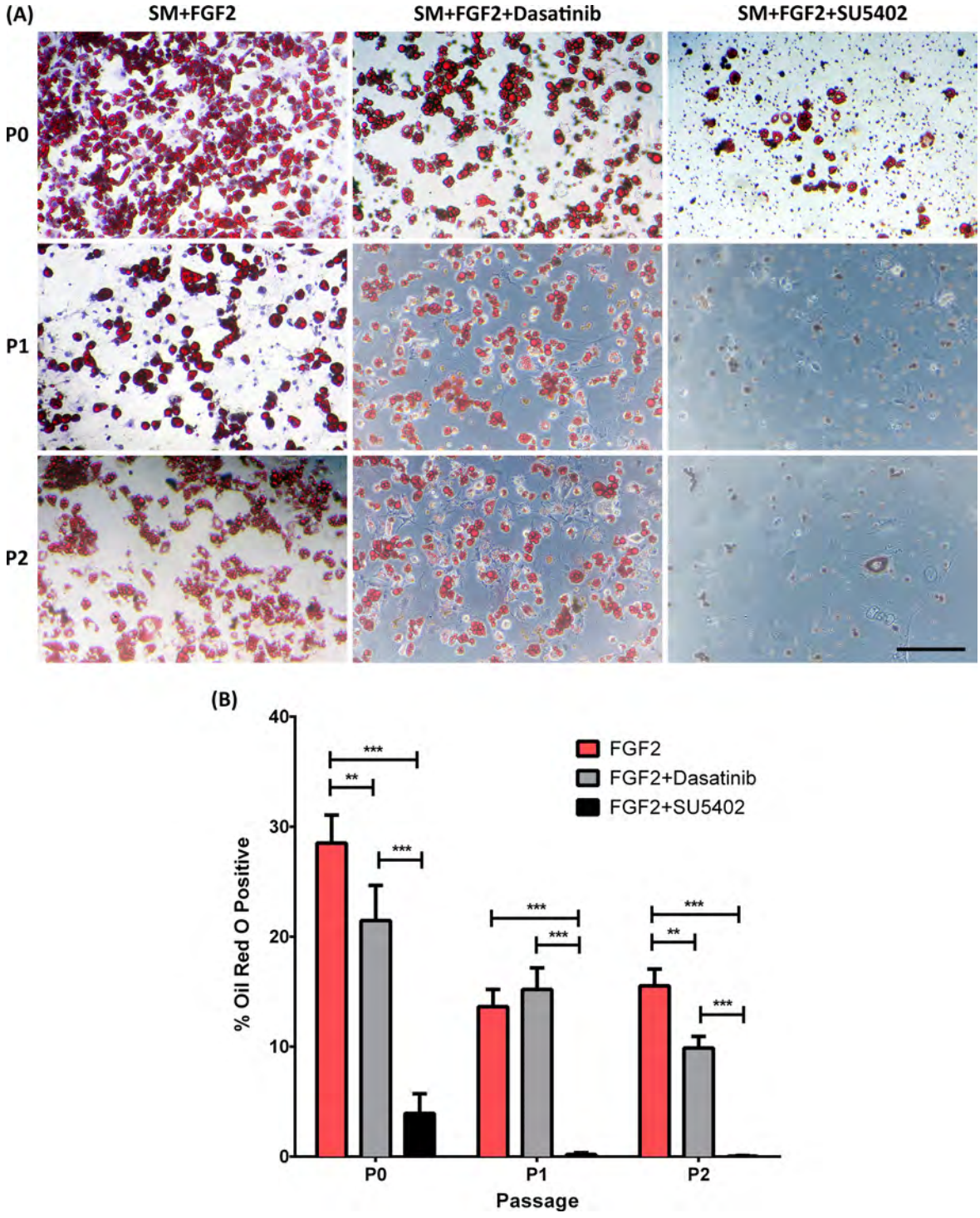


Figure 5.17 | **Signalling pathway behind FGF2-mediated adipogenic priming**. Freshly isolated PαS MSCs were expanded in the presence of FGF2, FGF2+Dasatanib or FGF2+SU5402. Expanded cells were induced to undergo adipogenic differentiation whereupon GF and inhibitor treatment was halted. (A) Representative images of oil red O stained cultures. Images taken at 100x magnification. Bar, 20µm. (B) Quantification of total percentage area oil red O positive using Image J. Data represented as mean±SD, n=3 technical repeats per condition at each passage. Statistical analysis performed using One-way ANOVA with Bonferroni's Multiple Comparison Test.

### 5.2.6.2 Adipogenic priming by PDGF-BB

The PDGF ligand family consists of four members that form homo- or heterodimers to become active (Betsholtz, 2004). So far, five isoforms have been recorded: PDGF-AA, PDGF-AB, PDGF-BB, PDGF-CC, and PDGF-DD. Binding of these ligands to PDGF tyrosine kinase receptors causes receptor dimerisation and activation of downstream pathways (Andrae et al., 2008). PDGF-BB (the ligand used in this study) binds to all receptor isoforms, and is therefore used as a promiscuous activator of PDGF signalling (Figure 5.18). PDGF-AA is selective for PDGFRα only (Fredriksson et al., 2004).

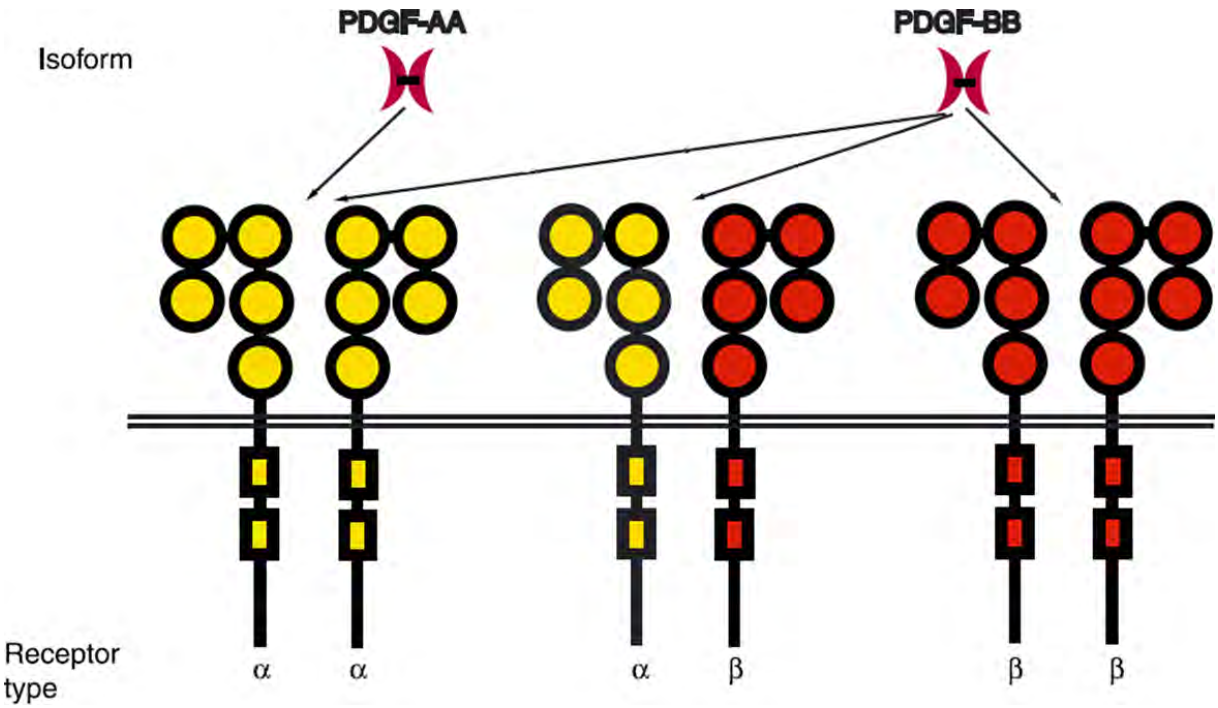


Figure 5.18 | **PDGF receptor signalling**. PDGF-BB can signal through all three receptor combinations, making it a promiscuous activator of the PDGF signalling pathway. In contrast, PDGF-AA signals exclusively through the PDGFRα homodimer. Figure modified from Fredriksson et al. (2004).

The selectivity of PDGF ligands for specific receptor combinations has been exploited in previous studies of PDGFR signalling (Ball et al., 2007, Cao et al., 2002, Lemström and Koskinen, 1997). We adopted the same procedure to identify which PDGF receptor was responsible for priming PαS MSCs down the adipogenic lineage in the presence of PDGF. Freshly-isolated PαS MSCs were expanded in SM containing either PDGF-BB or PDGF-AA. Adipogenic differentiation was then induced and GF treatment stopped. As shown previously, PαS MSCs expanded in PDGF-BB readily differentiated down the adipogenic lineage across all passages tested (Figure 5.19). However, PαS MSCs expanded in PDGF-AA underwent sporadic adipogenic differentiation that diminished by P3. This is similar to the fat differentiation seen when PαS MSCs were expanded in SM alone (Figure 5.13). These results suggest that adipogenic priming seen using PDGF is not exclusively mediated downstream of PDGFRα, as PDGF-AA was not able to recreate the same effects that were seen with PDGF-BB.

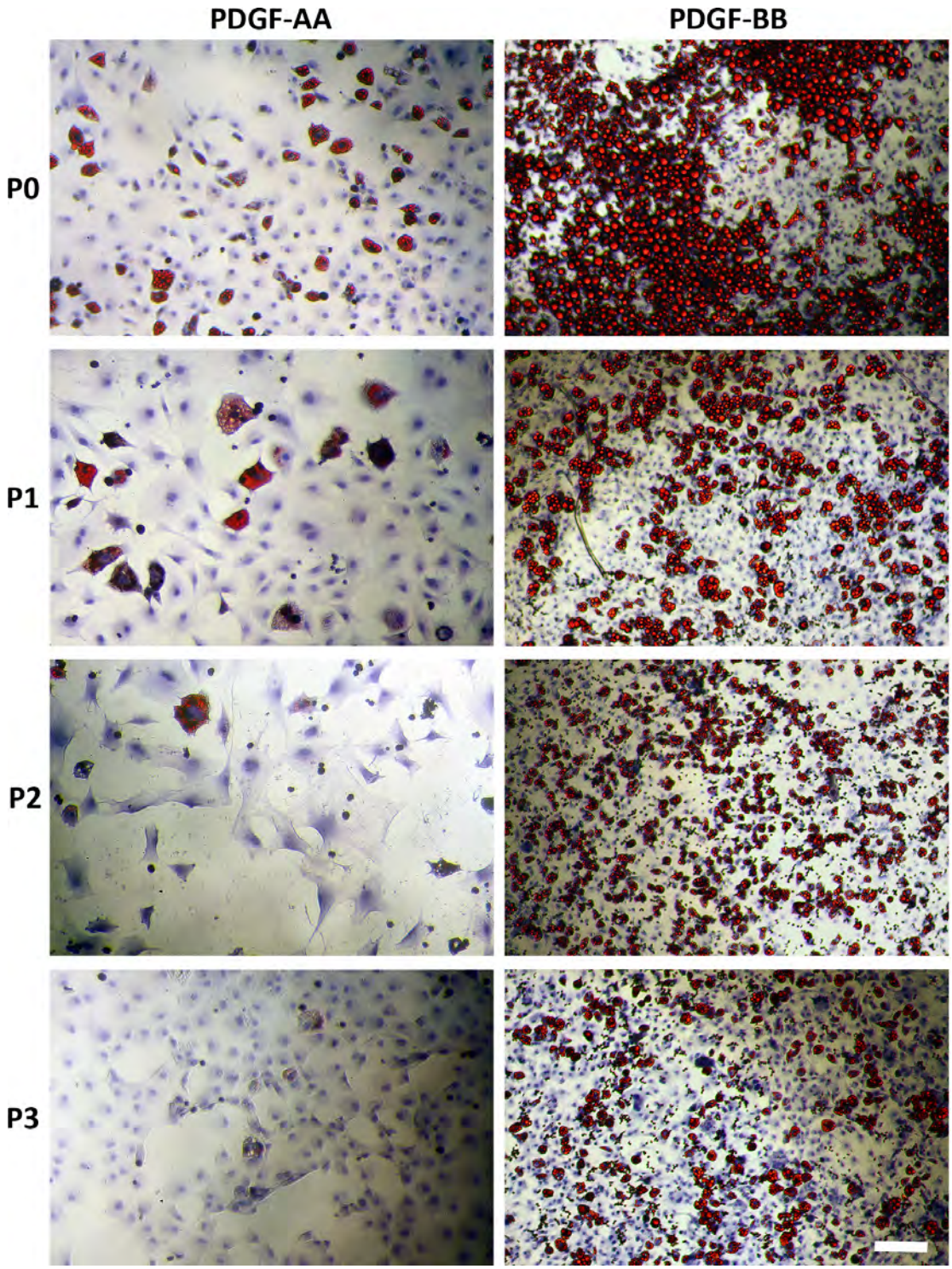


Figure 5.19 | **Receptor complex behind PDGF-mediated adipogenic priming**. Representative images of oil red O stained adipogenic differentiation of PαS MSCs expanded in SM containing PDGF-AA (n=3) or PDGF-BB (n=3). Samples were counterstained with haematoxylin prior to imaging. All images were taken at 100x magnification. Bar, 25µm. In all experiments, n is indicative of technical repeats using the same culture of PαS MSCs.

### 5.2.7 Effect of GFs on Immunosuppression

There is currently very little literature on the effect of MSC culture conditions on their immunosuppressive phenotype. We first examined the expression of previously reported immunosuppressive genes from the microarray but failed to identify any clear patterns between groups (Figure 5.20). This was because PαS MSCs were not exposed to inflammatory conditions prior to RNA isolation for the microarray, hence their immunomodulatory functions were 'switched off' (Ryan et al., 2007, Krampera et al., 2006).

We then performed $CD4^+$ T cell suppression assays to identify whether GF-treated Balb/c-derived PαS MSCs had varying capacities for immunomodulation. Passage 3 MSCs expanded in SM±GFs were co-cultured with $CD4^+CD25^-$ T cells that were activated with anti-CD3e antibody and $CD19^+$ B cells. Cultures were maintained for 72 hours and the total number of $CD4^+$ cells quantified using flow cytometry. Our data shows profound differences between the immunomodulatory capacities of PαS MSCs depending on their culture conditions (Figure 5.21). PαS MSCs expanded in SM were the most suppressive, achieving significant drops in T cell proliferation across all ratio's tested compared to the GF-treated cells. TGF-β1 primed MSCs achieved similar levels of suppression as SM MSCs at higher doses (1:8 and 1:4). Significant decreases in T cell proliferation were also seen in TGF-β primed cells compared to FGF and PDGF-primed MSCs at 1:16, 1:8 and 1:4 doses. In contrast, MSCs expanded in FGF or PDGF-supplemented medium had an attenuated immunosuppressive phenotype. FGF-primed MSCs were able to reach 50% suppression of SM cells at the highest dose, but PDGF-primed cells failed to pass the 20% mark across all tested ratios.

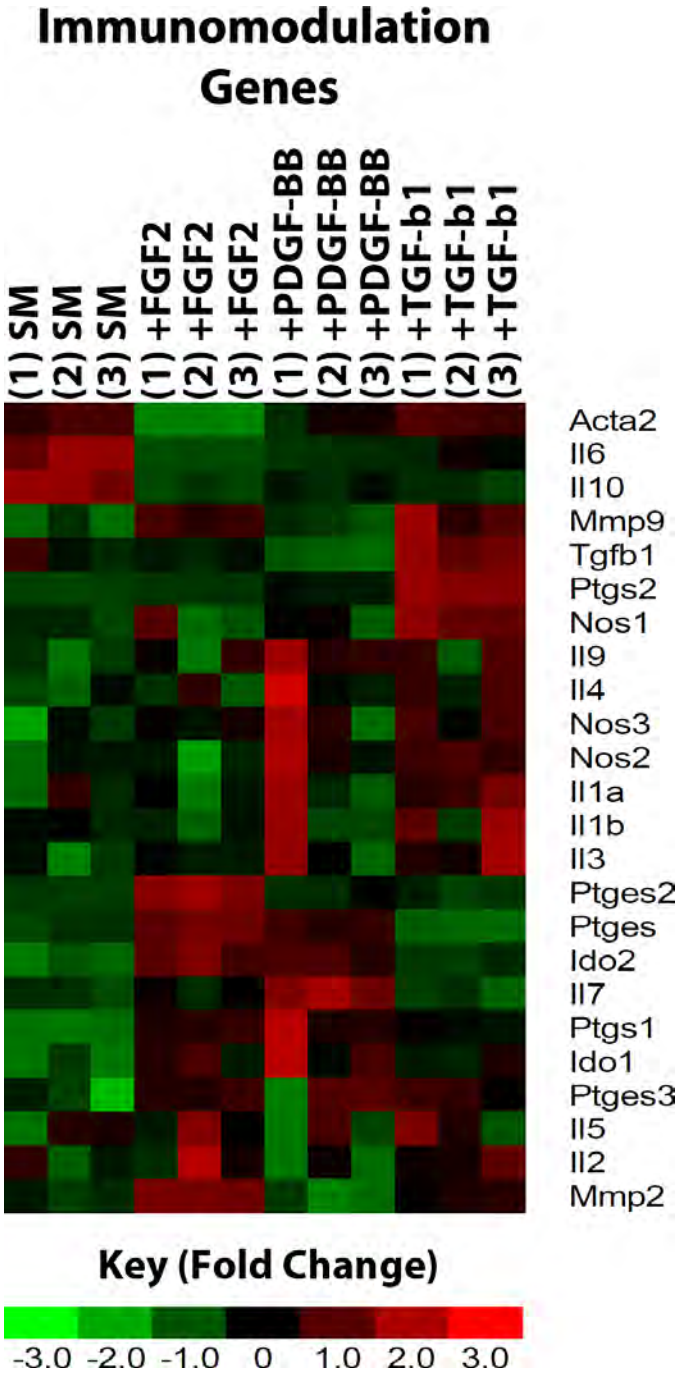


Figure 5.20 | **Effect of GF treatment on the expression of 'immunosuppressive' genes**. RNA isolated from undifferentiated, P1 PαS MSCs grown in SM±GFs were hybridised onto separate Affymetrix whole genome microarrays (n=3 per condition). The expression of previously reported 'immunosuppressive genes' were examined. The mean expression value for each gene across all samples was set as 0 (black box). A relative fold decrease in gene expression (compared to the mean) is represented by a green square, and a relative fold increase is represented by a red square.

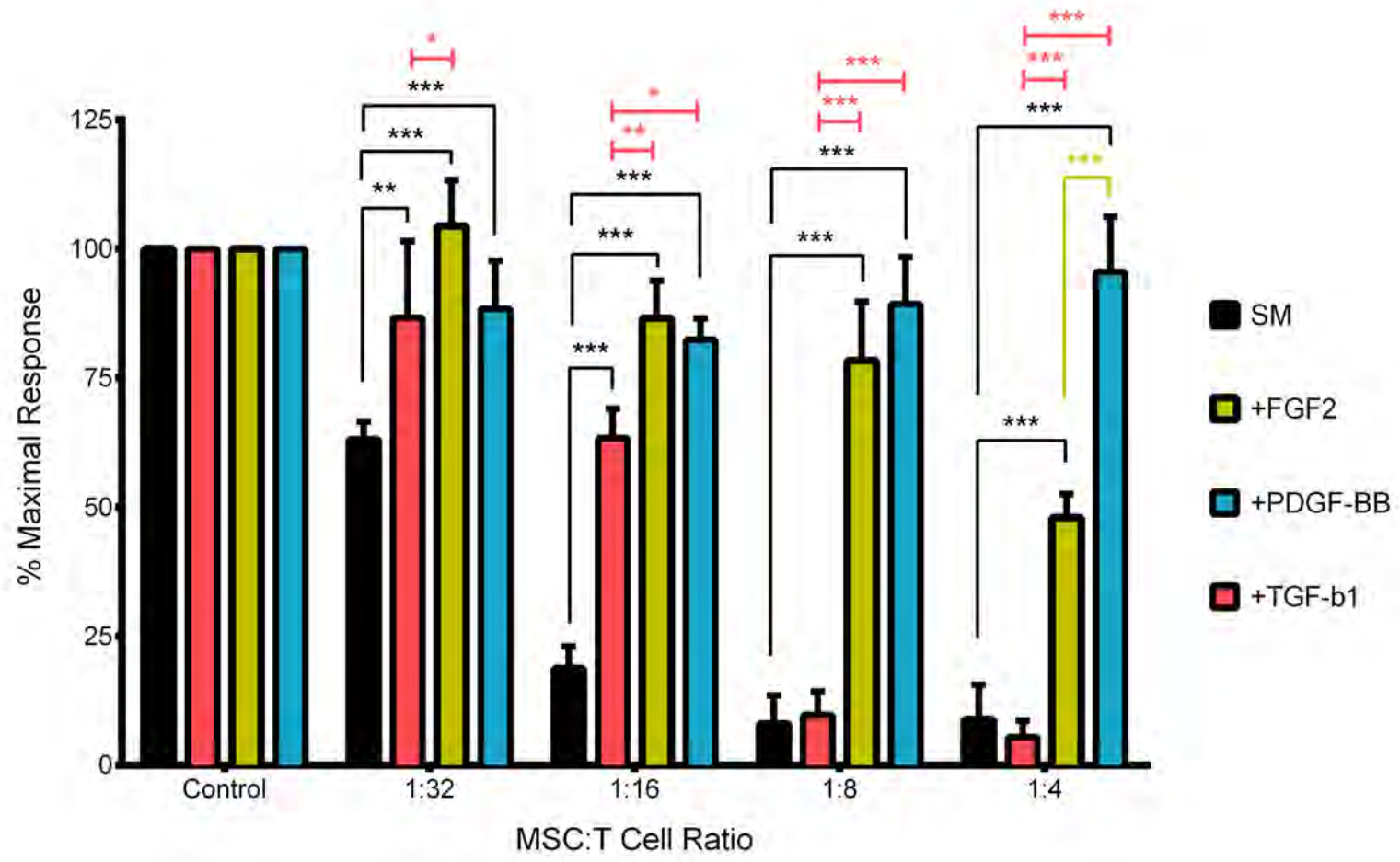


Figure 5.21 | **Effect of GFs on PαS MSC immunomodulation**. P3 PαS MSCs isolated from Balb/c mice were cultured and expanded in SM±GFs. MSCs were co-cultured with activated $CD4^+$ T cells for 72 hours. Samples were then analysed by flow cytometry and total CD4 numbers counted and expressed as a percentage to the no-MSC control. Data shown as mean±SD, n≥3 technical repeats per culture condition. Statistical analysis performed using Two-way ANOVA with Bonferroni's Multiple Comparison Test. Black bars represent significance compared to SM MSCs, red bars to TGF-β1 primed cells and yellow bars to FGF2-primed MSCs.

As NO secretion was the mechanism behind Balb/c-derived PαS MSC immunosuppression, we examined the effect of GF-priming on NO production to explain whether differences in immunomodulation were due to differential NO secretion. Our results validate this hypothesis, as PαS MSCs expanded in SM produced significantly more nitrite than GF-supplemented cultures (Figure 5.22). TGF-β1 primed cells, the next most suppressive group, also produced significantly more nitrite than FGF or PDGF-supplemented MSCs. FGF and PDGF produced less than half the NO of the other groups, which explains their poor immunomodulatory phenotype in CD4 T cell suppression assays. Interestingly, no differences in NO production were observed between FGF and PDGF-primed cells even though significant differences in CD4 T cell number were observed in the suppression assay.

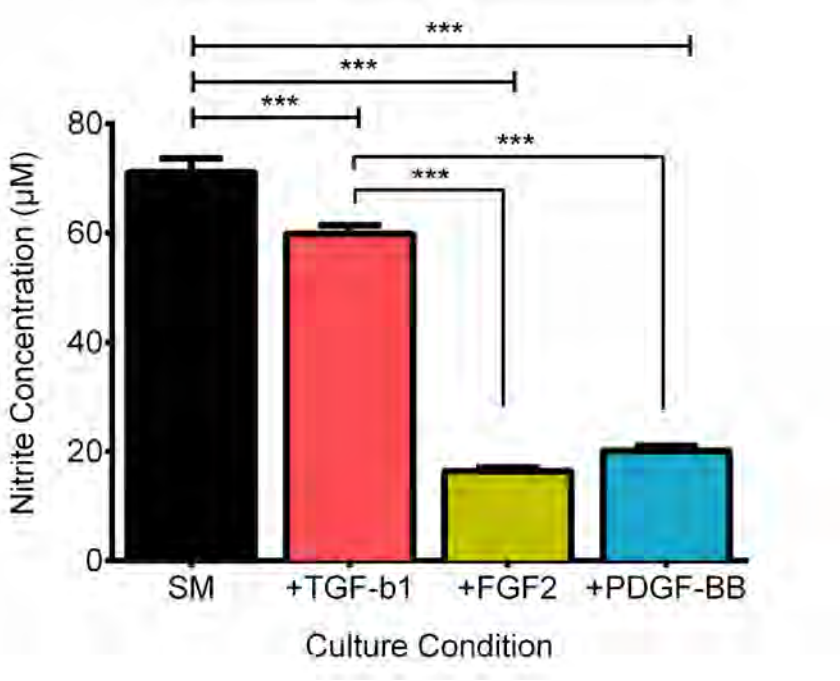


Figure 5.22 | **Effect of GF-priming on NO secretion**. PαS MSCs were expanded in SM±GFs until P3. Cells were cultured overnight with 20ng/ml IFNγ and TNFα and their supernatants examined for NO production using the Griess Assay. Data shown as mean±SD, n=3 technical repeats per condition. Statistical analysis performed using One-way ANOVA with Bonferroni's Multiple Comparison Test.

#### 5.2.7.1 TGF-β1 maintains Immunosuppressive Potential

The suppressive phenotype of PαS MSCs cultured in SM was lost at later passages due to increases in the number of senescent cells and a reduction in NO secretion. Our data demonstrates that TGF-β1 supplementation reduces the senescence of MSC cultures and has a similar immunomodulatory profile to SM cells at P3. We hypothesised that TGF-β1 treatment could maintain the immunosuppressive phenotype of MSCs after extended culture, allowing us to expand PαS MSC populations to reach cell numbers required for therapeutic infusions.

Balb/c-derived PαS MSCs were cultured in SM±TGF-β1 and expanded until P7. Graded numbers of MSCs were co-cultured with activated $CD4^+$ T cells as before, and the total number of $CD4^+$ cells quantified using flow cytometry after 72 hours. As expected, P7 MSCs expanded in SM failed to suppress T cell proliferation across all ratios tested (Figure 5.23A). However, P7 MSCs expanded in TGF-β1 supplemented medium retained their immunosuppressive phenotype and were able to significantly reduce T cell proliferation. Examination of NO production via the Griess Assay revealed that P7 TGF-β1 MSCs produced significantly more NO after overnight stimulation with IFNγ and TNFα (Figure 5.23B). Our findings clearly demonstrate that the suppressive potential of PαS MSCs changes over time and is closely linked with NO production. TGF-β1 primed cells retain their suppressive phenotype after extended due to enhanced NO secretion over SM cells. Thus, expansion of MSCs in TGF-β1 containing medium may be beneficial for future uses of these cells in autoimmune diseases.

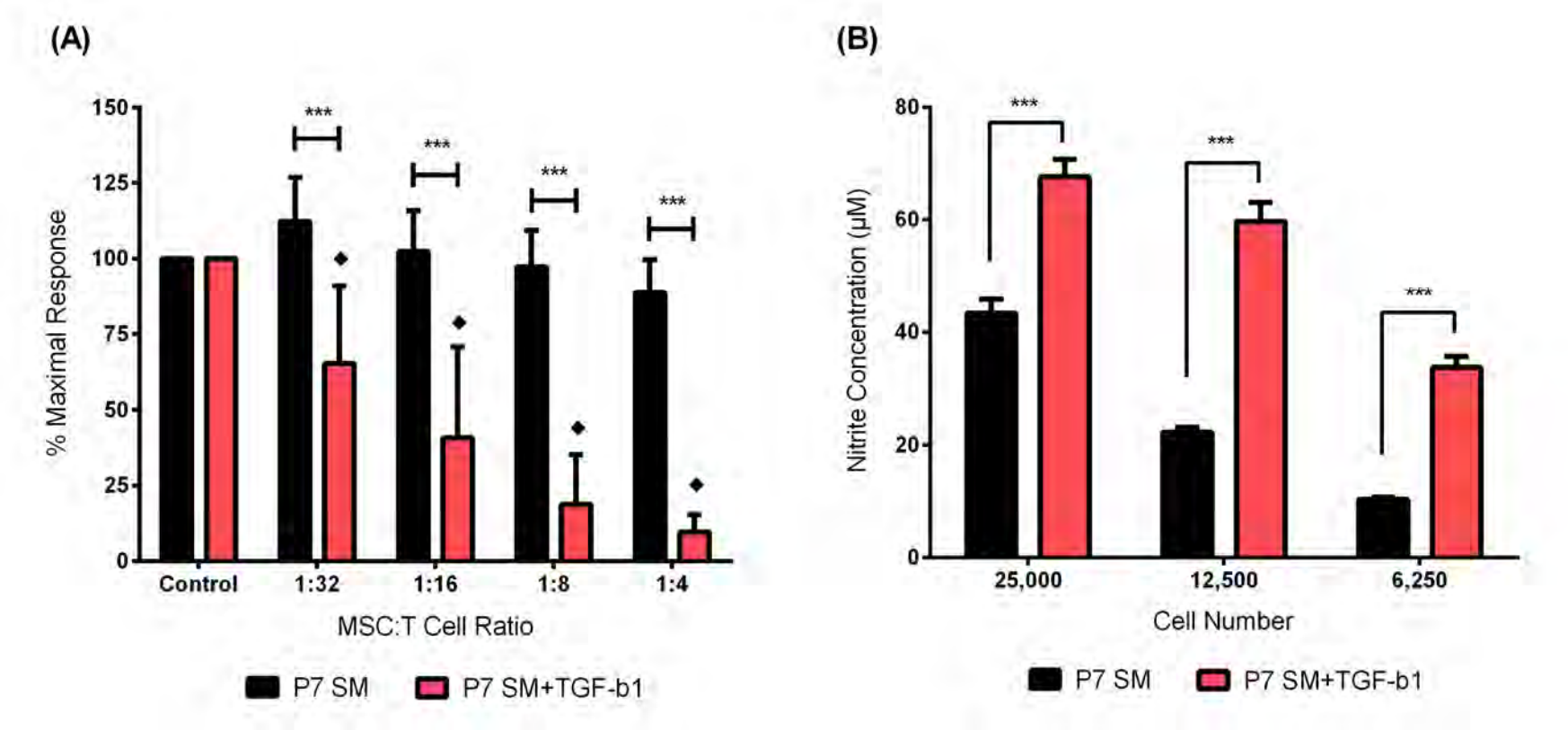


Figure 5.23 | **TGF-β1 maintains the immunosuppressive phenotype of PαS MSCs**. (A) *In vitro* T cell suppression assay. Balb/c-derived PαS MSCs were expanded in SM±TGF-β1 until P7. Graded numbers of cells were co-cultured with activated CD4 T cells for 72 hours. Total CD4 numbers are expressed as a percentage to the no-MSC control. Data shown as mean±SD, n=7 technical repeats per condition. Statistical analysis represented by asterisks (*) performed using One-way ANOVA with Bonferroni's Correction. Statistical analysis represented by diamonds (◆) denote significant differences (P<0.01) performed using One-sample T test compared to the no-MSC controls. (B) NO production as measured using the Griess Assay. Cells were cultured overnight with 20ng/ml IFNγ and TNFα and their supernatants examined for NO production. Data shown as mean±SD, n=3 technical repeats per condition. Statistical analysis performed using One-way ANOVA with Bonferroni's Correction.

## 5.3 Discussion

### 5.3.1 Chapter Summary

The rarity of PαS MSCs and their susceptibility to undergo replicative senescence after extended culture limits their use as a pre-clinical population of purified MSCs. We have been able to overcome senescence and increase the growth potential of PαS MSCs via the use of FGF2, PDGF-BB and TGF-β1 supplementation. These GFs were chosen as their respective signalling pathways have been reported previously to control MSC proliferation and differentiation down specific lineages (Ng et al., 2008). FGF2 had the most potent effect on PαS MSC proliferation, while PDGF-BB and TGF-β1 had more modest mitogenic effects.

We have also reported the karyotype of cultured PαS MSCs for the first time. Plastic-adherent murine MSCs are prone to culture-induced karyotypic abnormalities that lead to neoplastic transformation and tumour formation *in vivo* (Miura et al., 2006). No cytogenetic evidence of neoplastic transformation could be observed in PαS MSCs cultured±GFs at P3 or P5, suggesting that prospectively-isolated cells are more stable than their plastic-adherent counterparts. We did observe cases of polyploidy in TGF-β1 cultures and the presence of quadriradial chromosomes in PDGF-BB supplemented cells. More work is required to elucidate the significance of this finding for PαS MSC cultures.

The findings of Delorme et al. (2009) show that MSCs are 'primed' at the genetic level towards the lineages they can differentiate into. FGF, PDGF and TGF-β signalling pathways

were the key regulators controlling MSC differentiation down these lineages (Ng et al., 2008). We hypothesised that the addition of their respective ligands to MSC cultures could enhance MSC differentiation down pre-determined fates. Microarray analysis revealed evidence of 'lineage priming' following GF supplementation in PαS MSCS. Culture in SM enhanced the expression of osteogenic lineage genes in undifferentiated MSCs. When induced to undergo differentiation, SM cultures readily went down the osteogenic lineage, producing significantly more calcium than GF-supplemented cells. FGF2 and PDGF-BB supplementation upregulated key adipogenic lineage genes in undifferentiated MSCs, and we saw increased lipid droplet formation in these cultures when induced to undergo differentiation. Evidence for chondrogenic lineage priming was less clear, however our phenotypic data suggests that culture in FGF2 is beneficial for cartilage formation. In contrast, PαS MSCs expanded in TGF-β1 supplemented medium had attenuated tri-lineage differentiation but enhanced immunosuppressive potential. This was due to a reduction in the number of senescent cells and an increase in NO production in late-passage TGF-β1 MSCs compared to SM MSCs.

The findings of this chapter have significant implications for downstream therapeutic uses as we reveal that culture conditions can functionally 'prime' MSC fate (Figure 5.24). The maintenance of immunomodulatory capacity with TGF-β1 is useful for systemic immune disorders where multiple doses of MSCs are required. Additionally, the use of a 'lineage primed' population in regenerative medicine would allow clinicians to infuse lower numbers of MSCs to reach the same beneficial outcome in patients, thereby reducing the risk of any adverse events occurring.

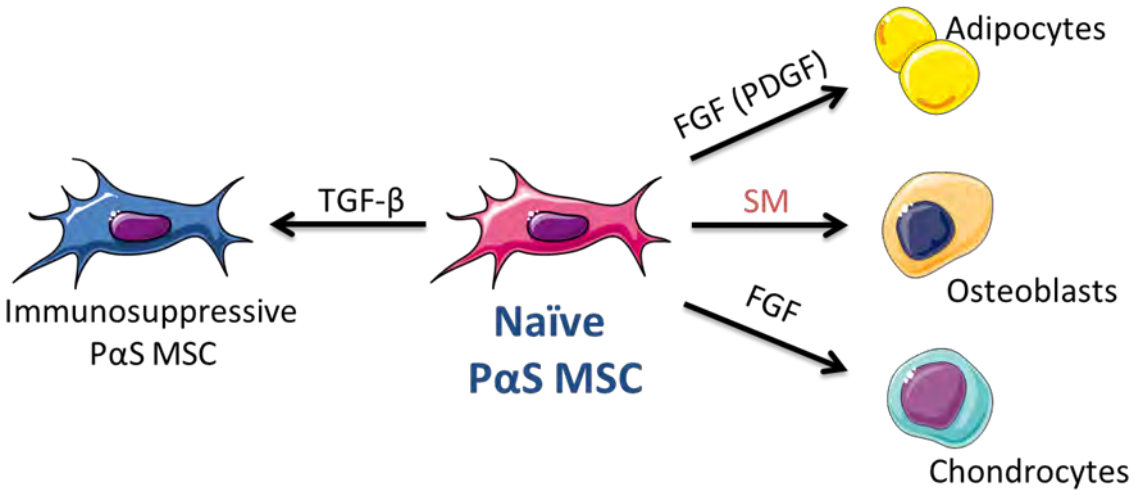


Figure 5.24 | **Summary of lineage priming experiments**. Expansion of PαS MSCs in SM promotes osteogenic differentiation, while FGF2 supplementation favours chondrogenesis and adipogenesis. TGF-β1 treatment is able to maintain the immunosuppressive potential of PαS MSCs over extended passage.

### 5.3.2 Effect of GF supplementation on PαS MSC Growth

GF supplementation has been used by many groups to enhance the growth of human and mouse MSC populations (Gharibi and Hughes, 2012, Rodrigues et al., 2010). FGF2 had the most mitogenic effect on PαS MSCs, followed by PDGF-BB and TGF-β1. FGFs are historical mitogens for stromal cell populations and are commonly added to MSC expansion medium (Lai et al., 2011, Coutu et al., 2011, Jung et al., 2010, Ito et al., 2008). FGF2 has also been used to enhance proliferation and reduce the differentiation potential of immunodepleted murine MSCs (Baddoo et al., 2003, Phinney et al., 1999). FGF primed cells also appeared smaller and more slender than SM MSCs. The infusion of smaller cells can reduce the risk of emboli formation and entrapment of MSCs in small capillaries *in vivo*, which can lead to further ischaemic injury (Furlani et al., 2009).

The *in vivo* role for FGF2 in maintaining BM MSC and HSC populations was described in a recent publication by Itkin et al. (2012). Wild type mice treated with FGF2 for seven consecutive days displayed a 2-fold increase in the number of HSCs in BM. Concurrent increases in the number of Nestin$^+$ MSCs was also observed after FGF2 treatment. FGF-treated Nestin$^+$ MSCs had 2-fold increased CFU-F and formed significantly more 'mesenspheres' compared to control cells. FGF2 treatment also reduced CXCL12 production and increased SCF secretion by Nestin$^+$ MSCs, thereby allowing HSCs to re-enter the cell cycle and increase in number. This study provides further proof of the close relationship between MSCs and HSCs in the BM niche and demonstrates how an FGF2-dependent increase in MSC number can restore and expand the HSC pool during times of stress or injury.

PDGF-BB is another commonly added supplement to MSC expansion media (Jung et al., 2010). Phinney et al. (1999) reported a 2-fold increase in plastic-adherent murine MSC number after expansion in PDGF-BB for 14 days. Interestingly, they observed no effect on MSC growth following culture in FGF2, which is contradictory to both our findings and to other published papers. PDGF-BB is crucial for the survival and proliferation of pericytes during embryonic development (Lindahl et al., 1997). Therefore it is not surprising that MSCs, who share many features with pericytes, respond to PDGF-BB stimulation in the same way (Meirelles et al., 2008). Further evidence comes from a study that showed MSCs cultured in serum-free media containing fresh frozen plasma (rich in PDGFs) exhibited enhanced growth characteristics compared to FCS-supplemented cells (Müller et al., 2006).

TGF-β1 supplementation is less commonly used in MSC literature to enhance proliferation. Jian et al. (2006) showed that TGF-β1 stimulated human MSC proliferation via cross-talk with the Wnt signalling pathway. Walenda and colleagues also reported pro-proliferative effects of TGF-β1 on human MSC populations (Walenda et al., 2013). Interestingly, the authors also report that addition of TGF-β1 to human MSCs caused them to grow in clusters rather than as a homogenous monolayer. We observed similar morphological changes in mouse MSCs following TGF-β1 in this study, with PαS cells growing in discrete colonies containing tightly packed cells. This could be due to an increase in actin expression in MSCs after TGF-β1 treatment (Wang et al., 2004). In contrast, PDGF-BB treatment has been shown to reduce the expression of actin in human MSC cultures, which may explain the more elongated, spindle-shaped morphology of PDGF-primed PαS MSCs (Kinner et al., 2002).

### 5.3.3 Effect of GF supplementation on PαS MSC Senescence

The accumulation of senescent cells limits the therapeutic applications of MSCs, especially in cases where large numbers of cells are required to see a clinical benefit. We have shown that PαS MSCs are susceptible to replicative senescence, resulting in reduced differentiation and loss of immunomodulation. The effects of GF-supplementation was tested in this study as a way of overcoming senescence in PαS MSC cultures. Our results demonstrate significant reductions in the number of senescent cells at days 30 and 50 in GF-supplemented cultures compared to SM. There is plenty of published evidence that highlights the importance of FGF signalling in regulating senescence of stem cells (Coutu and Galipeau, 2011). Ito and colleagues report a reduction in senescence and restoration of proliferation in human MSC

cultures following FGF2 treatment due to downregulation of cell cycle inhibitors p21, p16 and p53 (Ito et al., 2007). Coutu et al. (2011) show that FGF2 signalling is required to avoid replicative senescence of mouse MSCs. A three-fold increase in cell number was observed after FGF2 supplementation, however removal of the GF immediately induced cell cycle arrest, which suggests that immortalisation had not taken place. Further mechanistic studies revealed that FGF2 treatment caused hyper-phosphorylation and activation of MDM2, a key regulator of senescence in mammalian cells (Coutu et al., 2011).

Addition of PDGF-BB or TGF-β1 in PαS MSC cultures also caused drops in the number of SA-β-gal$^+$ cells at days 30 and 50. The effect of TGF-β1 is interesting as it has been shown previously to induce the onset of senescence in healthy, non-transformed stromal cells (Debacq-Chainiaux et al., 2005). Murine C57BL/6 MSCs also demonstrated a dose-dependent increase in the number of SA-β-gal$^+$ cells after 24h exposure to TGF-β1 (Wu et al., 2014). Our results contradict these findings, with TGF-β1 supplementation reducing the number of SA-β-gal$^+$ PαS MSCs compared to SM controls. The reasons behind these contradictory findings could be due to differences in the cell population used and the duration of TGF-β1 stimulation between studies. Whereas Wu et al. (2014) exposed heterogeneous plastic-adherent MSCs to TGF-β1 for 24 hours, we studied the long-term effects of TGF-β supplementation on a purified population of cells. Future work investigating the expression of key senescence-associated genes (p16, p21) in GF-supplemented MSCs is required to elucidate how GF treatment is reducing senescence in PαS MSC cultures.

### 5.3.4 Karyotypic stability of PαS MSCs

Mouse MSCs are susceptible to karyotypic abnormalities after *in vitro* expansion. Previous studies have shown that C57BL/6-derived plastic-adherent MSCs lost contact inhibition from P3 onwards and accumulated karyotypic errors with extended passage (Zhou et al., 2006). Analysis of 50 metaphase spreads revealed aneuploidy in all 50 samples, with chromosome numbers ranging between 66 and 82 per cell. Similar findings were reported by both Miura et al. (2006) and Tolar et al. (2007), who identified that continuous passaging of murine MSCs led to cytogenetic abnormalities and eventual malignant transformation. *In vivo* infusion of transformed MSCs formed sarcomas in *nude* mice in both studies.

In contrast, human MSCs demonstrate a good degree of genetic stability after extended culture and no reports of tumour formation have been reported in clinical trials that have used these cells (Lalu et al., 2012). There are some isolated reports of karyotypic abnormalities involving human MSCs, although these changes in chromosome number did not result in malignant transformation (Wang et al., 2013, Tarte et al., 2010). Nonetheless, the use of minimally-manipulated cells for therapy would be ideal to avoid any risk of culture-induced aberrations (Trounson et al., 2011).

Pinpointing the reasons behind why murine MSCs are more prone to genetic instability than their human counterparts is difficult but could be due to species differences. Human fibroblasts have evolved to require alterations in six tumour suppressor signalling pathways

for oncogenic transformation, whereas murine fibroblasts need alterations in only two (Rangarajan et al., 2004). Additionally, it also remains to be seen whether prospectively-isolated PαS MSCs are more karyotypically stable than plastic-adherent cells, and whether GF-treatment has a detrimental effect on the stability of these cells.

G-banding analysis and chromosome breakage studies revealed that PαS MSCs were genetically stable *in vitro*. There was no cytogenetic evidence of neoplastic transformation in SM or GF-supplemented cultures at P3 or P5, suggesting that these cells are more stable than plastic-adherent murine MSCs. Compared to numerous previous studies that report several abnormal chromosome numbers in early passage murine cells, we show that <10 out of 60 analysed metaphase spreads were abnormal. Interestingly, we observed an increase in the number of tetraploid chromosomes (80, XXYY) in TGF-β1 supplemented PαS MSCs. Past literature has reported polyploidisation to be a protective mechanism against tumourigenesis in murine MSC cultures (Shoshani et al., 2012). In their study, injection of tetraploid MSCs (4N) resulted in a 13-fold reduction of tumour formation in *nude* mice, while the injection of over-tetraploid MSCs (>4N) did not form any tumours at all. Mature cells such as hepatocytes undergo dynamic changes in chromosome number as a mechanism to adapt to the genotoxic stresses present in liver tissue (Duncan et al., 2010). However, changes in chromosome number are also a hallmark of cancers (Davoli and de Lange, 2011). Further work is required to understand whether polyploidisation occurs as a 'stress' response in PαS MSC cultures following growth in TGF-β1 supplemented medium and experiments involving injection into *nude* mice are required to find out whether polyploidisation protects against transformation and malignancy in PαS cells.

Chromosome breakage studies were performed to identify DNA damage events that manifests as gaps or breakages in chromosomes rather than changes in overall chromosome number. Again, GF-supplementation had a protective effect over SM cultures, with FGF2-treated cultures having the least number of errors. Interestingly, we did observe the formation of quadriradial chromosomes exclusively in PDGF-supplemented cultures. QR chromosomes are formed when chromosome breaks in two homologous or non-homologous chromosomes are misrepaired and joined together (Joenje and Patel, 2001). QR chromosomes are defining characteristic of human genetic instability syndromes Bloom's disease and Fanconi's anaemia (Singh et al., 2010, Joenje and Patel, 2001). Patients suffering from these rare conditions are much more likely to develop cancer at an early age. Patients with Bloom syndrome display several incidences of chromosome breaks and QR chromosome formation due to an inactivating mutation of the BLM DNA helicase protein (Amor-Guéret, 2006). The significance of QR formation in PDGF-supplemented cultures is unclear. The fact that only ≈7/60 PDGF-supplemented metaphase spreads showed evidence of QR chromosome formation, and the fact that we did not see an increased incidence of chromosome gaps or breaks at a later passage would be argue against a 'genetically unstable' phenotype. Additionally, these DNA damage events did not cause changes in the gross number of chromosomes in PDGF samples. Further studies analysing the karyotype of PDGF-supplemented at later passages are required to identify whether QR chromosome formation preludes further karyotypic abnormalities in PDGF samples.

### 5.3.5 'Lineage Priming' using GFs

Human and murine MSCs are routinely cultured in medium containing GFs to enhance their growth characteristics; however, the effect of extended culture in GF-supplemented medium on the tri-lineage differentiation and immunosuppressive properties of MSCs has not received much research attention. Expanding on the findings of Delorme et al. (2009) and Ng et al. (2008), we hypothesised that GFs may 'prime' MSCs down specific fates while maintaining them in a proliferative, undifferentiated state. To prove that priming did occur in PαS MSCs, we examined the expression of key osteogenic, adipogenic and chondrogenic transcripts in undifferentiated cells. Our results demonstrate profound changes in gene expression after expansion in GF-supplemented media, resulting in altered differentiation and immunosuppressive potential after expansion. Thus, the choice of GF used for MSC expansion must be tailored to the clinical setting in order to maximise the efficacy of MSCs in pre-clinical models and in human clinical trials.

#### 5.3.5.1 Osteogenic Lineage Priming

Microarray analysis revealed that key osteogenic lineage genes were significantly upregulated in undifferentiated SM cultures compared to GF-supplemented cells. These included the master osteogenic regulators *Runx2* and *Osterix*. Runx2$^{-/-}$ and Osterix$^{-/-}$ mice show a complete lack of mature osteoblasts, highlighting the importance of these transcription factors in bone formation (Tu et al., 2008, Nakashima et al., 2002). *Runx2* also inhibits the differentiation of mesenchymal cells into adipocytes or chondrocytes (Komori, 2006b), and it is interesting to note that FGF and PDGF-primed cells (that readily differentiated into fat and cartilage) expressed low levels of this transcription factor.

As suggested by the microarray, MSCs expanded in SM readily underwent osteogenic differentiation and produced significantly more calcium than GF-supplemented cells. FGF2 and PDGF-BB primed cells produced similar levels of calcium, while TGF-β1 supplemented MSCs lost the ability to differentiate towards bone at earlier passages. The decreased osteogenic differentiation seen in FGF2-primed PαS MSCs is surprising, as FGF has been shown to support osteogenic differentiation in previous studies (Ng et al., 2008, Minamide et al., 2007, Tsutsumi et al., 2001). However, there is some recent data that suggests FGF2 signalling might inhibit osteogenesis in MSC cultures (Gharibi and Hughes, 2012, Lai et al., 2011, Osathanon et al., 2011). Similarly, PDGF-BB and TGF-β1 have also been shown to have both pro- and anti-osteogenic effects on MSC differentiation in past studies (Zhen et al., 2013, Zhao and Hantash, 2011, Tokunaga et al., 2008, Ng et al., 2008).

The contradictory findings in past literature could be due to species differences or due to the heterogeneous populations of MSCs used in past studies. Additionally, the experimental design used in this study and past literature is also subtly different. Here, GF treatment was stopped prior to the induction of differentiation to ensure that any differences observed between groups were due to differences in their expansion culture medium only. Past studies were examining the contribution of certain signalling pathways to MSC growth and differentiation by scrutinising the effect of GF-supplementation for short periods of time (24-48 hours; Wu et al., 2014) or during the differentiation process itself (Ng et al., 2008, Zhao and Hantash, 2011). As shown here, long-term culture in GFs increases the proliferation of PαS MSCs but skews their differentiation towards specific fates.

### 5.3.5.2 Adipogenic Lineage Priming

Analysis of adipogenic lineage genes revealed that key transcripts of this pathway were significantly upregulated in FGF and PDGF-supplemented PαS MSCs compared to SM controls. These included master regulators *Cebpa* and *Pparg*, which were expressed approximately 2-fold and 3-fold higher than SM cells. In contrast, TGF-β1 supplemented cells expressed these master regulators approximately 3-fold lower than SM cells, suggesting a loss in fat differentiation potential. Cebpa$^{-/-}$ mice suffer from defects in glycogen and lipid storage (Wang et al., 1995), and PPARγ-GFP$^{+}$ adipocyte precursors were able to form ectopic GFP$^{+}$ fat after *in vivo* infusion, demonstrating the importance of the *Cebpa*/*Pparg* axis in fat development (Tontonoz and Spiegelman, 2008).

When induced to undergo differentiation, FGF or PDGF-primed cells readily differentiated towards fat as suggested by the microarray. The differentiation protocol had to be shortened from 24 to 8 days to avoid cell death due to excessive lipid droplet formation in these cultures. FGF and PDGF supplemented cells also maintained their adipogenic differentiation potential until P5, while SM-expanded cells lost this ability by P3. These findings back up previous work in the MSC field that have identified FGF2 and PDGF-BB as pro-adipogenic factors (Ahn et al., 2009, Ng et al., 2008, Kratchmarova et al., 2005). TGF-β1 primed MSCs failed to differentiate towards fat across all passages tested. TGF-β has historically been described as a potent inhibitor of adipogenic differentiation in MSCs and other adipogenic precursors (Wang et al., 2012, Watabe and Miyazono, 2009). Smad3/4, a key intracellular signalling protein in the TGF-β pathway, has been shown to directly interact

with the master adipogenic regulator Cebpa to inhibit its transcriptional activity in mouse fibroblasts (Choy and Derynck, 2003). It would be interesting to examine the kinetics behind TGF-β1 mediated inhibition of adipogenesis to see whether GF-removal restores the adipogenic potential of TGF-β1 primed MSCs.

#### 5.3.5.3 Chondrogenic Lineage Priming

Cartilage loss is a major cause of disability in the western world (Arden and Nevitt, 2006). Cartilage repair following injury is a slow and limited process due to the avascular and non-innervated nature of mature cartilage. MSCs are an ideal tool for cartilage repair due to their ability to replace lost chondrocytes and their ability to prevent further immune-mediated damage from taking place (Boeuf and Richter, 2010, Chen and Tuan, 2008).

Unlike the other two 'main' lineages, chondrogenic differentiation of MSCs is technically more challenging, requiring the use of 3D culture and specialised differentiation media (Gupta et al., 2012, Solchaga et al., 2011, Koga et al., 2009, Raghunath et al., 2007, Heng et al., 2004). We examined the effect of GF-priming on PαS MSCs in an attempt to improve chondrogenic differentiation efficiencies and maximise the therapeutic potential of these cells. Microarray analysis for chondrogenic lineage genes showed significant increases in the expression of master regulators *Sox9* and *Sox5* in FGF and PDGF supplemented cells compared to SM or TGF-β1 MSCs. *Sox9* and *Sox5* expression is essential for the formation of cartilage and endochondral bone development (Akiyama, 2008). $Sox9^{-/-}$ mouse embryos

display generalised chondrodysplasia due to mesenchymal progenitor cells being unable to terminally differentiate into chondrocytes (Akiyama et al., 2003, Akiyama et al., 2002). Analysis of downstream effector genes gave mixed results, which suggests that it is more difficult to prime MSCs down the chondrogenic lineage using GFs alone and could explain why complex 3D culture systems are required for efficient chondrogenic differentiation.

Micromass pellet cultures were used to induce chondrogenic differentiation of GF-primed PαS MSCs. As suggested by the microarray, FGF and PDGF-primed cells made the largest cartilage pellets that were rich in Col2 and proteoglycans. PαS MSCs expanded in SM made pellets that were of similar collagen and proteoglycan content to GF-supplemented cells, but their pellets were significantly smaller in size. TGF-β1 primed cells made the smallest cartilage pellets that with the lowest Col2:Col1 ratio, indicating the formation of fibrocartilage, an inferior alternative to hyaline cartilage.

The pro-chondrogenic effects of FGF2 and PDGF-BB supplementation in MSC cultures has been described previously, and our results further back up these findings (Handorf and Li, 2011, Ng et al., 2008, Ito et al., 2008). Interestingly, TGF-β1 treatment prevented chondrogenic differentiation in PαS MSCs, which contradicts the findings of several other groups (Mueller et al., 2010, Xu et al., 2008, Ng et al., 2008, Liu et al., 2007, Barry et al., 2001). Again, species differences and variations in the timing and duration of GF treatment may explain the differences observed between studies.

#### 5.3.5.3.1 Tissue Engineered Cartilage

MSC therapy for cartilage disorders faces many challenges, including the need for therapies suitable for larger cartilage injuries. While micromass pellets are suitable for studying the pathways controlling MSC differentiation, the amount of cartilage produced is too small to be of practical value in animal models. To address this issue, cartilage tissue engineering experiments using PGA scaffolds were performed to increase the amount of ECM produced by PαS MSCs. PGA scaffolds undergo hydrolysis and degrade over time to leave behind MSC-derived ECM proteins. FGF-primed cells were chosen for analysis due to their superior growth and cartilage differentiation properties. SM-expanded MSCs were used as controls.

After 35 days differentiation, significant increases in weight and proteoglycan content were observed in FGF-primed samples compared to SM cells. FGF2-primed cells also produced more Col2 and had a higher Col2:Col1 ratio, but the increase was non-significant. These findings match the results obtained using the micromass pellet culture system. However, there was a 4-fold increase in size and 2-fold increase in collagen and proteoglycan content using PGA scaffolds compared to micromass pellets. These improvements were achieved with a small increase in initial MSC seeding number ($5x10^5$ per pellet compared to $6x10^5$ per PGA scaffold), demonstrating the power of scaffolds in improving chondrogenic differentiation of MSCs.

Testing cartilage repair in murine models and optimising strategies for MSC differentiation would significantly reduce the cost and increase the clinical benefit seen in human patients (Helminen et al., 2002). However, tissue engineering murine cartilage has been challenging due to difficulties in isolating pure populations of mouse MSCs (Zhang, 2014, Frenette et al., 2013). Our results show that PαS MSCs can differentiate into good quality cartilage, which can be further improved via the use of scaffolds. PαS cells can therefore be used as a model pre-clinical population of cells to design and optimise novel cartilage repair therapies. Future studies can investigate the use of bioreactors or the effect of physical stimulation such as shear stress and surface coatings on tissue-engineered constructs as a way to improve chondrogenic differentiation even further (Schulz and Bader, 2007).

### 5.3.6 Maintenance of Immunosuppression using TGF-β1

The immunosuppressive properties of MSCs make them an attractive cell source for future stem cell therapies. We have shown that early-passage (P3) PαS MSCs were able to strongly suppress $CD4^+$ T cell proliferation via the secretion of NO. However, as PαS MSCs become increasingly senescent, their ability to secrete NO is lost, resulting in a complete reversal of their immunosuppressive phenotype. Due to the rarity of PαS MSCs in BM, a degree of *ex vivo* expansion is required to reach cell doses needed for therapeutic infusions. To address this issue, we examined the effect of GF-supplementation on the immunomodulatory functions of PαS MSCs to identify culture conditions that could enhance or maintain their suppressive properties over extended *in vitro* culture.

Our results demonstrated that MSCs expanded in SM were the most suppressive, closely followed by TGF-β1 primed cells. FGF2 and PDGF-BB supplemented cultures fared much worse and had significantly less suppressive capacity. Examination of NO secretion using the Griess Assay followed the same trend, with SM cells producing the most NO and PDGF-BB primed MSCs producing the least. There is very little published literature that examines the effect of senescence on murine MSC-mediated immunosuppression. Li et al. (2012) show that human MSCs at P7 lost their ability to suppress T cell proliferation due to an increase in the number of SA-β-$gal^+$ cells in culture. Sepulveda and colleagues report loss of *in vivo* immunosuppression of aged human MSCs but demonstrate no differences in their *in vitro* function (Sepulveda et al., 2014). Methods used to overcome senescence and boost immunomodulatory functions include hypoxia (Roemeling-Van Rhijn et al., 2013, Haque et

al., 2013) and the use of 'MSC licensing' agents such as TNFα, IFNγ and TLR agonists (Krampera, 2011, DelaRosa and Lombardo, 2010, Waterman et al., 2010). GF-priming is one avenue that has not received much attention. One study which examined this option was performed by Auletta et al. (2011), who examined the effect of long-term culture in FGF2-containing medium. Their findings contradict ours, as they report that FGF2 supplementation can expand human MSC numbers without diminishing their immunosuppressive potential. However, preservation of immunomodulatory functions was only observed in 3/5 BM donors, which suggests that the effect is not entirely reproducible.

In our T cell suppression assay, P3 TGF-β1 primed MSCs were equally as suppressive as SM cells at the higher MSC doses. However, P7 TGF-β cells were significantly more suppressive than SM cells across all ratios tested due to significant increases in NO secretion. Reductions in SA-β-gal$^+$ MSCs following TGF-β1 supplementation could be one reason behind the maintenance of immunosuppressive function; however, FGF and PDGF primed cells had lower numbers of SA-β-gal$^+$ cells than TGF-β samples but failed to perform in the T cell suppression assay. FGF2 has been shown to inhibit *iNOS* expression in human microglial cells (Colasanti et al., 1995) and bovine epithelial cells (Goureau et al., 1995) after LPS and TNFα stimulation. There is no literature that proves a causal link between TGF-β1 signalling and increased NO production in mammalian cells. On the other hand, there is plenty of evidence which proves NO can negatively regulate TGF-β1 signalling in models of organ injury (Saura et al., 2005, Dreieicher et al., 2009). TGF-β1 is itself a potent immunosuppressive compound which is secreted by MSCs and Tregs to downregulate the activity of immune cells (English et

al., 2009). Transfer of residual TGF-β1 on the surface of MSCs to the T cell co-culture is unlikely as MSCs were washed thoroughly before experimentation.

Microarray analysis revealed that TGF-β1 primed cells expressed significantly higher levels of *Nos2* (iNOS) compared to the other culture conditions, but the relevance of this finding is debatable as the cells were not pre-stimulated to 'switch on' their immunosuppressive properties (Krampera et al., 2013). It is interesting to note that TGF-β1 prevented the tri-lineage differentiation of MSCs but maintained their immunosuppressive phenotype. Conversely, FGF and PDGF treatment enhanced tri-lineage differentiation but failed to maintain immunosuppression. Future work should try to identify how TGF-β1 treatment maintains NO production in PαS MSCs. Further genetic and phenotypic analysis is required to identify the lineage TGF-β1 is priming PαS MSCs towards. It would also be interesting to examine whether C57BL/6-derived MSCs, which suppress via a NO-independent mechanism, also maintain their immunosuppressive phenotype when expanded in TGF-β1.

In summary, these findings highlight the need to tailor culture conditions to the intended future use of these cells and have significant implications for translational studies. Although FGF2 or PDGF-BB treatment increases MSC yield *in vitro*, it may not be ideal for use in patients with bone injuries or for immunosuppressive indications. Conversely, TGF-β1 primed MSCs do not appear suitable for regenerative medicine purposes but are ideal for immune-mediated disorders.

# CHAPTER 6

# IN VIVO EFFICACY IN A MOUSE MODEL OF ALLOIMMUNE LIVER INJURY

## 6.1 Chapter Rationale and Aims

We have been able to overcome senescence in MSC cultures via the use of GFs, which increase the proliferative capacity of PαS MSCs and also 'primes' them down specific lineages. In particular, TGF-β1 supplementation was able to maintain the immunosuppressive phenotype of PαS MSCs over extended culture, which is of interest for future uses in immune-mediated disorders. In this chapter we tested the efficacy of PαS MSCs in a transgenic mouse model of alloimmune liver injury to examine their immunosuppressive phenotype *in vivo* and see whether late-passage TGF-β1 primed cells retained their immunomodulatory functions.

### 6.1.1 Autoimmune Liver Disease

The liver is the largest organ in the human body and has a number of important functions including metabolism, detoxification and protein synthesis that are essential for survival. The liver also plays an important role as a first-line defence against foreign antigens entering from the gut (Racanelli and Rehermann, 2006). It must maintain a balance between tolerance to dietary antigens and the need to generate an immune response against pathogenic microorganisms. The coordinated action of Kupffer cells, dendritic cells, NKT cells and others is required to maintain this balance, which, when disrupted, can trigger the onset of autoimmune liver disease (Liaskou et al., 2012).

Autoimmune hepatitis (AIH), primary biliary cirrhosis (PBC) and primary sclerosing cholangitis (PSC) are all chronic, inflammatory liver diseases of unknown aetiology that fall under the category of autoimmune liver diseases. These conditions make up an estimated 5% of all liver disease cases (Decock et al., 2009). Patients with AIH typically present with altered serum biochemistry, showing elevated levels of alanine transaminase (ALT), a biomarker of hepatocellular damage, but normal levels of alkaline phosphatase (ALP), a marker of biliary injury (Manns et al., 2010). Examination of liver histology should reveal the presence of interface hepatitis (disruption of the portal tract by a mononuclear cell infiltrate), the defining hallmark of AIH (Czaja, 2006). This infiltrate consists mainly of lymphocytes and plasma cells. Unfortunately, treatment options for patients with AIH are limited. First-line therapy for patients with AIH are high-dose corticosteroids (e.g. prednisone) to control the inflammation (Manns et al., 2010). Those that fail to respond to steroids alone are supplemented with an immunosuppressive agent such as azathioprine to further control the injury. Common side-effects with corticosteroids or azathioprine treatment include weight gain, acne, osteopenia and cytopenia (Czaja, 2008). Corticosteroid-related side effects are the most common causes for premature drug withdrawal in AIH, and there are subgroups of patients (children, cirrhotics and pregnant women) for whom this therapy regimen is unsuitable due to an increased risk of drug toxicity (Selvarajah et al., 2012, Levy, 2012).

Patients that do not respond to therapy (approximately 10%), or were unsuitable for corticosteroids or were simply left undiagnosed develop liver cirrhosis and require liver transplantation (Manns et al., 2010). Transplantation carries a risk of further morbidity and

mortality and patients need to be placed on life-long immunosuppression to avoid rejection (Jain et al., 2000). However, advances in surgical techniques and management have improved the 5 and 10 year survivals of patients with AIH that underwent transplantation to approximately 75% (NHS Blood and Transplant, 2010, Vogel et al., 2004). The main disadvantages of liver transplantation are the shortage of suitable donor organs, resulting in an average waiting time of 142 days for adults and 78 days for children (NHS, 2013). Up to 30% of AIH patients who received a transplant suffer from recurrent AIH in allografts, resulting in the reintroduction of prednisone/azathioprine dual-therapy and the side-effects that come with these medicines (Ratziu et al., 1999). Due to these issues, the search is on for alternative therapies to combat autoimmune liver diseases.

Due to their ability to module immune cell responses, MSC transplantation could complement existing treatment regimens to dampen the proliferation of autoreactive T cells and reduce liver injury (Czaja, 2009). As mentioned in the Introduction (1.6.3 – Clinical evidence for Immunosuppression), MSCs have been used clinically in a variety of immune-mediated and autoimmune conditions including GvHD, SLE and Crohn's Disease (Le Blanc and Mougiakakos, 2012). However, the evidence supporting MSC therapy in early-to-medium stage AIH is limited to pre-clinical animal models. Chen and colleagues demonstrate that the systemic administration of murine MSCs ameliorated experimental AIH in mice (Chen et al., 2014). Interestingly, they observed an improved response on serum ALT after repeated dosing of MSCs. The majority of pre-clinical and clinical studies have examined the effect of MSC infusion in patients with late-stage AIH, often those with decompensated liver

disease that require transplantation (Houlihan and Newsome, 2008). As with most early-stage MSC trials, the results are varied with some studies showing clinical improvements following infusion and others proving only the safety of MSC therapy (Meier et al., 2013, Zhang and Wang, 2013). Additionally, the majority of studies had poorly defined endpoints, short-term follow-up or the lack of a comparator arm which makes it difficult to evaluate therapeutic efficacy. Early work by Mohamadnejad et al. (2007) demonstrated MSC infusion to be safe in a small-scale trial involving four patients with decompensated cirrhosis. Improvements in liver function were detected in 2/4 patients and improvements in QoL questionnaire scores were seen in 4/4 patients after 12 months. A later study by the same group recruited 27 patients with decompensated cirrhosis and randomised them to receive either MSCs or placebo in a single-blinded fashion (Mohamadnejad et al., 2013). Although no adverse effects were seen after MSC infusion, no differences in liver function or liver synthesis scores were observed between both arms of the study one year after treatment. As such, the efficacy of MSC therapy in autoimmune liver disease still needs to be proven in larger-scale studies and questions still remain about the mechanism of action behind any clinical improvements seen in patients after infusion.

### 6.1.2 Mouse model of Autoimmune Liver Injury (OVA-Bil)

To test the *in vivo* efficacy of PαS MSCs, we utilised a transgenic mouse model of immune-mediated liver injury first described by Marion Peters' group in 2006 (Buxbaum et al., 2006). OVA-Bil mice express membrane bound ovalbumin (OVA) under the control of a bile acid transporter promoter (ASBT – apical sodium-dependent bile acid transporter). This limits the

expression of OVA to the biliary epithelium of their livers. OVA-Bil mice are maintained on a C57BL/6 background and develop normally with no signs of liver inflammation when assessed using histology (Figure 6.1A), serum ALT or ALP. To induce immune-mediated liver injury, OVA-specific $CD8^+$ T cells (isolated from OT-1 transgenic mice) and $CD4^+$ T cells (isolated from OT-2 transgenic mice) are adoptively transferred into OVA-Bil mice. These OVA-specific T cells migrate to the biliary tree where they proliferate and induce necro-inflammatory damage (Figure 6.1A). Regions of interphase hepatitis, the characteristic histological marker of AIH, could be seen around the portal triad in injured mice. The authors identified through a series of dose-titration experiments that co-infusion of $10x10^6$ OT1 splenocytes and $4x10^6$ OT2 splenocytes were optimal to cause peak liver injury. Interestingly, infusion of up to $10x10^6$ OT2 splenocytes by itself does not result in any liver injury, and infusion of OT1 splenocytes alone only caused mild increases in liver transaminases, suggesting that there is a synergistic partnership between OVA-specific CD8 and CD4 T cells in mediating liver injury in these animals.

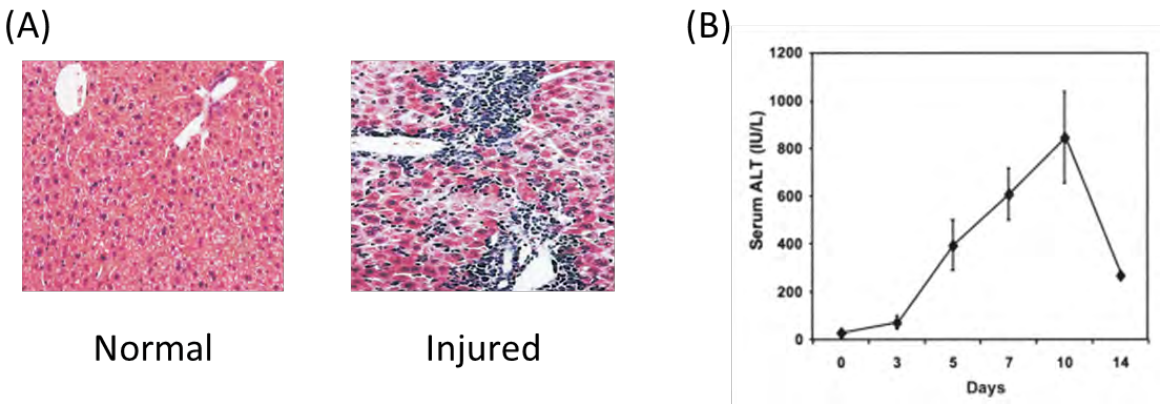


Figure 6.1 | **Induction of liver injury in OVA-Bil mice**. (A) H+E stained liver sections from normal and injured OVA-Bil mice. (B) Time course of serum ALT following adoptive transfer of OVA-specific CD4 and CD8 T cells. Figure modified from Buxbaum et al. (2006).

A time-dependent 30-fold increase in serum ALT was observed following adoptive transfer of OT1/OT2 T cells (Figure 6.1B). ALT readings peak at day 10 post adoptive transfer and drops thereafter. The authors' report that histology and ALT readings return to baseline after 28 days due to loss of adoptively transferred cells. Interestingly, only a two-fold increase in ALP was observed by Buxbaum and colleagues, demonstrating significant spillover of injury towards hepatocytes from the $OVA^{+}$ biliary epithelium. In addition to changes in liver transaminase enzymes, the authors also report a sharp increase in liver-infiltrating mononuclear cells, with the majority being $V\alpha2^{+}$ T cells, corresponding to the adoptively-transferred population. An increase in inflammatory cytokine (IFNγ and TNFα) production was also observed during hepatobiliary inflammation.

As such, OVA-Bil mice are an antigen- and organ-specific model of immune-mediated tissue injury. Uninjured mice develop normally and show no signs of liver damage. Inflammation is dependent on the adoptive transfer of OT1 and OT2 splenocytes, with OT1 cells being absolutely required and OT2 cells augmenting the damage seen. Therefore, OVA-Bil mice are a model of *alloimmune* liver injury as host T cells are tolerant to the OVA antigen. The symptoms displayed by injured mice closely resemble patients with AIH as we could observe regions of interface hepatitis in injured animals. Additionally, significant increases ALT, but not ALP give further evidence for their AIH phenotype. One key disadvantage of this model is the transient nature of inflammation, which peaks at day 10 and falls thereafter due to the loss of adoptively-transferred cells. The natural resolution of injury in OVA-Bil mice mean that these animals do not develop liver cirrhosis or undergo liver failure, which are frequently observed in patients with late-stage AIH (Manns et al., 2010).

### 6.1.3 Chapter Aims

Our previous findings show that PαS MSCs can suppress the proliferation of CD4 and CD8 T cells *in vitro*, and that TGF-β1 supplementation can maintain the immunomodulatory properties of these cells over extended *in vitro* culture. The aims of this chapter were to characterise the immunosuppressive properties of PαS *in vivo* using the OVA-Bil model of hepatobiliary injury. The specific aims of this chapter were to:

1. Establish the transgenic mouse colonies required to perform the OVA-Bil model
2. Characterise the inflammatory damage seen in OVA-Bil mice
3. Examine the effect of early-passage PαS MSC infusion on overall liver damage, infiltrating leukocyte numbers and their activation status
4. Examine the effect of late-passage TGF-β1 primed PαS MSCs *in vivo*

## 6.2 Results

### 6.2.1 Genotyping and Confirmation of OVA Expression

OVA-Bil mice were maintained as heterozygotes on a C57BL/6 background. Confirmation of OVA expression was performed using conventional PCR as described by Buxbaum et al. (2006). OVA$^+$ mice produce a band approximately 990bp in size (Figure 6.2A). OT-1 mice are also maintained on a C57BL/6 background and confirmation of OVA-specific transgenic T cell receptor expression was performed using PCR as described by Wright et al. (2005). OT-1$^+$ mice produce a band approximately 250bp in size (Figure 6.2B). OT-2 mice were maintained as homozygotes and genotyping of breeders was outsourced to Transnetyx (Cordova, USA).

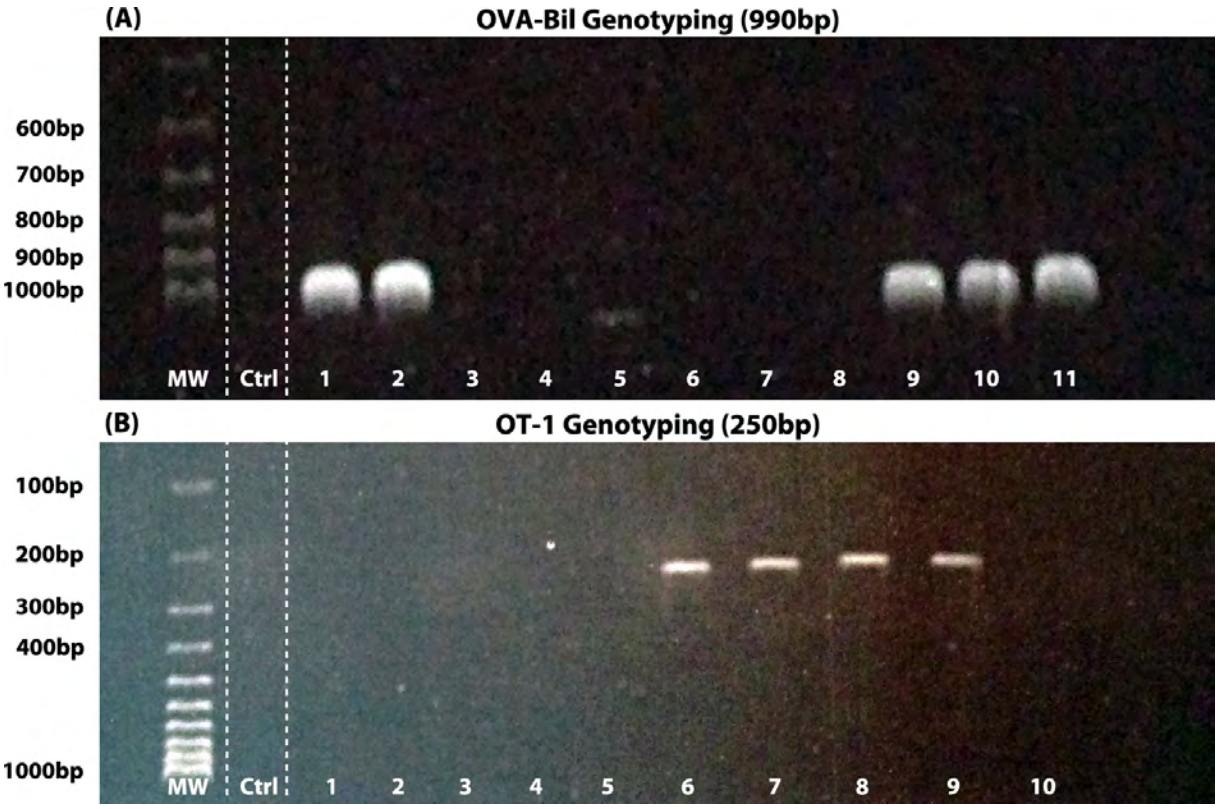


Figure 6.2 | **Genotyping OVA-Bil and OT-1 mice**. (A) OVA$^+$ mice produce a band 990bp in size. Mice in lanes 3-8 were negative for the OVA transgene. (B) OT-1$^+$ mice produce a band 250bp in size. Mice in lanes 1-5 and 10 were negative for the OT-1 transgene. Control (Ctrl) lanes contained no DNA in PCR reaction.

Chromogenic immunohistochemistry (IHC) was used to confirm expression of ovalbumin at the protein level. Liver sections from 12-week old $OVA^+$ OVA-Bil mice were cut, incubated with an anti-ovalbumin antibody and counterstained using H&E. No positive staining could be seen in the isotype-matched controls (Figure 6.3). Although the DAB stain was very faint, expression of ovalbumin was confined to biliary epithelial cells of the liver (Figure 6.3 arrowheads). No signs of liver damage or leukocytic infiltrate could be observed in the livers of uninjured animals, confirming the previous findings of Buxbaum et al. (2006).

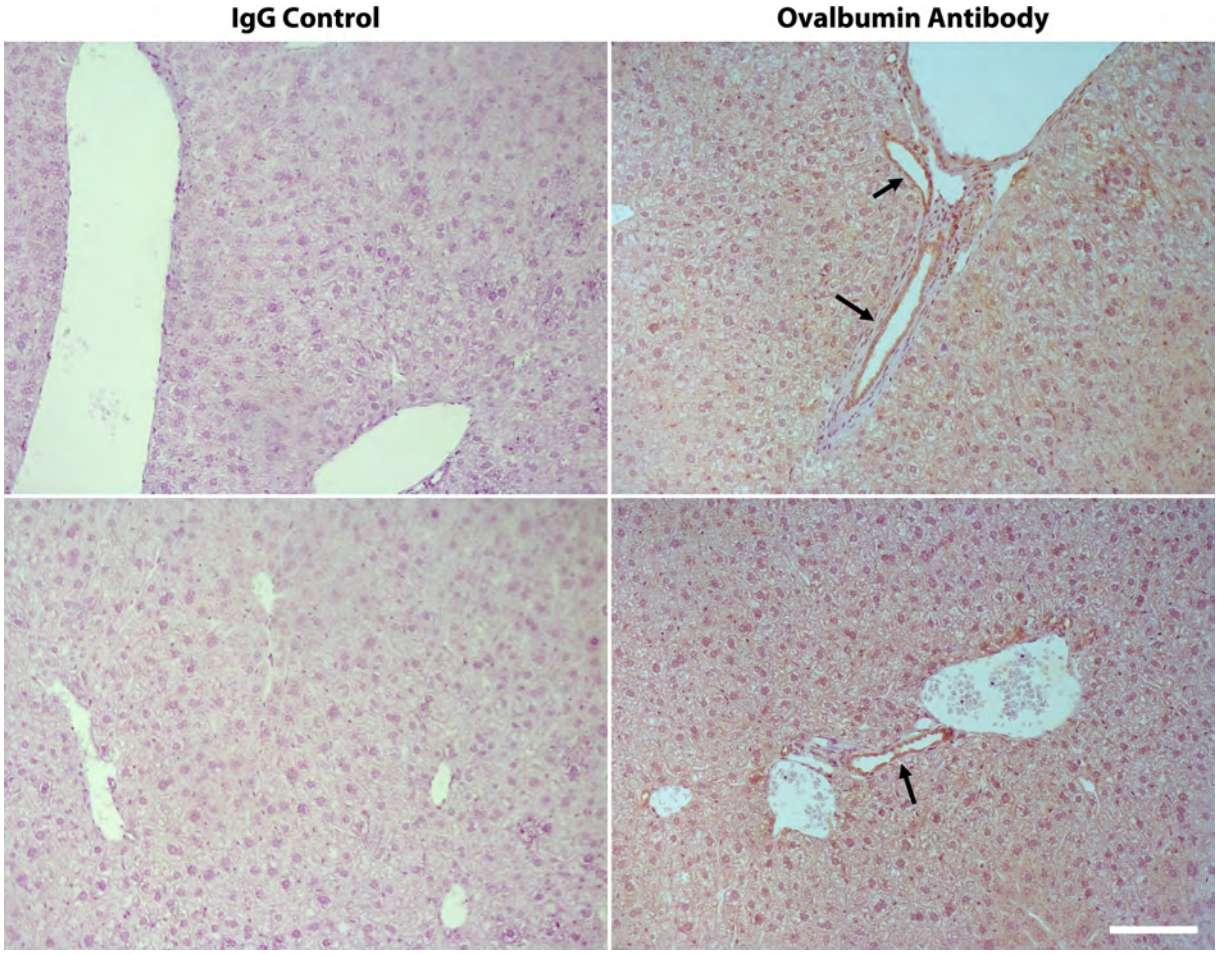


Figure 6.3 | **Localisation of ovalbumin expression in OVA-Bil mice**. 12-week old male OVA-Bil mice livers were cut and incubated with an isotype matched control or ovalbumin antibody. Sections were counterstained using H&E prior to imaging. Images taken at 200x magnification. Scale bar, 100µm.

### 6.2.2 Time course of Liver Injury

Adoptive transfer of $10x10^6$ OT-1 splenocytes and $4x10^6$ OT-2 splenocytes via intraperitoneal (IP) infusion into OVA-Bil mice results in their migration to the liver where they proliferate and cause damage. To assess the time course of liver injury, serum ALT and ALP readings were taken at different periods after adoptive transfer. Significant increases in serum ALT was observed between uninjured controls (22±8.5 IU/L) and days eight (264±140 IU/L), nine (294±141 IU/L) and ten (643±184 IU/L) post-adoptive transfer (Figure 6.4A). As described by Buxbaum et al. (2006), we too observed a peak in serum ALT at day 10 followed by a sharp drop by day 11 (164±36 IU/L) due to loss of adoptively transferred cells. Compared to ALT, which rose approximately 30-fold compared to controls, serum ALP levels only rose 2-fold in injured mine and remained elevated at day 11 (Figure 6.4B). Due to its increased sensitivity, serum ALT was chosen as a marker of overall liver injury for downstream experiments.

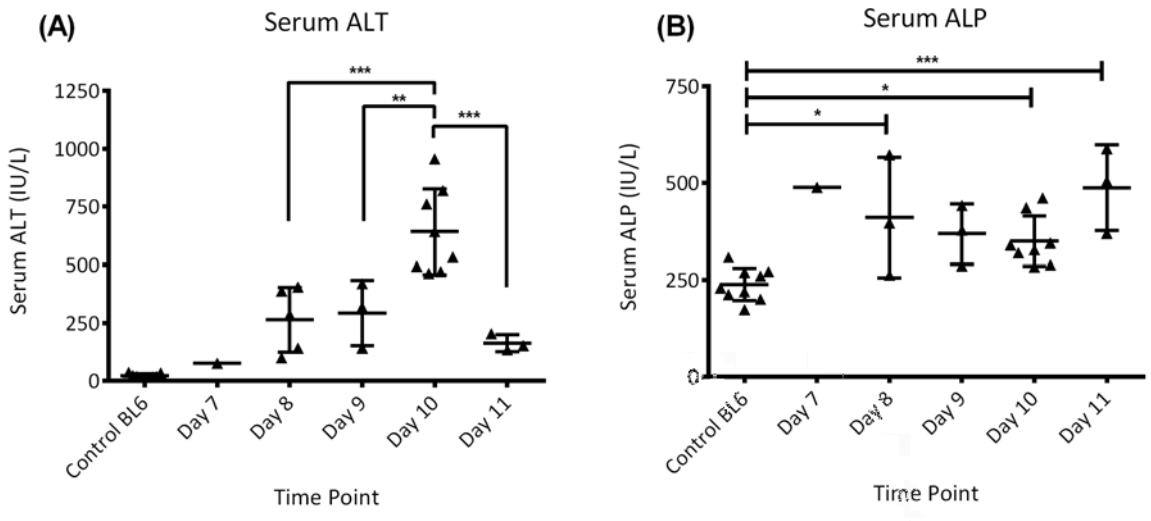


Figure 6.4 | **Time course of liver injury in OVA-Bil mice**. Mouse serum was analysed for the activity of liver enzymes ALT (A) and ALP (B) following adoptive transfer of OT-1 and OT-2 splenocytes. Data represented as mean±SD. Each data point represents one animal. Statistical analysis performed using One-way ANOVA with Bonferroni's Multiple Comparison Test.

### 6.2.3 Liver Histology after Injury

Liver sections from uninjured and day 10 injured OVA-Bil mice were fixed in formalin and processed for IHC. H&E staining revealed normal liver architecture in uninjured animals with no visible immune reaction against $OVA^+$ biliary cells in the portal areas of the liver (Figure 6.5A). Following injury, a widespread disruption of portal areas by infiltrating immune cells could be seen (Figure 6.5B). Regions of interphase hepatitis could be seen around the bile ducts, and clusters of lymphocytes could also be observed in the wider liver parenchyma (Figure 6.5C). As ovalbumin is not expressed on hepatocytes, it was interesting to see substantial spillover of lymphocytes into lobular regions.

CD45 was used to mark all leukocytes (Fedorcsák et al., 2007) and the F4/80 antigen used to mark murine macrophages in the livers of OVA-Bil mice (Austyn and Gordon, 1981). Low numbers of $CD45^+$ leukocytes or $F4/80^+$ macrophages were detected in uninjured mice (Figure 6.5D,G). A sharp increase in the number of cells expressing either antigen was observed in portal areas after injury. Matching the observations of the H&E stained sections, spillover of $CD45^+$ cells into lobular regions was also observed, with clusters of leukocytes present in parenchymal areas after injury (Figure 6.5E,F). The numbers of $F4/80^+$ hepatic macrophages in portal and lobular regions also increased after injury (Figure 6.5H,I). These findings suggest that although the damage is primarily targeted against biliary epithelium in OVA-Bil mice, there is considerable spillover of mononuclear infiltrate into lobular regions resulting in moderate interphase hepatitis. This spillover of damage-causing OT-1 and OT-2 cells into lobular areas could account for the increase in serum ALT observed in this model.

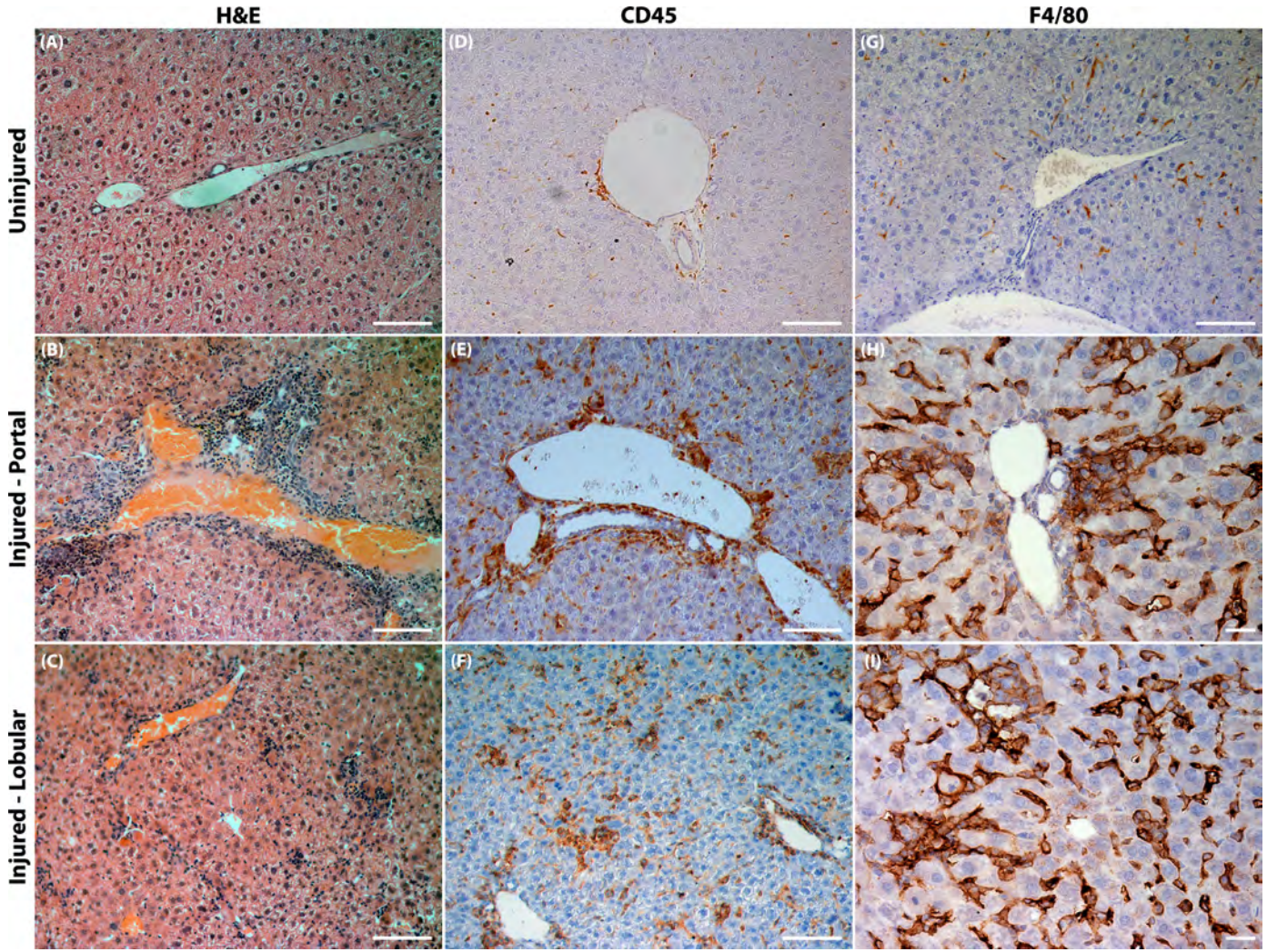


Figure 6.5 | **Liver Histology of OVA-Bil mice after injury.** Representative images of uninjured and injured mice (Day 10) stained using H&E (A-C) and antibodies against CD45 (D-F) and F4/80 (G-I). Images A-G were taken at 200x magnification. Images H & I were taken at 400x magnification. Scale bar, 100µm.

### 6.2.4 Effects of Early-Passage PαS MSC infusion in the OVA-Bil model

#### 6.2.4.1 Effect on Serum ALT

Our *in vitro* data shows that PαS MSCs cultured in SM were the most suppressive at early passages (P3), but this ability was lost as cells became increasingly senescent. Cells expanded in TGF-β1 medium were not as potent as SM cells early on, but TGF-β1 supplementation was able to maintain the immunosuppressive potential over several passages. To back up these *in vitro* findings, the OVA-Bil model was used to test the *in vivo* immunosuppressive effects of early-passage PαS MSCs to see whether they could dampen liver injury in these animals.

PαS MSCs expanded in SM±TGF-β1 were used at P4 for *in vivo* studies. Two doses of $1x10^6$ MSCs were given via IP infusions after the induction of injury at days 3 and 7. Animals were then sacrificed at day 10 for analysis of liver inflammation (Figure 6.6A). The timings and dosage of MSCs were chosen after reviewing recent literature, which suggested that MSCs were short-lived and need to be in an inflammatory environment to be active (Krampera et al., 2013). Day 10 was chosen as the end point from our earlier ALT time course data showing peak damage at this time (Figure 6.4A).

Serum ALT levels were recorded in control and MSC-treated animals to measure overall hepatic damage (Figure 6.6B). Significant reductions in ALT were observed in animals receiving SM MSC treatment (339±220 IU/L) compared to control animals (818±452 IU/L, p=0.005). TGF-β1 primed MSCs also caused a reduction in serum ALT (585±355 IU/L)

compared to controls, but this difference did not reach statistical significance (p=0.2). These findings back up our earlier *in vitro* data that showed early passage SM cells were more suppressive than TGF-β1 primed cells.

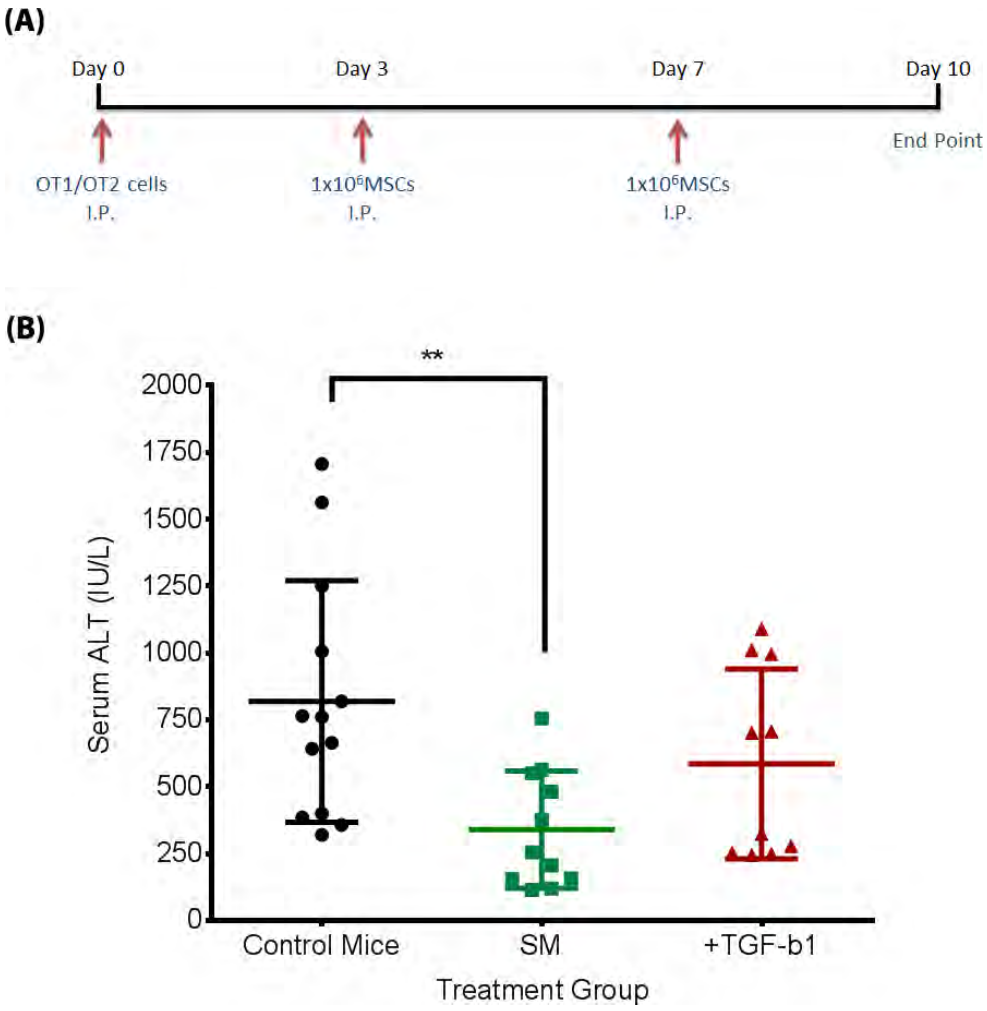


Figure 6.6 | **Effect of PαS MSC infusion on serum ALT readings from OVA-Bil mice**. (A) Experimental plan outlining initiation of injury (Day 0) followed by two MSC doses at days 3 and 7 and the end point at day 10. (B) Serum ALT from untreated control mice (n=13), P4 SM-primed MSC treated animals (n=11) and P4 TGF-β1 primed MSC treated animals (n=10). All mice were age and sex-matched for each experiment. Data shown as mean±SD. Statistical analysis performed using One-way ANOVA with Bonferroni's Multiple Comparison Test.

### 6.2.4.2 Characterisation of Liver Lymphocyte Populations

Flow cytometric analysis of liver-infiltrating lymphocytes was performed to elucidate how PαS MSCs were reducing serum ALT in injured animals. Liver lobes from day 10 animals were weighed and processed to form a single cell suspension. Lymphocytes were then isolated and stained with relevant antibodies. A live/dead marker was used to remove dead cells from downstream analysis and absolute counts from the flow cytometer were then normalised to the weights of the starting liver lobes to allow comparison between mice.

One potential mechanism behind the beneficial effects seen with MSC infusion is via the reduction of total leukocyte numbers in models of injury (Ma et al., 2014, Le Blanc and Mougiakakos, 2012, Uccelli et al., 2008). Analysis of viable $CD3^+$ lymphocytes revealed a significant drop in the numbers of cells isolated from the livers of SM-primed MSC-treated animals (225,119±150,669 cells per gram of liver tissue) compared to control animals (421,551±169,367 cells /g liver, p=0.03, Figure 6.7A). A non-significant reduction was observed in TGF-β1 primed MSC-treated animals (305,848±173,589 cells /g liver). Division of $CD3^+$ T lymphocytes into $CD3^+CD4^+$ T helper cells (Figure 6.7B) and $CD3^+CD8^+$ cytotoxic T cells (Figure 6.7C) revealed non-significant reductions in MSC-treated animals. Approximately 2 to 3-fold higher numbers of $CD8^+$ T cells were isolated than their $CD4^+$ counterparts. These findings suggest that MSC infusion produces improvements in serum ALT by reducing the total numbers of damage-causing lymphocytes in the livers of OVA-Bil animals.

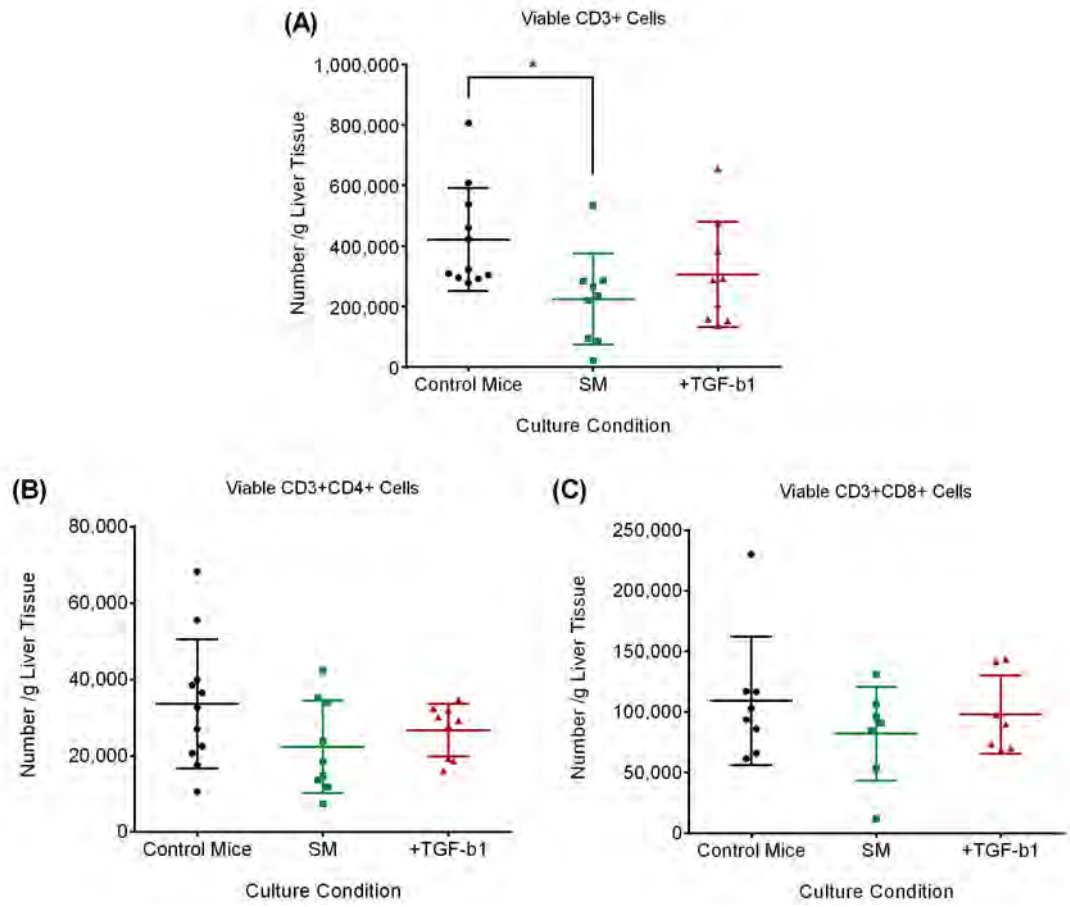


Figure 6.7 | **Quantification of liver lymphocyte populations from OVA-Bil mice**. Lymphocytes were isolated using density gradient separation and absolute cell counts were normalised to the weights of the starting liver lobe to allow comparison between animals. (A) Number of viable $CD3^+$ lymphocytes. (B) Number of viable $CD4^+$ T helper cells. (C) Number of viable $CD8^+$ cytotoxic T cells. Data shown as mean±SD. Each data point represents one animal. Statistical analysis performed using One-way ANOVA with Bonferroni's Multiple Comparison Test.

In addition to their ability to decrease total lymphocyte numbers at sites of injury, MSCs have also been reported to reduce the activation status of lymphocytes *in vivo* (Hof-Nahor et al., 2012, Park et al., 2011, Ding et al., 2009, Le Blanc et al., 2004a). To test this hypothesis, we examined the expression of the early T cell activation marker CD69 (Ziegler et al., 1994) and the IL-2 receptor alpha chain CD25 (Caruso et al., 1997) on CD4 and CD8 populations isolated from OVA-Bil mouse livers (Figure 6.8). In general, there was considerable variation in the activation status of lymphocytes isolated from control or MSC treated animals but the

mean values across all samples were broadly similar. CD25 expression on $CD8^+$ T cells gave mixed results, with one population of high expressers (5-15%) and another population of low expressers (<2%; Figure 6.8D). More repeats are necessary to discern whether this was due to operator error or whether this is a reproducible biological finding. In summary, the results show that PαS MSC infusion significantly reduces total numbers of lymphocytes in OVA-Bil mice, but the activation status of the cells that remain seems unchanged.

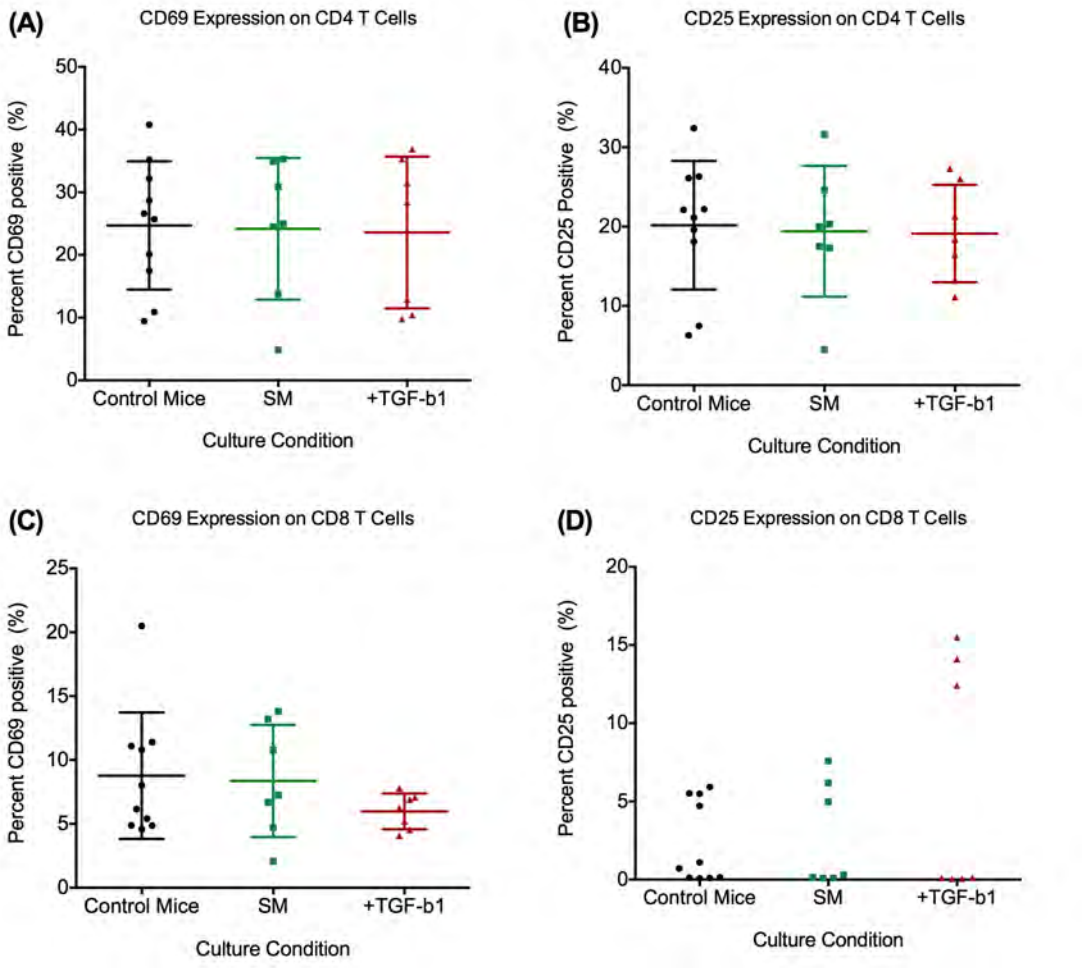


Figure 6.8 | **Activation marker expression of liver lymphocyte populations from OVA-Bil mice**. Lymphocytes were isolated using density gradient separation from day 10 OVA-Bil animals and analysed using flow cytometry. The percentage of CD69 and CD25 positive T helper cells (A and B) and cytotoxic T cells (C and D) were recorded. Data shown as mean±SD. Each data point represents one animal.

### 6.2.4.3 Histological Analysis of MSC-treated Animals

Liver sections from day 10 MSC-treated OVA-Bil animals were processed to examine inflammation in more detail. H&E staining was performed to examine the numbers of infiltrating immune cells and overall liver morphology. As suggested by the flow cytometry data (Figure 6.7), there appears to be a decrease in the number of infiltrating cells in MSC-treated animals compared to injured controls (Figure 6.9). However, disruption of portal areas by infiltrating immune cells could be seen in all groups, and there were clusters of immune cells located in the wider liver parenchyma as well.

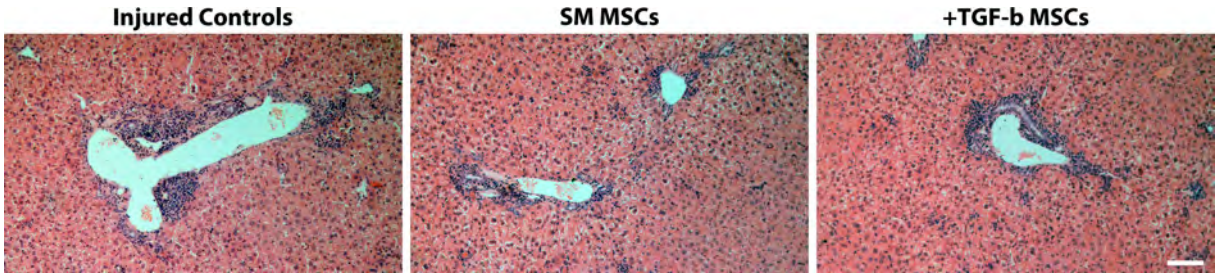


Figure 6.9 | **H&E stained livers of MSC-treated OVA-Bil mice**. Representative images of H&E stained liver sections from injured and MSC-treated animals. All images taken at 100x magnification. Bar, 100µm.

Expression of the pan-leukocyte marker CD45 was used to quantify the differences in immune cell number seen between groups. Multiple images of portal and lobular areas of the liver were taken from each mouse under high magnification (Figure 6.10A) and the amount of staining quantified using Image J software (Figure 6.10B). As expected, there was a significant increase in CD45 staining after injury in both portal and lobular regions compared to uninjured controls. A significant reduction in CD45 staining was seen in animals receiving SM-primed MSCs compared to injured controls in portal regions (20.5±9.1% vs.

9.0±5.1% CD45 positive, p=0.02). Animals receiving TGF-β1 primed MSCs also displayed significant reductions in CD45 staining in portal regions compared to controls (20.5±9.1% vs. 9.7±2.8% CD45 positive, p=0.03). Reductions in CD45 staining were also observed in lobular regions following MSC infusion, although these failed to reach statistical significance.

Expression of F4/80 antigen was then examined to quantify murine macrophages in the livers of OVA-Bil animals after MSC treatment. Multiple images were taken of both portal and lobular regions of the liver (Figure 6.11A) and the amount of staining quantified using Image J software (Figure 6.11B). As expected, significant increases in F4/80 staining was observed in injured animals compared to uninjured controls. Interestingly, SM-primed MSC treatment resulted in a small, non-significant reduction in macrophage numbers compared to injured controls in both portal (19.1±4.6% vs. 15.9±3.7% F4/80 positive, p=0.7) and lobular regions (19.6±6.0% vs. 16.2±3.2% positive, p=0.7). In contrast, animals receiving TGF-β1 primed MSC treatment had significant reductions in F4/80 staining in both portal (19.1±4.6% vs. 11.1±4.3% positive, p=0.006) and lobular (19.6±6.0% vs. 12.3±2.9% positive, p=0.02) regions compared to injured controls. The reason behind the selective retention of macrophage numbers following SM-primed, but not TGF-β1 primed MSC treatment is currently unknown, and further work looking at macrophage polarisation is required to elucidate the significance of this finding.

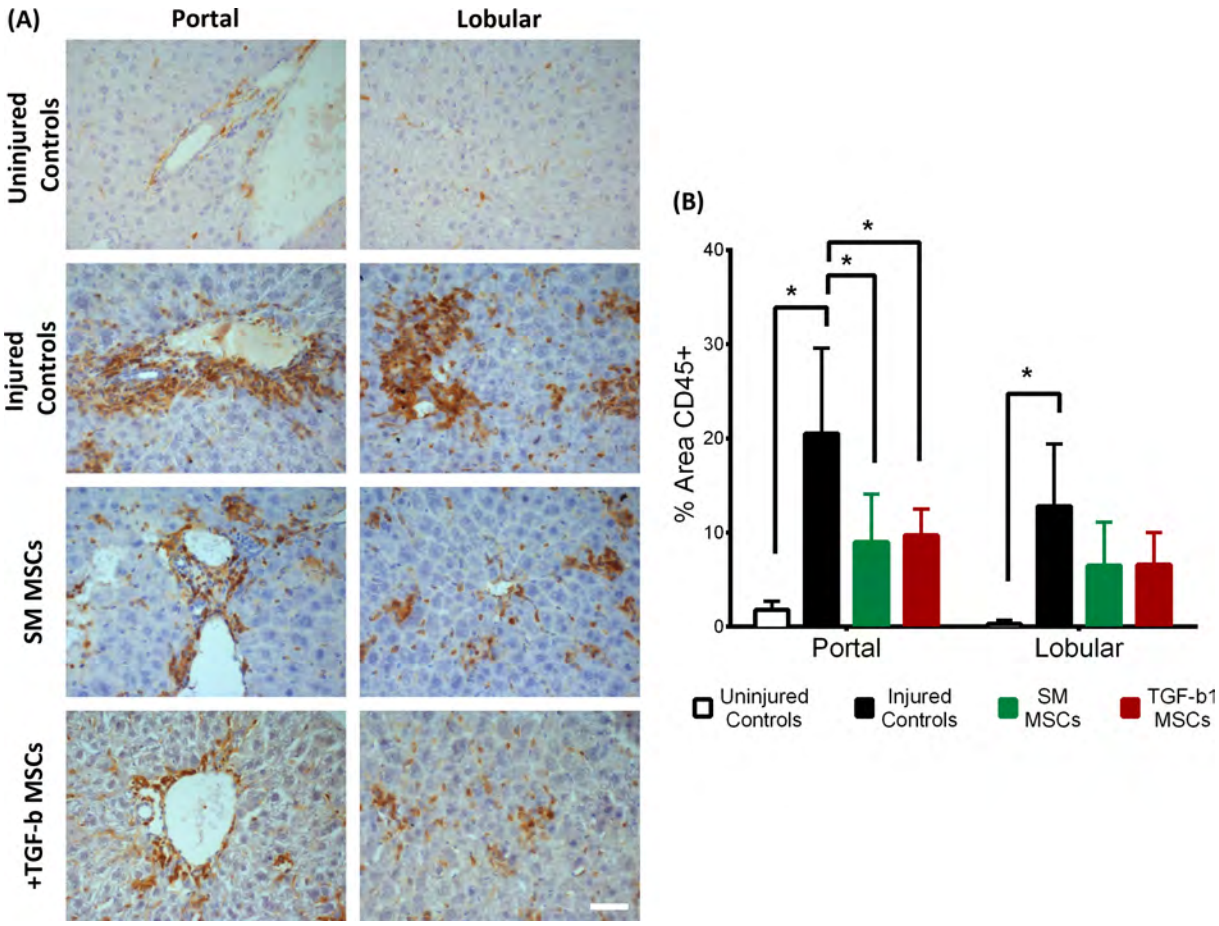


Figure 6.10 | **CD45 expression in the livers of OVA-Bil mice**. (A) Representative images of CD45 staining from control and MSC-treated OVA-Bil mouse livers. All images taken at 400x magnification. Bar, 100µm. (B) Quantification of CD45 staining using Image J. Five images each were taken of portal and lobular areas for quantification from uninjured controls (n=2), injured controls (n=7), SM-primed MSCs (n=6) and TGF-β primed MSCs (n=6). Data shown as mean±SD. Statistical analysis performed using One-way ANOVA with Bonferroni's Multiple Comparison Test.

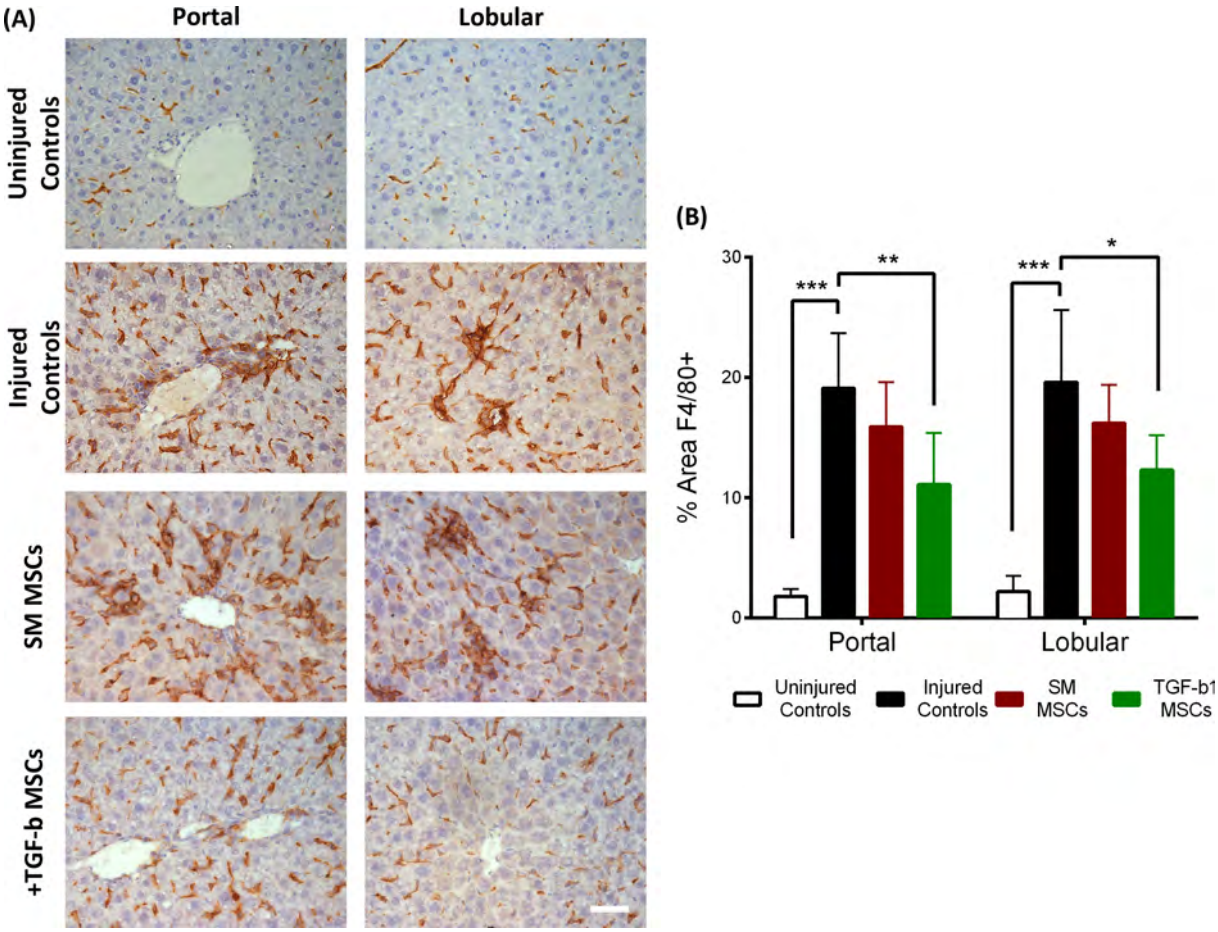


Figure 6.11 | **F4/80 expression in the livers of OVA-Bil mice**. (A) Representative images of F4/80 staining from control and MSC-treated OVA-Bil mouse livers. All images taken at 400x magnification. Bar, 100µm. (B) Quantification of F4/80 staining using Image J. Five images each were taken of portal and lobular areas for quantification from uninjured controls (n=2), injured controls (n=8), SM-primed MSCs (n=9) and TGF-β primed MSC animals (n=7). Data shown as mean±SD. Statistical analysis performed using One-way ANOVA with Bonferroni's Correction.

### 6.2.5 Effects of Late-Passage PαS MSC infusion in the OVA-Bil model

#### 6.2.5.1 Effect on Serum ALT

Our *in vitro* and *in vivo* findings demonstrate that early-passage (P4 or lower) PαS MSCs expanded in SM were more immunosuppressive than TGF-β1 supplemented cells. However, SM-primed MSCs lost their suppressive potential by P7 due to the onset of senescence. TGF-β1 supplementation was shown to maintain their immunomodulatory properties *in vitro* by delaying the onset of senescence. Here, we again used the OVA-Bil model to examine the effect of late-passage (P7) MSCs to see whether SM-primed cells lost their ability to reduce liver injury and observe whether TGF-β1 primed cells maintained their immunosuppressive properties *in vivo*.

Two doses of $1x10^6$ MSCs were given via IP infusions after the induction of liver injury as described before (Figure 6.6A). Animals were sacrificed at day 10 and serum ALT levels were recorded in controls and P7 MSC-treated animals to measure overall hepatic damage (Figure 6.12). No significant differences were observed between control animals (680±194 IU/L) and P7 SM-primed MSCs (580±77 IU/L), validating our previous *in vitro* findings. Late-passage TGF-β primed MSC infused caused the biggest mean reduction in serum ALT (410±300 IU/L), but the small sample size and variation observed between animals prevents this from being statistically significant. Further repeats are required to increase our sample size to pick out any potential significant differences between groups.

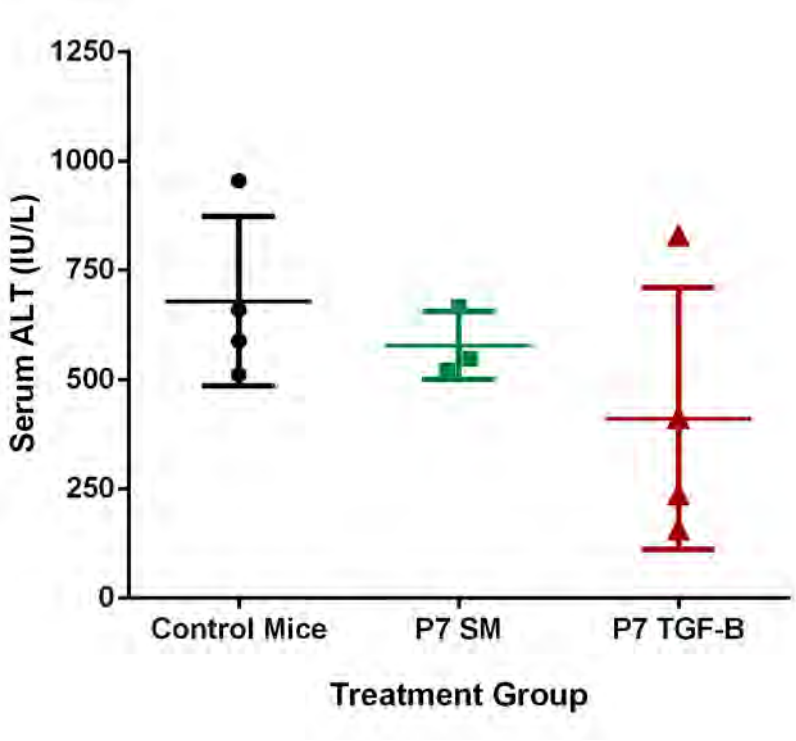


Figure 6.12 | **Effect of late-passage PαS MSCs on serum ALT readings in OVA-Bil mice**. Serum ALT was quantified from control animals (n=4), P7 SM-primed MSC-treated animals (n=3) and P7 TGF-β1 primed MSC-treated animals (n=4). All mice were age and sex-matched for each experiment. Data shown as mean±SD. Statistical analysis performed using One-way ANOVA with Bonferroni's Multiple Comparison Test.

### 6.2.5.2 Characterisation of Liver Lymphocyte Populations

Flow cytometric analysis of liver-infiltrating lymphocytes was performed to examine how late-passage PαS MSCs were working in this model. Total lymphocyte numbers were quantified from all animals to examine whether late-passage MSC treatment caused a reduction in overall lymphocyte numbers in OVA-Bil mice. Analysis of total viable $CD3^+$ lymphocytes revealed a significant drop in animals receiving P7 TGF-β1 primed MSCs (90,220±30,000 cells per gram of liver tissue) compared to injured control mice (245,600±76,000 cells /g liver, p=0.02, Figure 6.13A). A mean reduction was also observed in

P7 SM-primed MSC-treated animals (160,000±87,000 cells /g liver) but this failed to reach statistical significance. Sub-division of $CD3^+$ T lymphocytes into $CD4^+$ T helper cells revealed non-significant reductions in MSC-treated animals (Figure 6.13B). However, quantification of viable $CD8^+$ cytotoxic T cells revealed a significant reduction in the TGF-β1 group compared to controls (71,100±18,000 vs. 31,400±14,000 cells /g liver tissue, p=0.03, Figure 6.13C).

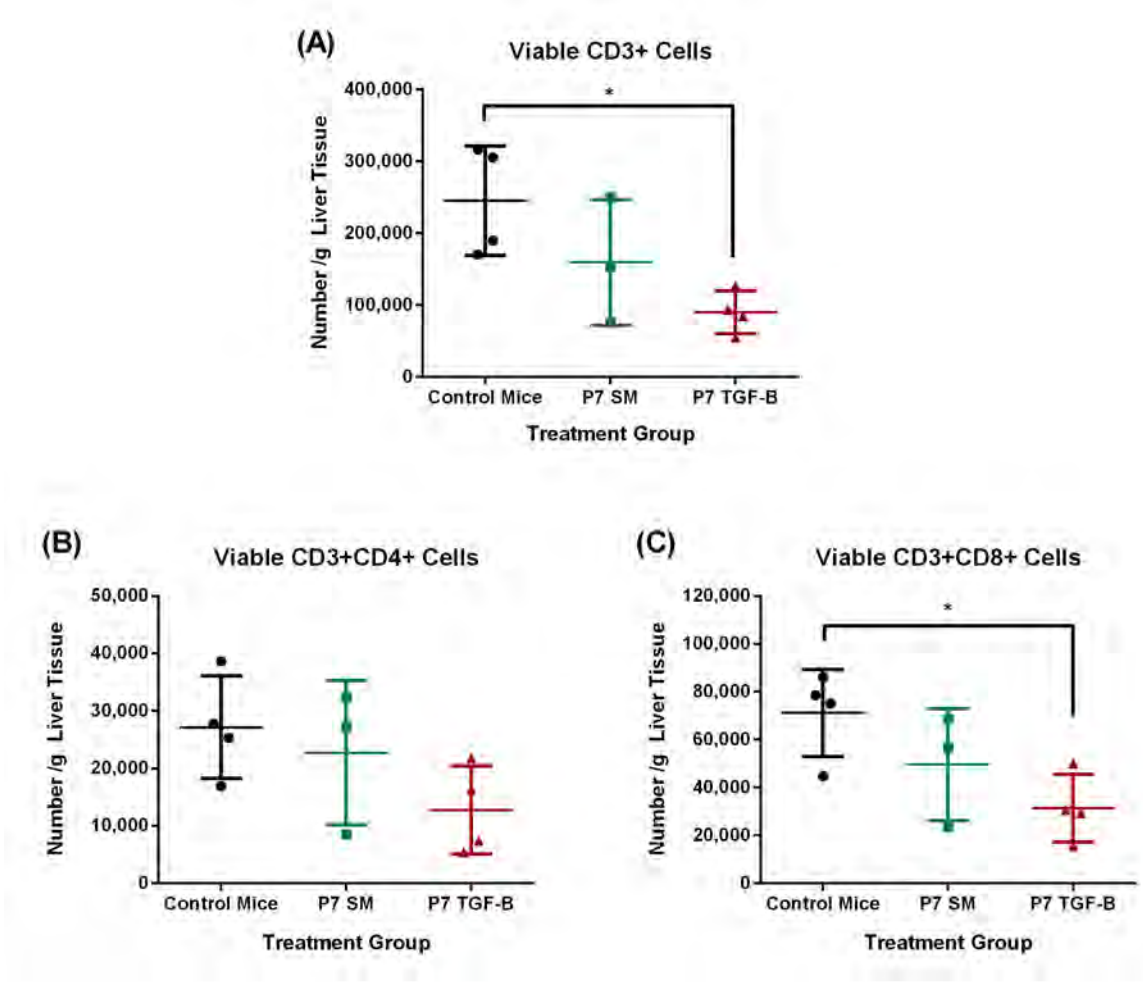


Figure 6.13 | **Quantification of liver lymphocyte populations after late-passage MSC treatment**. Viable lymphocytes were isolated using density gradient separation and absolute cell counts were normalised to the weights of the starting liver lobe to allow comparison between animals. (A) Total number of viable $CD3^+$ lymphocytes. (B) Number of viable $CD4^+$ T helper cells. (C) Number of viable $CD8^+$ cytotoxic T cells. Data shown as mean±SD. Each data point represents one animal. Statistical analysis performed using One-way ANOVA with Bonferroni's Multiple Comparison Test.

The activation status of lymphocytes was examined by recording CD69 and CD25 expression. In general, there was some variation but the mean values across all samples were broadly similar. However, a significant reduction in CD69 expression on $CD4^+$ T helper cells was observed in animals receiving TGF-β1 primed MSC treatment compared to controls (29±3% vs. 21±1% CD69 positive, p=0.01, Figure 6.14A). Due to the low sample size, the interpretation of these results is limited. Nevertheless, these findings suggest that late-passage MSCs work in a similar fashion to early-passage cells by significantly reducing total lymphocyte numbers but having a more modest effect on lymphocyte activation status.

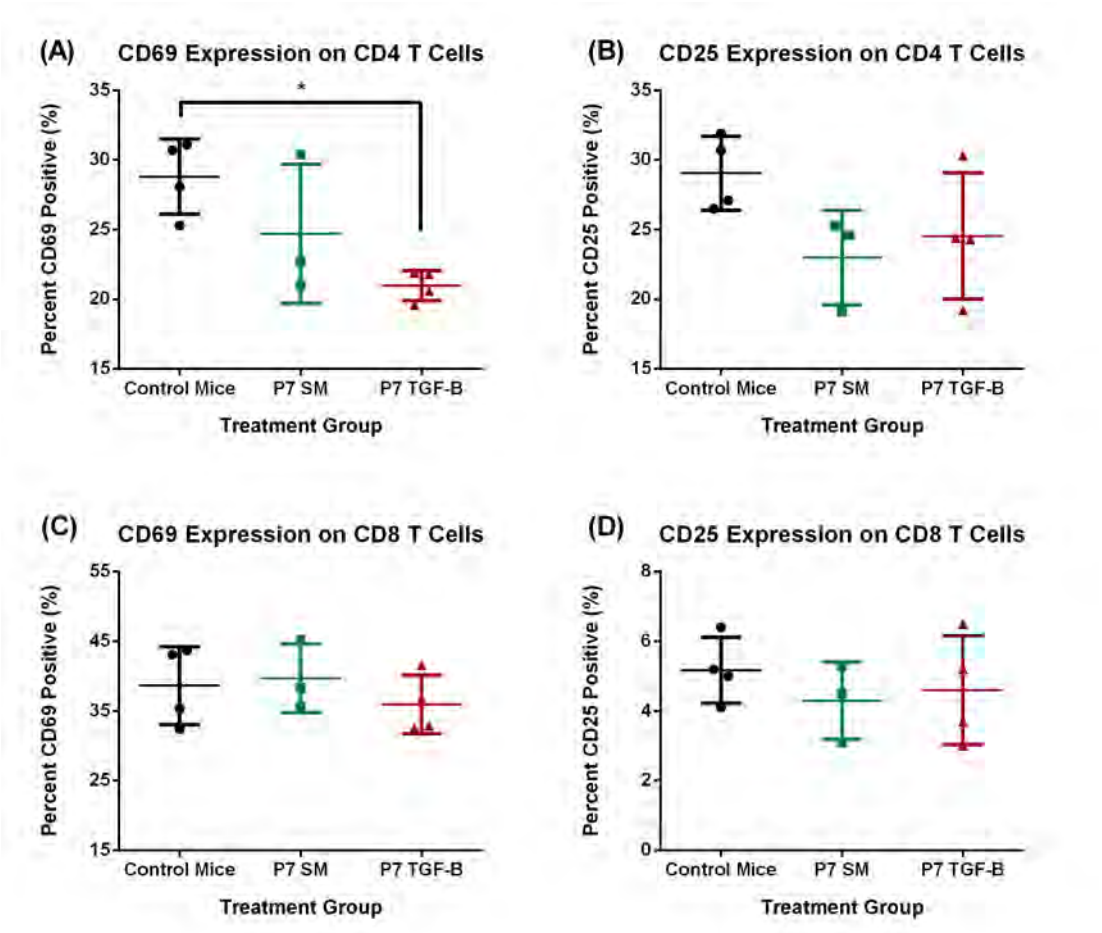


Figure 6.14 | **Activation status of liver lymphocyte populations after late-passage MSC treatment**. The percentage of CD69 and CD25 positive T helper cells (A and B) and cytotoxic T cells (C and D) was recorded. Data shown as mean±SD. Each data point represents one animal. Statistical analysis performed using One-way ANOVA with Bonferroni's Multiple Comparison Test.

#### 6.2.5.2.1 Analysis of Adoptively-transferred Cells

The OVA-Bil model is based on the adoptive transfer of damage-causing OVA-specific OT-1 and OT-2 T cells into recipient $OVA^+$ mice. All OT-1 and OT-2 donor lymphocytes express Vα2 Vβ5 chains on their T cell receptor (Gray et al., 2012, Lei et al., 2011, Gallegos and Bevan, 2004, Clarke et al., 2000) compared to <2% of host T cells (Buxbaum et al., 2006). Therefore, a monoclonal antibody against Vα2 was used to selectively isolate the damage-causing, adoptively transferred OVA-specific T cell population from the livers of OVA-Bil mice (Figure 6.15). Total numbers of $V\alpha2^+$ T cells were then quantified and their activation status examined to elucidate the effect of late-passage MSCs on these donor T cells compared to the bulk lymphocyte population.

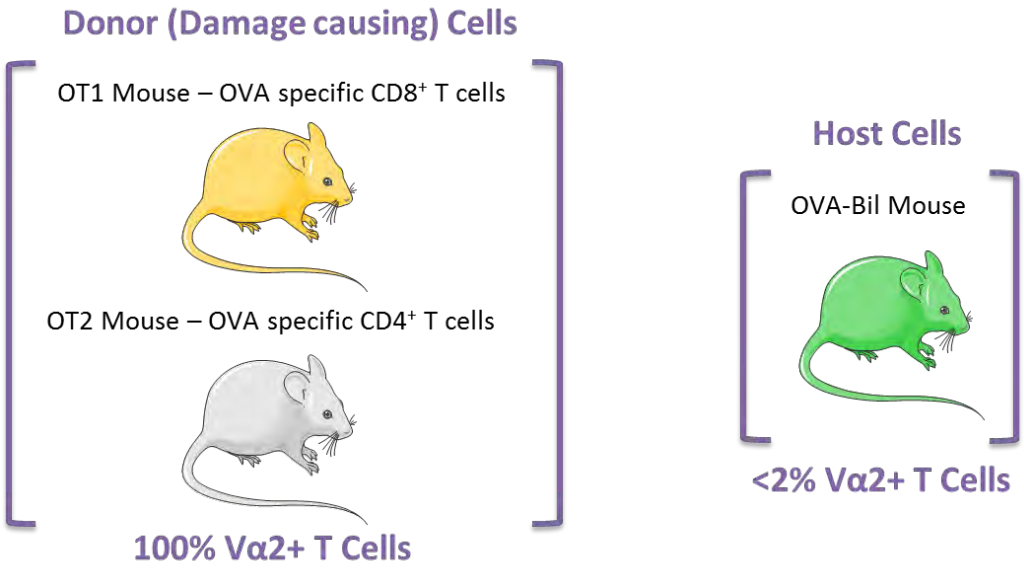


Figure 6.15 | **Identification of adoptively transferred OT-1 and OT-2 T cells**. Expression of the Vα2 chain on T cells isolated from OT-1 and OT-2 T cells allows us to mark damage-causing adoptively-transferred cells to a reasonable degree of accuracy over the host's own lymphocytes.

Analysis of the total numbers of adoptively-transferred CD4 T cells revealed a significant reduction in animals receiving TGF-β1 primed MSC treatment compared to injured controls (3900±1100 vs. 1600±980 cells /g liver tissue, p=0.03, Figure 6.16A). Significant reductions were also observed in the adoptively transferred CD8 T cell population in the TGF-β1 group (45,000±15,200 vs. 18,000±5900 cells /g liver, p=0.03, Figure 6.16B). Infusion of P7 SM-primed PαS MSCs failed to elicit significant drops in either population, suggesting that these cells have lost their *in vivo* immunosuppressive functionality at later passages.

Examination of the activation marker status of adoptively-transferred cells revealed that expression of the early T cell activation marker CD69 was significantly reduced in the CD4 and CD8 population following TGF-β1 primed MSC infusion (Figure 6.16C and E). In both cases, a reduction was also observed in animals receiving SM-primed MSCs, but this stopped short of reaching statistical significance. In contrast, expression of the late-stage activation marker CD25 was unchanged following MSC treatment on both CD4 and CD8 T cell populations (Figure 6.16D and F).

These results show that P7 TGF-β1 primed MSCs were able to reduce the number and activation status of OT-1 and OT-2 cells in OVA-Bil mice. By comparison, P7 SM-primed cells failed to produce any clinical benefit. Further repeats are required to generate significant reductions in serum ALT to further back up our hypothesis that culture and expansion in TGF-β1 maintains the immunosuppressive potential of MSCs over extended culture.

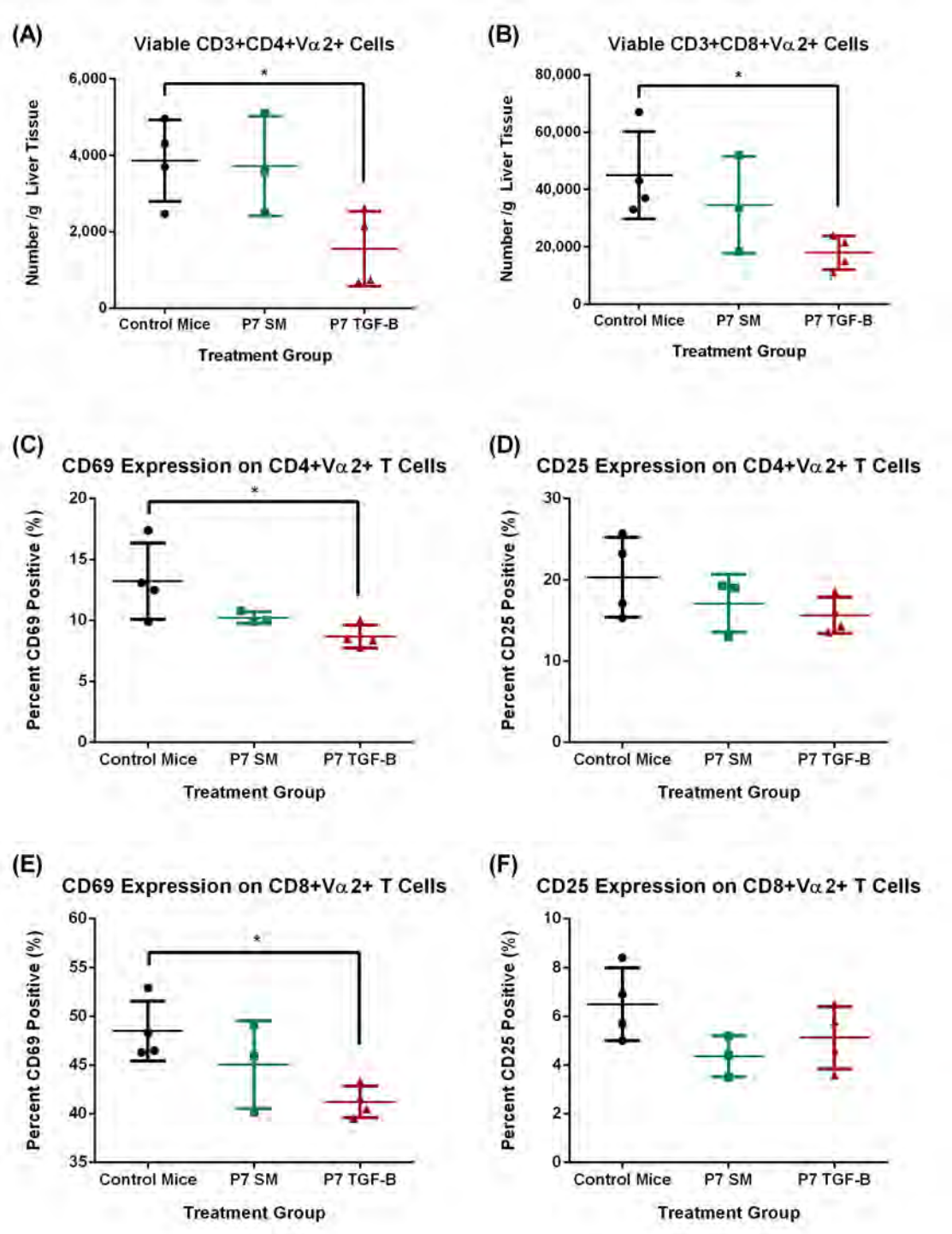


Figure 6.16 | **Effect of late-passage PαS MSCs on adoptively transferred OT-1 and OT-2 T cells**. Lymphocytes were isolated from the livers of OVA-Bil mice and analysed using flow cytometry. A monoclonal antibody for Vα2 was used to selectively identify adoptively transferred cells. (A) Total number of viable $V\alpha2^+$ CD4 T cells (from OT-2 mice) and (B) viable $V\alpha2^+$ CD8 T cells (from OT-1 mice). The percentage of CD69 and CD25 positive OT-2 (C and D) and OT-1 (E and F) T cells were also recorded. Data shown as mean±SD. Each data point represents one animal. Statistical analysis performed using One-way ANOVA with Bonferroni's Correction.

## 6.3 Discussion

### 6.3.1 Chapter Summary

The findings of this chapter show that adoptive transfer of OVA-specific CD4 and CD8 T cells into recipient OVA-Bil mice resulted in a sharp but transient immune-mediated hepatic injury. A 30-fold increase in serum ALT was observed in injured animals, alongside a significant increase in the number of $CD45^+$ leukocytes and $F4/80^+$ macrophages. As suggested by our *in vitro* data, mice treated with early-passage P4 SM-primed MSCs, but not TGF-β1 primed MSCs, displayed significantly reduced serum ALT readings. This was due to drops in the total number of CD3 T lymphocytes and CD45 leukocytes in the livers of OVA-Bil animals. Interestingly, quantification of $F4/80^+$ macrophages revealed no differences in animals receiving SM-primed MSCs but a significant reduction in animals receiving TGF-β1 primed cells. Further work is required to elucidate the significance of this finding.

Infusion of late-passage MSCs in the OVA-Bil model backed up our *in vitro* findings with P7 TGF-β1 primed MSCs performing better than their SM-primed counterparts. Although significant reductions in serum ALT were not achieved, we did observe a reduction in CD3 lymphocyte number and CD69 expression in animals receiving TGF-β1 primed cells. Significant reductions in OT-1 and OT-2 T cell number and activation status were also observed in the TGF-β MSC group. Taken together, these findings clearly demonstrate the importance of tailoring MSC culture and expansion conditions to the intended use of these cells, and should be taken into account for future translational research using human cells.

### 6.3.2 Characterisation of Liver Injury in OVA-Bil Mice

OVA-based models of injury have been used previously for various immune-mediated conditions including asthma (Zosky et al., 2008), type I diabetes (Van Belle et al., 2009), dermatitis (Wang et al., 2007) and autoimmune hepatitis (Cebula et al., 2013). The OVA-Bil mice used in this study express OVA under the control of a bile acid transporter promoter (ASBT), thereby limiting its expression to the biliary epithelium of the liver (Buxbaum et al., 2006). IHC analysis of OVA expression revealed positive staining around biliary structures, although the intensity was weak. This could be due to inefficient antigen retrieval or issues with the monoclonal antibody used. However, no staining was observed on surrounding hepatocytes which suggests that OVA expression is limited to biliary epithelium. Interestingly, similar issues with OVA staining were also reported by Buxbaum et al. (2006), who used a fluorescence-based approach to identify (but not localise) OVA expression in the liver.

We observed normal serum ALT, normal liver architecture and no signs of overt damage or inflammation in OVA-Bil mice prior to the infusion of OVA-specific T cells, demonstrating that these animals were tolerant to the OVA transgene. Adoptive transfer of $10x10^6$ OT-1 splenocytes and $4x10^6$ OT-2 splenocytes resulted in a time-dependent increase in serum ALT, peaking 10 days after infusion. Our mean ALT reading (643±184 IU/L) was slightly lower than the one reported by Buxbaum and colleagues (846±415 IU/L), but the spread of data was more restricted in this study. There was a 4-fold reduction in serum ALT by day 11 in OVA-Bil mice, which could be due to loss of adoptively transferred cells or due to the host mounting an active immune response against foreign cells. Similar transient injury profiles have been

reported in other OT-1/OT-2 adoptive transfer studies (Derkow et al., 2007). Further evidence for an active host immune response is provided by Buxbaum et al. (2006), who reported that adoptive transfer of OVA-specific T cells into OVA-Bil mice bred on a $Rag^{-/-}$ background produced an inflammatory reaction that remained constant over time.

Interestingly, for a biliary-specific damage model, we only observed a 2-fold increase in serum ALP after injury. ALP is an enzyme found in the biliary cells of the liver, as well as bone, kidney and placental tissue, with increases in serum ALP indicative of biliary damage or bone diseases (Shipman et al., 2013). Therefore, as the antigen-specific response seen in this model is targeted against biliary epithelium, we should have seen elevated levels of ALP. We did observe significant increases in the number of infiltrating lymphocytes, $CD45^{+}$ cells and $F4/80^{+}$ macrophages in portal regions of the liver after adoptive transfer, but this inflammatory response was insufficient to induce biliary cell death. The reasons behind a poor ALP response in OVA-Bil mice are currently unknown. One potential explanation could be due to the transient nature of inflammation not lasting long enough to cause cholestasis, which eventually results in biliary cell death and ALP release. It would be interesting to measure other serum markers of biliary injury, such as gamma-glutamyl transferase or bilirubin in future studies to further characterise the biliary injury seen in OVA-Bil animals.

In contrast, a significant (30-fold) increase in serum ALT was observed in OVA-Bil animals after adoptive transfer of OT-1 and OT-2 cells. ALT is an enzyme found in hepatocytes and an increase in serum ALT is almost exclusively indicative of hepatocyte damage or death (Limdi

and Hyde, 2003). There are several possible reasons for the hepatitis seen in OVA-Bil mice. Leakage of OVA expression from the biliary epithelium into neighbouring areas can result in an immune reaction against these cells. Histologically, we did not observe OVA expression on hepatocytes but we did observe widespread infiltration of hepatic architecture by lymphocytic cells with regions of interphase hepatitis and clear 'spreading' of immune cells towards the wider liver parenchyma. Clusters of $CD45^+$ were found in lobular regions after injury, which can induce hepatocyte injury and death. Future experiments using the TUNEL assay and IHC for caspases 3 and 7 can be used to quantify hepatocyte death to back up this hypothesis (Kyrylkova et al., 2012). Apoptotic hepatocytes can cause further injury via a feed-forward loop involving Kupffer cells (Malhi et al., 2010). Apoptotic bodies phagocytosed by Kupffer cells results in the expression of death ligands on its surface, causing further hepatocyte apoptosis by binding to their death receptors. Release of intracellular components during necrosis can also illicit an immune response (Nanji and Hiller-Sturmhofel, 1997). Intrahepatic accumulation of CD8+ T cells in other antigen-mediated models of liver injury has been associated with hepatitis, whereby activated CD8+ cells release TNF-α and IFN-γ to mediate non-specific hepatocyte damage (Bowen et al., 2002). Finally, bystander activation of naïve host T cells could also contribute to hepatocyte injury (Boyman, 2010).

An independent study by Derkow et al. (2007) also generated transgenic mice expressing OVA under the control of the ASBT promoter (ASBT-OVA mice). Interestingly, they too struggled to visualise OVA staining in small-to-medium size bile ducts, and only picked up a positive signal in large ducts. Unlike our study, which adoptively transferred un-purified $10x10^6$ OT-1 splenocytes and $4x10^6$ OT-2 splenocytes into OVA-Bil mice intraperitoneally,

Derkow and colleagues injected $8x10^6$ purified OT-1 $CD8^+$ T cells systemically via the tail vein. They report restricted localisation of injury to the portal/biliary areas of the liver after adoptive transfer, with no signs of lobular inflammation or interphase hepatitis. Only a 2-fold increase in ALT was observed in ASBT-OVA mice, demonstrating the specificity of injury. This increase in ALT was transient, peaking at day 6 and falling thereafter. However, the authors failed to observe any differences in biliary damage markers. One reason behind the more pronounced injury seen in OVA-Bil compared to ASBT-OVA mice might be due to the purity of adoptively transferred cells. The heterogeneous population of splenocytes used in the OVA-Bil model contains a mixture of other immune cells alongside naive T lymphocytes that may augment injury, including some activated T cells. Additionally, IP injection may predispose homing of infused cells to the liver compared to systemic injection.

In summary, while OVA-Bil mice appear on paper to be a murine model of human PBC, our results demonstrate that the injury more closely resembles AIH due to the lack of biliary-specific damage. More relevant mouse models of PBC include $Mdr2^{-/-}$ mice (Popov et al., 2005), IL-$2R\alpha^{-/-}$ mice (Wakabayashi et al., 2006) and NOD.c3c4 mice (Irie et al., 2006) which all share several symptoms seen in human patients that were not seen in OVA-Bil mice (e.g. biliary-specific damage, cholestasis, increases in serum ALP, and periportal fibrosis). However, these models develop symptoms over several weeks, which necessitate multiple doses of MSCs to see a clinical benefit. By comparison, although the OVA-Bil mice may not recreate fully the pathology seen in patients with PBC, it is still a good model to study the *in vivo* immunosuppressive effects of MSCs due to their reproducible injury profile and comparatively short 10-day 'incubation' times.

### 6.3.3 Effect of Early-Passage PαS MSC Infusion

Our *in vitro* data shows that early-passage (P3) MSCs expanded in SM were the most suppressive, but this ability was lost at P7 due to the onset of senescence. Expansion in TGF-β1 containing medium was able to maintain the suppressive phenotype of PαS MSCs until P7, however their suppressive potency at P3 was lower than that of SM cells. *In vivo* data using the OVA-Bil model fully backed up our *in vitro* findings, with animals receiving P3 SM-primed MSCs displaying significantly reduced serum ALT readings compared to injured controls. In contrast, animals receiving P3 TGF-β1 primed MSCs displayed a smaller, non-significant reduction in ALT. Liver digest data showed that SM MSC treatment reduced the total number of lymphocytes present in the liver after injury, however it does not appear to alter their activation status. IHC analysis revealed that MSC-treatment significantly reduced the number of $CD45^+$ leukocytes in portal areas, and caused a smaller, non-significant reduction in lobular regions. Interestingly, the number of $F4/80^+$ macrophages was unchanged following SM MSC treatment, and it remains to be seen whether skewed macrophage polarisation is a potential mechanism behind the improvements seen in OVA-Bil animals.

#### 6.3.3.1 Timing of PαS MSC Infusion

The timing of MSC infusion has been reported to have a major impact on clinical efficacy (Casiraghi et al., 2012, Casiraghi et al., 2008). We arbitrarily chose our infusion timings based on previous literature which report that MSCs need to be in an inflammatory environment to activate their immunosuppressive functions (Krampera, 2011, Polchert et al., 2008, Krampera et al., 2006). In a 10-day OVA-Bil model, this left us a narrow therapeutic window

in which MSC infusion could have had an optimal effect. Casiraghi *et al*. show that MSC infusion prior to transplantation had the best clinical outcome in their model of allograft survival, while MSCs given at the time of transplant had no effect (Casiraghi et al., 2008). A later study on kidney transplantation performed by the same group again demonstrated that pre-transplant infusion of MSCs caused a better outcome on graft function and survival (Casiraghi et al., 2012). Animals receiving MSCs post-transplant displayed signs of premature graft dysfunction and rejection, with all mice rejecting the graft within 20 days. Animals receiving a single or double dose of MSCs pre-transplant displayed long-term graft survival. Interestingly, the double-dose group displayed a trend towards better results. Other pre-clinical studies have also reported that multiple MSC doses tend towards better clinical outcomes than a single dose (Hao et al., 2013, Si et al., 2012), and published clinical trials using human MSCs have used multiple, large doses of MSCs in their studies (Lalu et al., 2012, Le Blanc et al., 2008). One key rationale for multiple doses is the finding that systemically administered MSCs are short lived and are rapidly cleared by the host after infusion (Eggenhofer et al., 2012). It is possible that our dosing regimen of days 3 and 7 post injury might miss the optimal therapeutic window for clinical improvements in OVA-Bil mice, and future work could focus on the effect of other infusion times to optimise efficacy.

#### 6.3.3.2 Route of PαS MSC Infusion

One limitation of this study is the intraperitoneal route of administration used, which is of limited translational feasibility in humans. IP injections are commonly used in veterinary practice due to its ease of application, but are rarely used in humans (Chaudhary et al., 2010).

Early studies in our lab reported the formation of PαS MSC clumps when stored in PBS prior to injection. Mechanical agitation of these clumps failed to disaggregate the cells, and systemic administration of clumped MSCs formed harmful emboli in recipient animals. Although MSCs remain viable for several hours when resuspended and stored in ice-cold PBS prior to infusion (Nikolaev et al., 2012, Pal et al., 2008), there is evidence for greater cellular aggregation of MSCs in ice-cold PBS compared to PBS at 37°C (Heng et al., 2008). The use of specialised media for resuspending and transporting MSCs prior to infusion is one option available to limit cellular aggregation and maintain viability (Gálvez-Martín et al., 2014).

Another limitation of systemic infusion is risk of infused cells being trapped in the lungs of recipient animals. Several studies using human and murine MSCs have reported that the majority of systemically infused MSCs are trapped in the lung due to their large size and expression of several adhesion proteins, preventing them from reaching the target organ (Nystedt et al., 2013, Fischer et al., 2009, Schrepfer et al., 2007, Barbash et al., 2003). Potential methods to bypass this pulmonary 'first-pass' effect include intraarterial infusion (Mitkari et al., 2013) and direct infusion into injured organs (Kean et al., 2013, Chen et al., 2004). Despite these limitations, it is important to note that several previous publications have reported favourable outcomes after IV administration of MSCs in models of injury, even in cases where MSC engraftment was not observed (Lee et al., 2009b).

Due to the issues with cell clumping and the other limitations listed above, an IP approach was used to deliver PαS MSCs to OVA-Bil animals. No adverse events were observed in OVA-

Bil mice after multiple IP injections and the reduction in injury seen demonstrate that IP-infused MSCs were functional. This finding raises some interesting questions regarding PαS MSC homing from the peritoneum to the liver. The peritoneum can be viewed as a large cavity with abundant vascularisation and lymphatic drainage systems (Parungo et al., 2007). The substantial vascular surface area on offer facilitates the rapid uptake and systemic delivery of injected drugs (Markman, 2009). However, the uptake and systemic diffusion of IP injected MSCs is less well understood. Castelo-Branco et al. (2012) show that IP-infused MSCs specifically migrate towards inflamed bowel in a mouse model of colitis while IV-infused MSCs were found in other organs. Ghionzoli and colleagues report similar findings following IP-MSC infusion in healthy rats, with injected cells localised in the intestine (67%), liver (25%), spleen (16%) and heart (15%; Ghionzoli et al., 2010). The reasons behind preferential homing towards intra-peritoneal organs over extra-peritoneal organs could be due to the proximity of intra-peritoneal organs to the infusion site.

Future work should study the migration of IP-infused PαS MSCs to see whether they engraft in the liver. Injection of quantum dot-labelled MSCs would allow real-time tracking using an imaging system such as IVIS® or CryoViz®. Engrafted MSCs can also be identified using IHC on serial sections of the liver. Furthermore, examination of draining lymph nodes of the peritoneal cavity for the presence of PαS MSCs would also be interesting, as this is one area where MSCs can directly interact with APCs and other immune cells to reduce the activation of OT-1 and OT-2 T cells, thereby preventing further hepatic injury.

#### 6.3.3.3 Liver Lymphocyte and Macrophage Populations

Flow cytometric analysis of liver-resident lymphocyte populations was performed to identify potential mechanisms of action. Quantification of total lymphocyte number revealed that SM-primed MSC treatment caused a significant reduction in the total numbers of $CD3^+$ lymphocytes in OVA-Bil mice after injury. A reduction was also seen following TGF-β1 primed MSC infusion, but this failed to reach significance. This finding fits our *in vitro* data and the anti-proliferative effect of MSCs on lymphocytes has also been described in detail elsewhere (Ma et al., 2014, Uccelli et al., 2008).

Interestingly, we did not observe any difference in the activation status of lymphocytes between injured and MSC-treated mice. This was surprising as there are several past reports describing the inhibition of lymphocyte activation after MSC co-culture (Park et al., 2011, Ding et al., 2009, Le Blanc et al., 2004a). However, analysis of 'bulk' lymphocyte populations (as done here) over adoptively transferred OT-1 and OT-2 populations could have masked any subtle effects MSCs were having on these damage-causing cells. As the OVA-Bil model does not have a significant autoimmune component, it is important to separate OVA-specific T cells from the total lymphocyte population when performing future experiments. Additionally, examination of the cytokine production of adoptively transferred cells should also be examined, as MSCs have previously been shown to skew the cytokine secretion of $CD4^+$ cells towards an anti-inflammatory $T_H2$ state (Aggarwal and Pittenger, 2005).

Analysis of liver macrophage populations using F4/80 expression revealed some very interesting findings following MSC infusion in OVA-Bil mice. Animals that received SM-primed MSCs (which displayed significant reductions in serum ALT and lymphocyte numbers) had similar numbers of liver-resident macrophages as injured control animals. By contrast, animals receiving TGF-β1 primed MSCs (which failed to show significant reductions in ALT or lymphocyte counts) had significantly less F4/80$^{+}$ compared to controls.

Our working hypothesis to explain this finding is that control mice may harbour a predominantly pro-inflammatory M1 macrophage population, but SM-primed MSC treated animals may have higher numbers of M2 macrophages. These anti-inflammatory M2 macrophages work synergistically with PαS MSCs to dampen the proliferation and activation of OVA-specific T cells and reduce overall liver injury. The effect of MSCs on macrophage polarisation towards M1 or M2 phenotypes is well understood, and there is a lot of evidence that demonstrates MSCs can skew macrophage polarisation towards a M2 phenotype *in vitro* and *in vivo* (Cho et al., 2014, Le Blanc and Mougiakakos, 2012, Choi et al., 2011, Nemeth et al., 2009). To address this hypothesis, future work should concentrate on identifying macrophage subsets in OVA-Bil mice after MSC treatment. Expression of characteristic markers of M1 (iNOS, MHC class II and CD86) and M2 macrophages (Arginase-1, CD206, CD163 and IL-10) macrophages can be examined using a combination of RT-PCR, IHC and functional assays (Barros et al., 2013). Additionally, the cytokine profile of isolated macrophages can also be used to identify their polarisation status (Martinez and Gordon, 2014, Martinez et al., 2006).

### 6.3.4 Effect of Late-Passage PαS MSC Infusion

Due to the rarity of PαS MSCs in BM, a degree of *in vitro* expansion is required to reach the cell numbers needed for therapeutic infusions. We were able to overcome senescence and maintain immunosuppression in MSC cultures via the use of TGF-β1 supplementation, which is of interest for future translational work in immune-mediated disorders. Here, we examined the effect of P7 PαS MSCs expanded in SM±TGF-β1 in the OVA-Bil model to back up our *in vitro* findings in a mouse model of injury.

Examination of serum ALT in day 10 OVA-Bil mice revealed no difference between injured controls and SM-MSC treated animals, which fits in nicely with our *in vitro* findings. Promisingly, animals receiving TGF-β1 primed MSCs tended to have much lower ALT readings, but the variation between animals prevented the data from reaching significance. This experiment is currently being repeated in our lab to increase the sample size to pick out any significant differences between groups.

#### 6.3.4.1 Liver Lymphocyte Populations after P7 PαS MSC treatment

Flow cytometric analysis of bulk lymphocyte populations provided further evidence for the maintenance of immunosuppressive phenotype in late-passage TGF-β1 primed PαS MSCs. Significant reductions in total $CD3^+$ lymphocytes, particularly $CD3^+CD8^+$ T cells were observed in animals receiving TGF-β primed MSCs. Animals receiving SM-primed MSCs failed to show significant reductions in lymphocyte numbers compared to control mice. These findings are

a reversal of the results obtained with early-passage cells, where SM-primed MSCs, but not TGF-β1 primed cells, caused significant reductions in lymphocyte number.

We were also able to specifically analyse the effect of late-passage MSC infusion on donor OT-1 and OT-2 lymphocyte populations using Vα2 expression. Unlike host OVA-Bil lymphocytes, donor lymphocytes express Vα2 Vβ5 chains on their transgenic TCR which allows us to separate the two populations (Buxbaum et al., 2006, Clarke et al., 2000). Significant reductions in the total number of adoptively transferred $CD4^+$ (OT-2) and $CD8^+$ (OT-1) lymphocytes were observed in animals receiving TGF-β1 primed MSC treatment compared to injured controls. We also observed a significant reduction in the expression of the early activation marker CD69 on $CD4^+$ and $CD8^+$ lymphocytes in the TGF-β group. No significant differences in lymphocyte number or activation status were observed in the SM-primed MSC group, providing further evidence for their loss of function. These findings demonstrate that late-passage TGF-β1 primed MSCs, but not SM-primed cells, can inhibit the proliferation and activation of damage-causing donor OT-1 & OT-2 cells, and could be a potential mechanism behind the improvements in serum ALT observed in TGF-β MSC-treated animals.

# CHAPTER 7

# CONCLUSIONS & FUTURE WORK

## 7.1 Summary of Principle Findings

MSCs are an attractive source of cells for future therapies due to their potent trophic and immunomodulatory characteristics, enabling their use in a wide variety of clinical indications (Ma et al., 2014, Mendicino et al., 2014, Ranganath et al., 2012). Promising pre-clinical studies in animal models have been quickly translated into small-scale human trials examining the efficacy of MSC infusion in GvHD, cardiovascular disease, liver failure and others. Although a recent meta-analysis of MSC trials has reported favourable safety outcomes, the degree of clinical benefit varied (Lalu et al., 2012). One possible reason behind the lack of efficacy could be due to the heterogeneous populations of plastic-adherent cells used in past studies, in which only a small percentage of cells were actually MSCs (Bianco et al., 2013, Bianco et al., 2008). Additionally, difficulties in isolating a purified population of murine MSCs has prevented the field from studying the biology and functions of these cells using the large number of transgenic mouse models currently available (Anjos-Afonso and Bonnet, 2011). Our current understanding of MSC biology is therefore inferred from the study of *in vitro* cultured human cells due to their ease of isolation. There is a pressing need to understand the biology of these cells in the murine system to better design culture conditions that optimise their therapeutic potential. These findings can then be translated into human trials to improve the efficacy of MSCs in patients.

Mouse MSC isolation has traditionally been hampered by the lack of specific markers and the persistence of contaminating cells in culture (Boxall and Jones, 2012). Three recent publications have comprehensively described markers and methods to isolate purified

murine MSCs and tested their function *in vivo* using traditional assays of stem cell function (Pinho et al., 2013, Mendez-Ferrer et al., 2010, Morikawa et al., 2009). However, the therapeutic or immunosuppressive properties of these prospectively isolated MSCs were not studied, and it remains to be seen whether purified cells function as effectively as their non-purified counterparts. To meet these needs, this thesis focused on the PαS ($PDGFR\alpha^{+}Sca\text{-}1^{+}$) population of murine MSCs and investigated their regenerative and immunosuppressive phenotype *in vitro* and *in vivo*.

### 7.1.1 Phenotype and Loss of Function of PαS MSCs

Although the original paper describing the identification and isolation of PαS MSCs was published over three years ago, there are no primary research articles published to date which have used this this population of cells in their studies. Reasons behind this are unknown, but could be due to difficulties in replicating the isolation procedure because of the subtle complexities involved in BM sample preparation and sorting. As described in Chapter 3, we have been able to successfully isolate PαS MSCs from multiple wild-type and transgenic mouse strains and test their functions *in vitro*. Early-passage PαS cells perform many of the functions expected of MSCs, including *in vitro* proliferation, tri-lineage differentiation and CFU-F formation. This study also describes for the first time the potent immunosuppressive phenotype of Balb/c-derived PαS MSCs, which was exclusively mediated via the release of NO. Preliminary analysis also revealed strain-specific differences in immunosuppressive mechanism, with MSCs isolated from C57BL/6 mice failing to suppress T cell proliferation in our standard assay. Immunosuppression was restored when we moved

away from a 'purified' system where no antigen presentation was required towards a more complex 'splenocyte reaction' containing several different immune cell subsets. Further work is ongoing to elucidate the mechanism behind C57BL/6-derived PαS MSC immunosuppression and the effects of GF-supplementation on this feature.

Due to the rarity of PαS MSCs in BM (approximately 5000-8000 cells per mouse), and the high numbers of MSCs required to see a clinical benefit in previous mouse models of injury (up to 1 million cells per animal; Nemeth et al., 2009, Casiraghi et al., 2008), a degree of *in vitro* expansion is therefore required to reach cell numbers needed for experimentation. The findings of Chapter 4 demonstrate that PαS MSCs are susceptible to senescence, resulting in reduced proliferative capacity and upregulation of SA-β-gal expression. Increased senescence has implications for future therapeutic uses of these cells, as PαS MSCs become increasingly lineage-restricted towards bone and lose their chondrogenic and adipogenic differentiation ability at later passages. Importantly, PαS MSCs also displayed a progressive loss of immunomodulatory functions at later passages due to decreased NO production.

### 7.1.2 Overcoming Senescence using GF-priming

Growth factors are frequently added to MSC growth media to increase MSC growth and function (Inamdar and Inamdar, 2013, Rodrigues et al., 2010). However, there are many contradictory findings on the effects of GF-supplementation on MSC cultures, which could again be due to the heterogeneous populations of plastic-adherent cells used in past studies.

Previous studies have also not addressed the effect of long-term exposure to GFs on the tri-lineage and immunosuppressive phenotype of MSCs. Although GFs increase the proliferation and differentiation of MSCs during the short term, they may also prime MSCs down specific lineages after extended culture. Defining culture conditions that prime MSCs towards pre-determined fates is of significant interest for future medical uses as it would allow culture conditions to be tailor-made for the clinical indication.

Chapter 5 describes the effect of FGF2, PDGF-BB and TGF-β1 supplementation on MSC growth and function. These GFs were chosen as their respective signalling pathways were reported to control MSC proliferation and differentiation down specific lineages (Ng et al., 2008). Our findings demonstrate enhanced growth and reduced senescence in the presence of GFs, with FGF2 having the most potent effect. We also report novel data on the karyotype of PαS MSCs, and observed no cytogenetic evidence of neoplastic transformation in SM or GF-supplemented cultures at P3 and P5, suggesting that prospectively-isolated cells are more stable than their plastic-adherent counterparts (Tolar et al., 2007, Miura et al., 2006).

The findings of Chapter 5 also provides evidence of 'lineage priming' in PαS MSC cultures after expansion in GF-supplemented media (Delorme et al., 2009). Microarray analysis revealed significant upregulation of osteogenic lineage genes in undifferentiated MSCs expanded in SM media. When induced to undergo differentiation, SM cultures readily went down the osteogenic lineage, producing significantly more calcium than GF-supplemented cells. FGF2 and PDGF-BB supplementation upregulated key adipogenic lineage genes in

undifferentiated MSCs, and we saw increased lipid droplet formation in these cultures when induced to undergo differentiation. Evidence for chondrogenic lineage priming was less clear than the other two lineages, however our phenotypic data suggests that culture in FGF2 is beneficial for cartilage formation. Interestingly, late-passage PαS MSCs expanded in TGF-β1 supplemented medium had attenuated tri-lineage differentiation but enhanced immunosuppressive potential. This was due to a reduction in the number of senescent cells and an increase in NO production in TGF-β1 MSCs compared to SM MSCs.

### 7.1.3 *In vivo* Immunosuppression in the OVA-Bil Model

The OVA-Bil model of alloimmune liver injury was used to demonstrate *in vivo* immunosuppressive functions of PαS MSCs and examine whether TGF-β1 supplementation could maintain the suppressive potential of late-passage cells. Characterisation of the liver injury observed in OVA-Bil mice following adoptive transfer of OT-1 and OT-2 cells revealed a sharp but transient immune-mediated hepatic injury. A 30-fold increase in serum ALT was observed in injured animals, alongside significant increases in the number of liver-resident $CD45^+$ leukocytes and $F4/80^+$ macrophages. As suggested by our *in vitro* data, mice treated with early-passage P4 SM-primed MSCs, but not TGF-β1 primed MSCs, displayed significantly reduced serum ALT readings compared to control animals. This was due to drops in the total number of $CD3^+$ T lymphocytes and $CD45^+$ leukocytes in the livers of OVA-Bil animals after MSC treatment. We also observed selective retention of $F4/80^+$ macrophages in animals receiving SM-primed MSC treatment, and further work studying macrophage polarisation is currently underway to examine the significance of this finding.

Infusion of late-passage PαS MSCs again backed up our *in vitro* findings, with P7 TGF-β1 primed MSCs performing substantially better than P7 SM-primed cells. Although significant reductions in serum ALT were not reached, we did observe significant reductions in 'bulk' lymphocyte number and activation status following TGF-β1 primed MSC infusion. Analysis of the adoptively transferred population revealed significant reductions in the total number and activation status of OT-1 and OT-2 cells in the TGF-β group but not the SM group.

These results have significant implications for downstream therapeutic uses as we reveal that culture conditions can functionally 'prime' MSCs down specific fates. For example, MSCs expanded in SM media are best suited for bone repair, while FGF-supplemented cells are best suited for cartilage regeneration. Conversely, TGF-β1 primed MSCs do not appear suitable for regenerative medicine purposes but are ideal for immune-mediated disorders. The use of a lineage-primed population would allow us to infuse lower numbers of MSCs to reach the same beneficial outcome, thereby reducing the risk of any adverse events.

## 7.2 Implications for Future Translational Work

Our findings have significant implications for downstream therapeutic uses as we reveal that culture conditions can functionally 'prime' MSCs down specific fates. For example, MSCs expanded in SM media are best suited for bone repair, while FGF-supplemented cells are best suited for cartilage regeneration. Conversely, TGF-β1 primed MSCs do not appear suitable for regenerative medicine purposes but are ideal for immune-mediated disorders. The use of a lineage-primed population in future clinical trials would allow us to infuse lower numbers of MSCs to reach the same beneficial outcome, thereby reducing the risk of any adverse events occurring.

Difficulties in isolating a purified population of murine MSCs has drawn criticism from certain groups and hampered attempts to reach agreement on potential mechanisms of action (Bianco et al., 2013, Haniffa et al., 2009). The recent publication of three murine MSC isolation methods have the potential to transform the field, but the uptake of these methods by the wider scientific community has been slow. No primary research article has used the PαS MSC population in their publication to date, and there has only been a handful which have used the Nestin$^{+}$ MSCs in their work (Ding et al., 2012, Itkin et al., 2012). The reasons behind the lack of uptake of PαS MSCs are unknown, but could be due to subtle intricacies involved in BM sample preparation prior to sorting. We have been able to successfully isolate and culture PαS MSCs from multiple mouse strains and the methods section of this thesis describes these steps in detail to allow replication from other groups. We have also been able to describe their regenerative and immunosuppressive potential and identified

culture conditions that enhance these properties. These findings can be directly translated to the human MSC field, and it would be very interesting to observe whether lineage specification with FGF, PDGF or TGF-β occurs in a purified population of human MSCs as well.

This thesis also evaluated PαS MSCs in clinically-relevant models of cartilage regeneration and immune-mediated liver injury. Cartilage injures are a major cause of disabilities in the western world, and repair following injury is a slow and limited process due to the avascular nature of mature cartilage (Arden and Nevitt, 2006). Individual case studies and small-scale trials have described MSC infusion to be as effective as ACI in repairing cartilage defects, however, there are other studies which describe a more modest benefit of MSC therapy, suggesting that there is still scope for optimisation (Nejadnik et al., 2010, Chen and Tuan, 2008). Testing cartilage repair in mouse models of injury and optimising protocols for chondrocyte differentiation *in vitro* would significantly reduce the cost and improve the efficacy of future clinical studies (Helminen et al., 2002). However, tissue engineering murine cartilage has been challenging due to difficulties in isolating a pure population of mouse MSCs (Zhang, 2014, Frenette et al., 2013), and the requirement for 3D culture and specialised differentiation media (Gupta et al., 2012, Solchaga et al., 2011, Koga et al., 2009). We have shown for the first time that PαS MSCs can differentiate into good quality cartilage in both micromass pellet cultures and biodegradable PGA scaffolds, making them a good pre-clinical model population of cells to design and optimise novel cartilage repair therapies. Notably, we were able to demonstrate the power of tissue engineering approaches by showing a 4-fold increase in size and a 2-fold increase in collagen and proteoglycan content

in tissue-engineered cartilage compared to micromass pellets when starting with a similar number of MSCs in both experiments ($5x10^5$ MSCs per micromass pellet compared to $6x10^5$ MSCs per PGA scaffold). These *in vitro* findings lay the groundwork for future *in vivo* studies in mouse models of cartilage repair to further optimise our differentiation strategies even further (Chu et al., 2010).

This thesis also demonstrates for the first time the potent immunosuppressive properties of PαS MSCs and the effect of TGF-β1 in maintaining the suppressive potential over extended *in vitro* culture. Nitric oxide was identified as the key molecule responsible for PαS MSC-mediated immunosuppression, with fits in nicely with previous murine MSC literature (Ren et al., 2009, Ren et al., 2008). The most promising clinical examples of MSC therapy for immune-mediated disorders occur in patients with GvHD, in whom MSC therapy has been shown to be safe and efficacious in phase I and II trials (Le Blanc et al., 2008, Le Blanc and Ringden, 2007, Ringdén et al., 2006). However, a larger-scale, phase III randomised trial involving 244 GvHD patients showed no difference in the complete response rate in patients receiving MSCs or placebo (Martin et al., 2010). One reason for this failure is that the infused MSCs were culture-expanded using a "proprietary" method to yield almost $20x10^9$ cells from a single donor (Galipeau, 2013). The importance of passage number was also made clear by von Bahr et al. (2012), who described a significant reduction in 1-year survival of GvHD patients receiving P3-4 MSCs compared to those that received P1-2 cells (21% vs 75% respectively). Furthermore, Moll and colleagues demonstrated that older MSCs (>P5) were cleared by the host quicker than younger cells, resulting in diminished *in vivo* efficacy (Moll

et al., 2014, Moll et al., 2012). In this context, our finding that TGF-β1 can maintain the immunosuppressive potential of PαS MSCs over extended passage is of significant interest for translational work. Future studies on purified populations of human MSCs should examine whether TGF-β1 can maintain the suppressive phenotype of human MSCs in a similar fashion to their murine counterparts. If the effects are transferrable, then clinical-grade MSCs should be expanded in TGF-β1 as a method to bypass the long standing hurdle of diminished efficacy after culture expansion.

## 7.3 Limitations of this Study

The identification, isolation and characterisation of PαS MSCs represent a major advance for the murine MSC field, however this technique does have some limitations which limit its translational feasibility. Firstly, the isolation method places a high tally on the number of animals required to isolate MSCs over the course of this PhD, which both incurs high costs for mice and goes against the guidance of the NC3Rs committee (Festing and Wilkinson, 2007). The delicate isolation method and requirement to use a cell sorter for several hours also adds to the costs involved and can limit access to some research groups wanting to use PαS MSCs in their studies.

Secondly, it is currently unknown whether PαS MSCs exist in human BM. A negative finding will severely limit the relevance of PαS MSCs as a model pre-clinical population of MSCs, and future work should try and identify whether the same marker combination pulls out MSCs from humans. However, the lineage priming aspects of this study may still be transferrable

across species. Another factor limiting the translational feasibility of PαS MSCs is the requirement for BM isolation. Although BM aspiration is a relatively routine and safe process, the procedure itself is a painful and costly process and carries with it certain risks such as infection and bleeding (Bain, 2005). This limits the number of cells which could be successfully isolated from BM aspirates (Mosna et al., 2010). By comparison, adipose-derived MSCs share many of the functionalities of BM-derived MSCs, but have some key advantages including 'ease-of-harvesting' through a less invasive liposuction procedure (Locke et al., 2011, Yarak and Okamoto, 2010). Adipose tissue is also abundant and accessible due to it being classified as a "waste product" of many routine cosmetic surgeries, allowing a larger yield of cells to be isolated (Gupta et al., 2013). Isolation of PαS MSCs from other sources in mice was outside the scope of this study, but it has been performed by other groups (Sara Rankin, personal communication). Further work is necessary to perform a comparative analysis of PαS MSCs from BM and adipose tissue, as there are reports of differences in the molecular phenotype, differentiation potential and immunosuppressive capacity of MSCs isolated from different sources (Al-Nbaheen et al., 2013, Ribeiro et al., 2013, Pendleton et al., 2013, Wagner et al., 2005). If both populations behave similarly, then adipose-derived PαS MSCs may be more suitable for clinical translation.

Another technical limitation of this work was due to the use of FBS in PαS MSC culture medium in experiments involving GF-priming. Although batch-to-batch variation in FBS was minimised by bulk purchasing, FBS is by nature an undefined product with varying concentrations of cytokines and growth factors (Zheng et al., 2006, Jochems et al., 2002).

Strictly speaking, the GF-priming experiments should be repeated in serum-free, chemically-defined medium to bypass any potential confounding effects of FBS (van der Valk et al., 2010). However, it is important to note that the effects of GFs were clear and reproducible over numerous experiments spanning several years with different batches of FBS, which argues against a confounding role for this undefined substrate in our experiments.

Finally, the use of FBS is again a limitation as it carries a risk of xenoantigen incorporation in MSC cultures and goes against Good Manufacturing Practice (GMP) guidelines (Copland and Galipeau, 2011, Sensebe et al., 2011). An interesting study by Spees et al. (2004) showed that a standard preparation of $10x10^7$ human MSCs (a dose equivalent to those used in human trials) internalised between 7 to 30mg of xeno-proteins which could make them immunogenic *in vivo*. A similar effect has been described for human embryonic stem cells (Martin et al., 2005) and adipose-derived MSCs (Komoda et al., 2009), which internalised and expressed the nonhuman sialic acid (N-glycolylneuraminic acid) after culture in animal serum-containing media. Although the stem cell therapy field as a whole is gradually moving towards xeno-free, GMP-compliant culture platforms (Tannenbaum et al., 2012), it is again important to note that a meta-analysis of safety in MSC clinical trials revealed no relationships between MSC infusion and "acute infusional toxicity" (Lalu et al., 2012). Out of the 36 trials examined, 27 used MSCs cultured in FBS, five used human serum and four used serum from an unknown source. Therefore, there is currently no evidence for increased toxicity or immunogenicity in MSCs cultured in FBS, although it would be wise to avoid xeno-products wherever possible in future studies.

## 7.4 Future Work

The findings of this study raise several interesting questions, particularly regarding potential mechanisms of action in the OVA-Bil model. These are summarised briefly below:

### 7.4.1 Mechanism of C57BL/6-derived PαS MSC Immunosuppression

One of the most interesting findings of this study is the observation that C57BL/6-derived PαS MSCs suppress via a different mechanism to Balb/c-derived MSCs. Strain-specific differences in immunosuppression have not received much research attention in MSC literature, but the implications of this finding could have an impact on the choice of mouse strain used in future *in vivo* experiments. Further studies using small molecule inhibitors of known immunosuppressive pathways (e.g IDO, L-NMMA, 1-MT or SB-3CT) can be used to identify a potential mechanism of action. Additionally, selective removal of immune cell subsets (e.g. monocytes/macrophages, B cells, DCs) can also be used to study possible indirect effects of PαS MSCs on T cell proliferation. Finally, it is also necessary to examine whether TGF-β1 can maintain the suppressive phenotype of C57BL/6 MSCs in a similar fashion to Balb/c-derived cells. Our *in vivo* findings in the OVA-Bil model suggest this may be the case, although further *in vitro* proof is required to substantiate this hypothesis.

### 7.4.2 Characterisation of PαS MSC Senescence

Senescence was defined as the appearance of β-gal$^+$ cells in this study. To further understand the kinetics of senescence in PαS MSCs, it is necessary to study the expression of senescence-associated genes and cell-cycle inhibitors p21, p16, p19 and p53 using a combination of RT-PCR and western blotting (Koch et al., 2012, Schallmoser et al., 2010, Wagner et al., 2010). It would also be interesting to observe whether late-passage PαS MSCs acquire a pro-inflammatory "senescence-associated secretory phenotype" which has been reported for other stromal cell subsets (Coppe et al., 2010, Fumagalli and Fagagna, 2009). Finally, to prove that immortalisation or transformation did not occur in PαS MSCs in the presence of GFs, it is necessary to demonstrate re-acquisition of senescence upon removal of GF-supplementation, as has been described previously by Coutu et al. (2011).

### 7.4.3 Karyotypic analysis of PαS MSCs

Metaphase karyotype analysis revealed no cytogenetic evidence of clonal abnormalities in PαS MSC cultures. However, we did observe increased tetraploidy in TGF-β1 supplemented cells compared to other culture conditions. Although tetraploidisation of murine MSCs has been reported to be a protective mechanism against malignancy *in vivo* (Shoshani et al., 2012), changes in chromosome number are also a hallmark of cancer (Albertson et al., 2003). Therefore, it is necessary to perform *in vivo* transplantation experiments in NOD/SCID mice to examine whether PαS MSCs also use tetraploidisation as a protective mechanism against malignancy (Hatakeyama et al., 2010).

Another interesting finding from our karyotype analysis was the occurrence of quadriradial chromosomes in PDGF-supplemented cells. QR chromosomes are indicative of an increased rate of sister chromatid exchange (SCE) in genetic instability disorders such as Bloom's Disease (Singh et al., 2010). The rate of SCE can be monitored by culturing cells in BrdU-containing medium to differentially stain sister chromatids. Metaphase spreads are prepared as before and analysed for regions of discontinuous staining that occur after reciprocal exchanges of genetic material (Moore and Best, 2001). This analysis would reveal whether PDGF-supplementation predisposes PαS MSCs towards genetic instability, and further work examining the karyotype of cells at later passages (P7 onwards) would reveal the downstream significance of elevated SCE and QR chromosome formation in PDGF cultures.

### 7.4.4 Kinetics of Growth Factor Action & Combination Studies

Growth factors were added to freshly isolated MSCs and maintained throughout their expansion period in this study. It would be interesting to examine whether short-term (24-48h) stimulation with GFs produces the same genotypic and phenotypic differences in PαS MSC differentiation and immunosuppression seen with long-term culture. Additionally, it would also be interesting to study whether removal of GFs results in a loss of priming 'memory' and observe the kinetics behind the possible loss in lineage-specific gene expression. Studies using combinations of GFs (e.g. FGF2 for growth and TGF-β1 for immunosuppression) can also be performed to overcome the limitations of each GF used individually.

### 7.4.5 Mechanism of Growth Factor Action

Addition of GFs caused profound genotypic and phenotypic changes in PαS MSCs, particularly in FGF2 and TGF-β1 supplemented cultures. Our preliminary analysis identified potential pathways regulating adipogenic priming in FGF2 and PDGF-BB supplemented cells. Future work should concentrate on how FGF2 enhances the growth and chondrogenic differentiation of PαS MSCs and how TGF-β1 maintains their immunosuppressive potential. The FGF pathway can be studied using dasatanib and SU5402 as before, and the TGF-β1 pathway examined using SB431542, a selective inhibitor of the type I TGF-β receptor (Stewart et al., 2010, Inman et al., 2002). Further analysis of PDGF-BB signalling can also be performed at the receptor level and on downstream signalling proteins using small-molecule inhibitors (CP-673,451; Roberts et al., 2005) or antibodies (Heldin, 2013).

### 7.4.6 Toll-like Receptor Priming

An emerging field in MSC biology involves the study of TLR stimulation and its effect on the immunosuppressive capacity of MSCs (Keating, 2012). Murine MSCs express TLRs 1-6, with TLR3 and TLR4 being key receptors controlling the switch between a pro-inflammatory and an anti-inflammatory phenotype (DelaRosa and Lombardo, 2010, Waterman et al., 2010, Tomchuck et al., 2008). It would be interesting to study the feasibility of TLR3 priming (using double stranded RNA) and TLR4 priming (using LPS) as a method to enhance the migratory and suppressive phenotype of PαS MSCs even further. Additionally, it would also be interesting to examine whether TGF-β1 treatment alters the expression of TLRs on PαS MSCs.

### 7.4.7 OVA-Bil model of Alloimmune Liver Injury

PαS MSCs were able to significantly reduce inflammatory liver damage in OVA-Bil mice by lowering the total numbers of damage-causing lymphocytes in their livers after infusion. The key unanswered questions in this model concern the localisation and mechanism of action of infused MSCs. The topic of MSC migration has always been a contentious issue in MSC literature, with some studies demonstrating efficient migration to areas of injury and others demonstrating a more systemic effect (Choi et al., 2011, Karp and Teol, 2009). Homing studies using labelled PαS MSCs could be performed to observe whether they migrate towards and engraft in the liver or work systemically from the peritoneal cavity. Examination of the draining lymph nodes of the peritoneum would also reveal whether MSCs directly affect lymphocyte activation at these sites. Alternatively, dual-colour labelling of adoptively transferred OT-1 and OT-2 cells and PαS MSCs would also allow us to study any direct interactions between these cells.

We observed a selective retention of macrophages in animals receiving early-passage SM MSC treatment, which could be a potential mechanism of action. Liver sections need to be stained for markers of M1 and M2 macrophages to study whether PαS MSC infusion skews macrophage polarisation towards an anti-inflammatory M2 phenotype. Alternatively, animals can be treated with clodronate to deplete macrophages to see whether the beneficial effect of PαS MSC infusion is lost (Weisser et al., 2012, Nemeth et al., 2009). Finally, further analyses using the TUNEL assay and IHC for caspases 3 and 7 would also reveal potential hepato-protective or trophic effects of PαS MSCs in this model of injury.

# CHAPTER 8

# REFERENCES

AGGARWAL, S. & PITTENGER, M. F. 2005. Human mesenchymal stem cells modulate allogeneic immune cell responses. *Blood,* 105**,** 1815-1822.

AHN, H.-J., LEE, W.-J., KWACK, K. & KWON, Y. D. 2009. FGF2 stimulates the proliferation of human mesenchymal stem cells through the transient activation of JNK signaling. *FEBS Letters,* 583**,** 2922-2926.

AKIYAMA, H. 2008. Control of chondrogenesis by the transcription factor Sox9. *Modern Rheumatology,* 18**,** 213-219.

AKIYAMA, H., CHABOISSIER, M.-C., MARTIN, J. F., SCHEDL, A. & DE CROMBRUGGHE, B. 2002. The transcription factor Sox9 has essential roles in successive steps of the chondrocyte differentiation pathway and is required for expression of Sox5 and Sox6. *Genes & Development,* 16**,** 2813-2828.

AKIYAMA, Y., AKIYAMA, H., ROWITCH, D. H. & DE CROMBRUGGHE, B. 2003. Sox9 is required for determination of the chondrogenic cell lineage in the cranial neural crest. *Proc Natl Acad Sci U S A,* 100**,** 9360-5.

AL-NBAHEEN, M., VISHNUBALAJI, R., ALI, D., BOUSLIMI, A., AL-JASSIR, F., MEGGES, M., PRIGIONE, A., ADJAYE, J., KASSEM, M. & ALDAHMASH, A. 2013. Human stromal (mesenchymal) stem cells from bone marrow, adipose tissue and skin exhibit differences in molecular phenotype and differentiation potential. *Stem Cell Rev,* 9**,** 32-43.

ALBERTSON, D. G., COLLINS, C., MCCORMICK, F. & GRAY, J. W. 2003. Chromosome aberrations in solid tumors. *Nat Genet,* 34**,** 369-76.

AMOR-GUÉRET, M. 2006. Bloom syndrome, genomic instability and cancer: the SOS-like hypothesis. *Cancer letters,* 236**,** 1-12.

ANDRAE, J., GALLINI, R. & BETSHOLTZ, C. 2008. Role of platelet-derived growth factors in physiology and medicine. *Genes & Development,* 22**,** 1276-1312.

ANJOS-AFONSO, F. & BONNET, D. 2011. Prospective identification and isolation of murine bone marrow derived multipotent mesenchymal progenitor cells. *Best Practice & Research Clinical Haematology,* 24**,** 13-24.

ANKRUM, J. A., ONG, J. F. & KARP, J. M. 2014. Mesenchymal stem cells: immune evasive, not immune privileged. *Nat Biotech,* 32**,** 252-260.

ARDEN, N. & NEVITT, M. C. 2006. Osteoarthritis: Epidemiology. *Best practice & research. Clinical rheumatology,* 20**,** 3-25.

ARINZEH, T. L., PETER, S. J., ARCHAMBAULT, M. P., VAN DEN BOS, C., GORDON, S., KRAUS, K., SMITH, A. & KADIYALA, S. 2003. Allogeneic Mesenchymal Stem Cells Regenerate Bone in a Critical-Sized Canine Segmental Defect. *The Journal of Bone & Joint Surgery,* 85**,** 1927-1935.

ASARI, S., ITAKURA, S., FERRERI, K., LIU, C. P., KURODA, Y., KANDEEL, F. & MULLEN, Y. 2009. Mesenchymal stem cells suppress B-cell terminal differentiation. *Exp Hematol,* 37**,** 604-15.

ASUMDA, F. Z. 2013. Age-associated changes in the ecological niche: implications for mesenchymal stem cell aging. *Stem Cell Res Ther,* 4**,** 47.

AULETTA, J. J., ZALE, E. A., WELTER, J. F. & SOLCHAGA, L. A. 2011. Fibroblast Growth Factor-2 Enhances Expansion of Human Bone Marrow-Derived Mesenchymal Stromal Cells without Diminishing Their Immunosuppressive Potential. *Stem Cells International,* 2011**,** 10.

AUSTYN, J. M. & GORDON, S. 1981. F4/80, a monoclonal antibody directed specifically against the mouse macrophage. *Eur J Immunol,* 11**,** 805-15.

BADDOO, M., HILL, K., WILKINSON, R., GAUPP, D., HUGHES, C., KOPEN, G. C. & PHINNEY, D. G. 2003. Characterization of mesenchymal stem cells isolated from murine bone marrow by negative selection. *Journal of Cellular Biochemistry,* 89**,** 1235-1249.

BAIN, B. J. 2005. Bone marrow biopsy morbidity: review of 2003. *J Clin Pathol,* 58**,** 406-8.

BAJADA, S., MARSHALL, M. J., WRIGHT, K. T., RICHARDSON, J. B. & JOHNSON, W. E. 2009. Decreased osteogenesis, increased cell senescence and elevated Dickkopf-1 secretion in human fracture non union stromal cells. *Bone,* 45**,** 726-35.

BALL, S. G., SHUTTLEWORTH, C. A. & KIELTY, C. M. 2007. Vascular endothelial growth factor can signal through platelet-derived growth factor receptors. *The Journal of Cell Biology,* 177**,** 489-500.

BARBASH, I. M., CHOURAQUI, P., BARON, J., FEINBERG, M. S., ETZION, S., TESSONE, A., MILLER, L., GUETTA, E., ZIPORI, D., KEDES, L. H., KLONER, R. A. & LEOR, J. 2003. Systemic delivery of bone marrow-derived mesenchymal stem cells to the infarcted myocardium: feasibility, cell migration, and body distribution. *Circulation,* 108**,** 863-8.

BARROS, M. H. M., HAUCK, F., DREYER, J. H., KEMPKES, B. & NIEDOBITEK, G. 2013. Macrophage Polarisation: an Immunohistochemical Approach for Identifying M1 and M2 Macrophages. *PLoS ONE,* 8**,** e80908.

BARRY, F., BOYNTON, R. E., LIU, B. & MURPHY, J. M. 2001. Chondrogenic differentiation of mesenchymal stem cells from bone marrow: differentiation-dependent gene expression of matrix components. *Exp Cell Res,* 268**,** 189-200.

BARTHOLOMEW, A., STURGEON, C., SIATSKAS, M., FERRER, K., MCINTOSH, K., PATIL, S., HARDY, W., DEVINE, S., UCKER, D., DEANS, R., MOSELEY, A. & HOFFMAN, R. 2002. Mesenchymal stem cells suppress lymphocyte proliferation in vitro and prolong skin graft survival in vivo. *Experimental Hematology,* 30**,** 42-48.

BEDORET, D., WALLEMACQ, H., MARICHAL, T., DESMET, C., QUESADA CALVO, F., HENRY, E., CLOSSET, R., DEWALS, B., THIELEN, C., GUSTIN, P., DE LEVAL, L., VAN ROOIJEN, N., LE MOINE, A., VANDERPLASSCHEN, A., CATALDO, D., DRION, P.-V., MOSER, M., LEKEUX, P. & BUREAU, F. 2009. Lung interstitial macrophages alter dendritic cell functions to prevent airway allergy in mice. *The Journal of Clinical Investigation,* 119**,** 3723-3738.

BEN-AMI, E., BERRIH-AKNIN, S. & MILLER, A. 2011. Mesenchymal stem cells as an immunomodulatory therapeutic strategy for autoimmune diseases. *Autoimmunity Reviews,* 10**,** 410-415.

BETSHOLTZ, C. 2004. Insight into the physiological functions of PDGF through genetic studies in mice. *Cytokine & Growth Factor Reviews,* 15**,** 215-228.

BEYTH, S., BOROVSKY, Z., MEVORACH, D., LIEBERGALL, M., GAZIT, Z., ASLAN, H., GALUN, E. & RACHMILEWITZ, J. 2004. Human mesenchymal stem cells alter antigen-presenting cell maturation and induce T-cell unresponsiveness. *Blood,* 105**,** 2214-2219.

BIANCO, P., CAO, X., FRENETTE, P. S., MAO, J. J., ROBEY, P. G., SIMMONS, P. J. & WANG, C. Y. 2013. The meaning, the sense and the significance: translating the science of mesenchymal stem cells into medicine. *Nat Med,* 19**,** 35-42.

BIANCO, P., ROBEY, P. G. & SIMMONS, P. J. 2008. Mesenchymal stem cells: Revisiting history, concepts, and assays. *Cell Stem Cell,* 2**,** 313-319.

BINGISSER, R. M., TILBROOK, P. A., HOLT, P. G. & KEES, U. R. 1998. Macrophage-Derived Nitric Oxide Regulates T Cell Activation via Reversible Disruption of the Jak3/STAT5 Signaling Pathway. *The Journal of Immunology,* 160**,** 5729-5734.

BOEUF, S. & RICHTER, W. 2010. Chondrogenesis of mesenchymal stem cells: role of tissue source and inducing factors. *Stem Cell Res Ther,* 1**,** 31.

BOGDAN, C. 2001. Nitric oxide and the immune response. *Nature Immunology,* 2**,** 907-916.

BOWEN, D. G., WARREN, A., DAVIS, T., HOFFMANN, M. W., MCCAUGHAN, G. W., DE ST. GROTH, B. F. & BERTOLINO, P. 2002. Cytokine-dependent bystander hepatitis due to intrahepatic murine CD8+ T-cell activation by bone marrow–derived cells. *Gastroenterology,* 123**,** 1252-1264.

BOXALL, S. A. & JONES, E. 2012. Markers for Characterization of Bone Marrow Multipotential Stromal Cells. *Stem Cells International,* 2012**,** 12.

BOYMAN, O. 2010. Bystander activation of CD4+ T cells. *European Journal of Immunology,* 40**,** 936-939.

BRANDAU, S., JAKOB, M., HEMEDA, H., BRUDEREK, K., JANESCHIK, S., BOOTZ, F. & LANG, S. 2010. Tissue-resident mesenchymal stem cells attract peripheral blood neutrophils and enhance

their inflammatory activity in response to microbial challenge. *Journal of Leukocyte Biology,* 88**,** 1005-1015.

BRITTBERG, M., LINDAHL, A., NILSSON, A., OHLSSON, C., ISAKSSON, O. & PETERSON, L. 1994. Treatment of deep cartilage defects in the knee with autologous chondrocyte transplantation. *N Engl J Med,* 331**,** 889-95.

BRUDER, S. P., KRAUS, K. H., GOLDBERG, V. M. & KADIYALA, S. 1998. The effect of implants loaded with autologous mesenchymal stem cells on the healing of canine segmental bone defects. *J Bone Joint Surg Am,* 80**,** 985-96.

BUETTNER, R., MESA, T., VULTUR, A., LEE, F. & JOVE, R. 2008. Inhibition of Src family kinases with dasatinib blocks migration and invasion of human melanoma cells. *Mol Cancer Res,* 6**,** 1766-74.

BUXBAUM, J., QIAN, P., KHUU, C., SHNEIDER, B. L., DAIKH, D. I., GERSHWIN, M. E., ALLEN, P. M. & PETERS, M. G. 2006. Novel Model of Antigen-Specific Induction of Bile Duct Injury. *Gastroenterology,* 131**,** 1899-1906.

CAMPISI, J. & FAGAGNA, F. 2007. Cellular senescence: when bad things happen to good cells. *Nat Rev Mol Cell Biol,* 8**,** 729-40.

CANTILE, M., PROCINO, A., D'ARMIENTO, M., CINDOLO, L. & CILLO, C. 2003. HOX gene network is involved in the transcriptional regulation of in vivo human adipogenesis. *J Cell Physiol,* 194**,** 225-36.

CAO, R., BRAKENHIELM, E., LI, X., PIETRAS, K., WIDENFALK, J., OSTMAN, A., ERIKSSON, U. & CAO, Y. 2002. Angiogenesis stimulated by PDGF-CC, a novel member in the PDGF family, involves activation of PDGFR-alphaalpha and -alphabeta receptors. *FASEB J,* 16**,** 1575-83.

CAPLAN, A. I. 1991. Mesenchymal Stem Cells. *Journal of Orthopaedic Research,* 9**,** 641-650.

CAPLAN, A. I. 1994. The Mesengenic Process. *Clinics in Plastic Surgery,* 21**,** 429-435.

CAPLAN, A. I. & CORREA, D. 2011. The MSC: an injury drugstore. *Cell Stem Cell,* 9**,** 11-5.

CARUSO, A., LICENZIATI, S., CORULLI, M., CANARIS, A. D., DE FRANCESCO, M. A., FIORENTINI, S., PERONI, L., FALLACARA, F., DIMA, F., BALSARI, A. & TURANO, A. 1997. Flow cytometric analysis of activation markers on stimulated T cells and their correlation with cell proliferation. *Cytometry,* 27**,** 71-6.

CASIRAGHI, F., AZZOLLINI, N., CASSIS, P., IMBERTI, B., MORIGI, M., CUGINI, D., CAVINATO, R. A., TODESCHINI, M., SOLINI, S., SONZOGNI, A., PERICO, N., REMUZZI, G. & NORIS, M. 2008. Pretransplant Infusion of Mesenchymal Stem Cells Prolongs the Survival of a Semiallogeneic Heart Transplant through the Generation of Regulatory T Cells. *The Journal of Immunology,* 181**,** 3933-3946.

CASIRAGHI, F., AZZOLLINI, N., TODESCHINI, M., CAVINATO, R. A., CASSIS, P., SOLINI, S., ROTA, C., MORIGI, M., INTRONA, M., MARANTA, R., PERICO, N., REMUZZI, G. & NORIS, M. 2012. Localization of Mesenchymal Stromal Cells Dictates Their Immune or Proinflammatory Effects in Kidney Transplantation. *American Journal of Transplantation,* 12**,** 2373-2383.

CASSATELLA, M. A., MOSNA, F., MICHELETTI, A., LISI, V., TAMASSIA, N., CONT, C., CALZETTI, F., PELLETIER, M., PIZZOLO, G. & KRAMPERA, M. 2011. Toll-Like Receptor-3-Activated Human Mesenchymal Stromal Cells Significantly Prolong the Survival and Function of Neutrophils. *STEM CELLS,* 29**,** 1001-1011.

CASTELO-BRANCO, M. T. L., SOARES, I. D. P., LOPES, D. V., BUONGUSTO, F., MARTINUSSO, C. A., DO ROSARIO, A., JR., SOUZA, S. A. L., GUTFILEN, B., FONSECA, L. M. B., ELIA, C., MADI, K., SCHANAIDER, A., ROSSI, M. I. D. & SOUZA, H. S. P. 2012. Intraperitoneal but Not Intravenous Cryopreserved Mesenchymal Stromal Cells Home to the Inflamed Colon and Ameliorate Experimental Colitis. *PLoS ONE,* 7**,** e33360.

CEBULA, M., OCHEL, A., HILLEBRAND, U., PILS, M. C., SCHIRMBECK, R., HAUSER, H. & WIRTH, D. 2013. An Inducible Transgenic Mouse Model for Immune Mediated Hepatitis Showing Clearance of Antigen Expressing Hepatocytes by CD8+ T Cells. *PLoS ONE,* 8**,** e68720.

CHAN, J. L., TANG, K. C., PATEL, A. P., BONILLA, L. M., PIEROBON, N., PONZIO, N. M. & RAMESHWAR, P. 2006. Antigen-presenting property of mesenchymal stem cells occurs during a narrow window at low levels of interferon-gamma. *Blood,* 107**,** 4817-24.

CHASE, L. G., LAKSHMIPATHY, U., SOLCHAGA, L. A., RAO, M. S. & VEMURI, M. C. 2010. A novel serum-free medium for the expansion of human mesenchymal stem cells. *Stem Cell Res Ther,* 1**,** 8.

CHAUDHARY, K., HADDADIN, S., NISTALA, R. & PAPAGEORGIO, C. 2010. Intraperitoneal drug therapy: an advantage. *Curr Clin Pharmacol,* 5**,** 82-8.

CHEN, F. H. & TUAN, R. S. 2008. Mesenchymal stem cells in arthritic diseases. *Arthritis Res Ther,* 10**,** 223.

CHEN, L., TREDGET, E. E., WU, P. Y. & WU, Y. 2008. Paracrine factors of mesenchymal stem cells recruit macrophages and endothelial lineage cells and enhance wound healing. *PLoS One,* 3**,** e1886.

CHEN, S.-L., FANG, W.-W., YE, F., LIU, Y.-H., QIAN, J., SHAN, S.-J., ZHANG, J.-J., CHUNHUA, R. Z., LIAO, L.-M., LIN, S. & SUN, J.-P. 2004. Effect on left ventricular function of intracoronary transplantation of autologous bone marrow mesenchymal stem cell in patients with acute myocardial infarction. *The American Journal of Cardiology,* 94**,** 92-95.

CHEN, Y., CHEN, S., LIU, L.-Y., ZOU, Z.-L., CAI, Y.-J., WANG, J.-G., CHEN, B., XU, L.-M., LIN, Z., WANG, X.-D. & CHEN, Y.-P. 2014. Mesenchymal stem cells ameliorate experimental autoimmune hepatitis by activation of the programmed death 1 pathway. *Immunology Letters,* 162**,** 222-228.

CHIESA, S., MORBELLI, S., MORANDO, S., MASSOLLO, M., MARINI, C., BERTONI, A., FRASSONI, F., BARTOLOME, S. T., SAMBUCETI, G., TRAGGIAI, E. & UCCELLI, A. 2011. Mesenchymal stem cells impair in vivo T-cell priming by dendritic cells. *Proc Natl Acad Sci U S A,* 108**,** 17384-9.

CHO, D.-I., KIM, M. R., JEONG, H.-Y., JEONG, H. C., JEONG, M. H., YOON, S. H., KIM, Y. S. & AHN, Y. 2014. Mesenchymal stem cells reciprocally regulate the M1/M2 balance in mouse bone marrow-derived macrophages. *Exp Mol Med,* 46**,** e70.

CHOI, H., LEE, R. H., BAZHANOV, N., OH, J. Y. & PROCKOP, D. J. 2011. Anti-inflammatory protein TSG-6 secreted by activated MSCs attenuates zymosan-induced mouse peritonitis by decreasing TLR2/NF-kappaB signaling in resident macrophages. *Blood,* 118**,** 330-8.

CHOY, L. & DERYNCK, R. 2003. Transforming growth factor-beta inhibits adipocyte differentiation by Smad3 interacting with CCAAT/enhancer-binding protein (C/EBP) and repressing C/EBP transactivation function. *J Biol Chem,* 278**,** 9609-19.

CHU, C. R., SZCZODRY, M. & BRUNO, S. 2010. Animal models for cartilage regeneration and repair. *Tissue Eng Part B Rev,* 16**,** 105-15.

CLARKE, S. R., BARNDEN, M., KURTS, C., CARBONE, F. R., MILLER, J. F. & HEATH, W. R. 2000. Characterization of the ovalbumin-specific TCR transgenic line OT-I: MHC elements for positive and negative selection. *Immunol Cell Biol,* 78**,** 110-117.

COLASANTI, M., DI PUCCHIO, T., PERSICHINI, T., SOGOS, V., PRESTA, M. & LAURO, G. M. 1995. Inhibition of inducible nitric oxide synthase mRNA expression by basic fibroblast growth factor in human microglial cells. *Neuroscience Letters,* 195**,** 45-48.

COPLAND, I. & GALIPEAU, J. 2011. Death and inflammation following somatic cell transplantation. *Seminars in Immunopathology,* 33**,** 535-550.

COPPE, J. P., DESPREZ, P. Y., KRTOLICA, A. & CAMPISI, J. 2010. The senescence-associated secretory phenotype: the dark side of tumor suppression. *Annu Rev Pathol,* 5**,** 99-118.

CORCIONE, A., BENVENUTO, F., FERRETTI, E., GIUNTI, D., CAPPIELLO, V., CAZZANTI, F., RISSO, M., GUALANDI, F., MANCARDI, G. L., PISTOIA, V. & UCCELLI, A. 2005. Human mesenchymal stem cells modulate B-cell functions. *Blood,* 107**,** 367-372.

COUTU, D. L., FRANÇOIS, M. & GALIPEAU, J. 2011. Inhibition of cellular senescence by developmentally regulated FGF receptors in mesenchymal stem cells. *Blood,* 117**,** 6801-6812.

COUTU, D. L. & GALIPEAU, J. 2011. Roles of FGF signaling in stem cell self-renewal, senescence and aging. *Aging (Albany NY),* 3**,** 920-33.

CUNHA, F. F., MARTINS, L., MARTIN, P. K., STILHANO, R. S. & HAN, S. W. 2013. A comparison of the reparative and angiogenic properties of mesenchymal stem cells derived from the bone marrow of BALB/c and C57/BL6 mice in a model of limb ischemia. *Stem Cell Res Ther,* 4**,** 86.

CUNNINGHAM, D. L., SWEET, S. M., COOPER, H. J. & HEATH, J. K. 2010. Differential phosphoproteomics of fibroblast growth factor signaling: identification of Src family kinase-mediated phosphorylation events. *J Proteome Res,* 9**,** 2317-28.

CZAJA, A. J. 2006. Autoimmune hepatitis--approach to diagnosis. *MedGenMed,* 8**,** 55.

CZAJA, A. J. 2008. Safety issues in the management of autoimmune hepatitis. *Expert Opin Drug Saf,* 7**,** 319-33.

CZAJA, A. J. 2009. Current and future treatments of autoimmune hepatitis. *Expert Review of Gastroenterology & Hepatology,* 3**,** 269-291.

DAS, R., JAHR, H., VAN OSCH, G. J. & FARRELL, E. 2010. The role of hypoxia in bone marrow-derived mesenchymal stem cells: considerations for regenerative medicine approaches. *Tissue Eng Part B Rev,* 16**,** 159-68.

DAVOLI, T. & DE LANGE, T. 2011. The causes and consequences of polyploidy in normal development and cancer. *Annu Rev Cell Dev Biol,* 27**,** 585-610.

DEBACQ-CHAINIAUX, F., BORLON, C., PASCAL, T., ROYER, V., ELIAERS, F., NINANE, N., CARRARD, G., FRIGUET, B., DE LONGUEVILLE, F., BOFFE, S., REMACLE, J. & TOUSSAINT, O. 2005. Repeated exposure of human skin fibroblasts to UVB at subcytotoxic level triggers premature senescence through the TGF-β1 signaling pathway. *Journal of Cell Science,* 118**,** 743-758.

DECOCK, S., MCGEE, P. & HIRSCHFIELD, G. M. 2009. Autoimmune liver disease for the non-specialist. *British Medical Journal,* 339.

DEEG, H. J. 2007. How I treat refractory acute GVHD. *Blood,* 109**,** 4119-4126.

DELAERE, P. R. 2013. Stem-cell-based, tissue-engineered tracheal replacement in a child. *The Lancet,* 381**,** 113.

DELAROSA, O. & LOMBARDO, E. 2010. Modulation of adult mesenchymal stem cells activity by toll-like receptors: implications on therapeutic potential. *Mediators Inflamm,* 2010**,** 865601.

DELORME, B., RINGE, J., PONTIKOGLOU, C., GAILLARD, J., LANGONNÉ, A., SENSEBÉ, L., NOËL, D., JORGENSEN, C., HÄUPL, T. & CHARBORD, P. 2009. Specific Lineage-Priming of Bone Marrow Mesenchymal Stem Cells Provides the Molecular Framework for Their Plasticity. *Stem Cells,* 27**,** 1142-1151.

DERKOW, K., LODDENKEMPER, C., MINTERN, J., KRUSE, N., KLUGEWITZ, K., BERG, T., WIEDENMANN, B., PLOEGH, H. L. & SCHOTT, E. 2007. Differential priming of CD8 and CD4 T-cells in animal models of autoimmune hepatitis and cholangitis. *Hepatology,* 46**,** 1155-65.

DESPARS, G., CARBONNEAU, C. L., BARDEAU, P., COUTU, D. L. & BEAUSÉJOUR, C. M. 2013. Loss of the Osteogenic Differentiation Potential during Senescence Is Limited to Bone Progenitor Cells and Is Dependent on p53. *PLoS ONE,* 8**,** e73206.

DI LEONARDO, A., LINKE, S. P., CLARKIN, K. & WAHL, G. M. 1994. DNA damage triggers a prolonged p53-dependent G1 arrest and long-term induction of Cip1 in normal human fibroblasts. *Genes Dev,* 8**,** 2540-51.

DI NICOLA, M., CARLO-STELLA, C., MAGNI, M., MILANESI, M., LONGONI, P. D., MATTEUCCI, P., GRISANTI, S. & GIANNI, A. M. 2002. Human bone marrow stromal cells suppress T-lymphocyte proliferation induced by cellular or nonspecific mitogenic stimuli. *Blood,* 99**,** 3838-3843.

DICKINSON, S. C., SIMS, T. J., PITTARELLO, L., SORANZO, C., PAVESIO, A. & HOLLANDER, A. P. 2005. Quantitative outcome measures of cartilage repair in patients treated by tissue engineering. *Tissue Eng,* 11**,** 277-87.

DIMRI, G. P. 2005. What has senescence got to do with cancer? *Cancer Cell,* 7**,** 505-12.

DING, L., SAUNDERS, T. L., ENIKOLOPOV, G. & MORRISON, S. J. 2012. Endothelial and perivascular cells maintain haematopoietic stem cells. *Nature,* 481**,** 457-62.

DING, Y., XU, D., FENG, G., BUSHELL, A., MUSCHEL, R. J. & WOOD, K. J. 2009. Mesenchymal Stem Cells Prevent the Rejection of Fully Allogenic Islet Grafts by the Immunosuppressive Activity of Matrix Metalloproteinase-2 and-9. *Diabetes,* 58**,** 1797-1806.

DOMINICI, M., LE BLANC, K., MUELLER, I., SLAPER-CORTENBACH, I., MARINI, F. C., KRAUSE, D. S., DEANS, R. J., KEATING, A., PROCKOP, D. J. & HORWITZ, E. M. 2006. Minimal criteria for defining multipotent mesenchymal stromal cells. The International Society for Cellular Therapy position statement. *Cytotherapy,* 8**,** 315-317.

DREIEICHER, E., BECK, K.-F., LAZAROSKI, S., BOOSEN, M., TSALASTRA-GREUL, W., BECK, M., FLEMING, I., SCHAEFER, L. & PFEILSCHIFTER, J. 2009. Nitric Oxide Inhibits Glomerular TGF-β Signaling via SMOC-1. *Journal of the American Society of Nephrology,* 20**,** 1963-1974.

DUIJVESTEIN, M., VOS, A. C. W., ROELOFS, H., WILDENBERG, M. E., WENDRICH, B. B., VERSPAGET, H. W., KOOY-WINKELAAR, E. M. C., KONING, F., ZWAGINGA, J. J., FIDDER, H. H., VERHAAR, A. P., FIBBE, W. E., VAN DEN BRINK, G. R. & HOMMES, D. W. 2010. Autologous bone marrow-derived mesenchymal stromal cell treatment for refractory luminal Crohn's disease: results of a phase I study. *Gut,* 59**,** 1662-1669.

DUNCAN, A. W., TAYLOR, M. H., HICKEY, R. D., HANLON NEWELL, A. E., LENZI, M. L., OLSON, S. B., FINEGOLD, M. J. & GROMPE, M. 2010. The ploidy conveyor of mature hepatocytes as a source of genetic variation. *Nature,* 467**,** 707-710.

EGGENHOFER, E., BENSELER, V., KROEMER, A., POPP, F., GEISSLER, E., SCHLITT, H., BAAN, C., DAHLKE, M. & HOOGDUIJN, M. J. 2012. Mesenchymal stem cells are short-lived and do not migrate beyond the lungs after intravenous infusion. *Frontiers in Immunology,* 3.

ENGLER, A. J., SEN, S., SWEENEY, H. L. & DISCHER, D. E. 2006. Matrix elasticity directs stem cell lineage specification. *Cell,* 126**,** 677-689.

ENGLISH, K., RYAN, J. M., TOBIN, L., MURPHY, M. J., BARRY, F. P. & MAHON, B. P. 2009. Cell contact, prostaglandin E2 and transforming growth factor beta 1 play non-redundant roles in human mesenchymal stem cell induction of CD4+CD25Highforkhead box P3+ regulatory T cells. *Clinical & Experimental Immunology,* 156**,** 149-160.

ESKO, J. D., KIMATA, K. & LINDAHL, U. 2009. Proteoglycans and Sulfated Glycosaminoglycans. *In:* VARKI, A., CUMMINGS, R. D., ESKO, J. D., FREEZE, H. H., STANLEY, P., BERTOZZI, C. R., HART, G. W. & ETZLER, M. E. (eds.) *Essentials of Glycobiology.* 2nd ed. Cold Spring Harbor (NY).

ESWARAKUMAR, V. P., LAX, I. & SCHLESSINGER, J. 2005. Cellular signaling by fibroblast growth factor receptors. *Cytokine Growth Factor Rev,* 16**,** 139-49.

FEDORCSÁK, P., RÁKI, M. & STORENG, R. 2007. Characterization and depletion of leukocytes from cells isolated from the pre-ovulatory ovarian follicle. *Human Reproduction,* 22**,** 989-994.

FERRARA, J. L. M., LEVINE, J. E., REDDY, P. & HOLLER, E. 2009. Graft-versus-host disease. *The Lancet,* 373**,** 1550-1561.

FESTING, S. & WILKINSON, R. 2007. The ethics of animal research. Talking Point on the use of animals in scientific research. *EMBO Rep,* 8**,** 526-30.

FISCHER, U. M., HARTING, M. T., JIMENEZ, F., MONZON-POSADAS, W. O., XUE, H., SAVITZ, S. I., LAINE, G. A. & COX, C. S., JR. 2009. Pulmonary passage is a major obstacle for intravenous stem cell delivery: the pulmonary first-pass effect. *Stem Cells Dev,* 18**,** 683-92.

FORSLÖW, U., BLENNOW, O., LEBLANC, K., RINGDÉN, O., GUSTAFSSON, B., MATTSSON, J. & REMBERGER, M. 2012. Treatment with mesenchymal stromal cells is a risk factor for pneumonia-related death after allogeneic hematopoietic stem cell transplantation. *European Journal of Haematology,* 89**,** 220-227.

FRANCOIS, M., ROMIEU-MOUREZ, R., LI, M. & GALIPEAU, J. 2012. Human MSC suppression correlates with cytokine induction of indoleamine 2,3-dioxygenase and bystander M2 macrophage differentiation. *Mol Ther,* 20**,** 187-95.

FRANQUESA, M., HOOGDUIJN, M. J., BESTARD, O. & GRINYÓ, J. M. 2012. Immunomodulatory effect of Mesenchymal Stem Cells on B cells. *Frontiers in Immunology,* 3.

FREDRIKSSON, L., LI, H. & ERIKSSON, U. 2004. The PDGF family: four gene products form five dimeric isoforms. *Cytokine & Growth Factor Reviews,* 15**,** 197-204.

FRENETTE, P. S., PINHO, S., LUCAS, D. & SCHEIERMANN, C. 2013. Mesenchymal Stem Cell: Keystone of the Hematopoietic Stem Cell Niche and a Stepping-Stone for Regenerative Medicine. *Annual Review of Immunology,* 31**,** 285-316.

FRIEDENSTEIN, A. J., CHAILAKH, R. K. & LALYKINA, K. S. 1970. DEVELOPMENT OF FIBROBLAST COLONIES IN MONOLAYER CULTURES OF GUINEA-PIG BONE MARROW AND SPLEEN CELLS. *Cell and Tissue Kinetics,* 3**,** 393-&.

FRIEDENSTEIN, A. J., PIATETZKY, S., II & PETRAKOVA, K. V. 1966. Osteogenesis in transplants of bone marrow cells. *J Embryol Exp Morphol,* 16**,** 381-90.

FUJISAKI, J., WU, J., CARLSON, A. L., SILBERSTEIN, L., PUTHETI, P., LAROCCA, R., GAO, W., SAITO, T. I., CELSO, C. L., TSUYUZAKI, H., SATO, T., COTE, D., SYKES, M., STROM, T. B., SCADDEN, D. T. & LIN, C. P. 2011. In vivo imaging of Treg cells providing immune privilege to the haematopoietic stem-cell niche. *Nature,* 474**,** 216-219.

FUMAGALLI, M. & FAGAGNA, F. 2009. SASPense and DDRama in cancer and ageing. *Nat Cell Biol,* 11**,** 921-3.

FURLANI, D., UGURLUCAN, M., ONG, L., BIEBACK, K., PITTERMANN, E., WESTIEN, I., WANG, W. W., YEREBAKAN, C., LI, W. Z., GAEBEL, R., LI, R. K., VOLLMAR, B., STEINHOFF, G. & MA, N. 2009. Is the intravascular administration of mesenchymal stem cells safe? Mesenchymal stem cells and intravital microscopy. *Microvascular Research,* 77**,** 370-376.

GALIPEAU, J. 2013. The mesenchymal stromal cells dilemma—does a negative phase III trial of random donor mesenchymal stromal cells in steroid-resistant graft-versus-host disease represent a death knell or a bump in the road? *Cytotherapy,* 15**,** 2-8.

GALLEGOS, A. M. & BEVAN, M. J. 2004. Central Tolerance to Tissue-specific Antigens Mediated by Direct and Indirect Antigen Presentation. *The Journal of Experimental Medicine,* 200**,** 1039-1049.

GÁLVEZ-MARTÍN, P., HMADCHA, A., SORIA, B., CALPENA-CAMPMANY, A. C. & CLARES-NAVEROS, B. 2014. Study of the stability of packaging and storage conditions of human mesenchymal stem cell for intra-arterial clinical application in patient with critical limb ischemia. *European Journal of Pharmaceutics and Biopharmaceutics,* 86**,** 459-468.

GARY, R. K. & KINDELL, S. M. 2005. Quantitative assay of senescence-associated beta-galactosidase activity in mammalian cell extracts. *Anal Biochem,* 343**,** 329-34.

GESTA, S., TSENG, Y. H. & KAHN, C. R. 2007. Developmental origin of fat: tracking obesity to its source. *Cell,* 131**,** 242-56.

GHARIBI, B. & HUGHES, F. J. 2012. Effects of medium supplements on proliferation, differentiation potential, and in vitro expansion of mesenchymal stem cells. *Stem Cells Transl Med,* 1**,** 771-82.

GHIONZOLI, M., CANANZI, M., ZANI, A., ROSSI, C. A., LEON, F. F., PIERRO, A., EATON, S. & DE COPPI, P. 2010. Amniotic fluid stem cell migration after intraperitoneal injection in pup rats: implication for therapy. *Pediatr Surg Int,* 26**,** 79-84.

GINIS, I., GRINBLAT, B. & SHIRVAN, M. H. 2012. Evaluation of bone marrow-derived mesenchymal stem cells after cryopreservation and hypothermic storage in clinically safe medium. *Tissue Eng Part C Methods,* 18**,** 453-63.

GLENNIE, S., SOEIRO, I., DYSON, P. J., LAM, E. W. F. & DAZZI, F. 2005. Bone marrow mesenchymal stem cells induce division arrest anergy of activated T cells. *Blood,* 105**,** 2821-2827.

GNECCHI, M., HE, H., NOISEUX, N., LIANG, O. D., ZHANG, L., MORELLO, F., MU, H., MELO, L. G., PRATT, R. E., INGWALL, J. S. & DZAU, V. J. 2006. Evidence supporting paracrine hypothesis for Akt-

modified mesenchymal stem cell-mediated cardiac protection and functional improvement. *FASEB J,* 20**,** 661-9.

GNECCHI, M., ZHANG, Z., NI, A. & DZAU, V. J. 2008. Paracrine mechanisms in adult stem cell signaling and therapy. *Circ Res,* 103**,** 1204-19.

GOLDRING, M. B., TSUCHIMOCHI, K. & IJIRI, K. 2006. The control of chondrogenesis. *J Cell Biochem,* 97**,** 33-44.

GOTOH, N., ITO, M., YAMAMOTO, S., YOSHINO, I., SONG, N., WANG, Y., LAX, I., SCHLESSINGER, J., SHIBUYA, M. & LANG, R. A. 2004. Tyrosine phosphorylation sites on FRS2α responsible for Shp2 recruitment are critical for induction of lens and retina. *Proceedings of the National Academy of Sciences of the United States of America,* 101**,** 17144-17149.

GOUREAU, O., FAURE, V. & COURTOIS, Y. 1995. Fibroblast Growth Factors Decrease Inducible Nitric Oxide Synthase mRNA Accumulation in Bovine Retinal Pigmented Epithelial Cells. *European Journal of Biochemistry,* 230**,** 1046-1052.

GRAY, D. H., KUPRESANIN, F., BERZINS, S. P., HEROLD, M. J., O'REILLY, L. A., BOUILLET, P. & STRASSER, A. 2012. The BH3-only proteins Bim and Puma cooperate to impose deletional tolerance of organ-specific antigens. *Immunity,* 37**,** 451-62.

GRAYSON, W. L., ZHAO, F., BUNNELL, B. & MA, T. 2007. Hypoxia enhances proliferation and tissue formation of human mesenchymal stem cells. *Biochem Biophys Res Commun,* 358**,** 948-53.

GUPTA, K., HERGRUETER, A. & OWEN, C. A. 2013. Adipose-derived stem cells weigh in as novel therapeutics for acute lung injury. *Stem Cell Res Ther,* 4**,** 19.

GUPTA, P. K., DAS, A. K., CHULLIKANA, A. & MAJUMDAR, A. S. 2012. Mesenchymal stem cells for cartilage repair in osteoarthritis. *Stem Cell Res Ther,* 3**,** 25.

HAMPEL, B., MALISAN, F., NIEDEREGGER, H., TESTI, R. & JANSEN-DURR, P. 2004. Differential regulation of apoptotic cell death in senescent human cells. *Exp Gerontol,* 39**,** 1713-21.

HANDLEY, C. J. & BUTTLE, D. J. 1995. Assay of proteoglycan degradation. *In:* ALAN, J. B. (ed.) *Methods in Enzymology.* Academic Press.

HANDORF, A. M. & LI, W.-J. 2011. Fibroblast Growth Factor-2 Primes Human Mesenchymal Stem Cells for Enhanced Chondrogenesis. *PLoS One,* 6**,** e22887.

HANIFFA, M. A., COLLIN, M. P., BUCKLEY, C. D. & DAZZI, F. 2009. Mesenchymal stem cells: the fibroblasts' new clothes? *Haematologica-the Hematology Journal,* 94**,** 258-263.

HAO, H., LIU, J., SHEN, J., ZHAO, Y., LIU, H., HOU, Q., TONG, C., TI, D., DONG, L., CHENG, Y., MU, Y., LIU, J., FU, X. & HAN, W. 2013. Multiple intravenous infusions of bone marrow mesenchymal stem cells reverse hyperglycemia in experimental type 2 diabetes rats. *Biochem Biophys Res Commun,* 436**,** 418-23.

HAQUE, N., RAHMAN, M. T., ABU KASIM, N. H. & ALABSI, A. M. 2013. Hypoxic Culture Conditions as a Solution for Mesenchymal Stem Cell Based Regenerative Therapy. *The Scientific World Journal,* 2013**,** 12.

HARE, J. M., TRAVERSE, J. H., HENRY, T. D., DIB, N., STRUMPF, R. K., SCHULMAN, S. P., GERSTENBLITH, G., DEMARIA, A. N., DENKTAS, A. E., GAMMON, R. S., HERMILLER, J. B., JR., REISMAN, M. A., SCHAER, G. L. & SHERMAN, W. 2009. A randomized, double-blind, placebo-controlled, dose-escalation study of intravenous adult human mesenchymal stem cells (prochymal) after acute myocardial infarction. *J Am Coll Cardiol,* 54**,** 2277-86.

HASHEMI, S. M., HASSAN, Z. M., POURFATHOLLAH, A. A., SOUDI, S., SHAFIEE, A. & SOLEIMANI, M. 2013. Comparative immunomodulatory properties of adipose-derived mesenchymal stem cells conditioned media from BALB/c, C57BL/6, and DBA mouse strains. *Journal of Cellular Biochemistry,* 114**,** 955-965.

HATAKEYAMA, S., YAMAMOTO, H. & OHYAMA, C. 2010. Tumor formation assays. *Methods in enzymology,* 479**,** 397-411.

HAYFLICK, L. 1965. The limited in vitro lifetime of human diploid cell strains. *Experimental Cell Research,* 37**,** 614-636.

HEALTH CANADA. 2012. *Summary Basis of Decision (SBD) for PROCHYMAL®* [Online]. Available: http://www.hc-sc.gc.ca/dhp-mps/prodpharma/sbd-smd/drug-med/sbd_smd_2012_prochymal_150026-eng.php [Accessed August 2014].

HEIDARI, B., SHIRAZI, A., AKHONDI, M. M., HASSANPOUR, H., BEHZADI, B., NADERI, M. M., SARVARI, A. & BORJIAN, S. 2013. Comparison of proliferative and multilineage differentiation potential of sheep mesenchymal stem cells derived from bone marrow, liver, and adipose tissue. *Avicenna J Med Biotechnol,* 5**,** 104-17.

HELDIN, C. H. 2013. Targeting the PDGF signaling pathway in tumor treatment. *Cell Commun Signal,* 11**,** 97.

HELMINEN, H. J., SÄÄMÄNEN, A. M., SALMINEN, H. & HYTTINEN, M. M. 2002. Transgenic mouse models for studying the role of cartilage macromolecules in osteoarthritis. *Rheumatology,* 41**,** 848-856.

HENG, B. C., CAO, T. & LEE, E. H. 2004. Directing Stem Cell Differentiation into the Chondrogenic Lineage In Vitro. *Stem Cells,* 22**,** 1152-1167.

HENG, B. C., COWAN, C. M. & BASU, S. 2008. Temperature and calcium ions affect aggregation of mesenchymal stem cells in phosphate buffered saline. *Cytotechnology,* 58**,** 69-75.

HERNIGOU, P., POIGNARD, A., BEAUJEAN, F. & ROUARD, H. 2005. Percutaneous autologous bone-marrow grafting for nonunions. Influence of the number and concentration of progenitor cells. *J Bone Joint Surg Am,* 87**,** 1430-7.

HEY, Y. Y. & O'NEILL, H. C. 2012. Murine spleen contains a diversity of myeloid and dendritic cells distinct in antigen presenting function. *J Cell Mol Med,* 16**,** 2611-9.

HIMENO, T., KAMIYA, H., NARUSE, K., CHENG, Z., ITO, S., KONDO, M., OKAWA, T., FUJIYA, A., KATO, J., SUZUKI, H., KITO, T., HAMADA, Y., OISO, Y., ISOBE, K. & NAKAMURA, J. 2013. Mesenchymal Stem Cell-Like Cells Derived from Mouse Induced Pluripotent Stem Cells Ameliorate Diabetic Polyneuropathy in Mice. *BioMed Research International,* 2013**,** 12.

HOF-NAHOR, I., LESHANSKY, L., SHIVTIEL, S., ELDOR, L., ABERDAM, D., ITSKOVITZ-ELDOR, J. & BERRIH-AKNIN, S. 2012. Human mesenchymal stem cells shift CD8+ T cells towards a suppressive phenotype by inducing tolerogenic monocytes. *J Cell Sci,* 125**,** 4640-50.

HOLLANDER, A. P., HEATHFIELD, T. F., WEBBER, C., IWATA, Y., BOURNE, R., RORABECK, C. & POOLE, A. R. 1994. Increased damage to type II collagen in osteoarthritic articular cartilage detected by a new immunoassay. *J Clin Invest,* 93**,** 1722-32.

HOLMES, C. & STANFORD, W. L. 2007. Concise Review: Stem Cell Antigen-1: Expression, Function, and Enigma. *STEM CELLS,* 25**,** 1339-1347.

HONMOU, O., HOUKIN, K., MATSUNAGA, T., NIITSU, Y., ISHIAI, S., ONODERA, R., WAXMAN, S. G. & KOCSIS, J. D. 2011. Intravenous administration of auto serum-expanded autologous mesenchymal stem cells in stroke. *Brain,* 134**,** 1790-807.

HORWITZ, E. M., PROCKOP, D. J., FITZPATRICK, L. A., KOO, W. W. K., GORDON, P. L., NEEL, M., SUSSMAN, M., ORCHARD, P., MARX, J. C., PYERITZ, R. E. & BRENNER, M. K. 1999. Transplantability and therapeutic effects of bone marrow-derived mesenchymal cells in children with osteogenesis imperfecta. *Nature Medicine,* 5**,** 309-313.

HORWITZ, E. M., PROCKOP, D. J., GORDON, P. L., KOO, W. W. K., FITZPATRICK, L. A., NEEL, M. D., MCCARVILLE, M. E., ORCHARD, P. J., PYERITZ, R. E. & BRENNER, M. K. 2001. Clinical responses to bone marrow transplantation in children with severe osteogenesis imperfecta. *Blood,* 97**,** 1227-1231.

HOULIHAN, D. D., MABUCHI, Y., MORIKAWA, S., NIIBE, K., ARAKI, D., SUZUKI, S., OKANO, H. & MATSUZAKI, Y. 2012. Isolation of mouse mesenchymal stem cells on the basis of expression of Sca-1 and PDGFR-α. *Nat. Protocols,* 7**,** 2103-2111.

HOULIHAN, D. D. & NEWSOME, P. N. 2008. Critical review of clinical trials of bone marrow stem cells in liver disease. *Gastroenterology,* 135**,** 438-450.

HSU, Y.-C. & FUCHS, E. 2012. A family business: stem cell progeny join the niche to regulate homeostasis. *Nat Rev Mol Cell Biol,* 13**,** 103-114.

HUANG, H., OSTROFF, G. R., LEE, C. K., SPECHT, C. A. & LEVITZ, S. M. 2010. Robust Stimulation of Humoral and Cellular Immune Responses following Vaccination with Antigen-Loaded β-Glucan Particles. *mBio,* 1.

HUANG, Y. L., QIU, R. F., MAI, W. Y., KUANG, J., CAI, X. Y., DONG, Y. G., HU, Y. Z., SONG, Y. B., CAI, A. P. & JIANG, Z. G. 2012. Effects of insulin-like growth factor-1 on the properties of mesenchymal stem cells in vitro. *J Zhejiang Univ Sci B,* 13**,** 20-8.

HUH, J. W., KIM, S.-Y., LEE, J. H., LEE, J.-S., VAN TA, Q., KIM, M., OH, Y.-M., LEE, Y.-S. & LEE, S.-D. 2011. Bone marrow cells repair cigarette smoke-induced emphysema in rats. *American Journal of Physiology - Lung Cellular and Molecular Physiology,* 301**,** L255-L266.

HUNG, S.-C., POCHAMPALLY, R. R., CHEN, S.-C., HSU, S.-C. & PROCKOP, D. J. 2007. Angiogenic Effects of Human Multipotent Stromal Cell Conditioned Medium Activate the PI3K-Akt Pathway in Hypoxic Endothelial Cells to Inhibit Apoptosis, Increase Survival, and Stimulate Angiogenesis. *STEM CELLS,* 25**,** 2363-2370.

IGURA, K., ZHANG, X., TAKAHASHI, K., MITSURU, A., YAMAGUCHI, S. & TAKASHI, T. A. 2004. Isolation and characterization of mesenchymal progenitor cells from chorionic villi of human placenta. *Cytotherapy,* 6**,** 543-53.

INAMDAR, A. A. & INAMDAR, A. C. 2013. Culture conditions for growth of clinical grade human tissue derived mesenchymal stem cells: comparative study between commercial serum-free media and human product supplemented media. *journal of Regenerative Medicine and Tissue Engineering,* 2.

INMAN, G. J., NICOLAS, F. J., CALLAHAN, J. F., HARLING, J. D., GASTER, L. M., REITH, A. D., LAPING, N. J. & HILL, C. S. 2002. SB-431542 is a potent and specific inhibitor of transforming growth factor-beta superfamily type I activin receptor-like kinase (ALK) receptors ALK4, ALK5, and ALK7. *Mol Pharmacol,* 62**,** 65-74.

IRIE, J., WU, Y., WICKER, L. S., RAINBOW, D., NALESNIK, M. A., HIRSCH, R., PETERSON, L. B., LEUNG, P. S., CHENG, C., MACKAY, I. R., GERSHWIN, M. E. & RIDGWAY, W. M. 2006. NOD.c3c4 congenic mice develop autoimmune biliary disease that serologically and pathogenetically models human primary biliary cirrhosis. *J Exp Med,* 203**,** 1209-19.

ISO, Y., SPEES, J. L., SERRANO, C., BAKONDI, B., POCHAMPALLY, R., SONG, Y. H., SOBEL, B. E., DELAFONTAINE, P. & PROCKOP, D. J. 2007. Multipotent human stromal cells improve cardiac function after myocardial infarction in mice without long-term engraftment. *Biochem Biophys Res Commun,* 354**,** 700-6.

ITKIN, T., LUDIN, A., GRADUS, B., GUR-COHEN, S., KALINKOVICH, A., SCHAJNOVITZ, A., OVADYA, Y., KOLLET, O., CANAANI, J., SHEZEN, E., COFFIN, D. J., ENIKOLOPOV, G. N., BERG, T., PIACIBELLO, W., HORNSTEIN, E. & LAPIDOT, T. 2012. FGF-2 expands murine hematopoietic stem and progenitor cells via proliferation of stromal cells, c-Kit activation, and CXCL12 down-regulation. *Blood,* 120**,** 1843-1855.

ITO, T., SAWADA, R., FUJIWARA, Y., SEYAMA, Y. & TSUCHIYA, T. 2007. FGF-2 suppresses cellular senescence of human mesenchymal stem cells by down-regulation of TGF-β2. *Biochemical and Biophysical Research Communications,* 359**,** 108-114.

ITO, T., SAWADA, R., FUJIWARA, Y. & TSUCHIYA, T. 2008. FGF-2 increases osteogenic and chondrogenic differentiation potentials of human mesenchymal stem cells by inactivation of TGF-beta signaling. *Cytotechnology,* 56**,** 1-7.

JAIN, A., REYES, J., KASHYAP, R., DODSON, S. F., DEMETRIS, A. J., RUPPERT, K., ABU-ELMAGD, K., MARSH, W., MADARIAGA, J., MAZARIEGOS, G., GELLER, D., BONHAM, C. A., GAYOWSKI, T., CACCIARELLI, T., FONTES, P., STARZL, T. E. & FUNG, J. J. 2000. Long-term survival after liver transplantation in 4,000 consecutive patients at a single center. *Ann Surg,* 232**,** 490-500.

JAMOUS, M., AL-ZOUBI, A., KHABAZ, M. N., KHALEDI, R., AL KHATEEB, M. & AL-ZOUBI, Z. 2010. Purification of mouse bone marrow-derived stem cells promotes ex vivo neuronal differentiation. *Cell Transplant,* 19**,** 193-202.

JIAN, H., SHEN, X., LIU, I., SEMENOV, M., HE, X. & WANG, X.-F. 2006. Smad3-dependent nuclear translocation of β-catenin is required for TGF-β1-induced proliferation of bone marrow-derived adult human mesenchymal stem cells. *Genes & Development,* 20**,** 666-674.

JIANG, X.-X., ZHANG, Y., LIU, B., ZHANG, S.-X., WU, Y., YU, X.-D. & MAO, N. 2005. Human mesenchymal stem cells inhibit differentiation and function of monocyte-derived dendritic cells. *Blood,* 105**,** 4120-4126.

JIANG, Y., JAHAGIRDAR, B. N., REINHARDT, R. L., SCHWARTZ, R. E., KEENE, C. D., ORTIZ-GONZALEZ, X. R., REYES, M., LENVIK, T., LUND, T., BLACKSTAD, M., DU, J., ALDRICH, S., LISBERG, A., LOW, W. C., LARGAESPADA, D. A. & VERFAILLIE, C. M. 2002. Pluripotency of mesenchymal stem cells derived from adult marrow. *Nature,* 418**,** 41-49.

JOCHEMS, C. E., VAN DER VALK, J. B., STAFLEU, F. R. & BAUMANS, V. 2002. The use of fetal bovine serum: ethical or scientific problem? *Altern Lab Anim,* 30**,** 219-27.

JOENJE, H. & PATEL, K. J. 2001. The emerging genetic and molecular basis of Fanconi anaemia. *Nat Rev Genet,* 2**,** 446-459.

JONES, D. G. & PETERSON, L. 2006. Autologous Chondrocyte Implantation. 88**,** 2501-2520.

JUNG, S., PANCHALINGAM, K. M., ROSENBERG, L. & BEHIE, L. A. 2012. Ex vivo expansion of human mesenchymal stem cells in defined serum-free media. *Stem Cells International,* 2012**,** 123030.

JUNG, S., SEN, A., ROSENBERG, L. & BEHIE, L. A. 2010. Identification of growth and attachment factors for the serum-free isolation and expansion of human mesenchymal stromal cells. *Cytotherapy,* 12**,** 637-657.

KAFIENAH, W., MISTRY, S., DICKINSON, S. C., SIMS, T. J., LEARMONTH, I. & HOLLANDER, A. P. 2007. Three-dimensional cartilage tissue engineering using adult stem cells from osteoarthritis patients. *Arthritis Rheum,* 56**,** 177-87.

KARP, J. M. & TEOL, G. S. L. 2009. Mesenchymal Stem Cell Homing: The Devil Is in the Details. *Cell Stem Cell,* 4**,** 206-216.

KEAN, T. J., LIN, P., CAPLAN, A. I. & DENNIS, J. E. 2013. MSCs: Delivery Routes and Engraftment, Cell-Targeting Strategies, and Immune Modulation. *Stem Cells International,* 2013**,** 13.

KEATING, A. 2012. Mesenchymal Stromal Cells: New Directions. *Cell Stem Cell,* 10**,** 709-716.

KIM, S.-Y., LEE, J.-H., KIM, H. J., PARK, M. K., HUH, J. W., RO, J. Y., OH, Y.-M., LEE, S.-D. & LEE, Y.-S. 2012. Mesenchymal stem cell-conditioned media recovers lung fibroblasts from cigarette smoke-induced damage. *American Journal of Physiology - Lung Cellular and Molecular Physiology,* 302**,** L891-L908.

KINNER, B., ZALESKAS, J. M. & SPECTOR, M. 2002. Regulation of Smooth Muscle Actin Expression and Contraction in Adult Human Mesenchymal Stem Cells. *Experimental Cell Research,* 278**,** 72-83.

KLEIFELD, O., KOTRA, L. P., GERVASI, D. C., BROWN, S., BERNARDO, M. M., FRIDMAN, R., MOBASHERY, S. & SAGI, I. 2001. X-ray absorption studies of human matrix metalloproteinase-2 (MMP-2) bound to a highly selective mechanism-based inhibitor. comparison with the latent and active forms of the enzyme. *J Biol Chem,* 276**,** 17125-31.

KNUDSON, C. B. & KNUDSON, W. 2001. Cartilage proteoglycans. *Seminars in Cell & Developmental Biology,* 12**,** 69-78.

KOCH, C. M., JOUSSEN, S., SCHELLENBERG, A., LIN, Q., ZENKE, M. & WAGNER, W. 2012. Monitoring of cellular senescence by DNA-methylation at specific CpG sites. *Aging Cell,* 11**,** 366-369.

KOGA, H., ENGEBRETSEN, L., BRINCHMANN, J. E., MUNETA, T. & SEKIYA, I. 2009. Mesenchymal stem cell-based therapy for cartilage repair: a review. *Knee Surg Sports Traumatol Arthrosc,* 17**,** 1289-97.

KOMODA, H., OKURA, H., LEE, C. M., SOUGAWA, N., IWAYAMA, T., HASHIKAWA, T., SAGA, A., YAMAMOTO-KAKUTA, A., ICHINOSE, A., MURAKAMI, S., SAWA, Y. & MATSUYAMA, A. 2009.

Reduction of N-Glycolylneuraminic Acid Xenoantigen on Human Adipose Tissue-Derived Stromal Cells/Mesenchymal Stem Cells Leads to Safer and More Useful Cell Sources for Various Stem Cell Therapies. *Tissue Engineering Part A,* 16**,** 1143-1155.

KOMORI, T. 2006a. Regulation of osteoblast differentiation by transcription factors. *J Cell Biochem,* 99**,** 1233-9.

KOMORI, T. 2006b. Regulation of osteoblast differentiation by transcription factors. *Journal of Cellular Biochemistry,* 99**,** 1233-1239.

KOPEN, G. C., PROCKOP, D. J. & PHINNEY, D. G. 1999. Marrow stromal cells migrate throughout forebrain and cerebellum, and they differentiate into astrocytes after injection into neonatal mouse brains. *Proceedings of the National Academy of Sciences,* 96**,** 10711-10716.

KRAMPERA, M. 2011. Mesenchymal stromal cell `licensing': a multistep process. *Leukemia,* 25**,** 1408-1414.

KRAMPERA, M., COSMI, L., ANGELI, R., PASINI, A., LIOTTA, F., ANDREINI, A., SANTARLASCI, V., MAZZINGHI, B., PIZZOLO, G., VINANTE, F., ROMAGNANI, P., MAGGI, E., ROMAGNANI, S. & ANNUNZIATO, F. 2006. Role for interferon-gamma in the immunomodulatory activity of human bone marrow mesenchymal stem cells. *Stem Cells,* 24**,** 386-398.

KRAMPERA, M., GALIPEAU, J., SHI, Y., TARTE, K. & SENSEBE, L. 2013. Immunological characterization of multipotent mesenchymal stromal cells—The International Society for Cellular Therapy (ISCT) working proposal. *Cytotherapy,* 15**,** 1054-1061.

KRAMPERA, M., GLENNIE, S., DYSON, J., SCOTT, D., LAYLOR, R., SIMPSON, E. & DAZZI, F. 2002. Bone marrow mesenchymal stem cells inhibit the response of naive and memory antigen-specific T cells to their cognate peptide. *Blood,* 101**,** 3722-3729.

KRATCHMAROVA, I., BLAGOEV, B., HAACK-SORENSEN, M., KASSEM, M. & MANN, M. 2005. Mechanism of Divergent Growth Factor Effects in Mesenchymal Stem Cell Differentiation. *Science,* 308**,** 1472-1477.

KRAUSE, D. S. 2002. Plasticity of marrow-derived stem cells. *Gene Ther,* 9**,** 754-8.

KRAUSE, D. S., THEISE, N. D., COLLECTOR, M. I., HENEGARIU, O., HWANG, S., GARDNER, R., NEUTZEL, S. & SHARKIS, S. J. 2001. Multi-organ, multi-lineage engraftment by a single bone marrow-derived stem cell. *Cell,* 105**,** 369-377.

KRETLOW, J., JIN, Y.-Q., LIU, W., ZHANG, W., HONG, T.-H., ZHOU, G., BAGGETT, L. S., MIKOS, A. & CAO, Y. 2008. Donor age and cell passage affects differentiation potential of murine bone marrow-derived stem cells. *Bmc Cell Biology,* 9**,** 60.

KUO, T. K., HUNG, S. P., CHUANG, C. H., CHEN, C. T., SHIH, Y. R., FANG, S. C., YANG, V. W. & LEE, O. K. 2008. Stem cell therapy for liver disease: parameters governing the success of using bone marrow mesenchymal stem cells. *Gastroenterology,* 134**,** 2111-21, 2121 e1-3.

KURTZBERG, J., PROCKOP, S., TEIRA, P., BITTENCOURT, H., LEWIS, V., CHAN, K. W., HORN, B., YU, L., TALANO, J.-A., NEMECEK, E., MILLS, C. R. & CHAUDHURY, S. 2014. Allogeneic Human Mesenchymal Stem Cell Therapy (Remestemcel-L, Prochymal) as a Rescue Agent for Severe Refractory Acute Graft-versus-Host Disease in Pediatric Patients. *Biology of blood and marrow transplantation : journal of the American Society for Blood and Marrow Transplantation,* 20**,** 229-235.

KYRYLKOVA, K., KYRYACHENKO, S., LEID, M. & KIOUSSI, C. 2012. Detection of apoptosis by TUNEL assay. *Methods Mol Biol,* 887**,** 41-7.

LAI, W.-T., KRISHNAPPA, V. & PHINNEY, D. G. 2011. Fibroblast Growth Factor 2 (Fgf2) Inhibits Differentiation of Mesenchymal Stem Cells by Inducing Twist2 and Spry4, Blocking Extracellular Regulated Kinase Activation, and Altering Fgf Receptor Expression Levels. *Stem Cells,* 29**,** 1102-1111.

LALU, M. M., MCINTYRE, L., PUGLIESE, C., FERGUSSON, D., WINSTON, B. W., MARSHALL, J. C., GRANTON, J., STEWART, D. J. & CANADIAN CRITICAL CARE TRIALS, G. 2012. Safety of Cell

Therapy with Mesenchymal Stromal Cells (SafeCell): A Systematic Review and Meta-Analysis of Clinical Trials. *PLoS ONE,* 7**,** e47559.

LE BLANC, K., FRASSONI, F., BALL, L., LOCATELLI, F., ROELOFS, H., LEWIS, I., LANINO, E., SUNDBERG, B., BERNARDO, M. E., REMBERGER, M., DINI, G., EGELER, R. M., BACIGALUPO, A., FIBBE, W., RINGDEN, O. & DEV COMMITTEE EUROPEAN GRP BLOOD, M. 2008. Mesenchymal stem cells for treatment of steroid-resistant, severe, acute graft-versus-host disease: a phase II study. *Lancet,* 371**,** 1579-1586.

LE BLANC, K. & MOUGIAKAKOS, D. 2012. Multipotent mesenchymal stromal cells and the innate immune system. *Nat Rev Immunol,* 12**,** 383-396.

LE BLANC, K., RASMUSSON, I., GOTHERSTROM, C., SEIDEL, C., SUNDBERG, B., SUNDIN, M., ROSENDAHL, K., TAMMIK, C. & RINGDEN, O. 2004a. Mesenchymal stem cells inhibit the expression of CD25 (interleukin-2 receptor) and CD38 on phytohaemagglutinin-activated lymphocytes. *Scand J Immunol,* 60**,** 307-15.

LE BLANC, K., RASMUSSON, I., SUNDBERG, B., GOTHERSTROM, C., HASSAN, M., UZUNEL, M. & RINGDEN, O. 2004b. Treatment of severe acute graft-versus-host disease with third party haploidentical mesenchymal stem cells. *Lancet,* 363**,** 1439-1441.

LE BLANC, K. & RINGDEN, O. 2007. Immunomodulation by mesenchymal stem cells and clinical experience. *Journal of Internal Medicine,* 262**,** 509-525.

LEE, B. Y., HAN, J. A., IM, J. S., MORRONE, A., JOHUNG, K., GOODWIN, E. C., KLEIJER, W. J., DIMAIO, D. & HWANG, E. S. 2006. Senescence-associated β-galactosidase is lysosomal β-galactosidase. *Aging Cell,* 5**,** 187-195.

LEE, J. S., HONG, J. M., MOON, G. J., LEE, P. H., AHN, Y. H., BANG, O. Y. & COLLABORATORS, S. 2010a. A long-term follow-up study of intravenous autologous mesenchymal stem cell transplantation in patients with ischemic stroke. *Stem Cells,* 28**,** 1099-106.

LEE, J. S., LEE, M. O., MOON, B. H., SHIM, S. H., FORNACE, A. J., JR. & CHA, H. J. 2009a. Senescent growth arrest in mesenchymal stem cells is bypassed by Wip1-mediated downregulation of intrinsic stress signaling pathways. *Stem Cells,* 27**,** 1963-75.

LEE, M.-J., JUNG, J., NA, K.-H., MOON, J. S., LEE, H.-J., KIM, J.-H., KIM, G. I., KWON, S.-W., HWANG, S.-G. & KIM, G. J. 2010b. Anti-fibrotic effect of chorionic plate-derived mesenchymal stem cells isolated from human placenta in a rat model of CCl4-injured liver: Potential application to the treatment of hepatic diseases. *Journal of Cellular Biochemistry,* 111**,** 1453-1463.

LEE, O. K., KUO, T. K., CHEN, W.-M., LEE, K.-D., HSIEH, S.-L. & CHEN, T.-H. 2004. Isolation of multipotent mesenchymal stem cells from umbilical cord blood. *Blood,* 103**,** 1669-1675.

LEE, R. H., PULIN, A. A., SEO, M. J., KOTA, D. J., YLOSTALO, J., LARSON, B. L., SEMPRUN-PRIETO, L., DELAFONTAINE, P. & PROCKOP, D. J. 2009b. Intravenous hMSCs improve myocardial infarction in mice because cells embolized in lung are activated to secrete the anti-inflammatory protein TSG-6. *Cell Stem Cell,* 5**,** 54-63.

LEI, F., ZHAO, B., HAQUE, R., XIONG, X., BUDGEON, L., CHRISTENSEN, N. D., WU, Y. & SONG, J. 2011. In vivo programming of tumor antigen-specific T lymphocytes from pluripotent stem cells to promote cancer immunosurveillance. *Cancer Res,* 71**,** 4742-7.

LEIKER, M., SUZUKI, G., IYER, V. S., CANTY, J. M., JR. & LEE, T. 2008. Assessment of a nuclear affinity labeling method for tracking implanted mesenchymal stem cells. *Cell Transplant,* 17**,** 911-22.

LEMSTRÖM, K. B. & KOSKINEN, P. K. 1997. Expression and Localization of Platelet-Derived Growth Factor Ligand and Receptor Protein During Acute and Chronic Rejection of Rat Cardiac Allografts. *Circulation,* 96**,** 1240-1249.

LENNON, D. P., EDMISON, J. M. & CAPLAN, A. I. 2001. Cultivation of rat marrow-derived mesenchymal stem cells in reduced oxygen tension: Effects on in vitro and in vivo osteochondrogenesis. *Journal of Cellular Physiology,* 187**,** 345-355.

LEVY, C. 2012. Treatment Side Effects and Associated Autoimmune Diseases. *In:* HIRSCHFIELD, G. M. & HEATHCOTE, E. J. (eds.) *Autoimmune Hepatitis.* Springer New York.

LI, C., HIRSCH, M., DIPRIMIO, N., ASOKAN, A., GOUDY, K., TISCH, R. & SAMULSKI, R. J. 2009. Cytotoxic-T-lymphocyte-mediated elimination of target cells transduced with engineered adeno-associated virus type 2 vector in vivo. *J Virol,* 83**,** 6817-24.

LI, X. Y., DING, J., ZHENG, Z. H., LI, X. Y., WU, Z. B. & ZHU, P. 2012. Long-term culture in vitro impairs the immunosuppressive activity of mesenchymal stem cells on T cells. *Mol Med Rep,* 6**,** 1183-9.

LI, Y.-P., PACZESNY, S., LAURET, E., POIRAULT, S., BORDIGONI, P., MEKHLOUFI, F., HEQUET, O., BERTRAND, Y., OU-YANG, J.-P., STOLTZ, J.-F., MIOSSEC, P. & ELJAAFARI, A. 2008. Human Mesenchymal Stem Cells License Adult CD34+ Hemopoietic Progenitor Cells to Differentiate into Regulatory Dendritic Cells through Activation of the Notch Pathway. *The Journal of Immunology,* 180**,** 1598-1608.

LIANG, J., ZHANG, H., HUA, B., WANG, H., LU, L., SHI, S., HOU, Y., ZENG, X., GILKESON, G. S. & SUN, L. 2010. Allogenic mesenchymal stem cells transplantation in refractory systemic lupus erythematosus: a pilot clinical study. *Annals of the Rheumatic Diseases,* 69**,** 1423-1429.

LIANG, J., ZHANG, H., WANG, D., FENG, X., WANG, H., HUA, B., LIU, B. & SUN, L. 2012. Allogeneic mesenchymal stem cell transplantation in seven patients with refractory inflammatory bowel disease. *Gut,* 61**,** 468-469.

LIASKOU, E., WILSON, D. V. & OO, Y. H. 2012. Innate Immune Cells in Liver Inflammation. *Mediators of Inflammation,* 2012**,** 21.

LIMDI, J. K. & HYDE, G. M. 2003. Evaluation of abnormal liver function tests. *Postgrad Med J,* 79**,** 307-12.

LIN, C. S., NING, H., LIN, G. & LUE, T. F. 2012. Is CD34 truly a negative marker for mesenchymal stromal cells? *Cytotherapy,* 14**,** 1159-63.

LINDAHL, P., JOHANSSON, B. R., LEVÉEN, P. & BETSHOLTZ, C. 1997. Pericyte Loss and Microaneurysm Formation in PDGF-B-Deficient Mice. *Science,* 277**,** 242-245.

LIU, T. M., MARTINA, M., HUTMACHER, D. W., HUI, J. H., LEE, E. H. & LIM, B. 2007. Identification of common pathways mediating differentiation of bone marrow- and adipose tissue-derived human mesenchymal stem cells into three mesenchymal lineages. *Stem Cells,* 25**,** 750-60.

LOCKE, M., FEISST, V. & DUNBAR, P. R. 2011. Concise review: human adipose-derived stem cells: separating promise from clinical need. *Stem Cells,* 29**,** 404-11.

MA, S., XIE, N., LI, W., YUAN, B., SHI, Y. & WANG, Y. 2014. Immunobiology of mesenchymal stem cells. *Cell Death Differ,* 21**,** 216-225.

MABUCHI, Y., HOULIHAN, D. D., AKAZAWA, C., OKANO, H. & MATSUZAKI, Y. 2013a. Prospective Isolation of Murine and Human Bone Marrow Mesenchymal Stem Cells Based on Surface Markers. *Stem Cells International,* 2013**,** 7.

MABUCHI, Y., MORIKAWA, S., HARADA, S., NIIBE, K., SUZUKI, S., RENAULT-MIHARA, F., HOULIHAN, D. D., AKAZAWA, C., OKANO, H. & MATSUZAKI, Y. 2013b. LNGFR(+)THY-1(+)VCAM-1(hi+) Cells Reveal Functionally Distinct Subpopulations in Mesenchymal Stem Cells. *Stem Cell Reports,* 1**,** 152-65.

MACCARIO, R., PODESTA, M., MORETTA, A., COMETA, A., COMOLI, P., MONTAGNA, D., DAUDT, L., IBATICI, A., PIAGGIO, G., POZZI, S., FRASSONI, F. & LOCATELLI, F. 2005. Interaction of human mesenchymal stem cells with cells involved in alloantigen-specific immune response favors the differentiation of CD4(+), T-cell subsets expressing a regulatory/suppressive phenotype. *Haematologica-the Hematology Journal,* 90**,** 516-525.

MAGGINI, J., MIRKIN, G., BOGNANNI, I., HOLMBERG, J., PIAZZÓN, I. M., NEPOMNASCHY, I., COSTA, H., CAÑONES, C., RAIDEN, S., VERMEULEN, M. & GEFFNER, J. R. 2010. Mouse Bone Marrow-Derived Mesenchymal Stromal Cells Turn Activated Macrophages into a Regulatory-Like Profile. *PLoS ONE,* 5**,** e9252.

MALHI, H., GUICCIARDI, M. E. & GORES, G. J. 2010. Hepatocyte Death: A Clear and Present Danger. *Physiological Reviews,* 90**,** 1165-1194.

MANNS, M. P., CZAJA, A. J., GORHAM, J. D., KRAWITT, E. L., MIELI-VERGANI, G., VERGANI, D. & VIERLING, J. M. 2010. Diagnosis and management of autoimmune hepatitis. *Hepatology,* 51**,** 2193-2213.

MÅNSSON, R., HULTQUIST, A., LUC, S., YANG, L., ANDERSON, K., KHARAZI, S., AL-HASHMI, S., LIUBA, K., THORÉN, L., ADOLFSSON, J., BUZA-VIDAS, N., QIAN, H., SONEJI, S., ENVER, T., SIGVARDSSON, M. & JACOBSEN, S. E. W. 2007. Molecular Evidence for Hierarchical Transcriptional Lineage Priming in Fetal and Adult Stem Cells and Multipotent Progenitors. *Immunity,* 26**,** 407-419.

MANUGUERRA-GAGNE, R., BOULOS, P. R., AMMAR, A., LEBLOND, F. A., KROSL, G., PICHETTE, V., LESK, M. R. & ROY, D.-C. 2013. Transplantation of Mesenchymal Stem Cells Promotes Tissue Regeneration in a Glaucoma Model Through Laser-Induced Paracrine Factor Secretion and Progenitor Cell Recruitment. *STEM CELLS,* 31**,** 1136-1148.

MARCACCI, M., KON, E., MOUKHACHEV, V., LAVROUKOV, A., KUTEPOV, S., QUARTO, R., MASTROGIACOMO, M. & CANCEDDA, R. 2007. Stem cells associated with macroporous bioceramics for long bone repair: 6- to 7-year outcome of a pilot clinical study. *Tissue Eng,* 13**,** 947-55.

MARKMAN, M. 2009. An update on the use of intraperitoneal chemotherapy in the management of ovarian cancer. *Cancer J,* 15**,** 105-9.

MARLOVITS, S., HOMBAUER, M., TRUPPE, M., VÈCSEI, V. & SCHLEGEL, W. 2004. Changes in the ratio of type-I and type-II collagen expression during monolayer culture of human chondrocytes. *Journal of Bone & Joint Surgery, British Volume,* 86-B**,** 286-295.

MAROLT, D., KNEZEVIC, M. & NOVAKOVIC, G. V. 2010. Bone tissue engineering with human stem cells. *Stem Cell Res Ther,* 1**,** 10.

MARTIN, M. J., MUOTRI, A., GAGE, F. & VARKI, A. 2005. Human embryonic stem cells express an immunogenic nonhuman sialic acid. *Nat Med,* 11**,** 228-232.

MARTIN, P. J., UBERTI, J. P., SOIFFER, R. J., KLINGEMANN, H., WALLER, E. K., DALY, A. S., HERRMANN, R. P. & KEBRIAEI, P. 2010. Prochymal Improves Response Rates In Patients With Steroid-Refractory Acute Graft Versus Host Disease (SR-GVHD) Involving The Liver And Gut: Results Of A Randomized, Placebo-Controlled, Multicenter Phase III Trial In GVHD. *Biology of blood and marrow transplantation : journal of the American Society for Blood and Marrow Transplantation,* 16**,** S169-S170.

MARTINEZ, F. O. & GORDON, S. 2014. The M1 and M2 paradigm of macrophage activation: time for reassessment. *F1000Prime Rep,* 6**,** 13.

MARTINEZ, F. O., GORDON, S., LOCATI, M. & MANTOVANI, A. 2006. Transcriptional profiling of the human monocyte-to-macrophage differentiation and polarization: new molecules and patterns of gene expression. *J Immunol,* 177**,** 7303-11.

MAZZONI, A., BRONTE, V., VISINTIN, A., SPITZER, J. H., APOLLONI, E., SERAFINI, P., ZANOVELLO, P. & SEGAL, D. M. 2002. Myeloid Suppressor Lines Inhibit T Cell Responses by an NO-Dependent Mechanism. *The Journal of Immunology,* 168**,** 689-695.

MCBEATH, R., PIRONE, D. M., NELSON, C. M., BHADRIRAJU, K. & CHEN, C. S. 2004. Cell shape, cytoskeletal tension, and RhoA regulate stem cell lineage commitment. *Dev Cell,* 6**,** 483-95.

MEIER, R. P. H., MÜLLER, Y. D., MOREL, P., GONELLE-GISPERT, C. & BÜHLER, L. H. 2013. Transplantation of mesenchymal stem cells for the treatment of liver diseases, is there enough evidence? *Stem Cell Research,* 11**,** 1348-1364.

MEIRELLES, L., FONTES, A. M., COVAS, D. T. & CAPLAN, A. I. 2009. Mechanisms involved in the therapeutic properties of mesenchymal stem cells. *Cytokine & Growth Factor Reviews,* 20**,** 419-427.

MEIRELLES, L. D., CAPLAN, A. I. & NARDI, N. B. 2008. In search of the in vivo identity of mesenchymal stem cells. *Stem Cells,* 26**,** 2287-2299.

MEIRELLES LDA, S. & NARDI, N. B. 2003. Murine marrow-derived mesenchymal stem cell: isolation, in vitro expansion, and characterization. *Br J Haematol,* 123**,** 702-11.

MEISEL, R., ZIBERT, A., LARYEA, M., GOBEL, U., DAUBENER, W. & DILLOO, D. 2004. Human bone marrow stromal cells inhibit allogeneic T-cell responses by indoleamine 2,3-dioxygenase-mediated tryptophan degradation. *Blood,* 103**,** 4619-21.

MENDEZ-FERRER, S., MICHURINA, T. V., FERRARO, F., MAZLOOM, A. R., MACARTHUR, B. D., LIRA, S. A., SCADDEN, D. T., MA'AYAN, A., ENIKOLOPOV, G. N. & FRENETTE, P. S. 2010. Mesenchymal and haematopoietic stem cells form a unique bone marrow niche. *Nature,* 466**,** 829-34.

MENDICINO, M., BAILEY, A. M., WONNACOTT, K., PURI, R. K. & BAUER, S. R. 2014. MSC-based product characterization for clinical trials: an FDA perspective. *Cell Stem Cell,* 14**,** 141-5.

MI, H., MURUGANUJAN, A. & THOMAS, P. D. 2013. PANTHER in 2013: modeling the evolution of gene function, and other gene attributes, in the context of phylogenetic trees. *Nucleic Acids Res,* 41**,** D377-86.

MIMURA, S., KIMURA, N., HIRATA, M., TATEYAMA, D., HAYASHIDA, M., UMEZAWA, A., KOHARA, A., NIKAWA, H., OKAMOTO, T. & FURUE, M. K. 2011. Growth factor-defined culture medium for human mesenchymal stem cells. *Int J Dev Biol,* 55**,** 181-7.

MINAMIDE, A., YOSHIDA, M., KAWAKAMI, M., OKADA, M., ENYO, Y., HASHIZUME, H. & BODEN, S. D. 2007. The Effects of Bone Morphogenetic Protein and Basic Fibroblast Growth Factor on Cultured Mesenchymal Stem Cells for Spine Fusion. *Spine,* 32**,** 1067-1071 10.1097/01.brs.0000261626.32999.8a.

MITCHELL, J. A., AKARASEREENONT, P., THIEMERMANN, C., FLOWER, R. J. & VANE, J. R. 1993. Selectivity of nonsteroidal antiinflammatory drugs as inhibitors of constitutive and inducible cyclooxygenase. *Proc Natl Acad Sci U S A,* 90**,** 11693-7.

MITKARI, B., KERKELA, E., NYSTEDT, J., KORHONEN, M., MIKKONEN, V., HUHTALA, T. & JOLKKONEN, J. 2013. Intra-arterial infusion of human bone marrow-derived mesenchymal stem cells results in transient localization in the brain after cerebral ischemia in rats. *Exp Neurol,* 239**,** 158-62.

MIURA, M., MIURA, Y., PADILLA-NASH, H. M., MOLINOLO, A. A., FU, B., PATEL, V., SEO, B.-M., SONOYAMA, W., ZHENG, J. J., BAKER, C. C., CHEN, W., RIED, T. & SHI, S. 2006. Accumulated Chromosomal Instability in Murine Bone Marrow Mesenchymal Stem Cells Leads to Malignant Transformation. *Stem Cells,* 24**,** 1095-1103.

MOERMAN, E. J., TENG, K., LIPSCHITZ, D. A. & LECKA-CZERNIK, B. 2004. Aging activates adipogenic and suppresses osteogenic programs in mesenchymal marrow stroma/stem cells: the role of PPAR-gamma2 transcription factor and TGF-beta/BMP signaling pathways. *Aging Cell,* 3**,** 379-89.

MOHAMADNEJAD, M., ALIMOGHADDAM, K., BAGHERI, M., ASHRAFI, M., ABDOLLAHZADEH, L., AKHLAGHPOOR, S., BASHTAR, M., GHAVAMZADEH, A. & MALEKZADEH, R. 2013. Randomized placebo-controlled trial of mesenchymal stem cell transplantation in decompensated cirrhosis. *Liver Int,* 33**,** 1490-6.

MOHAMADNEJAD, M., ALIMOGHADDAM, K., MOHYEDDIN-BONAB, M., BAGHERI, M., BASHTAR, M., GHANAATI, H., BAHARVAND, H., GHAVAMZADEH, A. & MALEKZADEH, R. 2007. Phase 1 trial of autologous bone marrow mesenchymal stem cell transplantation in patients with decompensated liver cirrhosis. *Arch Iran Med,* 10**,** 459-66.

MOHAMMADI, M., MCMAHON, G., SUN, L., TANG, C., HIRTH, P., YEH, B. K., HUBBARD, S. R. & SCHLESSINGER, J. 1997. Structures of the tyrosine kinase domain of fibroblast growth factor receptor in complex with inhibitors. *Science,* 276**,** 955-60.

MOLL, G., ALM, J. J., DAVIES, L. C., VON BAHR, L., HELDRING, N., STENBECK-FUNKE, L., HAMAD, O. A., HINSCH, R., IGNATOWICZ, L., LOCKE, M., LÖNNIES, H., LAMBRIS, J. D., TERAMURA, Y., NILSSON-EKDAHL, K., NILSSON, B. & LE BLANC, K. 2014. Do cryopreserved mesenchymal stromal cells display impaired immunomodulatory and therapeutic properties? *STEM CELLS***,** n/a-n/a.

MOLL, G., RASMUSSON-DUPREZ, I., VON BAHR, L., CONNOLLY-ANDERSEN, A.-M., ELGUE, G., FUNKE, L., HAMAD, O. A., LÖNNIES, H., MAGNUSSON, P. U., SANCHEZ, J., TERAMURA, Y., NILSSON-EKDAHL, K., RINGDÉN, O., KORSGREN, O., NILSSON, B. & LE BLANC, K. 2012. Are Therapeutic Human Mesenchymal Stromal Cells Compatible with Human Blood? *STEM CELLS,* 30**,** 1565-1574.

MONTERO, J. C., SEOANE, S., OCANA, A. & PANDIELLA, A. 2011. Inhibition of SRC family kinases and receptor tyrosine kinases by dasatinib: possible combinations in solid tumors. *Clin Cancer Res,* 17**,** 5546-52.

MOORE, C. M. & BEST, R. G. 2001. Chromosome Preparation and Banding. *eLS.* John Wiley & Sons, Ltd.

MORIKAWA, S., MABUCHI, Y., KUBOTA, Y., NAGAI, Y., NIIBE, K., HIRATSU, E., SUZUKI, S., MIYAUCHI-HARA, C., NAGOSHI, N., SUNABORI, T., SHIMMURA, S., MIYAWAKI, A., NAKAGAWA, T., SUDA, T., OKANO, H. & MATSUZAKI, Y. 2009. Prospective identification, isolation, and systemic transplantation of multipotent mesenchymal stem cells in murine bone marrow. *Journal of Experimental Medicine,* 206**,** 2483-2496.

MOSNA, F., SENSEBE, L. & KRAMPERA, M. 2010. Human bone marrow and adipose tissue mesenchymal stem cells: a user's guide. *Stem Cells Dev,* 19**,** 1449-70.

MUELLER, M. B., FISCHER, M., ZELLNER, J., BERNER, A., DIENSTKNECHT, T., PRANTL, L., KUJAT, R., NERLICH, M., TUAN, R. S. & ANGELE, P. 2010. Hypertrophy in mesenchymal stem cell chondrogenesis: effect of TGF-beta isoforms and chondrogenic conditioning. *Cells Tissues Organs,* 192**,** 158-66.

MÜLLER, I., KORDOWICH, S., HOLZWARTH, C., SPANO, C., ISENSEE, G., STAIBER, A., VIEBAHN, S., GIESEKE, F., LANGER, H., GAWAZ, M., HORWITZ, E., CONTE, P., HANDGRETINGER, R. & DOMINICI, M. 2006. Animal serum-free culture conditions for isolation and expansion of multipotent mesenchymal stromal cells from human BM. *Cytotherapy,* 8**,** 437-444.

MURRAY, I. R., WEST, C. C., HARDY, W. R., JAMES, A. W., PARK, T. S., NGUYEN, A., TAWONSAWATRUK, T., LAZZARI, L., SOO, C. & PEAULT, B. 2014. Natural history of mesenchymal stem cells, from vessel walls to culture vessels. *Cell Mol Life Sci,* 71**,** 1353-74.

MURRAY, P. J. & WYNN, T. A. 2011. Protective and pathogenic functions of macrophage subsets. *Nat Rev Immunol,* 11**,** 723-737.

NADRI, S. & SOLEIMANI, M. 2007. Isolation murine mesenchymal stem cells by positive selection. *In Vitro Cellular & Developmental Biology - Animal,* 43**,** 276-282.

NADRI, S., SOLEIMANI, M., HOSSENI, R. H., MASSUMI, M., ATASHI, A. & IZADPANAH, R. 2007. An efficient method for isolation of murine bone marrow mesenchymal stem cells. *International Journal of Developmental Biology,* 51**,** 723-729.

NAKASHIMA, K., ZHOU, X., KUNKEL, G., ZHANG, Z., DENG, J. M., BEHRINGER, R. R. & DE CROMBRUGGHE, B. 2002. The novel zinc finger-containing transcription factor osterix is required for osteoblast differentiation and bone formation. *Cell,* 108**,** 17-29.

NAM, S., KIM, D., CHENG, J. Q., ZHANG, S., LEE, J. H., BUETTNER, R., MIROSEVICH, J., LEE, F. Y. & JOVE, R. 2005. Action of the Src family kinase inhibitor, dasatinib (BMS-354825), on human prostate cancer cells. *Cancer Res,* 65**,** 9185-9.

NANJI, A. A. & HILLER-STURMHOFEL, S. 1997. Apoptosis and necrosis: two types of cell death in alcoholic liver disease. *Alcohol Health Res World,* 21**,** 325-30.

NAUTA, A. J., KRUISSELBRINK, A. B., LURVINK, E., WILLEMZE, R. & FIBBE, W. E. 2006. Mesenchymal stem cells inhibit generation and function of both CD34(+)-derived and monocyte-derived dendritic cells. *Journal of Immunology,* 177**,** 2080-2087.

NEJADNIK, H., HUI, J. H., FENG CHOONG, E. P., TAI, B. C. & LEE, E. H. 2010. Autologous bone marrow-derived mesenchymal stem cells versus autologous chondrocyte implantation: an observational cohort study. *Am J Sports Med,* 38**,** 1110-6.

NEMETH, K., LEELAHAVANICHKUL, A., YUEN, P. S. T., MAYER, B., PARMELEE, A., DOI, K., ROBEY, P. G., LEELAHAVANICHKUL, K., KOLLER, B. H., BROWN, J. M., HU, X., JELINEK, I., STAR, R. A. & MEZEY, E. 2009. Bone marrow stromal cells attenuate sepsis via prostaglandin E2-dependent reprogramming of host macrophages to increase their interleukin-10 production. *Nat Med,* 15**,** 42-49.

NEUSS, S., BECHER, E., WOLTJE, M., TIETZE, L. & JAHNEN-DECHENT, W. 2004. Functional expression of HGF and HGF receptor/c-met in adult human mesenchymal stem cells suggests a role in cell mobilization, tissue repair, and wound healing. *Stem Cells,* 22**,** 405-14.

NG, F., BOUCHER, S., KOH, S., SASTRY, K. S. R., CHASE, L., LAKSHMIPATHY, U., CHOONG, C., YANG, Z., VEMURI, M. C., RAO, M. S. & TANAVDE, V. 2008. PDGF, TGF-beta, and FGF signaling is important for differentiation and growth of mesenchymal stem cells (MSCs): transcriptional profiling can identify markers and signaling pathways important in differentiation of MSCs into adipogenic, chondrogenic, and osteogenic lineages. *Blood,* 112**,** 295-307.

NHS. 2013. *Liver Transplant - Waiting List* [Online]. Available: http://www.nhs.uk/Conditions/Liver-transplant/Pages/When-it-should-be-done.aspx [Accessed 06 December 2014].

NHS BLOOD AND TRANSPLANT. 2010. *Liver Success Rates* [Online]. Available: http://www.uktransplant.org.uk/ukt/about_transplants/success_rates/success_rates.jsp [Accessed 06 December 2014].

NIKOLAEV, N. I., LIU, Y., HUSSEIN, H. & WILLIAMS, D. J. 2012. The sensitivity of human mesenchymal stem cells to vibration and cold storage conditions representative of cold transportation. *Journal of The Royal Society Interface*.

NOISEUX, N., GNECCHI, M., LOPEZ-ILASACA, M., ZHANG, L., SOLOMON, S. D., DEB, A., DZAU, V. J. & PRATT, R. E. 2006. Mesenchymal Stem Cells Overexpressing Akt Dramatically Repair Infarcted Myocardium and Improve Cardiac Function Despite Infrequent Cellular Fusion or Differentiation. *Mol Ther,* 14**,** 840-850.

NYSTEDT, J., ANDERSON, H., TIKKANEN, J., PIETILA, M., HIRVONEN, T., TAKALO, R., HEISKANEN, A., SATOMAA, T., NATUNEN, S., LEHTONEN, S., HAKKARAINEN, T., KORHONEN, M., LAITINEN, S., VALMU, L. & LEHENKARI, P. 2013. Cell surface structures influence lung clearance rate of systemically infused mesenchymal stromal cells. *Stem Cells,* 31**,** 317-26.

OGAWA, Y., MORIKAWA, S., OKANO, H., MABUCHI, Y., SUZUKI, S., YAGUCHI, T., YAGUCHI, S., INABA, T., OKAMOTO, S., KAWAKAMI, Y., TSUBOTA, K., SHIMMURA, S. & MATSUZAKI, Y. 2012. *Donor mesenchymal stem cells trigger chronic graft-versus-host disease following minor antigen-mismatched bone marrow transplantation* [Online]. Available: http://hdl.handle.net/10101/npre.2012.6843.1 [Accessed 25 June 2014].

OH, S., BRAMMER, K. S., LI, Y. S., TENG, D., ENGLER, A. J., CHIEN, S. & JIN, S. 2009. Stem cell fate dictated solely by altered nanotube dimension. *Proc Natl Acad Sci U S A,* 106**,** 2130-5.

ORNITZ, D. M. & ITOH, N. 2001. Fibroblast growth factors. *Genome Biol,* 2**,** REVIEWS3005.

OSATHANON, T., NOWWAROTE, N. & PAVASANT, P. 2011. Basic fibroblast growth factor inhibits mineralization but induces neuronal differentiation by human dental pulp stem cells through a FGFR and PLCgamma signaling pathway. *J Cell Biochem,* 112**,** 1807-16.

PAL, R., HANWATE, M. & TOTEY, S. M. 2008. Effect of holding time, temperature and different parenteral solutions on viability and functionality of adult bone marrow-derived mesenchymal stem cells before transplantation. *J Tissue Eng Regen Med,* 2**,** 436-44.

PALACIOS, R. 1982. Concanavalin A triggers T lymphocytes by directly interacting with their receptors for activation. *J Immunol,* 128**,** 337-42.

PAN, R. L., WANG, P., XIANG, L. X. & SHAO, J. Z. 2011. Delta-like 1 serves as a new target and contributor to liver fibrosis down-regulated by mesenchymal stem cell transplantation. *J Biol Chem,* 286**,** 12340-8.

PARK, M. J., SHIN, J. S., KIM, Y. H., HONG, S. H., YANG, S. H., SHIN, J. Y., KIM, S. Y., KIM, B., KIM, J. S. & PARK, C. G. 2011. Murine mesenchymal stem cells suppress T lymphocyte activation through

IL-2 receptor alpha (CD25) cleavage by producing matrix metalloproteinases. *Stem Cell Rev,* 7**,** 381-93.

PARKIN, J. & COHEN, B. 2001. An overview of the immune system. *The Lancet,* 357**,** 1777-1789.

PARUNGO, C. P., SOYBEL, D. I., COLSON, Y. L., KIM, S. W., OHNISHI, S., DEGRAND, A. M., LAURENCE, R. G., SOLTESZ, E. G., CHEN, F. Y., COHN, L. H., BAWENDI, M. G. & FRANGIONI, J. V. 2007. Lymphatic drainage of the peritoneal space: a pattern dependent on bowel lymphatics. *Ann Surg Oncol,* 14**,** 286-98.

PATTEN, D. A. & COLLETT, A. 2013. Exploring the immunomodulatory potential of microbial-associated molecular patterns derived from the enteric bacterial microbiota. *Microbiology,* 159**,** 1535-1544.

PEISTER, A., MELLAD, J. A., LARSON, B. L., HALL, B. M., GIBSON, L. F. & PROCKOP, D. J. 2004. Adult stem cells from bone marrow (MSCs) isolated from different strains of inbred mice vary in surface epitopes, rates of proliferation, and differentiation potential. *Blood,* 103**,** 1662-1668.

PEK, Y. S., WAN, A. C. & YING, J. Y. 2010a. The effect of matrix stiffness on mesenchymal stem cell differentiation in a 3D thixotropic gel. *Biomaterials,* 31**,** 385-91.

PEK, Y. S., WAN, A. C. A. & YING, J. Y. 2010b. The effect of matrix stiffness on mesenchymal stem cell differentiation in a 3D thixotropic gel. *Biomaterials,* 31**,** 385-391.

PENDLETON, C., LI, Q., CHESLER, D. A., YUAN, K., GUERRERO-CAZARES, H. & QUINONES-HINOJOSA, A. 2013. Mesenchymal Stem Cells Derived from Adipose Tissue vs Bone Marrow: <italic>In Vitro</italic> Comparison of Their Tropism towards Gliomas. *PLoS ONE,* 8**,** e58198.

PENG, L., JIA, Z., YIN, X., ZHANG, X., LIU, Y., CHEN, P., MA, K. & ZHOU, C. 2008. Comparative analysis of mesenchymal stem cells from bone marrow, cartilage, and adipose tissue. *Stem Cells Dev,* 17**,** 761-73.

PENG, L., XIE, D.-Y., LIN, B.-L., LIU, J., ZHU, H.-P., XIE, C., ZHENG, Y.-B. & GAO, Z.-L. 2011. Autologous bone marrow mesenchymal stem cell transplantation in liver failure patients caused by hepatitis B: Short-term and long-term outcomes. *Hepatology,* 54**,** 820-828.

PERICO, N., CASIRAGHI, F., INTRONA, M., GOTTI, E., TODESCHINI, M., CAVINATO, R. A., CAPELLI, C., RAMBALDI, A., CASSIS, P., RIZZO, P., CORTINOVIS, M., MARASÀ, M., GOLAY, J., NORIS, M. & REMUZZI, G. 2011. Autologous Mesenchymal Stromal Cells and Kidney Transplantation: A Pilot Study of Safety and Clinical Feasibility. *Clinical Journal of the American Society of Nephrology,* 6**,** 412-422.

PHINNEY, D. G. 2008. Isolation of mesenchymal stem cells from murine bone marrow by immunodepletion. *In:* PROCKOP, D. J. P. D. G. B. B. A. (ed.) *Methods in Molecular Biology.*

PHINNEY, D. G., KOPEN, G., ISAACSON, R. L. & PROCKOP, D. J. 1999. Plastic adherent stromal cells from the bone marrow of commonly used strains of inbred mice: Variations in yield, growth, and differentiation. *Journal of Cellular Biochemistry,* 72**,** 570-585.

PIERDOMENICO, L., BONSI, L., CALVITTI, M., RONDELLI, D., ARPINATI, M., CHIRUMBOLO, G., BECCHETTI, E., MARCHIONNI, C., ALVIANO, F., FOSSATI, V., STAFFOLANI, N., FRANCHINA, M., GROSSI, A. & BAGNARA, G. P. 2005. Multipotent Mesenchymal Stem Cells with Immunosuppressive Activity Can Be Easily Isolated from Dental Pulp. *Transplantation,* 80**,** 836-842.

PINHO, S., LACOMBE, J., HANOUN, M., MIZOGUCHI, T., BRUNS, I., KUNISAKI, Y. & FRENETTE, P. S. 2013. PDGFRalpha and CD51 mark human nestin+ sphere-forming mesenchymal stem cells capable of hematopoietic progenitor cell expansion. *J Exp Med,* 210**,** 1351-67.

PITTENGER, M. F., MACKAY, A. M., BECK, S. C., JAISWAL, R. K., DOUGLAS, R., MOSCA, J. D., MOORMAN, M. A., SIMONETTI, D. W., CRAIG, S. & MARSHAK, D. R. 1999a. Multilineage potential of adult human mesenchymal stem cells. *Science,* 284**,** 143-147.

PITTENGER, M. F., MACKAY, A. M., BECK, S. C., JAISWAL, R. K., DOUGLAS, R., MOSCA, J. D., MOORMAN, M. A., SIMONETTI, D. W., CRAIG, S. & MARSHAK, D. R. 1999b. Multilineage potential of adult human mesenchymal stem cells. *Science,* 284**,** 143-7.

PLUMAS, J., CHAPEROT, L., RICHARD, M. J., MOLENS, J. P., BENSA, J. C. & FAVROT, M. C. 2005. Mesenchymal stem cells induce apoptosis of activated T cells. *Leukemia,* 19**,** 1597-1604.

POLCHERT, D., SOBINSKY, J., DOUGLAS, G., KIDD, M., MOADSIRI, A., REINA, E., GENRICH, K., MEHROTRA, S., SETTY, S., SMITH, B. & BARTHOLOMEW, A. 2008. IFN-gamma activation of mesenchymal stem cells for treatment and prevention of graft versus host disease. *Eur J Immunol,* 38**,** 1745-55.

PONS, J., HUANG, Y., ARAKAWA-HOYT, J., WASHKO, D., TAKAGAWA, J., YE, J., GROSSMAN, W. & SU, H. 2008. VEGF improves survival of mesenchymal stem cells in infarcted hearts. *Biochem Biophys Res Commun,* 376**,** 419-22.

POOLE, A. R., KOJIMA, T., YASUDA, T., MWALE, F., KOBAYASHI, M. & LAVERTY, S. 2001. Composition and Structure of Articular Cartilage: A Template for Tissue Repair. *Clinical Orthopaedics and Related Research,* 391**,** S26-S33.

POPOV, Y., PATSENKER, E., FICKERT, P., TRAUNER, M. & SCHUPPAN, D. 2005. Mdr2 (Abcb4)-/- mice spontaneously develop severe biliary fibrosis via massive dysregulation of pro- and antifibrogenic genes. *J Hepatol,* 43**,** 1045-54.

PRASAD, V. K., LUCAS, K. G., KLEINER, G. I., TALANO, J. A. M., JACOBSOHN, D., BROADWATER, G., MONROY, R. & KURTZBERG, J. 2011. Efficacy and Safety of Ex Vivo Cultured Adult Human Mesenchymal Stem Cells (Prochymal™) in Pediatric Patients with Severe Refractory Acute Graft-Versus-Host Disease in a Compassionate Use Study. *Biology of Blood and Marrow Transplantation,* 17**,** 534-541.

PUNWAR, S. & KHAN, W. S. 2011. Mesenchymal stem cells and articular cartilage repair: clinical studies and future direction. *Open Orthop J,* 5 Suppl 2**,** 296-301.

QUARTO, R., MASTROGIACOMO, M., CANCEDDA, R., KUTEPOV, S. M., MUKHACHEV, V., LAVROUKOV, A., KON, E. & MARCACCI, M. 2001. Repair of Large Bone Defects with the Use of Autologous Bone Marrow Stromal Cells. *New England Journal of Medicine,* 344**,** 385-386.

RACANELLI, V. & REHERMANN, B. 2006. The liver as an immunological organ. *Hepatology,* 43**,** S54-S62.

RAFFAGHELLO, L., BIANCHI, G., BERTOLOTTO, M., MONTECUCCO, F., BUSCA, A., DALLEGRI, F., OTTONELLO, L. & PISTOIA, V. 2008. Human mesenchymal stem cells inhibit neutrophil apoptosis: A model for neutrophil preservation in the bone marrow niche. *Stem Cells,* 26**,** 151-162.

RAFIQ, K., BERGTOLD, A. & CLYNES, R. 2002. Immune complex–mediated antigen presentation induces tumor immunity. *The Journal of Clinical Investigation,* 110**,** 71-79.

RAGHUNATH, J., ROLLO, J., SALES, K. M., BUTLER, P. E. & SEIFALIAN, A. M. 2007. Biomaterials and scaffold design: key to tissue-engineering cartilage. *Biotechnology and Applied Biochemistry,* 46**,** 73-84.

RANGANATH, S. H., LEVY, O., INAMDAR, M. S. & KARP, J. M. 2012. Harnessing the mesenchymal stem cell secretome for the treatment of cardiovascular disease. *Cell Stem Cell,* 10**,** 244-58.

RANGARAJAN, A., HONG, S. J., GIFFORD, A. & WEINBERG, R. A. 2004. Species- and cell type-specific requirements for cellular transformation. *Cancer Cell,* 6**,** 171-183.

RASMUSSON, I., LE BLANC, K., SUNDBERG, B. & RINGDÉN, O. 2007a. Mesenchymal Stem Cells Stimulate Antibody Secretion in Human B Cells. *Scandinavian Journal of Immunology,* 65**,** 336-343.

RASMUSSON, I., RINGDEN, O., SUNDBERG, B. & LE BLANC, K. 2005. Mesenchymal stem cells inhibit lymphocyte proliferation by mitogens and alloantigens by different mechanisms. *Exp Cell Res,* 305**,** 33-41.

RASMUSSON, I., UHLIN, M., LE BLANC, K. & LEVITSKY, V. 2007b. Mesenchymal stem cells fail to trigger effector functions of cytotoxic T lymphocytes. *Journal of Leukocyte Biology,* 82**,** 887-893.

RATZIU, V., SAMUEL, D., SEBAGH, M., FARGES, O., SALIBA, F., ICHAI, P., FARAHMAND, H., GIGOU, M., FERAY, C., REYNES, M. & BISMUTH, H. 1999. Long-term follow-up after liver transplantation for autoimmune hepatitis: evidence of recurrence of primary disease. *J Hepatol,* 30**,** 131-41.

REN, G., SU, J., ZHANG, L., ZHAO, X., LING, W., L'HUILLIE, A., ZHANG, J., LU, Y., ROBERTS, A. I., JI, W., ZHANG, H., RABSON, A. B. & SHI, Y. 2009. Species Variation in the Mechanisms of Mesenchymal Stem Cell-Mediated Immunosuppression. *Stem Cells,* 27**,** 1954-1962.

REN, G., ZHANG, L., ZHAO, X., XU, G., ZHANG, Y., ROBERTS, A. I., ZHAO, R. C. & SHI, Y. 2008. Mesenchymal Stem Cell-Mediated Immunosuppression Occurs via Concerted Action of Chemokines and Nitric Oxide. *Cell Stem Cell,* 2**,** 141-150.

REN, H., CAO, Y., ZHAO, Q., LI, J., ZHOU, C., LIAO, L., JIA, M., ZHAO, Q., CAI, H., HAN, Z. C., YANG, R., CHEN, G. & ZHAO, R. C. 2006. Proliferation and differentiation of bone marrow stromal cells under hypoxic conditions. *Biochemical and Biophysical Research Communications,* 347**,** 12-21.

RIBEIRO, A., LARANJEIRA, P., MENDES, S., VELADA, I., LEITE, C., ANDRADE, P., SANTOS, F., HENRIQUES, A., GRAOS, M., CARDOSO, C. M., MARTINHO, A., PAIS, M., DA SILVA, C. L., CABRAL, J., TRINDADE, H. & PAIVA, A. 2013. Mesenchymal stem cells from umbilical cord matrix, adipose tissue and bone marrow exhibit different capability to suppress peripheral blood B, natural killer and T cells. *Stem Cell Res Ther,* 4**,** 125.

RINGDÉN, O., UZUNEL, M., RASMUSSON, I., REMBERGER, M., SUNDBERG, B., LÖNNIES, H., MARSCHALL, H.-U., DLUGOSZ, A., SZAKOS, A., HASSAN, Z., OMAZIC, B., ASCHAN, J., BARKHOLT, L. & LE BLANC, K. 2006. Mesenchymal Stem Cells for Treatment of Therapy-Resistant Graft-versus-Host Disease. *Transplantation,* 81**,** 1390-1397 10.1097/01.tp.0000214462.63943.14.

ROBERTS, W. G., WHALEN, P. M., SODERSTROM, E., MORASKI, G., LYSSIKATOS, J. P., WANG, H. F., COOPER, B., BAKER, D. A., SAVAGE, D., DALVIE, D., ATHERTON, J. A., RALSTON, S., SZEWC, R., KATH, J. C., LIN, J., SODERSTROM, C., TKALCEVIC, G., COHEN, B. D., POLLACK, V., BARTH, W., HUNGERFORD, W. & UNG, E. 2005. Antiangiogenic and antitumor activity of a selective PDGFR tyrosine kinase inhibitor, CP-673,451. *Cancer Res,* 65**,** 957-66.

RODIER, F., COPPE, J. P., PATIL, C. K., HOEIJMAKERS, W. A., MUNOZ, D. P., RAZA, S. R., FREUND, A., CAMPEAU, E., DAVALOS, A. R. & CAMPISI, J. 2009. Persistent DNA damage signalling triggers senescence-associated inflammatory cytokine secretion. *Nat Cell Biol,* 11**,** 973-9.

RODRIGUES, M., GRIFFITH, L. G. & WELLS, A. 2010. Growth factor regulation of proliferation and survival of multipotential stromal cells. *Stem Cell Res Ther,* 1**,** 32.

ROELEN, B. A. J. & DIJKE, P. T. 2003. Controlling mesenchymal stem cell differentiation by TGF-B family members. *Journal of Orthopaedic Science,* 8**,** 740-748.

ROEMELING-VAN RHIJN, M., MENSAH, F. K., KOREVAAR, S. S., LEIJS, M. J., VAN OSCH, G. J., IJZERMANS, J. N., BETJES, M. G., BAAN, C. C., WEIMAR, W. & HOOGDUIJN, M. J. 2013. Effects of Hypoxia on the Immunomodulatory properties of Adipose tissue-derived Mesenchymal Stem Cells. *Frontiers in Immunology,* 4.

ROMBOUTS, W. J. & PLOEMACHER, R. E. 2003. Primary murine MSC show highly efficient homing to the bone marrow but lose homing ability following culture. *Leukemia,* 17**,** 160-70.

ROSOVÁ, I., DAO, M., CAPOCCIA, B., LINK, D. & NOLTA, J. A. 2008. Hypoxic Preconditioning Results in Increased Motility and Improved Therapeutic Potential of Human Mesenchymal Stem Cells. *STEM CELLS,* 26**,** 2173-2182.

RYAN, J. M., BARRY, F., MURPHY, J. M. & MAHON, B. P. 2007. Interferon-gamma does not break, but promotes the immunosuppressive capacity of adult human mesenchymal stem cells. *Clinical and Experimental Immunology,* 149**,** 353-363.

SACCHETTI, B., FUNARI, A., MICHIENZI, S., DI CESARE, S., PIERSANTI, S., SAGGIO, I., TAGLIAFICO, E., FERRARI, S., ROBEY, P. G., RIMINUCCI, M. & BIANCO, P. 2007. Self-renewing osteoprogenitors in bone marrow sinusoids can organize a hematopoietic microenvironment. *Cell,* 131**,** 324-36.

SALIM, A., NACAMULI, R. P., MORGAN, E. F., GIACCIA, A. J. & LONGAKER, M. T. 2004. Transient changes in oxygen tension inhibit osteogenic differentiation and Runx2 expression in osteoblasts. *J Biol Chem,* 279**,** 40007-16.

SATO, K., OZAKI, K., OH, I., MEGURO, A., HATANAKA, K., NAGAI, T., MUROI, K. & OZAWA, K. 2007. Nitric oxide plays a critical role in suppression of T-cell proliferation by mesenchymal stem cells. *Blood,* 109**,** 228-234.

SATO, Y., ARAKI, H., KATO, J., NAKAMURA, K., KAWANO, Y., KOBUNE, M., SATO, T., MIYANISHI, K., TAKAYAMA, T., TAKAHASHI, M., TAKIMOTO, R., IYAMA, S., MATSUNAGA, T., OHTANI, S., MATSUURA, A., HAMADA, H. & NIITSU, Y. 2005. Human mesenchymal stem cells xenografted directly to rat liver are differentiated into human hepatocytes without fusion. *Blood,* 106**,** 756-63.

SAURA, M., ZARAGOZA, C., HERRANZ, B., GRIERA, M., DIEZ-MARQUÉS, L., RODRIGUEZ-PUYOL, D. & RODRIGUEZ-PUYOL, M. 2005. Nitric Oxide Regulates Transforming Growth Factor-β Signaling in Endothelial Cells. *Circulation Research,* 97**,** 1115-1123.

SCHALLMOSER, K., BARTMANN, C., ROHDE, E., BORK, S., GUELLY, C., OBENAUF, A. C., REINISCH, A., HORN, P., HO, A. D., STRUNK, D. & WAGNER, W. 2010. Replicative senescence-associated gene expression changes in mesenchymal stromal cells are similar under different culture conditions. *Haematologica,* 95**,** 867-74.

SCHREPFER, S., DEUSE, T., REICHENSPURNER, H., FISCHBEIN, M. P., ROBBINS, R. C. & PELLETIER, M. P. 2007. Stem cell transplantation: the lung barrier. *Transplant Proc,* 39**,** 573-6.

SCHULZ, R. M. & BADER, A. 2007. Cartilage tissue engineering and bioreactor systems for the cultivation and stimulation of chondrocytes. *Eur Biophys J,* 36**,** 539-68.

SELMANI, Z., NAJI, A., ZIDI, I., FAVIER, B., GAIFFE, E., OBERT, L., BORG, C., SAAS, P., TIBERGHIEN, P., ROUAS-FREISS, N., CAROSELLA, E. D. & DESCHASEAUX, F. 2008. Human Leukocyte Antigen-G5 Secretion by Human Mesenchymal Stem Cells Is Required to Suppress T Lymphocyte and Natural Killer Function and to Induce CD4+CD25highFOXP3+ Regulatory T Cells. *Stem Cells,* 26**,** 212-222.

SELVARAJAH, V., MONTANO-LOZA, A. J. & CZAJA, A. J. 2012. Systematic review: managing suboptimal treatment responses in autoimmune hepatitis with conventional and nonstandard drugs. *Alimentary Pharmacology & Therapeutics,* 36**,** 691-707.

SENSEBE, L., BOURIN, P. & TARTE, K. 2011. Good manufacturing practices production of mesenchymal stem/stromal cells. *Hum Gene Ther,* 22**,** 19-26.

SEPULVEDA, J., TOME, M., EUGENIA FERNANDEZ, M., DELGADO, M., CAMPISI, J., BERNAD, A. & GONZALEZ, M. A. 2014. Cell senescence abrogates the therapeutic potential of human mesenchymal stem cells in the lethal endotoxemia model. *Stem Cells,* 32**,** 1865-77.

SETHE, S., SCUTT, A. & STOLZING, A. 2006. Aging of mesenchymal stem cells. *Ageing Research Reviews,* 5**,** 91-116.

SHENAQ, D. S., RASTEGAR, F., PETKOVIC, D., ZHANG, B. Q., HE, B. C., CHEN, L., ZUO, G. W., LUO, Q., SHI, Q., WAGNER, E. R., HUANG, E., GAO, Y., GAO, J. L., KIM, S. H., YANG, K., BI, Y., SU, Y., ZHU, G., LUO, J., LUO, X., QIN, J., REID, R. R., LUU, H. H., HAYDON, R. C. & HE, T. C. 2010. Mesenchymal Progenitor Cells and Their Orthopedic Applications: Forging a Path towards Clinical Trials. *Stem Cells Int,* 2010**,** 519028.

SHI, C., JIA, T., MENDEZ-FERRER, S., HOHL, T. M., SERBINA, N. V., LIPUMA, L., LEINER, I., LI, M. O., FRENETTE, P. S. & PAMER, E. G. 2011. Bone marrow mesenchymal stem and progenitor cells induce monocyte emigration in response to circulating toll-like receptor ligands. *Immunity,* 34**,** 590-601.

SHIPMAN, K. E., HOLT, A. D. & GAMA, R. 2013. *Interpreting an isolated raised serum alkaline phosphatase level in an asymptomatic patient*.

SHORT, B., BROUARD, N. & SIMMONS, P. 2009. Prospective Isolation of Mesenchymal Stem Cells from Mouse Compact Bone. *In:* AUDET, J. & STANFORD, W. (eds.) *Stem Cells in Regenerative Medicine.* Humana Press.

SHOSHANI, O., MASSALHA, H., SHANI, N., KAGAN, S., RAVID, O., MADAR, S., TRAKHTENBROT, L., LESHKOWITZ, D., RECHAVI, G. & ZIPORI, D. 2012. Polyploidization of murine mesenchymal cells is associated with suppression of the long noncoding RNA H19 and reduced tumorigenicity. *Cancer Res,* 72**,** 6403-13.

SI, Y., ZHAO, Y., HAO, H., LIU, J., GUO, Y., MU, Y., SHEN, J., CHENG, Y., FU, X. & HAN, W. 2012. Infusion of Mesenchymal Stem Cells Ameliorates Hyperglycemia in Type 2 Diabetic Rats: Identification of a Novel Role in Improving Insulin Sensitivity. *Diabetes,* 61**,** 1616-1625.

SIDNEY, L. E., BRANCH, M. J., DUNPHY, S. E., DUA, H. S. & HOPKINSON, A. 2014. Concise Review: Evidence for CD34 as a Common Marker for Diverse Progenitors. *STEM CELLS,* 32**,** 1380-1389.

SINGH, A., AMBUJAM, S. & UMA, A. N. 2010. The cytogenetics of Bloom's syndrome. *J Pediatr Neurosci,* 5**,** 171-2.

SMYTH, G. K. 2004. Linear models and empirical bayes methods for assessing differential expression in microarray experiments. *Stat Appl Genet Mol Biol,* 3**,** Article3.

SOLCHAGA, L. A., PENICK, K. J. & WELTER, J. F. 2011. Chondrogenic differentiation of bone marrow-derived mesenchymal stem cells: tips and tricks. *Methods Mol Biol,* 698**,** 253-78.

SOLEIMANI, M. & NADRI, S. 2009. A protocol for isolation and culture of mesenchymal stem cells from mouse bone marrow. *Nature Protocols,* 4**,** 102-106.

SONG, X., LI, Y., CHEN, X., YIN, G., HUANG, Q., CHEN, Y., XU, G. & WANG, L. 2014. bFGF promotes adipocyte differentiation in human mesenchymal stem cells derived from embryonic stem cells. *Genet Mol Biol,* 37**,** 127-34.

SOUNG DO, Y., DONG, Y., WANG, Y., ZUSCIK, M. J., SCHWARZ, E. M., O'KEEFE, R. J. & DRISSI, H. 2007. Runx3/AML2/Cbfa3 regulates early and late chondrocyte differentiation. *J Bone Miner Res,* 22**,** 1260-70.

SPAGGIARI, G. M., CAPOBIANCO, A., ABDELRAZIK, H., BECCHETTI, F., MINGARI, M. C. & MORETTA, L. 2008. Mesenchymal stem cells inhibit natural killer-cell proliferation, cytotoxicity, and cytokine production: role of indoleamine 2,3-dioxygenase and prostaglandin E2. *Blood,* 111**,** 1327-1333.

SPAGGIARI, G. M., CAPOBIANCO, A., BECCHETTI, S., MINGARI, M. C. & MORETTA, L. 2006. Mesenchymal stem cell-natural killer cell interactions: evidence that activated NK cells are capable of killing MSCs, whereas MSCs can inhibit IL-2-induced NK-cell proliferation. *Blood,* 107**,** 1484-1490.

SPEES, J. L., GREGORY, C. A., SINGH, H., TUCKER, H. A., PEISTER, A., LYNCH, P. J., HSU, S.-C., SMITH, J. & PROCKOP, D. J. 2004. Internalized Antigens Must Be Removed to Prepare Hypoimmunogenic Mesenchymal Stem Cells for Cell and Gene Therapy. *Mol Ther,* 9**,** 747-756.

SPEES, J. L., OLSON, S. D., YLOSTALO, J., LYNCH, P. J., SMITH, J., PERRY, A., PEISTER, A., WANG, M. Y. & PROCKOP, D. J. 2003. Differentiation, cell fusion, and nuclear fusion during ex vivo repair of epithelium by human adult stem cells from bone marrow stroma. *Proc Natl Acad Sci U S A,* 100**,** 2397-402.

STEWART, A., GUAN, H. & YANG, K. 2010. BMP-3 promotes mesenchymal stem cell proliferation through the TGF-beta/activin signaling pathway. *J Cell Physiol,* 223**,** 658-66.

STORCHOVA, Z. & KUFFER, C. 2008. The consequences of tetraploidy and aneuploidy. *Journal of Cell Science,* 121**,** 3859-3866.

TABERA, S., PÉREZ-SIMÓN, J. A., DÍEZ-CAMPELO, M., SÁNCHEZ-ABARCA, L. I., BLANCO, B., LÓPEZ, A., BENITO, A., OCIO, E., SÁNCHEZ-GUIJO, F. M., CAÑIZO, C. & SAN MIGUEL, J. F. 2008. The effect of mesenchymal stem cells on the viability, proliferation and differentiation of B-lymphocytes. *Haematologica,* 93**,** 1301-1309.

TAMAMA, K., FAN, V. H., GRIFFITH, L. G., BLAIR, H. C. & WELLS, A. 2006. Epidermal growth factor as a candidate for ex vivo expansion of bone marrow-derived mesenchymal stem cells. *Stem Cells,* 24**,** 686-95.

TANNENBAUM, S. E., TURETSKY, T. T., SINGER, O., AIZENMAN, E., KIRSHBERG, S., ILOUZ, N., GIL, Y., BERMAN-ZAKEN, Y., PERLMAN, T. S., GEVA, N., LEVY, O., ARBELL, D., SIMON, A., BEN-MEIR, A., SHUFARO, Y., LAUFER, N. & REUBINOFF, B. E. 2012. Derivation of xeno-free and GMP-grade human embryonic stem cells--platforms for future clinical applications. *PLoS One,* 7**,** e35325.

TAO, X. R., LI, W. L., SU, J., JIN, C. X., WANG, X. M., LI, J. X., HU, J. K., XIANG, Z. H., LAU, J. T. & HU, Y. P. 2009. Clonal mesenchymal stem cells derived from human bone marrow can differentiate into hepatocyte-like cells in injured livers of SCID mice. *J Cell Biochem,* 108**,** 693-704.

TARTE, K., GAILLARD, J., LATAILLADE, J.-J., FOUILLARD, L., BECKER, M., MOSSAFA, H., TCHIRKOV, A., ROUARD, H., HENRY, C., SPLINGARD, M., DULONG, J., MONNIER, D., GOURMELON, P., GORIN, N.-C., SENSEBÉ, L. & CELLULAIRE, O. B. O. S. F. D. G. D. M. E. T. 2010. Clinical-grade production of human mesenchymal stromal cells: occurrence of aneuploidy without transformation. *Blood,* 115**,** 1549-1553.

TERADA, N., HAMAZAKI, T., OKA, M., HOKI, M., MASTALERZ, D. M., NAKANO, Y., MEYER, E. M., MOREL, L., PETERSEN, B. E. & SCOTT, E. W. 2002. Bone marrow cells adopt the phenotype of other cells by spontaneous cell fusion. *Nature,* 416**,** 542-5.

TOKUNAGA, A., OYA, T., ISHII, Y., MOTOMURA, H., NAKAMURA, C., ISHIZAWA, S., FUJIMORI, T., NABESHIMA, Y., UMEZAWA, A., KANAMORI, M., KIMURA, T. & SASAHARA, M. 2008. PDGF receptor beta is a potent regulator of mesenchymal stromal cell function. *J Bone Miner Res,* 23**,** 1519-28.

TOLAR, J., NAUTA, A. J., OSBORN, M. J., PANOSKALTSIS MORTARI, A., MCELMURRY, R. T., BELL, S., XIA, L., ZHOU, N., RIDDLE, M., SCHROEDER, T. M., WESTENDORF, J. J., MCIVOR, R. S., HOGENDOORN, P. C. W., SZUHAI, K., OSETH, L., HIRSCH, B., YANT, S. R., KAY, M. A., PEISTER, A., PROCKOP, D. J., FIBBE, W. E. & BLAZAR, B. R. 2007. Sarcoma Derived from Cultured Mesenchymal Stem Cells. *Stem Cells,* 25**,** 371-379.

TOMA, C., PITTENGER, M. F., CAHILL, K. S., BYRNE, B. J. & KESSLER, P. D. 2002. Human Mesenchymal Stem Cells Differentiate to a Cardiomyocyte Phenotype in the Adult Murine Heart. *Circulation,* 105**,** 93-98.

TOMA, C., WAGNER, W. R., BOWRY, S., SCHWARTZ, A. & VILLANUEVA, F. 2009. Fate Of Culture-Expanded Mesenchymal Stem Cells in The Microvasculature. *Circulation Research,* 104**,** 398-402.

TOMCHUCK, S. L., ZWEZDARYK, K. J., COFFELT, S. B., WATERMAN, R. S., DANKA, E. S. & SCANDURRO, A. B. 2008. Toll-Like Receptors on Human Mesenchymal Stem Cells Drive Their Migration and Immunomodulating Responses. *Stem Cells,* 26**,** 99-107.

TONTONOZ, P. & SPIEGELMAN, B. M. 2008. Fat and beyond: the diverse biology of PPARgamma. *Annu Rev Biochem,* 77**,** 289-312.

TROPEL, P., NOËL, D., PLATET, N., LEGRAND, P., BENABID, A.-L. & BERGER, F. 2004. Isolation and characterisation of mesenchymal stem cells from adult mouse bone marrow. *Experimental Cell Research,* 295**,** 395-406.

TROPEL, P., PLATET, N., PLATEL, J.-C., NOËL, D., ALBRIEUX, M., BENABID, A.-L. & BERGER, F. 2006. Functional Neuronal Differentiation of Bone Marrow-Derived Mesenchymal Stem Cells. *STEM CELLS,* 24**,** 2868-2876.

TROUNSON, A., THAKAR, R. G., LOMAX, G. & GIBBONS, D. 2011. Clinical trials for stem cell therapies. *BMC Med,* 9**,** 52.

TSAI, C.-C., CHEN, Y.-J., YEW, T.-L., CHEN, L.-L., WANG, J.-Y., CHIU, C.-H. & HUNG, S.-C. 2010. Hypoxia inhibits senescence and maintains mesenchymal stem cell properties through down-regulation of E2A-p21 by HIF-TWIST. *Blood,* 117**,** 459-469.

TSUTSUMI, S., SHIMAZU, A., MIYAZAKI, K., PAN, H., KOIKE, C., YOSHIDA, E., TAKAGISHI, K. & KATO, Y. 2001. Retention of Multilineage Differentiation Potential of Mesenchymal Cells during Proliferation in Response to FGF. *Biochemical and Biophysical Research Communications,* 288**,** 413-419.

TU, Q., ZHANG, J., PAZ, J., WADE, K., YANG, P. & CHEN, J. 2008. Haploinsufficiency of Runx2 results in bone formation decrease and different BSP expression pattern changes in two transgenic mouse models. *Journal of Cellular Physiology,* 217**,** 40-47.

UCCELLI, A., MORETTA, L. & PISTOIA, V. 2008. Mesenchymal stem cells in health and disease. *Nature Reviews Immunology,* 8**,** 726-736.

URBAN, V. S., KISS, J., KOVACS, J., GOCZA, E., VAS, V., MONOSTORI, E. & UHER, F. 2008. Mesenchymal stem cells cooperate with bone marrow cells in therapy of diabetes. *Stem Cells,* 26**,** 244-53.

VALLIER, L., ALEXANDER, M. & PEDERSEN, R. A. 2005. Activin/Nodal and FGF pathways cooperate to maintain pluripotency of human embryonic stem cells. *Journal of Cell Science,* 118**,** 4495-4509.

VAN BELLE, T. L., TAYLOR, P. & VON HERRATH, M. G. 2009. Mouse Models for Type 1 Diabetes. *Drug Discov Today Dis Models,* 6**,** 41-45.

VAN DER VALK, J., BRUNNER, D., DE SMET, K., FEX SVENNINGSEN, A., HONEGGER, P., KNUDSEN, L. E., LINDL, T., NORABERG, J., PRICE, A., SCARINO, M. L. & GSTRAUNTHALER, G. 2010. Optimization of chemically defined cell culture media--replacing fetal bovine serum in mammalian in vitro methods. *Toxicol In Vitro,* 24**,** 1053-63.

VIGNALI, D. A., COLLISON, L. W. & WORKMAN, C. J. 2008. How regulatory T cells work. *Nat Rev Immunol,* 8**,** 523-32.

VINATIER, C., MRUGALA, D., JORGENSEN, C., GUICHEUX, J. & NOËL, D. 2009. Cartilage engineering: a crucial combination of cells, biomaterials and biofactors. *Trends in Biotechnology,* 27**,** 307-314.

VIVIER, E., TOMASELLO, E., BARATIN, M., WALZER, T. & UGOLINI, S. 2008. Functions of natural killer cells. *Nat Immunol,* 9**,** 503-510.

VOGEL, A., HEINRICH, E., BAHR, M. J., RIFAI, K., FLEMMING, P., MELTER, M., KLEMPNAUER, J., NASHAN, B., MANNS, M. P. & STRASSBURG, C. P. 2004. Long-term outcome of liver transplantation for autoimmune hepatitis. *Clin Transplant,* 18**,** 62-9.

VON BAHR, L., BATSIS, I., MOLL, G., HÄGG, M., SZAKOS, A., SUNDBERG, B., UZUNEL, M., RINGDEN, O. & LE BLANC, K. 2012. Analysis of Tissues Following Mesenchymal Stromal Cell Therapy in Humans Indicates Limited Long-Term Engraftment and No Ectopic Tissue Formation. *STEM CELLS,* 30**,** 1575-1578.

WAGNER, W., BORK, S., LEPPERDINGER, G., JOUSSEN, S., MA, N., STRUNK, D. & KOCH, C. 2010. How to track cellular aging of mesenchymal stromal cells? *Aging (Albany NY),* 2**,** 224-30.

WAGNER, W. & HO, A. 2007. Mesenchymal Stem Cell Preparations—Comparing Apples and Oranges. *Stem Cell Reviews,* 3**,** 239-248.

WAGNER, W., HORN, P., CASTOLDI, M., DIEHLMANN, A., BORK, S., SAFFRICH, R., BENES, V., BLAKE, J., PFISTER, S., ECKSTEIN, V. & HO, A. D. 2008. Replicative Senescence of Mesenchymal Stem Cells: A Continuous and Organized Process. *PLoS One,* 3.

WAGNER, W., WEIN, F., SECKINGER, A., FRANKHAUSER, M., WIRKNER, U., KRAUSE, U., BLAKE, J., SCHWAGER, C., ECKSTEIN, V., ANSORGE, W. & HO, A. D. 2005. Comparative characteristics of mesenchymal stem cells from human bone marrow, adipose tissue, and umbilical cord blood. *Exp Hematol,* 33**,** 1402-16.

WAKABAYASHI, K., LIAN, Z. X., MORITOKI, Y., LAN, R. Y., TSUNEYAMA, K., CHUANG, Y. H., YANG, G. X., RIDGWAY, W., UENO, Y., ANSARI, A. A., COPPEL, R. L., MACKAY, I. R. & GERSHWIN, M. E. 2006. IL-2 receptor alpha(-/-) mice and the development of primary biliary cirrhosis. *Hepatology,* 44**,** 1240-9.

WAKITANI, S., IMOTO, K., YAMAMOTO, T., SAITO, M., MURATA, N. & YONEDA, M. 2002. Human autologous culture expanded bone marrow mesenchymal cell transplantation for repair of cartilage defects in osteoarthritic knees. *Osteoarthritis and Cartilage,* 10**,** 199-206.

WAKITANI, S., NAWATA, M., TENSHO, K., OKABE, T., MACHIDA, H. & OHGUSHI, H. 2007. Repair of articular cartilage defects in the patello-femoral joint with autologous bone marrow mesenchymal cell transplantation: three case reports involving nine defects in five knees. *J Tissue Eng Regen Med,* 1**,** 74-9.

WALENDA, G., ABNAOF, K., JOUSSEN, S., MEURER, S., SMEETS, H., RATH, B., HOFFMANN, K., FRÖHLICH, H., ZENKE, M., WEISKIRCHEN, R. & WAGNER, W. 2013. TGF-beta1 Does Not Induce Senescence of Multipotent Mesenchymal Stromal Cells and Has Similar Effects in Early and Late Passages. *PLoS ONE,* 8**,** e77656.

WANG, D., PARK, J. S., CHU, J. S. F., KRAKOWSKI, A., LUO, K., CHEN, D. J. & LI, S. 2004. Proteomic Profiling of Bone Marrow Mesenchymal Stem Cells upon Transforming Growth Factor β1 Stimulation. *Journal of Biological Chemistry,* 279**,** 43725-43734.

WANG, G., SAVINKO, T., WOLFF, H., DIEU-NOSJEAN, M. C., KEMENY, L., HOMEY, B., LAUERMA, A. I. & ALENIUS, H. 2007. Repeated epicutaneous exposures to ovalbumin progressively induce atopic dermatitis-like skin lesions in mice. *Clin Exp Allergy,* 37**,** 151-61.

WANG, M. K., SUN, H. Q., XIANG, Y. C., JIANG, F., SU, Y. P. & ZOU, Z. M. 2012. Different roles of TGF-beta in the multi-lineage differentiation of stem cells. *World J Stem Cells,* 4**,** 28-34.

WANG, N., FINEGOLD, M., BRADLEY, A., OU, C., ABDELSAYED, S., WILDE, M., TAYLOR, L., WILSON, D. & DARLINGTON, G. 1995. Impaired energy homeostasis in C/EBP alpha knockout mice. *Science,* 269**,** 1108-1112.

WANG, X., WILLENBRING, H., AKKARI, Y., TORIMARU, Y., FOSTER, M., AL-DHALIMY, M., LAGASSE, E., FINEGOLD, M., OLSON, S. & GROMPE, M. 2003. Cell fusion is the principal source of bone-marrow-derived hepatocytes. *Nature,* 422**,** 897-901.

WANG, Y., ZHANG, Z., CHI, Y., ZHANG, Q., XU, F., YANG, Z., MENG, L., YANG, S., YAN, S., MAO, A., ZHANG, J., YANG, Y., WANG, S., CUI, J., LIANG, L., JI, Y., HAN, Z. B., FANG, X. & HAN, Z. C. 2013. Long-term cultured mesenchymal stem cells frequently develop genomic mutations but do not undergo malignant transformation. *Cell Death Dis,* 4**,** e950.

WATABE, T. & MIYAZONO, K. 2009. Roles of TGF-[beta] family signaling in stem cell renewal and differentiation. *Cell Res,* 19**,** 103-115.

WATERMAN, R. S., TOMCHUCK, S. L., HENKLE, S. L. & BETANCOURT, A. M. 2010. A New Mesenchymal Stem Cell (MSC) Paradigm: Polarization into a Pro-Inflammatory MSC1 or an Immunosuppressive MSC2 Phenotype. *PLoS One,* 5**,** e10088.

WEISSER, S. B., VAN ROOIJEN, N. & SLY, L. M. 2012. Depletion and reconstitution of macrophages in mice. *J Vis Exp***,** 4105.

WELTER, J. F., PENICK, K. J. & SOLCHAGA, L. A. 2013. Assessing Adipogenic Potential of Mesenchymal Stem Cells: A Rapid Three-Dimensional Culture Screening Technique. *Stem Cells International,* 2013**,** 8.

WIEDER, E. 2003. Dendritic cells: a basic review. *International Society for Cellular Therapy*.

WLODKOWIC, D., TELFORD, W., SKOMMER, J. & DARZYNKIEWICZ, Z. 2011. Apoptosis and beyond: cytometry in studies of programmed cell death. *Methods Cell Biol,* 103**,** 55-98.

WOODBURY, D., SCHWARZ, E. J., PROCKOP, D. J. & BLACK, I. B. 2000. Adult rat and human bone marrow stromal cells differentiate into neurons. *J Neurosci Res,* 61**,** 364-70.

WRIGHT, K. O., MURRAY, D. A., CRISPE, N. I. & PIERCE, R. H. 2005. Quantitative PCR for detection of the OT-1 transgene. *BMC Immunol,* 6**,** 20.

WU, J., NIU, J., LI, X., WANG, X., GUO, Z. & ZHANG, F. 2014. TGF-beta1 induces senescence of bone marrow mesenchymal stem cells via increase of mitochondrial ROS production. *BMC Dev Biol,* 14**,** 21.

XU, Y., JAMES, A. W. & LONGAKER, M. T. 2008. Transforming Growth Factor-[beta]1 Stimulates Chondrogenic Differentiation of Posterofrontal Suture-Derived Mesenchymal Cells In Vitro. *Plastic and Reconstructive Surgery,* 122**,** 1649-1659 10.1097/PRS.0b013e31818cbf44.

YANG, K. G. A., SARIS, D. B. F., GEUZE, R. E., VAN RIJEN, M. H. P., VAN DER HELM, Y. J. M., VERBOUT, A. J., CREEMERS, L. B. & DHERT, W. J. A. 2006. Altered in vitro chondrogenic properties of chondrocytes harvested from unaffected cartilage in osteoarthritic joints. *Osteoarthritis and cartilage / OARS, Osteoarthritis Research Society,* 14**,** 561-570.

YANG, S.-H., PARK, M.-J., YOON, I.-H., KIM, S.-Y., HONG, S.-H., SHIN, J.-Y., NAM, H.-Y., KIM, Y.-H., KIM, B. & PARK, C.-G. 2009. Soluble mediators from mesenchymal stem cells suppress T cell proliferation by inducing IL-10. *Experimental and Molecular Medicine,* 41**,** 315-324.

YANG, Z., ZHANG, F., MA, W., CHEN, B., ZHOU, F., XU, Z., ZHANG, Y., ZHANG, D., ZHU, T., WANG, L., WANG, H., DING, Z. & ZHANG, Y. 2010. A Novel Approach to Transplanting Bone Marrow Stem Cells to Repair Human Myocardial Infarction: Delivery via a Noninfarct-relative Artery. *Cardiovascular Therapeutics,* 28**,** 380-385.

YARAK, S. & OKAMOTO, O. K. 2010. Human adipose-derived stem cells: current challenges and clinical perspectives. *An Bras Dermatol,* 85**,** 647-56.

YOSHIKI, A. & MORIWAKI, K. 2006. Mouse Phenome Research: Implications of Genetic Background. *ILAR Journal,* 47**,** 94-102.

YU, J., YIN, S., ZHANG, W., GAO, F., LIU, Y., CHEN, Z., ZHANG, M., HE, J. & ZHENG, S. 2013. Hypoxia preconditioned bone marrow mesenchymal stem cells promote liver regeneration in a rat massive hepatectomy model. *Stem Cell Res Ther,* 4**,** 83.

YU, K. R. & KANG, K. S. 2013. Aging-Related Genes in Mesenchymal Stem Cells: A Mini-Review. *Gerontology,* 59**,** 557-563.

ZANINI, C., BRUNO, S., MANDILI, G., BACI, D., CERUTTI, F., CENACCHI, G., IZZI, L., CAMUSSI, G. & FORNI, M. 2011. Differentiation of Mesenchymal Stem Cells Derived from Pancreatic Islets and Bone Marrow into Islet-Like Cell Phenotype. *PLoS ONE,* 6**,** e28175.

ZAPPIA, E., CASAZZA, S., PEDEMONTE, E., BENVENUTO, F., BONANNI, I., GERDONI, E., GIUNTI, D., CERAVOLO, A., CAZZANTI, F., FRASSONI, F., MANCARDI, G. & UCCELLI, A. 2005. Mesenchymal stem cells ameliorate experimental autoimmune encephalomyelitis inducing T-cell anergy. *Blood,* 106**,** 1755-1761.

ZHANG, B., LIU, R., SHI, D., LIU, X., CHEN, Y., DOU, X., ZHU, X., LU, C., LIANG, W., LIAO, L., ZENKE, M. & ZHAO, R. C. H. 2008a. Mesenchymal stem cells induce mature dendritic cells into a novel Jagged-2–dependent regulatory dendritic cell population. *Blood,* 113**,** 46-57.

ZHANG, L., HU, J. & ATHANASIOU, K. A. 2009. The role of tissue engineering in articular cartilage repair and regeneration. *Crit Rev Biomed Eng,* 37**,** 1-57.

ZHANG, S. 2014. *Mesenchymal stem cells, cartilage regeneration and immune privilege.* Doctor of Philosophy Thesis, University of Bristol, UK.

ZHANG, Z. & WANG, F.-S. 2013. Stem cell therapies for liver failure and cirrhosis. *Journal of Hepatology,* 59**,** 183-185.

ZHANG, Z. X., GUAN, L. X., ZHANG, K., ZHANG, Q. & DAI, L. J. 2008b. A combined procedure to deliver autologous mesenchymal stromal cells to patients with traumatic brain injury. *Cytotherapy,* 10**,** 134-9.

ZHAO, L. & HANTASH, B. M. 2011. TGF-beta1 regulates differentiation of bone marrow mesenchymal stem cells. *Vitam Horm,* 87**,** 127-41.

ZHEN, G., WEN, C., JIA, X., LI, Y., CRANE, J. L., MEARS, S. C., ASKIN, F. B., FRASSICA, F. J., CHANG, W., YAO, J., CARRINO, J. A., COSGAREA, A., ARTEMOV, D., CHEN, Q., ZHAO, Z., ZHOU, X., RILEY, L., SPONSELLER, P., WAN, M., LU, W. W. & CAO, X. 2013. Inhibition of TGF-[beta] signaling in mesenchymal stem cells of subchondral bone attenuates osteoarthritis. *Nat Med,* 19**,** 704-712.

ZHENG, X., BAKER, H., HANCOCK, W. S., FAWAZ, F., MCCAMAN, M. & PUNGOR, E. 2006. Proteomic Analysis for the Assessment of Different Lots of Fetal Bovine Serum as a Raw Material for Cell Culture. Part IV. Application of Proteomics to the Manufacture of Biological Drugs. *Biotechnology Progress,* 22**,** 1294-1300.

ZHOU, Y. F., BOSCH-MARCE, M., OKUYAMA, H., KRISHNAMACHARY, B., KIMURA, H., ZHANG, L., HUSO, D. L. & SEMENZA, G. L. 2006. Spontaneous Transformation of Cultured Mouse Bone Marrow–Derived Stromal Cells. *Cancer Research,* 66**,** 10849-10854.

ZHU, H., GUO, Z. K., JIANG, X. X., LI, H., WANG, X. Y., YAO, H. Y., ZHANG, Y. & MAO, N. 2010. A protocol for isolation and culture of mesenchymal stem cells from mouse compact bone. *Nature Protocols,* 5**,** 550-560.

ZIEGLER, S. F., RAMSDELL, F. & ALDERSON, M. R. 1994. The activation antigen CD69. *Stem Cells,* 12**,** 456-65.

ZOSKY, G. R., LARCOMBE, A. N., WHITE, O. J., BURCHELL, J. T., JANOSI, T. Z., HANTOS, Z., HOLT, P. G., SLY, P. D. & TURNER, D. J. 2008. Ovalbumin-sensitized mice are good models for airway hyperresponsiveness but not acute physiological responses to allergen inhalation. *Clin Exp Allergy,* 38**,** 829-38.

ZUK, P. A., ZHU, M., ASHJIAN, P., DE UGARTE, D. A., HUANG, J. I., MIZUNO, H., ALFONSO, Z. C., FRASER, J. K., BENHAIM, P. & HEDRICK, M. H. 2002. Human Adipose Tissue Is a Source of Multipotent Stem Cells. *Mol. Biol. Cell,* 13**,** 4279-4295.